NEDO-32229
Class 1
AUGUST, 2000

MODEL 2000
RADIOACTIVE MATERIAL TRANSPORT PACKAGE
HFIR FUEL BASKET AND LINER
SAFETY ANALYSIS REPORT

GE NUCLEAR ENERGY IRRADIATION PROCESSING OPERATION
VALLECITOS NUCLEAR CENTER
PLEASANTON, CALIFORNIA

NOTICE AND DISCLAIMER

This report was prepared by General Electric Company solely for the use of the U.S. Nuclear Regulatory Commission (NRC) in licensing the Model 2000 Transport Package HFIR Fuel Basket and Liner. General Electric assumes no responsibility for liability or damage which may result from any other use of the information disclosed in this report.

The information contained in this report is believed to be an accurate and true representation of the facts known by or provided to General Electric at the time this report was prepared. General Electric Company and the individual contributors to this report make no express or implied warranty with respect to the accuracy, completeness, or usefulness of the information contained in this report, other than for the licensing of the Model 2000 Transport Package HFIR Fuel Basket and Liner or that the use of any information disclosed in this report may not infringe privately owned rights, including patent rights.

The following endorsements apply to the Safety Analysis Report:

Checked By: _____ Date 7/30/93

Harold Durlofsky, Ph.D., Consultant
Structural Mechanics Analysis
Sunnyvale, California

Checked By: _____ Date 7/30/93

George E. Cunningham
Senior Licensing Engineer

Approved By: _____ Date 7/30/93

Raul J. Pomares, Manager
Engineering Projects

TABLE OF CONTENTS

TABLE OF CONTENTS (CONTINUED)

TABLE OF CONTENTS (CONTINUED)

TABLE OF CONTENTS (CONTINUED)

TABLE OF CONTENTS (CONTINUED)

TABLE OF CONTENTS (CONTINUED)

TABLES

TABLES (CONTINUED)

TABLES (CONTINUED)

ILLUSTRATIONS

ILLUSTRATIONS (CONTINUED)

ILLUSTRATIONS (CONTINUED)

ILLUSTRATIONS (CONTINUED)

1.0 GENERAL INFORMATION

This Safety Analysis Report describes and evaluates the basket and liner developed for transportation of High Flux Isotope Reactor (HFIR) fuel assembly in a Model 2000 Transport Package. Drawings of the subject basket and liner are included in Subsection 1.3.2.

The complete description and evaluation of the Model 2000 Transport Package is described in the Model 2000 Radioactive Material Transport Package Safety Analysis Report, Reference 1.1.

1.1 INTRODUCTION

The HFIR fuel basket and liner have been developed as a means to transport one fuel assembly on its entirety of the HFIR reactor in the Model 2000 Packaging (United State Nuclear Regulatory Commission, USNRC, Model 2000, Certificate of Compliance No. 9228). No modifications to the Model 2000 packaging containment boundary is required to accommodate the HFIR fuel basket and liner. Neither would the basket and liner have significant effect on the design, operating characteristics, or safety performance of the packaging, as described in the its Safety Analysis Report [1.1].

The Model 2000 Package is currently licensed for transport of irradiated fuel rods which may be cut or segmented, byproduct, and source or special nuclear material, in solid form. The material or content is limited to a maximum decay heat of 600 watts. Also its weight including carrier racks, shoring or secondary containers must not exceed 5450 lbs. The fissile contents of the allowed irradiated fuel must have the following characteristics:

a) "Not to exceed 1175 grams U-235 equivalent mass with initial enrichment not to exceed 5 weight percent in the fissile isotope; minimum pellet diameter of 0.3 inch, maximum burnup of 45 GWd/MTU, and minimum cooling time of 120 days," or

b) "Not to exceed 1750 grams U-235 equivalent mass with initial enrichment not to exceed 5 weight percent in the fissile isotope; minimum pellet diameter of 0.35 inch, maximum burnup of 38 GWd/MTU, and minimum cooling time of 120 days."

The HFIR fuel assembly consists of two concentric cylindrical elements of involute-shaped U(93%)-Al fuel plates clad with aluminum. The outer element has 6872 grams of U-235 maximum and the inner element has 2628 grams of U-235 maximum. Appendix 1.4.2 gives a summary of the HFIR fuel assembly characteristics.

Authorization is sought for the use of the basket and liner for shipment of HFIR spent fuel assembly in the Model 2000 Package under 10CFR71.13 [1.2] provisions for modifications of contents of a Type B package.

1.2 PACKAGE DESCRIPTION

1.2.1 Packaging

The Model 2000 Packaging is a cylindrical cask transported in the upright position inside an overpack structure. The overpack has toroidal shell impact limiters at each end (see Figure 1.1). The approximate overall packaging dimensions are 131.5 inches in height and 72 inches in diameter. The approximate gross weight of the package is 33,350 lbs.

The cask is constructed of two 1-inch thick type 304 stainless steel concentric cylindrical shells (see Figure 1.2). The shells are joined at the bottom end to a 6-inch thick type 304 stainless steel forging. The annulus between the two shells is approximately 4 inches wide and is filled with lead. The cask has an approximate height of 71 inches and an outer diameter of 38.5 inches. The cask cavity is approximately 26.5 inches in diameter and 54 inches in depth. The cask lid is made

FIGURE WITHHELD UNDER 10 CFR 2.390

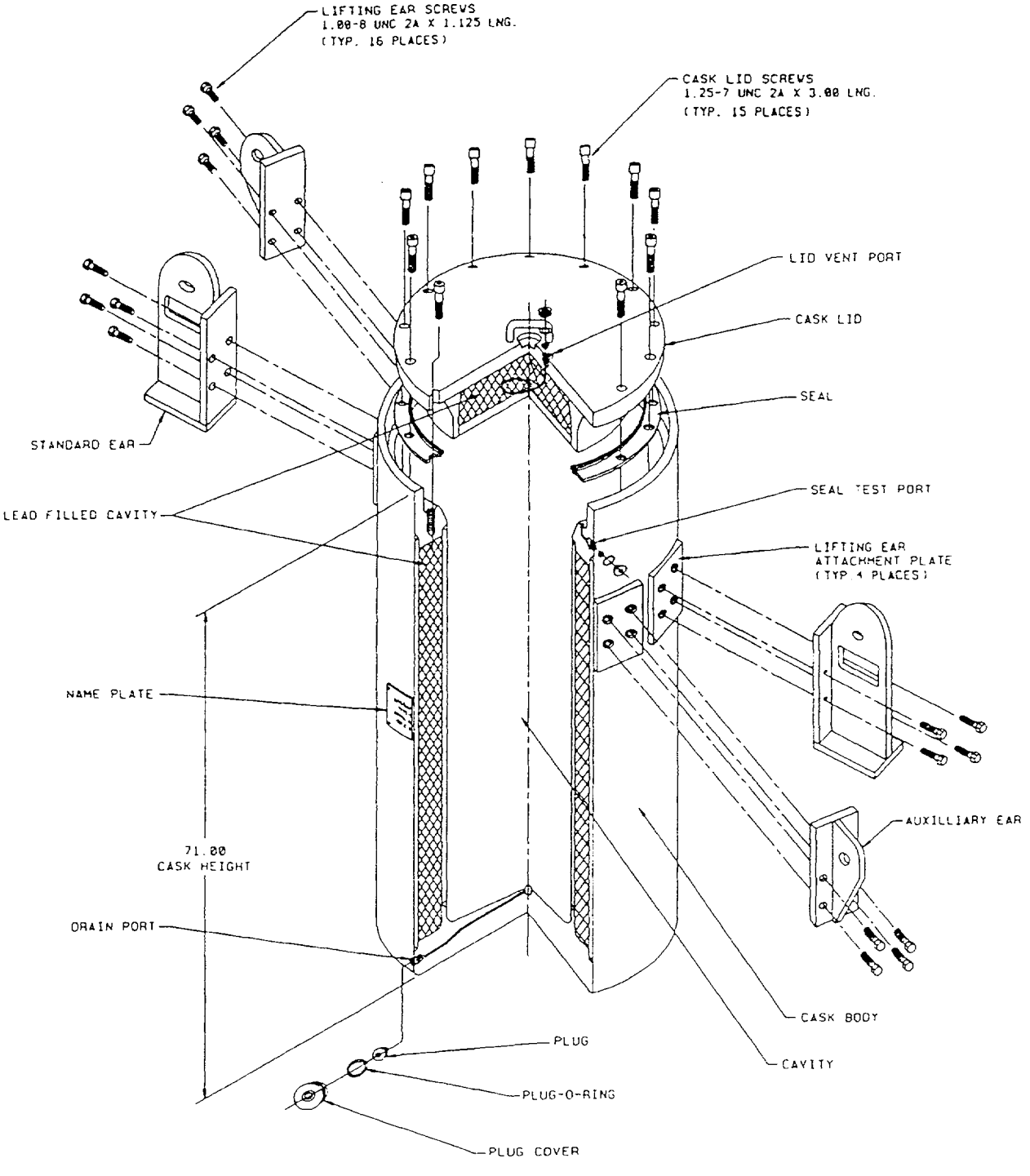

Figure 1.2. Model 2000 Transport Packaging, Cask

of type 304 stainless steel and lead. It has a stepped design, and is fully recessed into the cask top flange. The lid is secured to the cask body by 15 1-1/4 inch diameter socket head screws. The cask is sealed by elastomeric O-rings bonded to a thin aluminum disc-shaped ring. The cask has a seal test port in the side of the cask body, a vent port in the cask lid, and a drain port near the bottom of the cask. The cask body has attachment plates for lifting devices which are detached during transport.

The cask is positioned within an overpack constructed from two 0.5-inch thick type 304 stainless steel concentric cylindrical shells (see Figure 1.3). The shells are separated radially by eight equally spaced tubes along the length of the shells and by two tube sections around the perimeter of the shells. A toroidal shell impact limiter made of type 304 stainless steel is attached to each end of the overpack shells. The overpack opens just above the lower impact limiter for access to the cask. The top section of the overpack is joined to the base by 15 1-3/8 inch diameter shoulder screws. Gussets on the top and bottom impact limiters provide tie-down points for the package.

The HFIR fuel basket and liner is assembled in the Model 2000 cask cavity to maintain fuel element separation and provide additional shielding. Figure 1.4 depicts such assembly. The basket and liner house the inner and outer HFIR elements respectively. The outer element sits at the bottom of the liner supported by its outer shell while the inner element hangs by the upper edge of its outer shell inside the basket. This arrangement is the same as used to support the inner element in the HFIR Reactor.

The basket is a tubular structure of an inside diameter of 10.63 inches and a changing cross section (see Figure 1.5). The wall thickness varies from 0.25 inches for the top approximately 22.50 inches of length to 0.12 inches for a total length of 27.83 inches. A support tube 5.00 inches outside diameter, 0.13-inch wall and approximately 21.00 inches in length follows after a transition funnel section with a length of 4.71 inches. A 1.00-inch thick, 24.88 outside diameter flange is welded to the structure top end. A 3.00-inch thick tungsten alloy dish is attached to the bottom end of the support tube. A 0.38 inch diameter rod bail is bolted to the flange for handling. Three, equally spaced slots are provided on the flange, as an alternate arrangement, for lifting the basket. Six 1-inch thick rings or fins are part of the tube upper section on the outside diameter at 3.0-inch pitch. The basket is made of Type 304 stainless steel.

The HFIR fuel liner consists of a Type 304 stainless steel forging cylinder, machined to a length of 52.75 inches and with an inside diameter of 17.38 inches (see Figure 1.5). The outside diameter is machined to form a series of six rings 2 inches thick, with an 8 inch pitch and a 26.25 inches maximum diameter and approximately 23.13 inches minimum diameter. The seventh or bottom ring is 2.50-inches thick. At the bottom end of the liner cylinder there is a 2.13 inch thick tungsten alloy disk recessed into the liner wall. The tungsten alloy disk is held in place by twelve socket head cap screws. There is a 5.13 inch diameter hole at the center of the disk. This hole allows the basket support tube to penetrate the disk for the basket alignment and radial support.

Both structures, basket and liner, have features to facilitate water drainage during wet loading. See Figure 1.5 for their details.

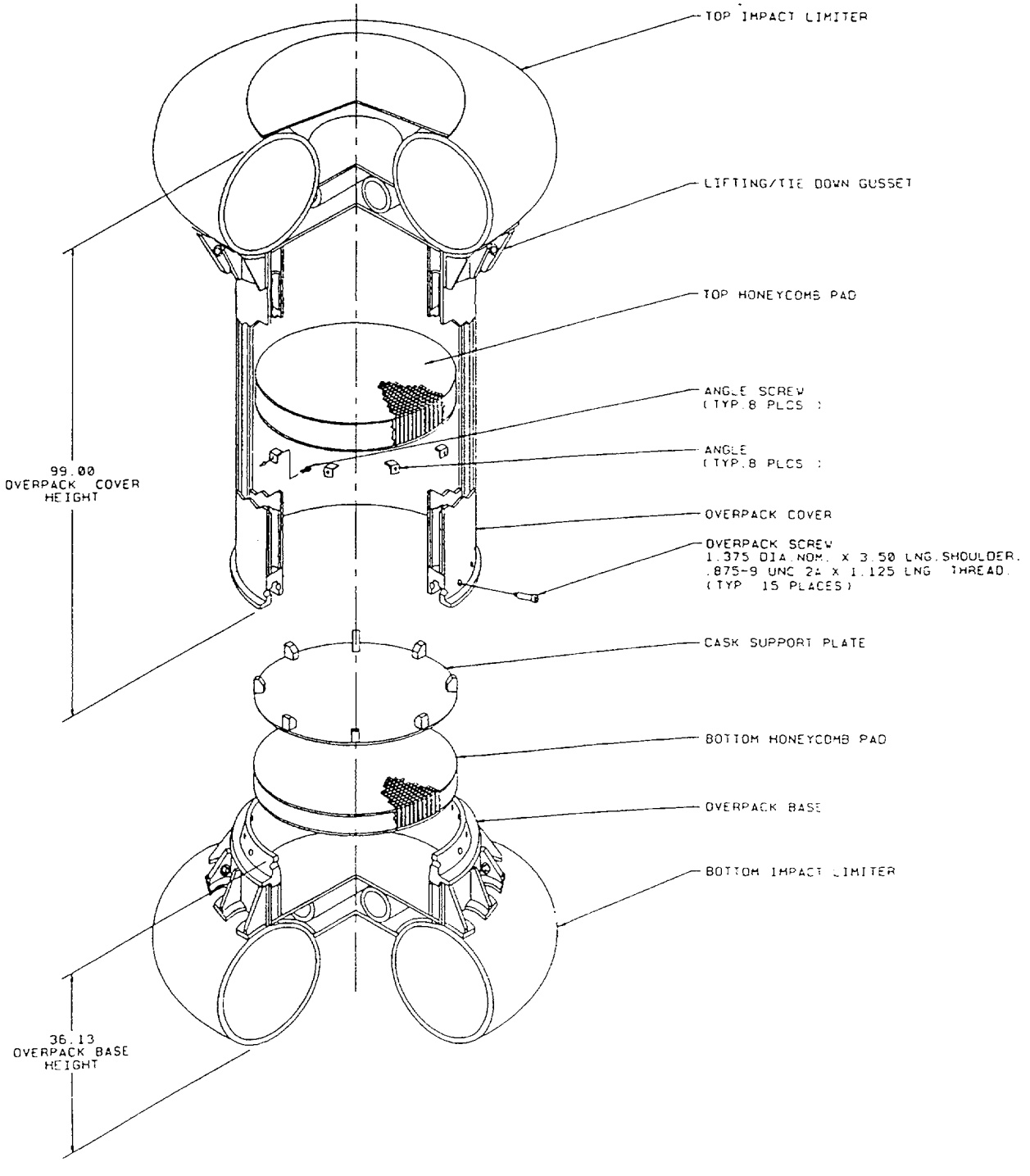

Figure 1.3. Model 2000 Transport Packaging, Overpack

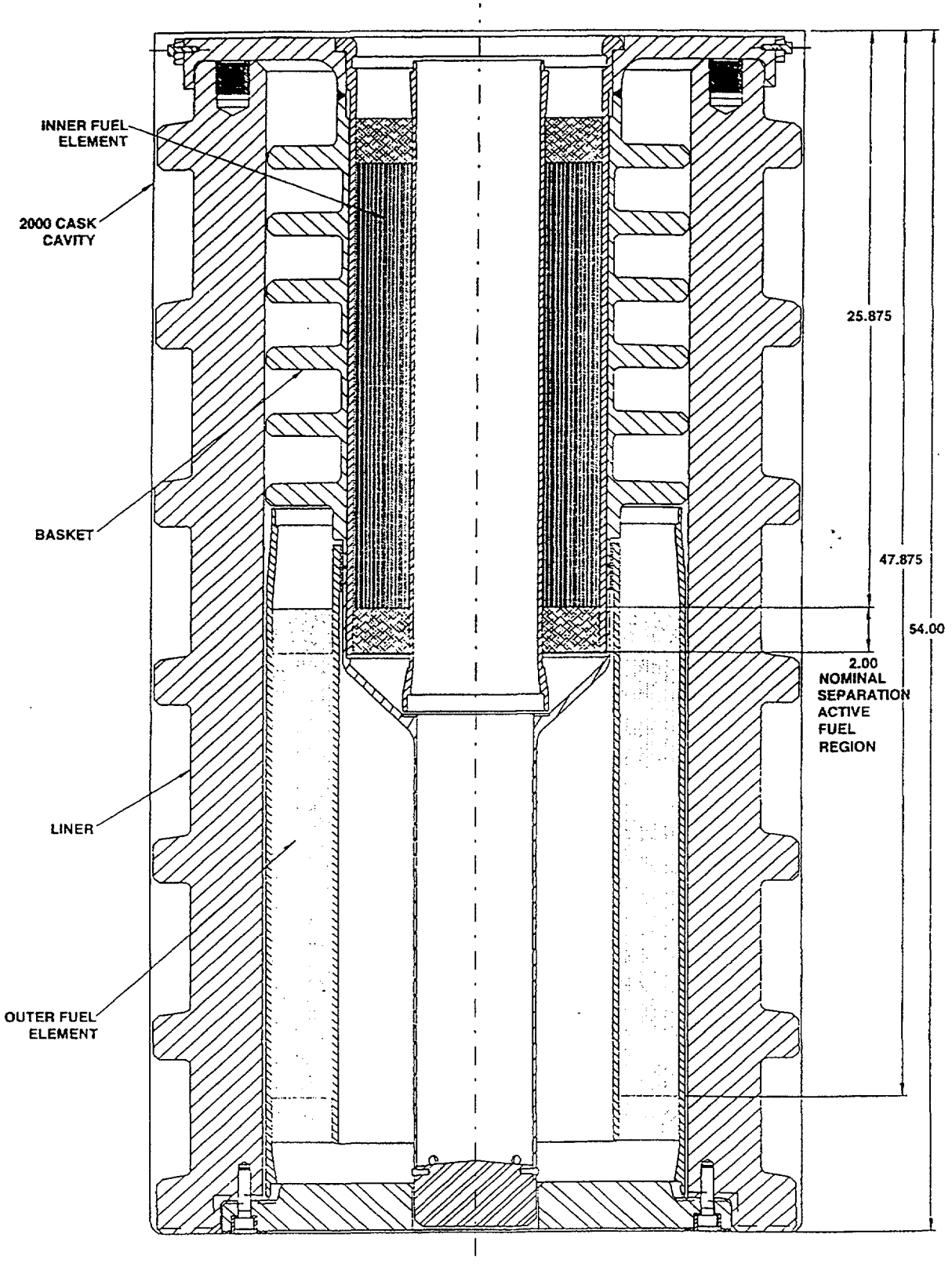

Figure 1.4. HFIR Fuel Elements Shipping Configuration

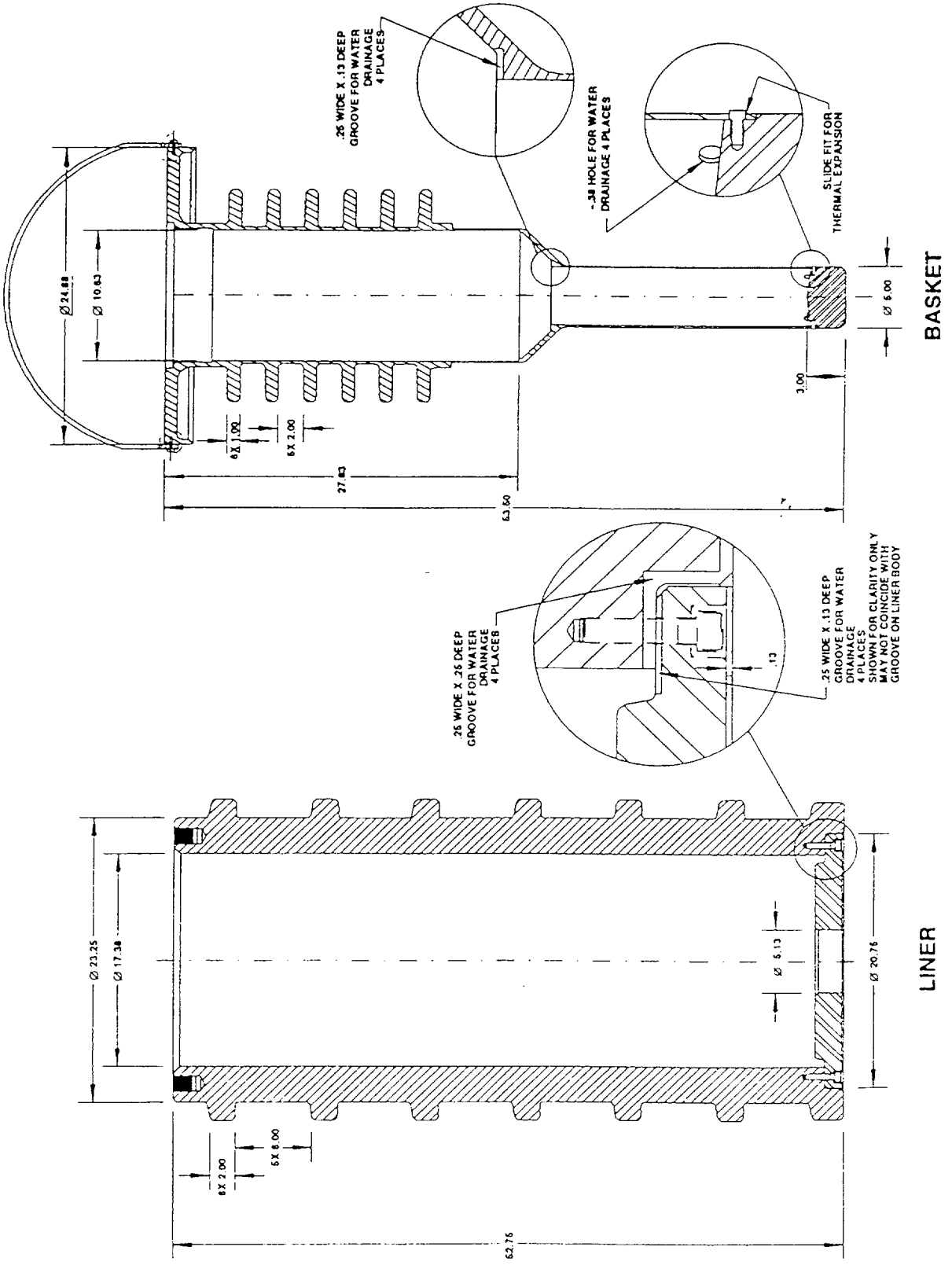

Figure 1.5. HFIR Fuel Shipping Basket and Liner

The General Electric Quality Assurance Program (QAP-1) used for the design, manufacture, and maintenance of the Model 2000 packaging and the HFIR fuel basket and liner satisfies the eighteen criteria of 10CFR71, Subpart H [1.2]. QAP-1 [1.3] has been approved by the USNRC under Docket 71-0170.

1.2.2 Operational Features

The use of the HFIR fuel basket and liner in the Model 2000 Package does not change or introduce any new operational features to the Package. The HFIR fuel elements are loaded in the Model 2000 cask underwater. All wet-loaded operation with this cask requires that the cask cavity be drained and vacuum dry to remove any residual moisture. To vacuum dry the cask, its cavity pressure is reduced below the vapor pressure of water and maintained at or below this pressure level for a period of time.

1.2.3 Contents of Packaging

The Model 2000 Package is used to transport Type B quantities of radioactive materials and fissile materials (Class III). This includes byproduct, source, and special nuclear materials. This Report addresses the addition of one HFIR spent fuel assembly limited to 600 watts of decay heat, as an authorized content when shipped in the basket and liner arrangement shown in Figure 1.4. No modification to either of the fuel elements, inner and outer, is required to place them within the basket and liner.

The HFIR fuel assembly consist of two concentric cylindrical elements. Each element is made of a series of involute-shaped U-AL fuel plates, 93% nominal, 93.2% maximum enrichment, with aluminum clad. The outer element has 6872 grams of U-235 maximum and the inner element has 2628 grams of U-235 maximum. Subsection 1.4.2 gives a summary of the HFIR fuel assembly.

1.3 REFERENCE

1.1. Model 2000 Radioactive Material Transport Package Safety Analysis Report, NEDO-31581 April 1988.

1.2. Code of Federal Regulations, Title 10, Part 71, 1992.

1.3. General Electric Quality Assurance Program for Shipping Packages for Radioactive Material, QAP-1, Revision 5, 1990.

1.4 APPENDIX

1.4.1 Drawings

1.4.2 HFIR Fuel Assembly Characteristics

APPENDIX 1.4.1

Drawing 105E9523 Rev 2: *HFIR Fuel Liner and Basket*

Drawing M-11524-0H-101-D: *HFIR Fuel Inner Element*

Drawing M-11524-0H-102-D: *HFIR Fuel Outer Element*

APPENDIX 1.4.2

HFIR FUEL ASSEMBLY CHARACTERISTICS

A nominal HFIR fuel assembly is shown in Figure 1.6. Table 1.1 provides relevant HFIR spent fuel data. Each assembly is constructed primarily of aluminum (6061 with additional 101 powder, 4043 filler, and 6061 cladding) and consists of a cylindrical inner element surrounded by a cylindrical outer element. The inner element contains 171 radially involuted fuel plates supported by inner and outer side plates. The outer element contains 369 fuel plates in a similar configuration. The radial involutes provide constant width coolant channels with widths comparable to those of the fuel plates. The side plates extend beyond the axial domain of the fuel plates to provide assembly support in the reactor.

Each fresh fuel plate contains a mixture of U_3O_8 and aluminum powder (cermet) housed within an aluminum cladding. Each inner fuel plate additionally contains a small amount of B_4C. The U_3O_8 (and, therefore, the aluminum powder) loading varies both along the path of the involute and between the inner and outer elements. Narrow aluminum radial rings (wings) exist adjacent to the inner and outer side plates of both elements. Additionally, aluminum upper and lower axial zones exist within each fuel plate.

Figures 1.7 and 1.8 show detail dimensions of the HFIR fuel inner and outer elements respectively. The information presented in these figures is based ORNL drawings M-11524-0H-101-D: *HFIR Fuel Inner Element* drawings M-11524-0H-102-D: *HFIR Fuel Outer Element*, which are included in this Subsection.

FIGURE WITHHELD UNDER 10 CFR 2.390

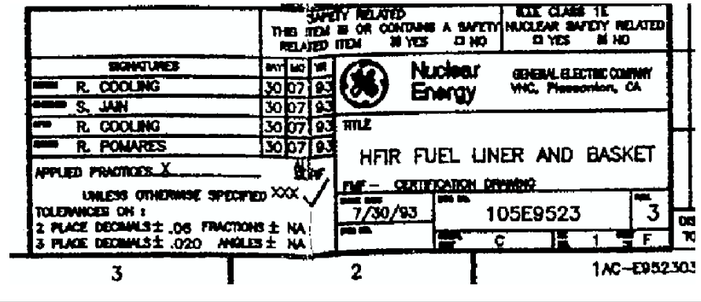

FIGURE WITHHELD UNDER 10 CFR 2.390

OAK RIDGE NATIONAL LABORATORY

MARTIN MARIETTA MARTIN MARIETTA ENERGY SYSTEMS, INC.

operated for the DEPARTMENT OF ENERGY under U.S. GOVERNMENT contract DE-AC-05-84OR21 400 eng 26

Oak Ridge, Tennessee • Paducah, Kentucky

FACILITY H.F.I.R. BLDG. NO. 7900

H.F.I.R. FUEL INNER ELEMENT
SHIPPING CASK
CERTIFICATION DRAWING

SUBMITTED		REQUESTOR		FACILITY APPROVAL			
R.W. KNIGHT		LARRY PROCTOR		M.B. FARRAR 5-10-95			
S.E. BURNETTE 5-10-95	M	11524	ØH	101	D	REV.	0

FIGURE WITHHELD UNDER 10 CFR 2.390

REFERENCE DRAWINGS	NUMBER

OAK RIDGE NATIONAL LABORATORY

MARTIN MARIETTA | MARTIN MARIETTA ENERGY SYSTEMS, INC.

operated for the DEPARTMENT OF ENERGY under U.S. GOVERNMENT contract DE-AC-05-840R21 400 eng 26
Oak Ridge, Tennessee • Paducah, Kentucky

FACILITY H.F.I.R. BLDG. NO. 7900

H.F.I.R. FUEL OUTER ELEMENT
G.E. 2000 SHIPPING CASK
CERTIFICATION DRAWING

SUBMITTED	REQUESTOR	FACILITY APPROVAL
R.W. KNIGHT	LARRY PROCTOR	W. B. FARMER 6-10-95

S.E. BURNETTE 5/10/95	M	11524	ØH	102	D	REV.	0

AS DESIGNED

2.0 STRUCTURAL EVALUATION

This Chapter presents the structural evaluation of the Model 2000 Cask HFIR fuel basket and liner and its conformance with all applicable structural criteria. Normal and hypothetical accident condition evaluations are performed in accordance with 10CFR71 [2.1] requirements.

The results of the engineering evaluations are presented to demonstrate that the HFIR fuel basket and liner remain functional under normal transport and hypothetical accident conditions, and as such, maintain the configuration of the contained HFIR fuel inner and outer elements to assure criticality and shielding safety.

The engineering evaluation consists of static, linear elastic finite element analyses of the HFIR fuel basket and liner design for each of the applicable loading conditions. The results of these analyses are compared against the allowable stress limit criteria specified by Regulatory Guide 7.6 [2.2]. LIBRA Finite Element Computer Code is used in this evaluation.

LIBRA is a multi-purpose finite element computer code applicable to both static and dynamic analyses of linear and nonlinear structural systems. In addition, there is a companion heat transfer program for the analysis of both steady-state and transient thermal distributions in structural systems. A series of exact solution type of problems and benchmark testing in the thermal and structural areas verify the accuracy of the analyses [2.3].

2.1 STRUCTURAL DESIGN

2.1.1 Discussion

The HFIR fuel basket and liner consist of an assembly of a tubular structure (basket) and a thick cylindrical shell (liner). The detailed design of each component is shown in the drawing included in Subsection 1.3.2. The basket and liner assembly accommodate one HFIR fuel assembly. The basket contains the inner fuel element, while the liner encloses the outer one. The total weight of the basket, liner, and HFIR fuel assembly is less than the allowable payload weight (5450 lbs) of the Model 2000 Package.

The HFIR basket and liner are designed to maintain separation of the fuel elements during all normal and accident conditions and to enhance the shielding characteristics of the Package.

2.1.1.1 General Description of The Finite Element Model. A two dimensional axisymmetric finite element model of the HFIR fuel basket and liner, shown in Figure 2.1, is developed and used for the analysis. The HFIR fuel basket and liner model employs primarily eight-node quadrilateral isoparametric elements which use second order shape functions for the displacement field. The only other type of element employed is the constant strain triangular element.

The constant strain triangular element is used in the thick fins positioned on the outer surface of the liner body which appear like ribs on the exterior of this cylindrical liner. These large fins can transfer lateral loads directly from the liner to the cask through bearing on the interior surface of the cask. However, their primary function is facilitating heat conduction to the cask, and they experience low stresses due to their large size and number which dictates small spacing. The triangular elements are used in the outer periphery of these rings as a transition zone between the mesh of the liner and the mesh of the cask to facilitate the finite element thermal analysis. In all, they total 36.

The finite element model of the HFIR fuel basket and liner has a total of 1589 nodes and 337 elements, which with the exception of the 36 triangular elements are all eight-node quadrilateral isoparametric elements. The basket portion has 637 nodes with 113 elements (Figure 2.2) all of which are eight-node quadrilateral isoparametric elements. The entire model is utilized in all structural analyses involving axisymmetric loading, i.e., vertical acceleration.

For the conditions involving lateral acceleration components only the basket portion is used as shown in Figure 2.2, since this portion is expected to be subjected to stresses exceeding those in the liner under these loading conditions. This is because the liner has much thicker walls than any segment of the basket. Extensions to the element formulations which accommodate non-axisymmetric loading of the axisymmetric model are utilized in the analyses involving the lateral acceleration components.

The interface area between the lower part of the basket support tube and its tungsten plug is modeled so that there is no contact between them except at the common node near the bottom as shown in Figure 2. l and Figure 2.2. The common node at the interface simulates the pinned joint of these components.

Therefore, only the radial and vertical forces are transmitted through the common node, not the moments. Similarly, the basket support tube and the liner base are also modeled with a gap, thus preventing any physical contact between them except for the side drop loading case where the radial movement of the basket support tube is restricted by the liner base.

Since there is a 0.25 inch gap between the basket support tube and the bottom surface of the cask cavity, the basket hangs inside the liner from its top flange on the liner top surface. The interface between the basket top flange and the liner are modeled with "double" nodes, one set belonging to the basket and the other to the liner. For each loading case, constraining conditions and/or merging of nodes are imposed selectively on these nodes.

A detailed description of the loading and boundary conditions used is further discussed in the sections (Section 2.6 and Section 2.7) describing each loading condition analyzed. For dimensions and various interfaces discussed in this Section, refer to the GE Certification Drawing, "HFIR FUEL BASKET AND LINER" [2.21].

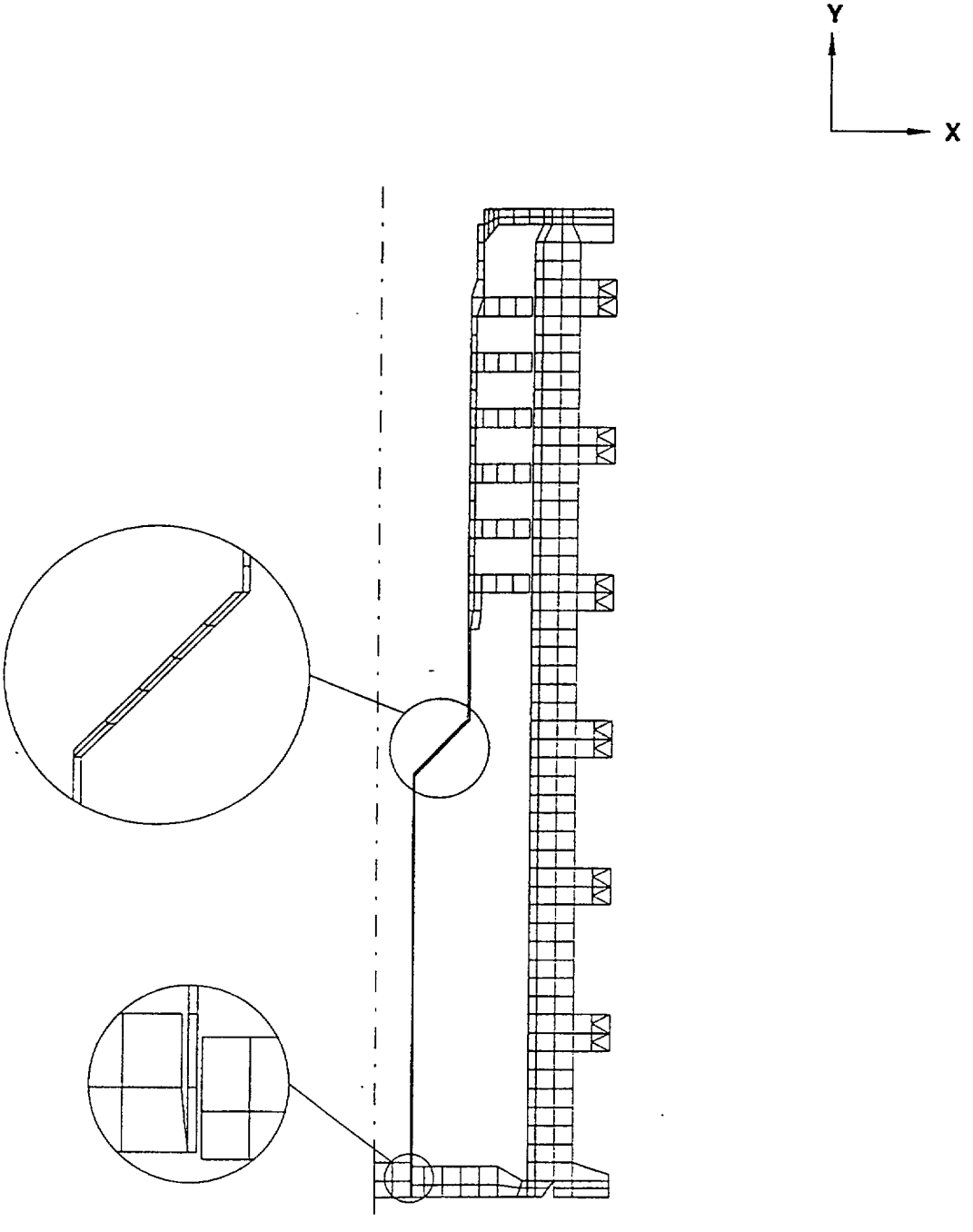

Figure 2.1. HFIR Basket and Liner Finite Element Model (1589 Nodes, 337 Elements)

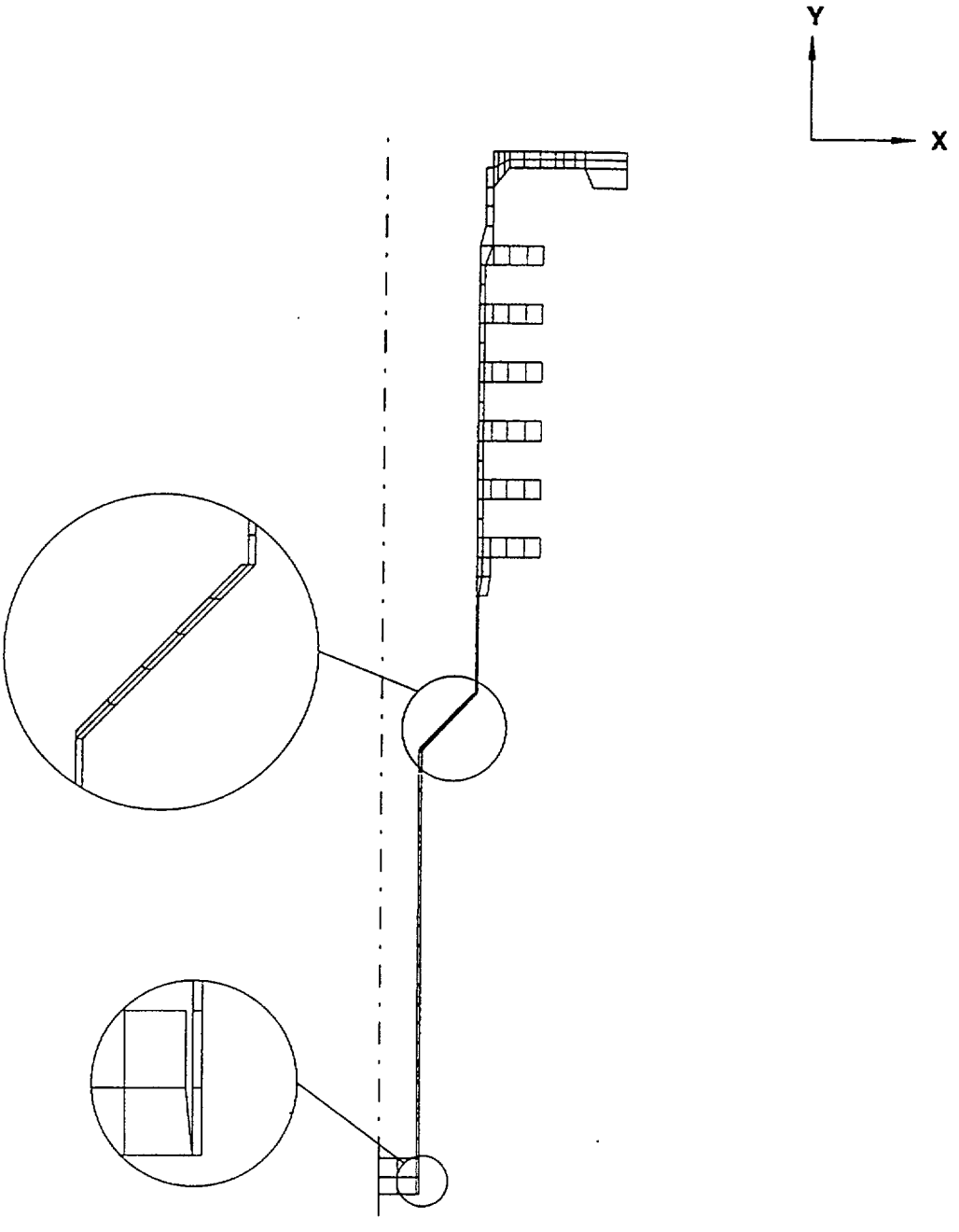

Figure 2.2. HFIR Basket Finite Element Model (637 Nodes, 113 Elements)

2.1.2 Design Criteria

2.1.2.1 Allowable Stresses. This section defines the allowable limits for primary membrane (Pm), primary bending (Pb), secondary (Q), bearing, and shear stresses and the required factor of safety against instability (i.e. buckling) for all components in the HFIR fuel basket and liner assembly. The basket is designed in accordance with the Regulatory Guide 7.6 [2.2] and Subsection NG [2.4]. Table 2.1 summarizes the allowable criteria used in this analysis.

2.1.2.2 Load Combinations. The load combinations used in the HFIR fuel basket and liner assembly analysis are developed in accordance with Regulatory Guide 7.8 [2.5] for the applicable basket loads. The resulting load combinations are shown in Table 2.2.

2.1.2.3 Miscellaneous Structural Criteria

2.1.2.3.1 Brittle Fracture. All structural components of the HFIR fuel basket and liner are fabricated from austenitic stainless steels Type 304 and Tungsten Alloy. Since these materials do not undergo a ductile to brittle transition in the temperature range of interest (down to -40°F), they are not subject to brittle fracture on this application.

2.1.2.3.2 Fatigue. A fatigue analysis of the basket assembly is required to evaluate the effects of cyclic loads. The fatigue analysis is performed in accordance with the requirements of Regulatory Guide 7.6 [2.2]. All significant cyclic loads, including thermal cycling and vibration, are evaluated to determine the cumulative usage factor.

Stress Condition	Allowable Stress
Normal Condition	
Pm	Sm
Pm+Pb	1.5 Sm
Pm+Pb+Q	3 Sm
Bearing Stress	Sy
Pure Shear	0.6 Sm
Fatigue, S_{alt}	Sa @ Life Cycles (1)
Accident Condition	
Pm	Lesser of 2.5 Sm and 0.7 Su
Pm+Pb	Lesser of 3.6 Sm and Su
Pm+Pb+Q	Need not be evaluated
Bearing Stress	Need not be evaluated
Pure Shear	0.42 Su
Buckling	<0.67 PCR (2)
Sum of All Peak Stress Components	<Sa at 10 Cycle (3)
Notes: (1) Sa obtained from fatigue curves Figure I-9.2.2, Appendix I [2.6] (2) PCR represents the elastic collapse-load (3) Sa obtained from fatigue curve Figure I-9.2.1, Appendix I [2.6]	

Table 2.1. Allowable Stress Limit Criteria [2.6]

Load Combination (1) Number	Load Definition [2.3]
1. One Foot Drop + Normal Thermal	Top/Btm 69 g's; Side 69 g's
2. Thirty Foot Drop	Top/Btm 133 g's; Side 133 g's CG/corner 63 g's
3. Accident Thermal(2)	
4. Vibration and Shock + Normal Thermal(3)	10 g's Vertical and 5 g's Lateral
Notes: (1) All other load combinations specified by Regulatory Guide 7.8 [2.5] are not applicable for the HFIR fuel basket and liner assembly. (2) Evaluation of the accident thermal (fire accident) case is performed to demonstrate it has no adverse effect on the HFIR fuel basket and liner. (3) Evaluated for fatigue.	

Table 2.2 Load Combination Definitions

2.2 COMPONENT WEIGHTS

The total weight of the HFIR fuel elements, basket, and liner assembly is 4,545 lbs. A summary of the HFIR fuel shipping assembly component weights is provided in Table 2.3.

2.3 MECHANICAL PROPERTIES OF MATERIALS

The HFIR fuel basket and liner assembly is fabricated from austenitic stainless steels Type 304 (ASME SA-182 and SA-213) and tungsten alloy (ASTM B777). Type 304 stainless steel is an ASME Code approved material with high corrosion resistance. The density of this stainless steel used in the analysis is 0.285 lb-in^3 [2.6] and the density of tungsten is 0.61 lb/in^3 [2.7]. A listing of the material properties used in the analysis is included in Table 2.4.

2.4 GENERAL STANDARDS FOR ALL PACKAGES

The existing Model 2000 Package SAR [2.3] provides justification that the general standards for the packaging are met. Additional information specifically applicable to the HFIR fuel basket and liner assembly is provided in the following sections.

2.4.1 Minimum Package Size

The HFIR fuel basket and liner assembly has no effect on package size.

Component	Maximum Weight (lbs)
HFIR Fuel Assembly	325
Liner	3700
Basket	520
Total	4545

Notes:

(1) Component weights are calculated based on the dimensions shown on the drawings in Section 1.3.2 and the material densities discussed in Section 2.3.

(2) HFIR fuel weight is based on an inner element weight of 110 lbs and an outer element weight of 215 lbs.

Table 2.3. HFIR Fuel Shipping Assembly Component Weights

Steel Material Spec.	Type or Grade	Stress (ksi)				Young's Modulus (106 psi)	Coef of Thermal Expansion (10^{-6} in/in°F)
		Temp °F	Yield Sy	Ultimate Su	Elastic Allowable Sm		
SA 182(1) and SA213	304	70	—	—		28.3	—
		100	30.0	75.0	20.0	—	8.55
		200	25.0	71.0	20.0	27.6	8.79
		300	22.5	66.0	20.0	27.0	9.00
		400	20.7	64.4	18.7	26.5	9.19
		500	19.4	63.5	17.5	25.8	9.37
		600	18.2	63.5	16.4	25.3	9.53
Tungsten Alloy ASTM B777	I	80	80.0	110.0	27.5(2)	40.0	5.4

Notes:

1. Reference 3 Tables, I-1.2, I-2.2, I-3.2, I-5.0 and I-6.0
2. Calculated per paragraph III-3310, Article III 3000, ASME Code Section III, Division I [2.6].

Table 2.4. Mechanical Properties of Materials

2.4.2 Tamperproof Feature

Since the HFIR fuel basket and liner assembly is contained within the cask body, it does not affect the tamperproof features of the packaging.

2.4.3 Positive Closure

Since the HFIR fuel basket and liner assembly is contained within the cask body, it does not affect the positive closure of the packaging.

2.4.4 Chemical and Galvanic Reactions

The cask body surfaces and the fuel baskets are constructed of stainless steel and tungsten alloy. These materials do not react in steam or water either chemically or galvanically. The fuel is designed to be chemically non reactive in water filled systems. In addition, the cask cavity is vacuum dried to eliminate moisture from the wet loading operation and made inert with He gas.

2.5 LIFTING AND TIE-DOWN STANDARDS FOR ALL PACKAGES

The payload weight of the HFIR fuel basket and liner assembly is below the maximum payload weight of 5450 lbs. specified by the Model 2000 Package SAR [2.3]. The existing cask lifting devices and tie downs are not affected by the HFIR fuel basket and liner assembly and are therefore not addressed herein. However, in addition to the two standard and four auxiliary ears

designed for lifting the cask [2.3], two optional ears are designed, which may be used exclusively to lift the cask using a crane with a special size hook [2.14].

The lifting load and stress analysis is presented under Appendix 2.11.5.

2.6 NORMAL CONDITIONS OF TRANSPORT

The HFIR fuel basket and liner assembly, when subjected to the normal conditions of transport as specified in 10CFR71.71, meets the performance requirements specified in Subpart E of 10CFR71 [2.1]. This is demonstrated in the following sections where each normal condition is addressed and shown to meet the applicable design criteria.

2.6.1 Heat

The thermal evaluation for the normal and off-normal events is performed in Chapter 3.0. The structural evaluation of the resulting thermal distributions is presented later in this section.

2.6.1.1 Summary of Pressures and Temperatures. The basket and liner assembly is not a pressure boundary. Therefore, pressure loads need not be addressed in the structural analysis. The controlling design temperatures for normal conditions of transport used in the structural analysis are listed in Table 2.5.

Package Component	Max Temp (°F)	Design Temperature Criteria
HFIR		
Inner Element	255	<400
Outer Element	255	<400
Basket	254	
Liner	244	
Cask Cavity	223	<600
Lead Shield	222	<600
Cask Seal Area	216	<400
Overpack Accessible Outer Surface	171	<180

Table 2.5. Maximum Normal Condition Temperatures

2.6.1.2 Differential Thermal Expansion. The effects of thermal gradients on the HFIR fuel basket and liner are investigated by finite element analysis. For normal conditions of transport the maximum stress occurs at the joint of the tungsten bottom plug (Part 6) with the basket support tube (Part 4). This is attributed to the differential radial displacement because of dissimilar materials. The basket is free to move axially upward under normal conditions of transport. See drawing given in Subsection 1.3.2 for Part numbers.

Under the normal conditions of transport, the temperature difference between the basket and the cask cavity under steady state condition is calculated to be 32°F. However, a maximum temperature difference of 100°F is used conservatively, due to the thermal inertia of the two components. Differential thermal axial expansion of the basket against the cask cavity is estimated to be approximately 0.053 inch, which is significantly less than the actual gap of 0.25 inch between the basket tube and the cask cavity.

2.6.1.3 Stress Calculation. The analysis results from the HFIR fuel basket and liner thermal evaluation, presented in Section 3.0, show that the temperature of the cask cavity increases from the 70°F ambient temperature to 223°F for normal operating conditions. This thermal gradient produces a maximum stress intensity in the basket of 18.43 ksi. Figure 2.3 shows the maximum stress locations. Thermal stress intensity for all normal conditions are given in Table 2.6. To establish the accuracy of the finite element analysis results, the resulting stresses at the -40°F condition are compared to the results found from close form solutions. The results of this comparison are given in Subsection 2.11.1.

2.6.1.4 Comparison With Allowable Stresses. Load combinations and comparisons with allowable stress limits are presented in Subsection 2.6.11. In that Subsection the resulting stresses from all normal conditions of transport are combined and compared against the criteria given in Subsection 2.1.2.

2.6.2 Cold

For the cold condition, a -40°F steady state ambient temperature is specified in Reference 2.5. This temperature in conjunction with no fuel load in the cask will result in a minimum temperature throughout the cask of -40°F. The materials of construction for the HFIR fuel basket and liner assembly are not adversely affected by the -40°F condition.

2.6.3 Reduced External Pressure

The basket assembly is not a pressure boundary and the effects of external pressure on the cask body have no effect on the HFIR fuel basket and liner assembly.

2.6.4 Increased External Pressure

The basket assembly is not a pressure boundary and the effects of external pressure on the cask body have no effect on the HFIR fuel basket and liner assembly.

2.6.5 Vibration

The stresses induced by vibration normally incident to handling and transportation of the package are considered to be negligible. The basket loads resulting from the nomad vibration accelerations will conservatively be less than 10 g's vertical and 5 g's lateral that are selected as loading condition. When compared to the stresses resulting from the nomad condition one foot drop loads (Subsection 2.6.7), the stresses due to a 10 g/5 g combined vibration load will be enveloped by those due to the drop condition. The resulting stress intensity values resulting from this analysis are presented in Tables 2.7 and 2.8 for the -20°F and the normal thermal conditions respectively. Vibration fatigue is addressed in Paragraph 2.6.5.1.

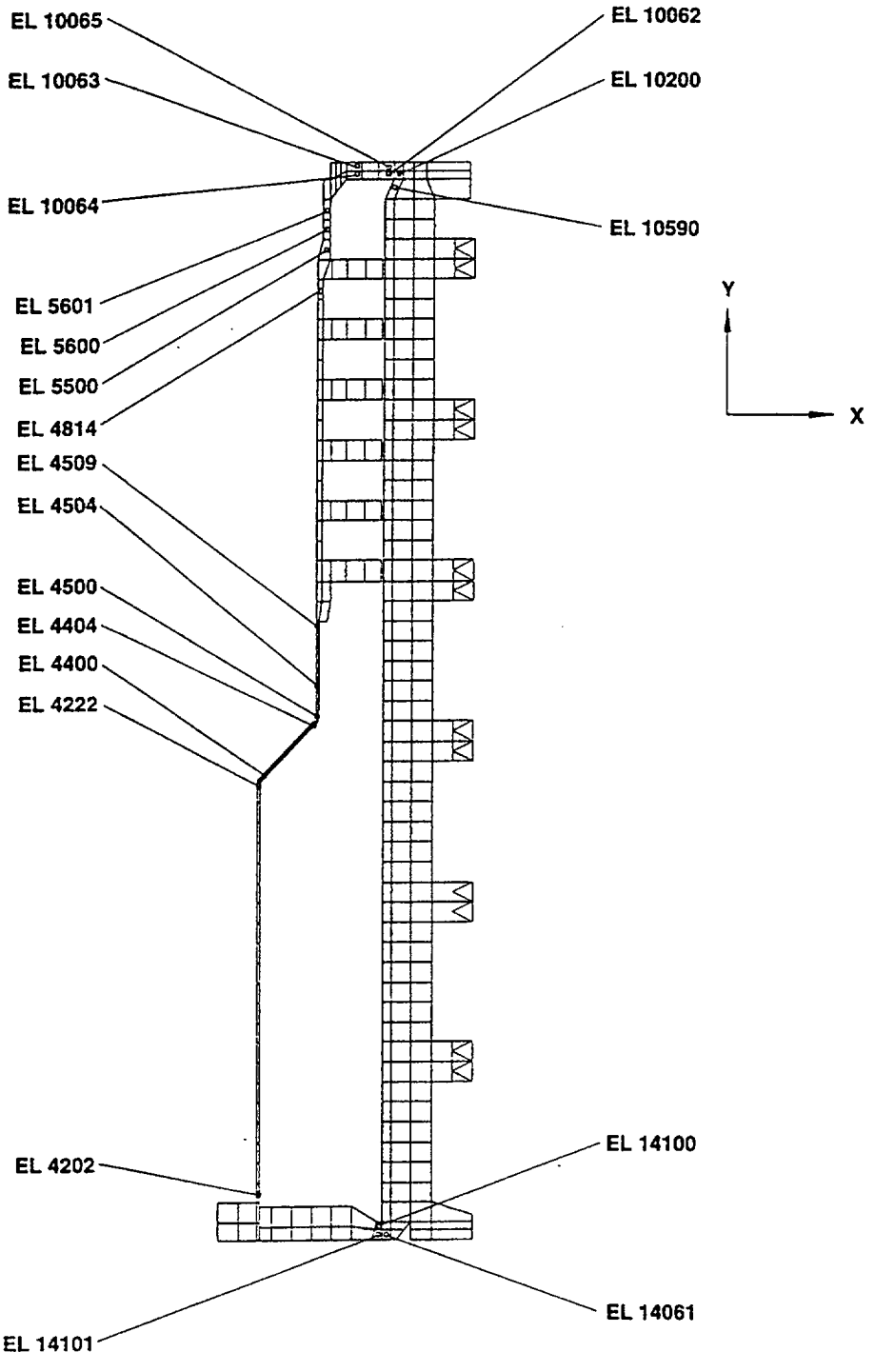

Figure 2.3. Elements of High Stress

Condition	S (ksi)	Location
Cold, -40°F	23.80	Basket support tube and bottom plug interface
-20°F	11.12	Basket support tube and bottom plug interface
100°F Ambt., decay heat, and solar	18.43	Basket support tube and bottom plug interface

Table 2.6. Maximum Thermal Stress Intensity, Normal Conditions

2.6.5.1 Vibration Fatigue. The analysis is performed using axisymmetric structure with non symmetric loading option of the LIBRA Computer Code. The effect of each acceleration response is separately analyzed, and the resulting stresses are combined by the square root of the sum of the square (SRSS) procedure to obtain the net effect on the basket. The liner is not analyzed because its cross sectional area is much larger than that of the basket. The evaluation is performed for the vibration loads, and for the cumulative effects of vibration and thermal loads for the expected life of the basket.

A number of stress concentration factors are used at applicable locations shown in Figure 2.4. The resultant stress intensities of the elements shown are multiplied by these factors leading to conservative results. For a number of locations a conservative stress concentration factor of 4.0 is used just for convenience. The other value used is discussed in Subsection 2.11.2. These factors have been applied to specified locations of maximum stress, taken from Tables 2.7 and 2.8.

The basket fatigue usage factor is calculated to be +0.00 after rounding off. The calculation assumed 100 sets of 12 round trips, with 10 hours duration each way between inspection periods. The calculation of the fatigue usage factor is presented in Subsection 2. 11.3. Section 8.0 gives inspection requirements and their schedules. It also uses the first mode of vibration equal to 287 Hz. The method used here is conservative given the unrealistic 287 cycles per second to calculate the number of stress cycles and the unrealistic applied transportation loads of 10 g's vertical and 5 g's lateral. Based on these results, fatigue is not a concern in this design.

2.6.6 Water Spray

The HFIR fuel basket and liner assembly need not be subject to the water spray test.

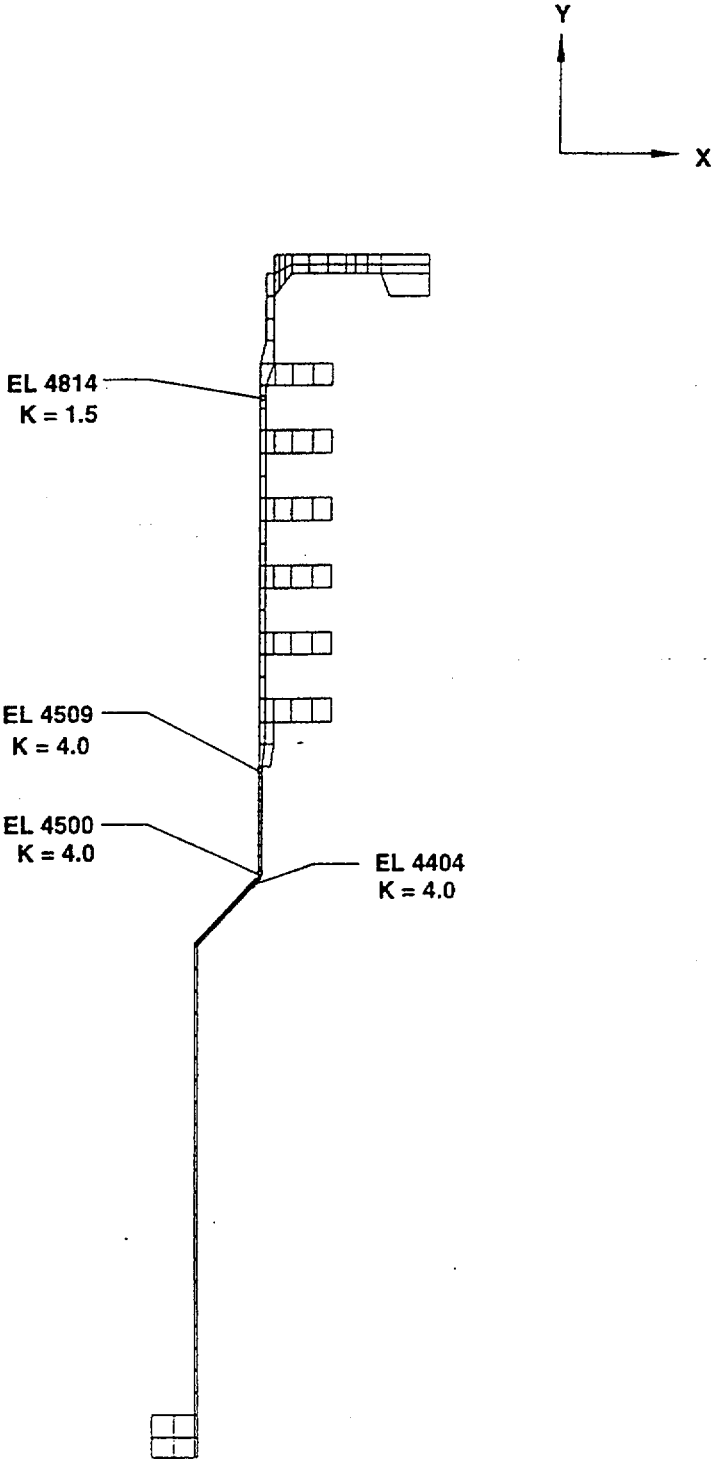

Figure 2.4. Elements with Applied Stress Concentration Factors, K

NORMAL CONDITION

(-20 degrees Fahrenheit)

STRESS COMPONENTS	Pm	Pm+Pb	Pm+Pb+Q	Shear (1)
ALLOWABLE CRITERIA	Sm	1.5Sm	3Sm	.6Sm
ALLOWABLE VALUES (KSI)	16.2	24.3	48.6	9.7

LOADING CONDITION	MAX STRESS LOCATION	Component Pm	Allowable Sm	Component Pm+Pb	Allowable 1.5Sm	Component Pm+Pb+Q	Allowable 3Sm
	Basket Flange						
	10062	0.14	16.2	0.65	24.3	0.65	48.6
	10063 (3)	1.61	16.2	2.29	24.3	2.29	48.6
	10064 (3)	1.47	16.2	1.89	24.3	1.89	48.6
	10065	0.66	16.2	0.96	24.3	0.96	48.6
	10200	0.13	16.2	0.38	24.3	0.38	48.6
	Basket						
VIBRATION	4202	0.15	16.2	0.18	24.3	8.35	48.6
	4222	0.20	16.2	0.32	24.3	1.95	48.6
	4400	0.16	16.2	0.24	24.3	10.52 (2)	48.6
	4404	0.26	16.2	0.37	24.3	1.28	48.6
	4500	0.41	16.2	0.64	24.3	0.58	48.6
	4504	0.26	16.2	0.31	24.3	0.31	48.6
	4509	0.38	16.2	0.46	24.3	1.32 (2)	48.6
	4814	0.59	16.2	0.68	24.3	0.47	48.6
	5500	0.30	16.2	0.65	24.3	0.60	48.6
	5600	0.52	16.2	0.73	24.3	0.69	48.6
	5601	1.01	16.2	1.90	24.3	1.90	48.6

Note 1: There were no elements in pure shear.

Note 2: This stress number was multiplied by 4 to account for a stress concentration factor in this area.

Note 3: The stress number was multiplied by 2.2 to account for a stress concentration factor in this area.

Table 2.7. Vibration Analysis at -20 Degrees Fahrenheit

NORMAL CONDITION
(100 degrees Fahrenheit)

STRESS COMPONENTS	Pm	Pm+Pb	Pm+Pb+Q	Shear (1)
ALLOWABLE CRITERIA	Sm	1.5Sm	3Sm	.6Sm
ALLOWABLE VALUES (KSI)	16.2	24.3	48.6	9.7

LOADING CONDITION	MAX STRESS LOCATION	Component Pm	Allowable Sm	Component Pm+Pb	Allowable 1.5Sm	Component Pm+Pb+Q	Allowable 3Sm
	Basket Flange						
	10062	0.14	16.2	0.65	24.3	2.01	48.6
	10063 (3)	1.61	16.2	2.29	24.3	6.23	48.6
	10064 (3)	1.47	16.2	1.89	24.3	4.05	48.6
	10065	0.66	16.2	0.96	24.3	1.38	48.6
	10200	0.13	16.2	0.38	24.3	1.08	48.6
	Basket						
VIBRATION	4202	0.15	16.2	0.18	24.3	14.78	48.6
	4222	0.20	16.2	0.32	24.3	0.36	48.6
	4400	0.16	16.2	0.24	24.3	1.12 (2)	48.6
	4404	0.26	16.2	0.37	24.3	0.42	48.6
	4500	0.41	16.2	0.64	24.3	0.69	48.6
	4504	0.26	16.2	0.31	24.3	0.32	48.6
	4509	0.38	16.2	0.46	24.3	3.56 (2)	48.6
	4814	0.59	16.2	0.68	24.3	1.63	48.6
	5500	0.30	16.2	0.65	24.3	1.23	48.6
	5600	0.52	16.2	0.73	24.3	1.74	48.6
	5601	1.01	16.2	1.90	24.3	3.32	48.6

Note 1: There were no elements in pure shear.
Note 2: This stress number was multiplied by 4 to account for a stress concentration factor in this area.
Note 3: This stress number was multiplied by 2.2 to account for a stress concentration factor in this area.

Table 2.8. Vibration Analysis at 100 Degrees Fahrenheit

2.6.7 Free Drop

The regulations [2.1] include a one-foot drop as part of the normal conditions of transport. The Model 2000 Package is transported vertically, an analysis of the basket and liner for postulated one foot drop is performed for the head on, bottom on, and side orientations to satisfy the intent of the regulations.

The one foot vertical and side drop load definition is taken from Reference 2.3, page 2-70, paragraph 1, which states "The g's force produced by the one foot drop for each drop configuration for a toroid with a wall thickness of 0.76 in are: Head On 69 g's; Side 20 g's; Cg-over-corner 14 g's ... ." However, the load used in the analysis for the side orientation was that of the head on. Consistent with the currently approved design basis for the package, this load definition represents an enveloping design basis for the HFIR fuel basket and liner assembly.

2.6.7.1 One Foot Head On Drop. A finite element analysis is used for the basket and liner one foot head on drop evaluation. For this drop orientation both structures, the basket and liner are included in the model. The loads, reactions and constraining conditions considered in the basket and liner one foot head on drop analysis are illustrated in Figure 2.5.A and Figure 2.5.B.

The force loading on the model is from the weight of the outer fuel on the basket and the body forces of the basket and the liner. Since the inner fuel weight does not make contact with the basket or liner. it is ignored. The weight of the outer fuel element, 110 lbs x 69 g, is applied as a concentrated force at the outer edge of the lowest cooling fin. Body forces of 69 g are also applied throughout the model.

The basket top flange surface is constrained in the vertical direction. Each set of "double" nodes at the interface between the basket top flange and the liner is constrained in vertical direction and free to move in radial direction. There are no other boundary conditions applied to the model. As discussed in Paragraph 2.1.1.1, there is no physical contact between the basket support tube and the liner base. The stress intensity values resulting from this analysis are presented in Tables 2.9 and 2.10 for the -20°F and the normal thermal conditions respectively.

2.6.7.2 One Foot Bottom On Drop. For this drop orientation, both structures, the basket and liner are included in the model. The loads, reactions and constraining conditions considered in the basket and liner one foot head on drop analysis are illustrated in Figure 2.6.A and Figure 2.6.B.

The force loading comes from three sources; the weight of the inner fuel, the weight of the outer fuel and the body forces of the basket and the liner. The weight of the inner fuel element, 110 lbs x 69 g, is applied as concentrated forces at the ledge in the basket top flange, from where the fuel element hangs. The weight of the outer fuel, 215 lbs x 69 g, is applied as concentrated forces at the liner base. A 69 g of body force is applied in the vertical direction throughout the model.

The bottom surface of the liner base is constrained in the vertical direction. Since the cask inner surface is slightly tapered, only a portion of the liner base is in full contact with the cask inner surface. This portion of the liner base is constrained. The bottom surface of the basket tube does not make contact with the cask inner surface. Since, by design, there is a 0.25 gap, the basket hangs from the top surface of the liner by its top flange. At the interface of the basket top flange

and the liner top surface, no constraining conditions are imposed on the "double" nodes except the innermost "double" nodes are merged into a single node to make it the hinged connection between the basket and the liner. Only forces, not moments, are allowed to be transmitted through this node. The top flange is free to rotate at the hinged node.

There are no other boundary conditions applied to the model. As discussed in Paragraph 2.1.1.1, there is no physical contact between the basket support tube and the liner base. The resulting stress intensity are given in Tables 2.11 and 2.12 for the -20°F and the normal thermal conditions respectively.

2.6.7.3 One Foot Side Drop. The model used in analyzing this drop condition includes only the basket structure because the liner has much thicker walls than any segment of the basket. Hence, it is assumed that the liner is more than sufficiently strong to accommodate the effect of this drop, when compared to the basket. Also, the analysis employed is that of an axisymmetric structure with non-axisymmetric loads. Loading and constraint conditions applied in this analysis are shown in Figure 2.7.A and Figure 2.7.B.

The force loading comes from the weight of the inner fuel and the body forces of the basket and the liner. The weight of the outer fuel is ignored, since it is confined within the liner not to exert force loading on the basket. The weight of the inner fuel element, 110 lbs x 69 g, is applied as distributed forces along the upper body of the basket. A 69 g of body force is applied in the lateral direction throughout the model.

Since, for the side drop loading condition, the lateral movement of the basket support tube is restricted by the liner base, the lower part of the basket support tube is constrained in the lateral direction but free to move in vertical direction. Similarly, every other basket fins, rather than all basket fins, are restrained in the lateral direction only.

The stresses are calculated at five meridian angles, 0°, 45°, 90°, 135° and 180°. For each element to be listed in the tables, only the maximum stresses are extracted, and the resulting stress intensities are given in Tables 2.13 and 2.14 for the -20°F and the normal thermal conditions respectively.

2.6.7.4 Summary of Results. The normal drop condition maximum stresses are summarized in Table 2.15. As can be seen, all stresses are well within allowable limits. Therefore, the integrity of the HFIR fuel basket and liner assembly is maintained and remains fully functional for all normal drop conditions. To establish the accuracy of the finite element analyses results, the resulting stresses from the one foot head on and bottom on are compared against close form solutions. Detail and results of this comparison are given in Subsection 2.11.4.

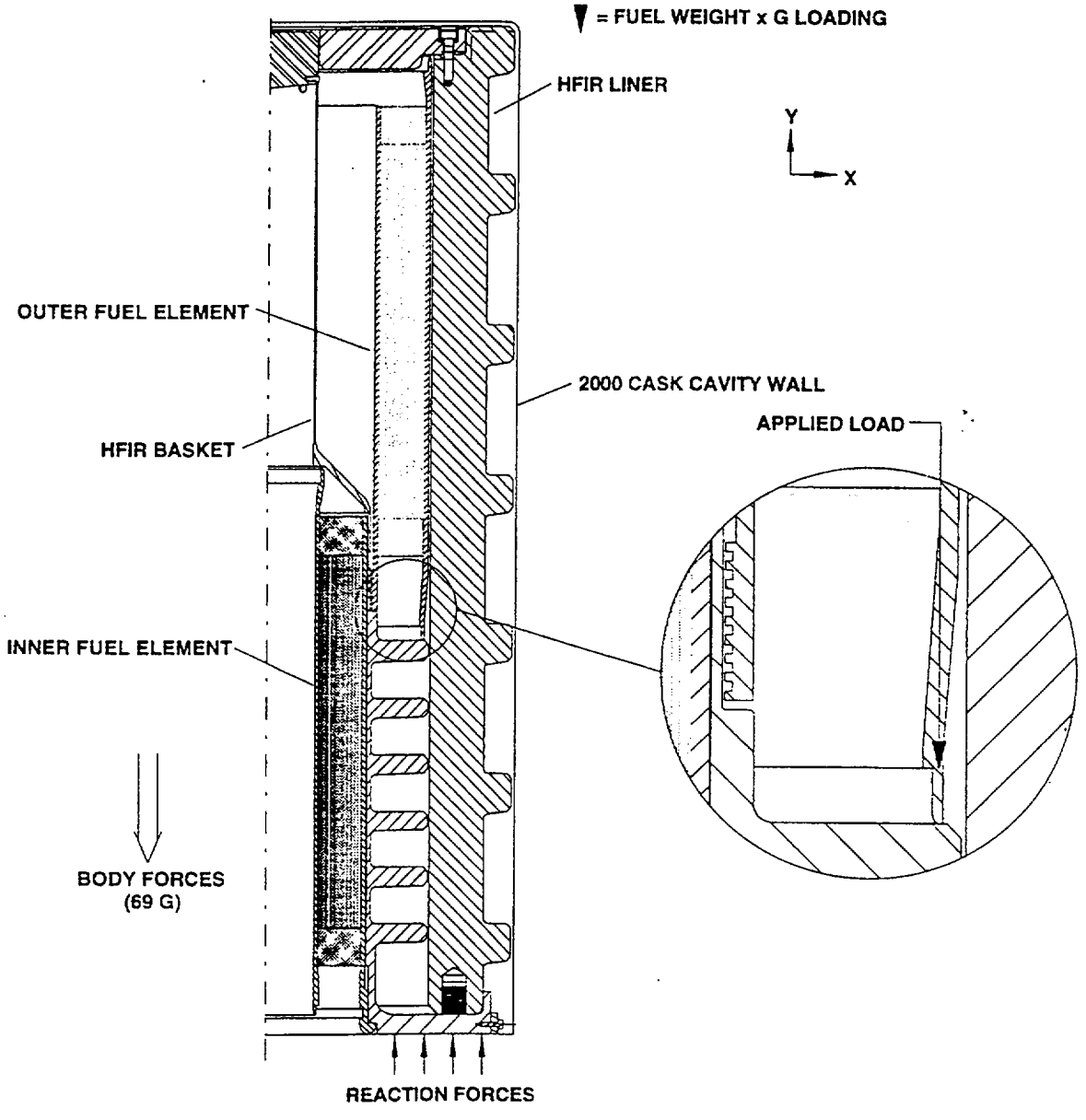

Figure 2.5.A. Normal Condition Head On Drop

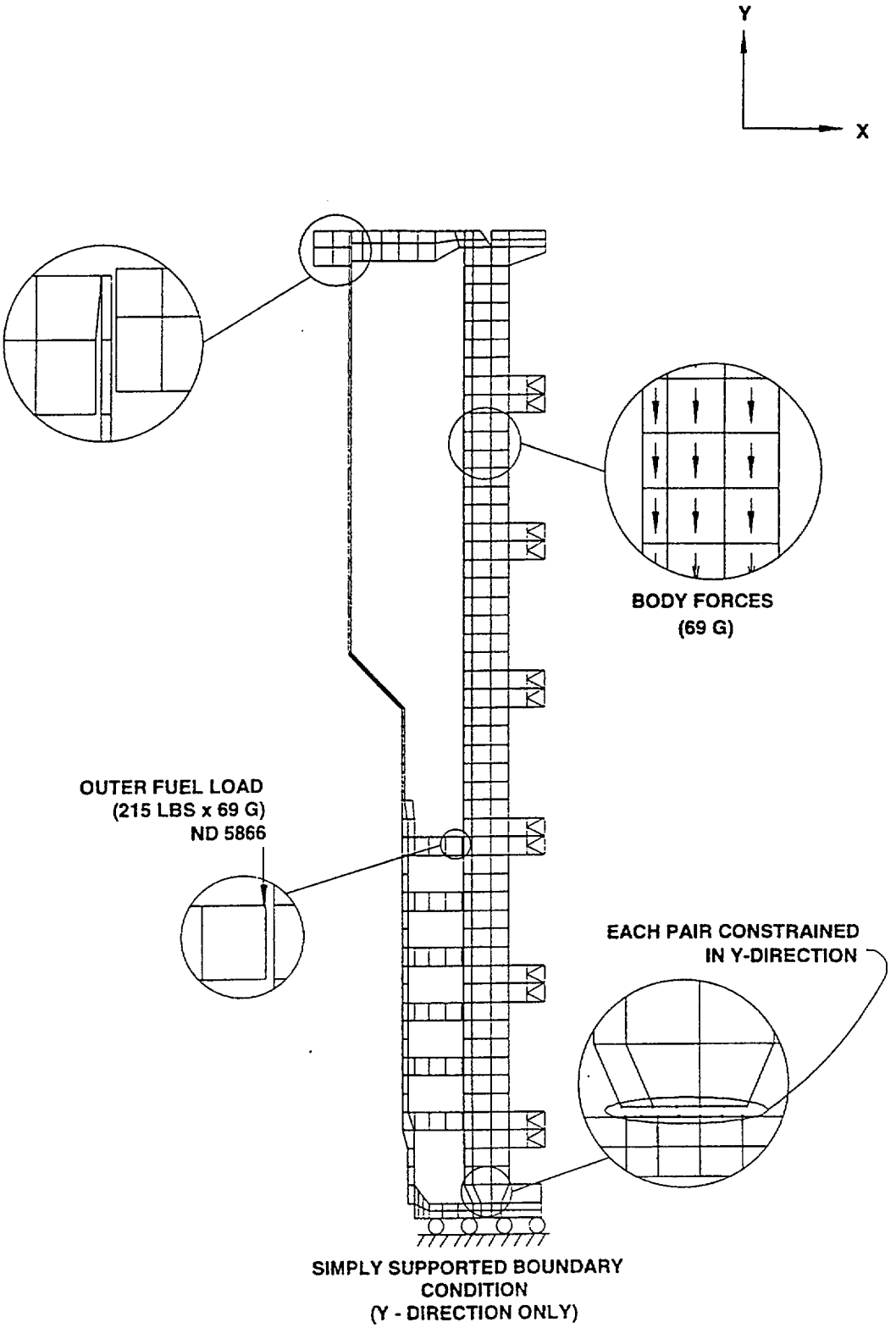

Figure 2.5.B. Normal Condition Head On Drop, FEM Model

NORMAL CONDITION
(-20 degrees Fahrenheit)

STRESS COMPONENTS	Pm	Pm+Pb	Pm+Pb+Q	Shear (1)
ALLOWABLE CRITERIA	Sm	1.5Sm	3Sm	.6Sm
ALLOWABLE VALUES (KSI)	16.2	24.3	48.6	9.7

LOADING CONDITION	MAX STRESS LOCATION	Component Pm	Allowable Sm	Component Pm+Pb	Allowable 1.5Sm	Component Pm+Pb+Q	Allowable 3Sm
	Basket Flange						
	10062	0.57	16.2	1.55	24.3	1.55	48.6
	10063 (3)	1.63	16.2	1.89	24.3	1.89	48.6
	10064 (3)	1.08	16.2	1.30	24.3	1.30	48.6
	10065	0.61	16.2	1.00	24.3	1.00	48.6
	10200	1.41	16.2	1.75	24.3	1.75	48.6
	Basket						
1 FOOT DROP ON TOP	4202	0.92	16.2	0.94	24.3	9.11	48.6
	4222	1.31	16.2	2.15	24.3	3.78	48.6
	4400	1.06	16.2	1.61	24.3	4.00	48.6
	4500	2.09	16.2	3.81	24.3	3.94	48.6
	4509	2.60	16.2	4.05	24.3	16.2(2)	48.6
	4814	4.07	16.2	4.73	24.3	4.73	48.6
	5500	2.38	16.2	3.53	24.3	3.53	48.6
	5600	2.83	16.2	3.89	24.3	3.89	48.6
	5601	2.83	16.2	4.84	24.3	4.84	48.6
	Liner						
	10590	1.36	16.2	2.24	24.3	2.24	48.6
	14061	0.75	16.2	1.07	24.3	1.07	48.6
	14100	0.73	16.2	1.71	24.3	1.71	48.6
	14101	0.79	16.2	1.25	24.3	1.25	48.6

Note 1: There were no elements in pure shear.
Note 2: This stress number was multiplied by 4 to account for a stress concentration factor in this area.
Note 3: This stress number was multiplied by 2.2 to account for a stress concentration factor in this area.

Table 2.9. Normal Condition Head On Drop at -20 Degrees Fahrenheit

NORMAL CONDITION
(100 degrees Fahrenheit)

STRESS COMPONENTS	Pm	Pm+Pb	Pm+Pb+Q	Shear (1)
ALLOWABLE CRITERIA	Sm	1.5Sm	3Sm	.6Sm
ALLOWABLE VALUES (KSI)	16.2	24.3	48.6	9.7

LOADING CONDITION	MAX STRESS LOCATION	Component Pm	Allowable Sm	Component Pm+Pb	Allowable 1.5Sm	Component Pm+Pb+Q	Allowable 3Sm
	Basket Range						
	10062	0.57	16.2	1.55	24.3	2.92	48.6
	10063 (3)	1.63	16.2	1.69	24.3	5.85	48.6
	10064 (3)	1.08	16.2	1.30	24.3	3.43	48.6
	10065	0.61	16.2	1.00	24.3	1.42	48.6
	10200	1.41	16.2	1.75	24.3	2.43	48.6
	Basket						
1 FOOT DROP ON TOP	4202	0.92	16.2	0.94	24.3	15.54	48.6
	4222	1.31	16.2	2.15	24.3	2.19	48.6
	4400	1.06	16.2	1.61	24.3	1.65	48.6
	4500	2.09	16.2	3.81	24.3	3.85	48.6
	4509	2.60	16.2	4.05	24.3	17.88 (2)	48.6
	4814	4.07	16.2	4.73	24.3	5.68	48.6
	5500	2.38	16.2	3.53	24.3	4.11	48.6
	5600	2.83	16.2	3.89	24.3	4.91	48.6
	5601	2.83	16.2	4.84	24.3	8.26	48.6
	Liner						
	10590	1.36	16.2	2.24	24.3	3.30	48.6
	14061	0.75	16.2	1.07	24.3	1.95	48.6
	14100	0.73	16.2	1.71	24.3	2.37	48.6
	14101	0.79	16.2	1.25	24.3	2.40	48.6

Note 1: There were no elements in pure shear.
Note 2: This stress number was multiplied by 4 to account for a stress concentration factor in this area.
Note 3: This stress number was multiplied by 2.2 to account for a stress concentration factor in this area.

Table 2.10. Normal Condition Head On Drop at 100 Degrees Fahrenheit

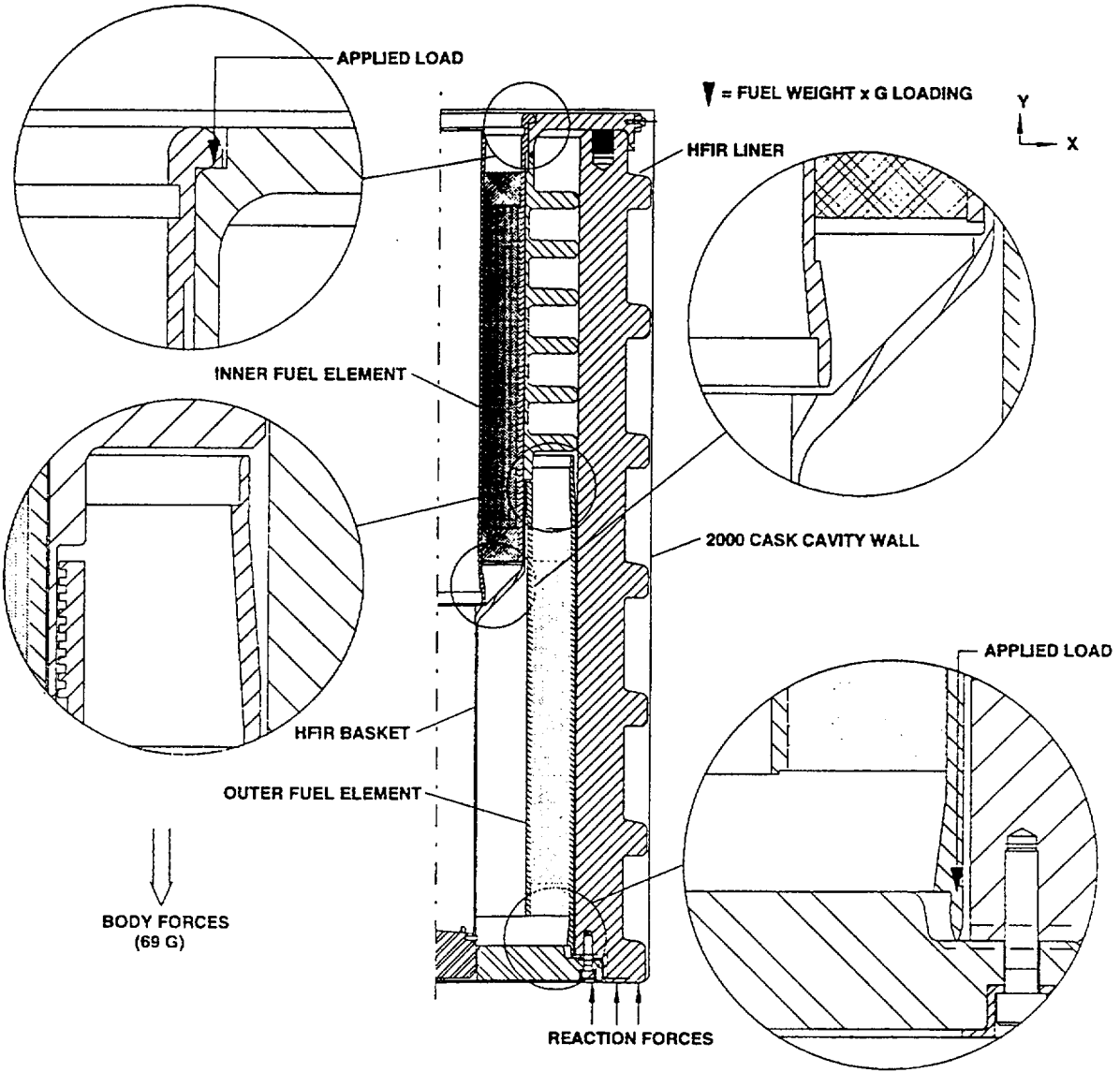

Figure 2.6.A. Normal Condition Bottom Drop

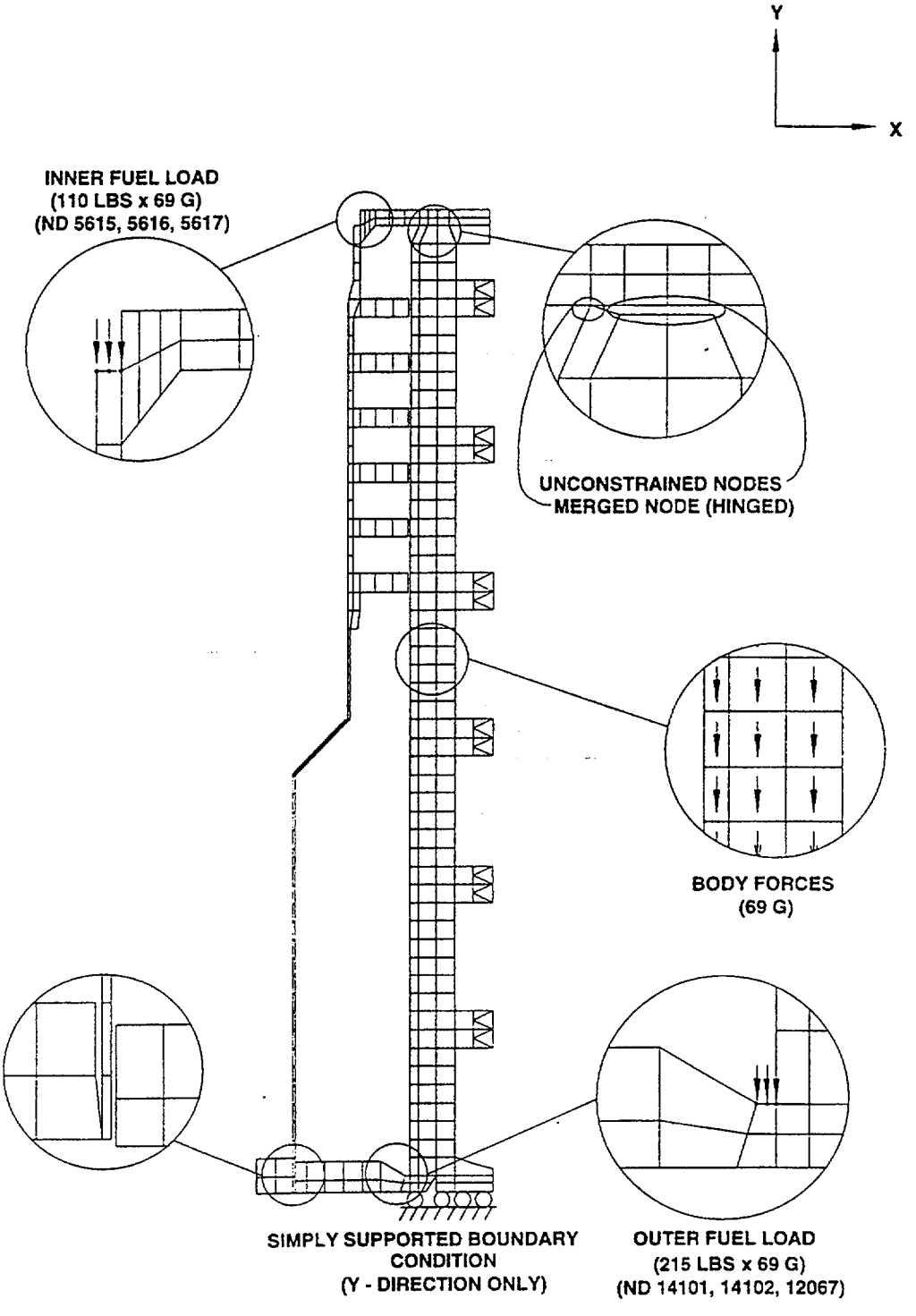

Figure 2.6.B. Normal Condition Bottom Drop, FEM Model

NORMAL CONDITION
(-20 degrees Fahrenheit)

STRESS COMPONENTS	Pm	Pm+Pb	Pm+Pb+Q	Shear (1)
ALLOWABLE CRITERIA	Sm	1.5Sm	3Sm	.6Sm
ALLOWABLE VALUES (KSI)	16.2	24.3	48.6	9.7

LOADING CONDITION	MAX STRESS LOCATION	Component Pm	Allowable Sm	Component Pm+Pb	Allowable 1.5Sm	Component Pm+Pb+Q	Allowable 3Sm
	Basket Flange						
	10062	1.97	16.2	4.42	24.3	4.42	48.6
	10063 (3)	11.09	16.2	15.75	24.3	15.75	48.6
	10064 (3)	10.01	16.2	13.09	24.3	13.09	48.6
	10065	4.53	16.2	6.66	24.3	6.66	48.6
	10200	0.85	16.2	2.41	24.3	2.41	48.6
	Basket						
1 FOOT DROP ON BOTTOM	4202	0.92	16.2	0.94	24.3	9.11	48.6
	4222	1.31	16.2	2.15	24.3	3.78	48.6
	4400	1.06	16.2	1.81	24.3	4.00	48.6
	4500	2.26	16.2	3.81	24.3	3.94	48.6
	4509	0.86	16.2	1.08	24.3	4.32(2)	48.6
	4814	2.36	16.2	3.04	24.3	3.04	48.6
	5500	1.47	16.2	4.10	24.3	4.10	48.6
	5600	3.21	16.2	4.70	24.3	4.70	48.6
	5601	6.88	16.2	13.03	24.3	13.03	48.6
	Liner						
	10590	1.31	16.2	2.72	24.3	2.72	48.6
	14061	1.66	16.2	2.24	24.3	2.24	48.6
	14100	1.55	16.2	2.69	24.3	2.69	48.6
	14101	1.14	16.2	2.54	24.3	2.54	48.6

Note 1: There were no elements in pure shear.
Note 2. This stress number was multiplied by 4 to account for a stress concentration factor in this area.
Note 3: This stress number was multiplied by 2.2 to account for a stress concentration factor in this area.

Table 2.11. Normal Condition Bottom Drop at -20 Degrees Fahrenheit

NORMAL CONDITION
(100 degrees Fahrenheit)

STRESS COMPONENTS	Pm	Pm+Pb	Pm+Pb+Q	Shear (1)
ALLOWABLE CRITERIA	Sm	1.5Sm	3Sm	.6Sm
ALLOWABLE VALUES (KSI)	16.2	24.3	48.6	9.7

LOADING CONDITION	MAX STRESS LOCATION	Component Pm	Allowable Sm	Component Pm+Pb	Allowable 1.5Sm	Component Pm+Pb+Q	Allowable 3Sm
	Basket Flange						
	10062	1.97	16.2	4.42	24.3	5.79	48.6
	10063 (3)	11.09	16.2	15.75	24.3	19.71	48.6
	10064 (3)	10.01	16.2	13.09	24.3	15.22	48.6
	10065	4.53	16.2	6.66	24.3	7.06	48.6
	10200	0.85	16.2	2.41	24.3	3.09	48.6
	Basket						
1 FOOT DROP ON BOTTOM	4202	0.92	16.2	0.94	24.3	15.54	48.6
	4222	1.31	16.2	2.15	24.3	2.19	48.6
	4400	1.06	16.2	1.61	24.3	1.65	48.6
	4500	2.26	16.2	3.81	24.3	3.86	48.6
	4509	0.86	16.2	1.08	24.3	8.01 (2)	48.6
	4814	2.36	16.2	3.04	24.3	3.99	48.6
	5500	1.47	16.2	4.10	24.3	4.68	48.6
	5600	3.21	16.2	4.70	24.3	5.72	48.6
	5601	6.88	16.2	13.03	24.3	14.45	48.6
	Liner						
	10590	1.31	16.2	2.72	24.3	3.78	48.6
	14061	1.66	16.2	2.24	24.3	3.12	48.6
	14100	1.55	16.2	2.69	24.3	3.35	48.6
	14101	1.14	16.2	2.54	24.3	3.69	48.6

Note 1: There were no elements in pure shear.
Note 2: This stress number was multiplied by 4 to account for a stress concentration factor in this area.
Note 3: This stress number was multiplied by 2.2 to account for a stress concentration factor in this area.

Table 2.12. Normal Condition Bottom Drop at 100 Degrees Fahrenheit

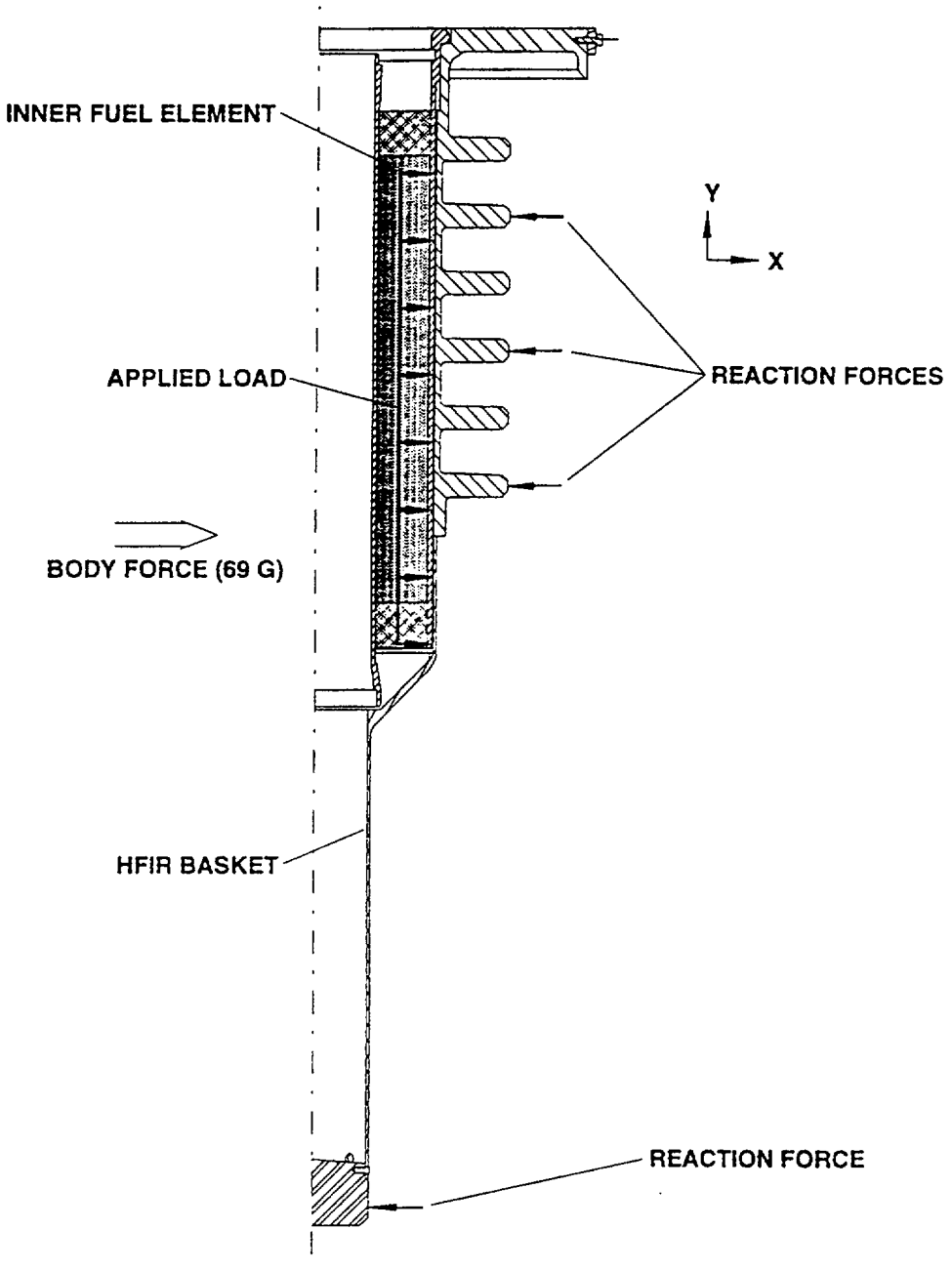

Figure 2.7.A. Normal Condition Side Drop

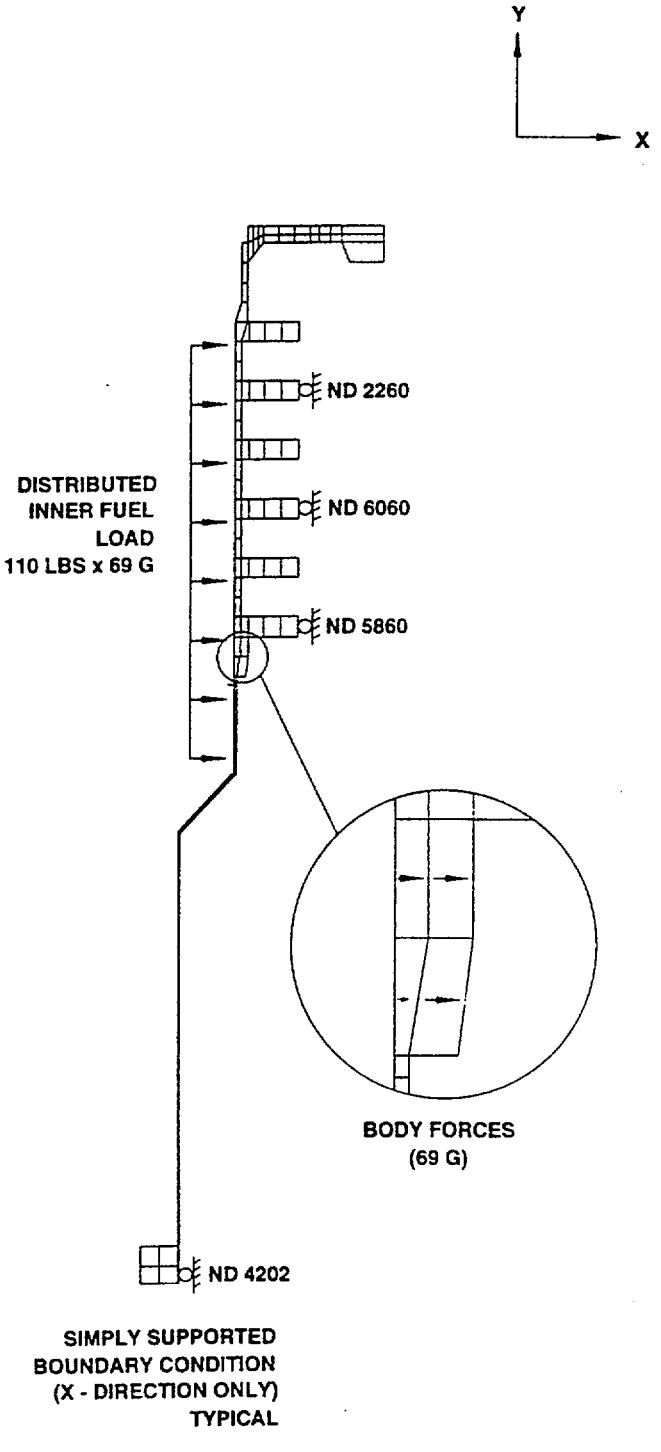

Figure 2.7.B. Normal Condition Side Drop, FEM Model

NORMAL CONDITION
(-20 degrees Fahrenheit)

STRESS COMPONENTS	Pm	Pm+Pb	Pm+Pb+Q	Shear (1)
ALLOWABLE CRITERIA	Sm	1.5Sm	3Sm	.6Sm
ALLOWABLE VALUES (KSI)	16.2	24.3	48.6	9.7

LOADING CONDITION	MAX STRESS LOCATION	Component Pm	Allowable Sm	Component Pm+Pb	Allowable 1.5Sm	Component Pm+Pb+Q	Allowable 3Sm
	Basket Flange						
	10062	0.61	16.2	1.15	24.3	1.15	48.6
	10063 (4)	0.92	16.2	1.83	24.3	1.83	48.6
	10064 (4)	1.21	16.2	1.96	24.3	1.96	48.6
	10065	0.88	16.2	1.54	24.3	1.54	48.6
	10200	0.67	16.2	2.08	24.3	2.08	48.6
	Basket						
1 FOOT DROP ON SIDE	4202	1.05	16.2	1.54	24.3	9.71	48.6
	4222	0.92	16.2	1.02	24.3	2.85	48.6
	4400	0.37	16.2	0.58	24.3	2.97	48.6
	4404	1.56	16.2	2.56	24.3	11.16 (2)	48.6
	4500	3.51	16.2	4.52	24.3	4.52	48.6
	4504	3.12	16.2	3.87	24.3	3.87	48.6
	4509	4.93	16.2	5.92	24.3	24.31 (2)	48.6
	4814	6.72	16.2	7.15	24.3	7.15	48.6
	5500	2.91	16.2	3.50	24.3	3.50	48.6
	5600	3.08	16.2	3.49	24.3	3.49	48.6
	5601	2.55	16.2	3.24	24.3	3.24	48.6

Note 1: There were no elements in pure shear.
Note 2: This stress number was multiplied by 4 to account for a stress concentration factor in this area.
Note 3: Each stress value represents the maximum of all meridan angles.
Note 4: This stress number was multiplied by 2.2 to account for a stress concentration factor in this area.

Table 2.13. Normal Condition Side Drop at -20 Degrees Fahrenheit

NORMAL CONDITION
(100 degrees Fahrenheit)

STRESS COMPONENTS	Pm	Pm+Pb	Pm+Pb+Q	Shear (1)
ALLOWABLE CRITERIA	Sm	1.5Sm	3Sm	.6Sm
ALLOWABLE VALUES (KSI)	16.2	24.3	48.6	9.7

LOADING CONDITION	MAX STRESS LOCATION	Component Pm	Allowable Sm	Component Pm+Pb	Allowable 1.5Sm	Component Pm+Pb+Q	Allowable 3Sm
	Basket Flange						
	10062	0.61	16.2	1.15	24.3	2.52	48.6
	10063 (4)	0.92	16.2	1.83	24.3	5.79	48.6
	10064 (4)	1.21	16.2	1.98	24.3	4.14	48.6
	10065	0.88	16.2	1.54	24.3	1.97	48.6
	10200	0.67	16.2	2.08	24.3	2.76	48.6
	Basket						
1 FOOT DROP ON SIDE	4202	1.05	16.2	1.54	24.3	16.14	48.6
	4222	0.92	16.2	1.02	24.3	1.06	48.6
	4400	0.37	16.2	0.58	24.3	0.62	48.6
	4404	1.56	16.2	2.56	24.3	10.84 (2)	48.6
	4500	3.51	16.2	4.52	24.3	4.57	48.6
	4504	3.12	16.2	3.87	24.3	3.88	48.6
	4509	4.93	16.2	5.92	24.3	26.00 (2)	48.6
	4814	6.72	16.2	7.15	24.3	8.10	48.6
	5500	2.91	16.2	3.50	24.3	4.09	48.6
	5600	3.08	16.2	3.49	24.3	4.51	48.6
	5601	2.55	16.2	3.24	24.3	4.66	48.6

Note 1: There were no elements in pure shear.
Note 2: This stress number was multiplied by 4 to account for a stress concentration factor in this area.
Note 3: Each Stress value represents the maximum of all meridian angles.
Note 4: This stress number was multiplied by 2.2 to account for a stress concentration factor in this area.

Table 2.14. Normal Condition Side Drop at 100 Degrees Fahrenheit

LOADING CONDITIONS	High Stress Element	Element Location	Stress Type	Stress (ksi) [1]	Allowable (ksi)	Margin of Safety
Normal Conditions						
1 foot head on drop (-20 degrees)	4509	transition funnel	Pm+Pb+Q	18.14	48.6	1.68
1 foot head on drop (100 degrees)	4509	transition funnel	Pm+Pb+Q	20.03	48.6	1.43
1 foot bottom drop (-20 degrees)	5601	basket flange/thin section transition	Pm+Pb	14.59	24.3	0.67
1 foot bottom drop (-20 degrees)	10063	basket flange	Pm	12.42	16.2	0.30
1 foot bottom drop (100 degrees)	5601	basket flange/thin section transition	Pm+Pb	14.59	24.3	0.67
1 foot bottom drop (100 degrees)	10063	basket flange	Pm	12.42	16.2	0.30
1 foot side drop (-20 degrees)	4509	transition funnel	Pm+Pb+Q	27.23	48.6	0.78
1 foot side drop (100 degrees)	4509	transition funnel	Pm+Pb+Q	29.12	48.6	0.67
vibration analysis (-20 degrees)	4400	transition funnel	Pm+Pb+Q	11.78	48.6	3.12
vibration analysis (100 degrees)	4202	support tube/bottom plug interface	Pm+Pb+Q	14.78	48.6	2.29
thermal analysis (-40 degrees)	4202	support tube/bottom plug interface	Pm+Pb	15.09	24.3	0.61
thermal analysis (100 degrees)	4202	support tube/bottom plug interface	Pm+Pb	16.35	24.3	0.49

[1] Stress numbers increased by 12% to reflect basket weight increase.

Table 2.15. Summary of Results for Normal Conditions

2.6.8 Compression

The HFIR fuel basket and liner assembly need not be evaluated for compression. This test does not apply to the Model 2000 Transport Package, since the package weight is in excess of 5,000 kg (11,000 lbs).

2.6.9 Penetration

This test does not apply to the HFIR fuel basket and liner assembly. The puncture surface is the Model 2000 Package Overpack.

2.7 HYPOTHETICAL ACCIDENT CONDITIONS

The Model 2000 Package HFIR fuel basket and liner assembly, when subjected to hypothetical accident conditions as specified in 10CFR71.73, meet the performance requirements specified in Subpart E of 10CFR71 [2.1]. This is demonstrated in the following sections where each accident condition is addressed and shown to meet the applicable design criteria.

2.7.1 Free Drop

Subpart F of 10CFR71 [2.1] requires that a 30 foot free drop be considered for the package, which includes the basket assembly. Consistent with the approved Model 2000 Safety Analysis Report [2.3], four different load orientations are considered for the basket assembly. These include the head on, bottom on, side, and cg-over-corner. The basket and liner loads vary in the different orientations due to differences in the toroid energy absorption characteristics and in the interaction of the fuel elements with the basket and liner. Oblique orientation drop is bounded by the evaluation of the horizontal and vertical drops, and is not addressed.

2.7.1.1 Head On Drop. The same finite element model used for the normal condition head on drop case is utilized in this analysis with the exception of the force loading. The same constraining conditions are applied. Two different scenarios depending on the location of the outer fuel weight loading are considered. The first case is the same as the normal condition, where the outer fuel weight is applied at the outer edge of the lowest cooling fin. Figure 2.8.A and Figure 2.8.B shows the loading and constraint conditions applied to the model for this case. The second case of the analysis is based on the assumption that the outer ring of the element fails completely and the inner ring makes a contact at the basket mid section. Figure 2.8.C and 2.8.D shows the loading and constraint conditions applied to the model for this type drop evaluation.

The 133 g's of body forces are applied to the basket and liner model for this orientation in both loading scenarios discussed above. In addition, the weight of the outer fuel element, 215 lb. x 133 g, is applied to the respective part of the basket. The inner fuel element does not impose any load on the basket for this drop configuration. The same constraining conditions as the normal condition head on drop case are applied. Table 2.16 and Table 2.16.A presents the resulting stress intensities under the first and second drop conditions, respectively.

2.7.1.2 Bottom Drop. The same finite element model used for the normal condition bottom drop case is utilized in this analysis with the exception of the force loading. The same constraining conditions are applied. Two different scenarios depending on the location of the inner fuel weight loading are considered. In both cases, it is assumed that the ledge structure on the inner element top ring has failed, and the fuel element is free to slide downward. This ledge structure is used to hang the inner fuel element inside the basket under normal conditions.

In the first case the inner fuel weight is applied at the lower funnel section of the basket. Figure 2.9.A and Figure 2.9.B shows the loading and constraint conditions applied to the model for this case. Similar to the head on drop condition, the second case of the analysis is based on the assumption that the inner ring of the element fails completely and the outer ring makes a contact at the upper funnel section. Figure 2.9.C and 2.9.D shows the loading and constraint conditions applied to the model for this type of drop evaluation.

The 133 g's of body forces are applied to the basket and liner model for this orientation. The weight of the inner fuel element, 110 lb. x 133 g, is applied to the respective part of the basket. In addition, the weight of the outer basket, 215 lbs x 133 g, is again applied at the liner base. The same constraining conditions as the normal condition bottom drop case are applied throughout the model. Table 2.17 and Table 2.17.A presents the resulting stress intensities under the first and second drop conditions, respectively.

2.7.1.3 Side Drop. Similar to the previous paragraphs, the same finite element model used for the normal condition side drop case is utilized in this analysis with the exception of the force loading. This approach of using only the basket model is based on the fact that the basket has the smallest cross sectional area of the two components (basket and liner) and that its structural integrity is important in maintaining separation of the HFIR fuel elements. The g-force applied is 133 8's. Force distributions and constraint conditions employed in the model are depicted in Figure 2.10.A and Figure 2.10.B and the resulting stresses are given in Table 2. 18.

2.7.1.4 Cg-over-corner Drop. The basket model only is considered in this analysis. Since the orientation of this drop is such that the Cg (center of gravity) of the basket and liner falls over the corner of the model, the 63 g's of inertia loading may be decomposed into 23.6 g's in the lateral direction and 58.4 g's in the vertical direction. The results of the accident bottom drop condition and those of the accident side drop conditions are linearly interpolated separately. These stresses are then combined by the square root of the sum of the square (SRSS) procedure to obtain the net effect on the basket for the Cg over corner drop condition.

Similar to the accident bottom condition, two scenarios are considered based on the location of the applied inner fuel weight loading. In both cases, it is assumed that the ledge structure on the inner element top ring has failed, and the fuel element is free to slide downward. In the first case the inner shell of the fuel is resting on the lower funnel section of the basket, while in the second case it is assumed that the inner shell of the element fails completely and the outer shell makes a contact at the upper funnel section.

Force distributions and constraint conditions employed in the model are depicted in Figure 2.11.A and Figure 2.11.B for the first case considered, and the resulting stresses are given in Table 2. 19. For the second case, the force distributions and constraint conditions are described in Figure 2.1 1.C and Figure 2.1 1 .D, and the resulting stresses are given in Table 2.1 9.A.

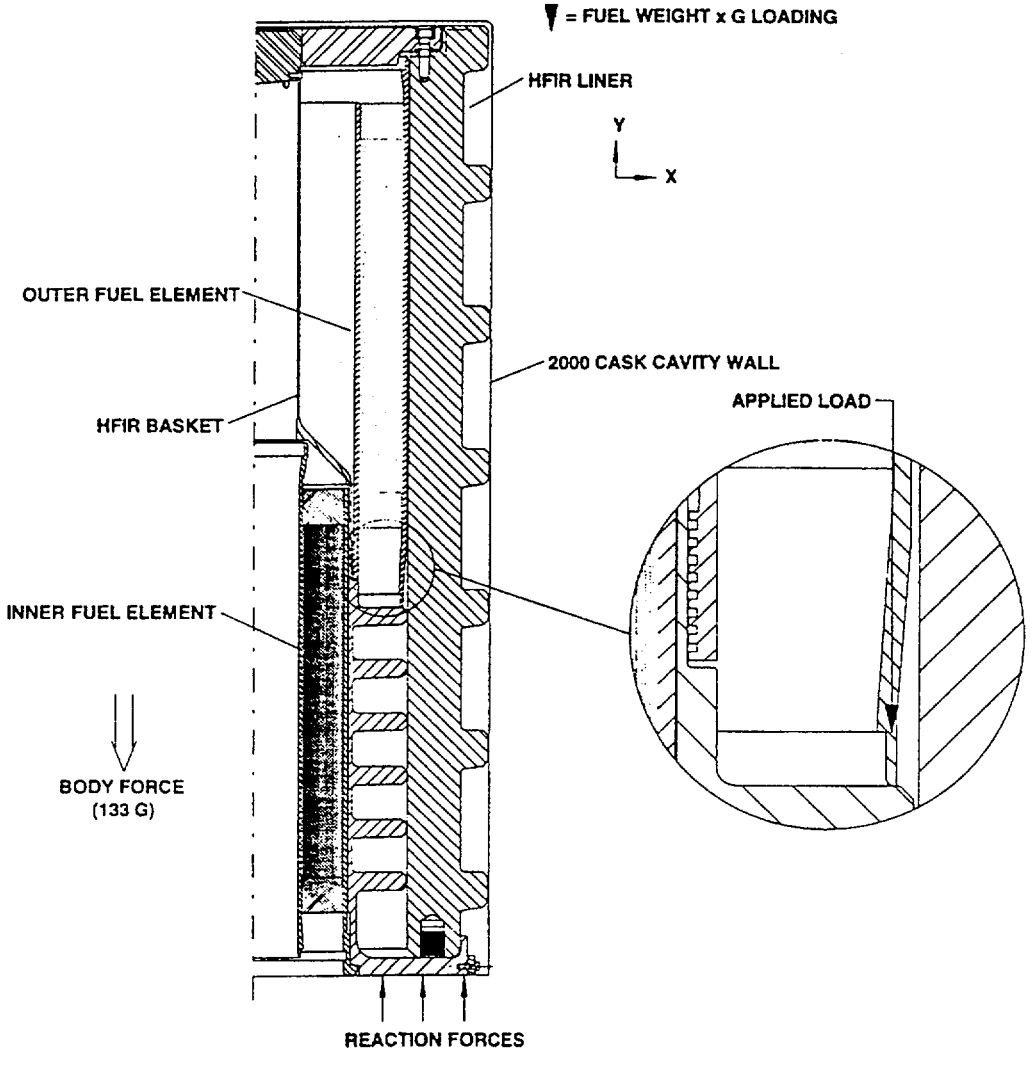

Figure 2.8.A. Accident Condition Head On Drop (Outer Fuel Load Applied at Cooling Fin)

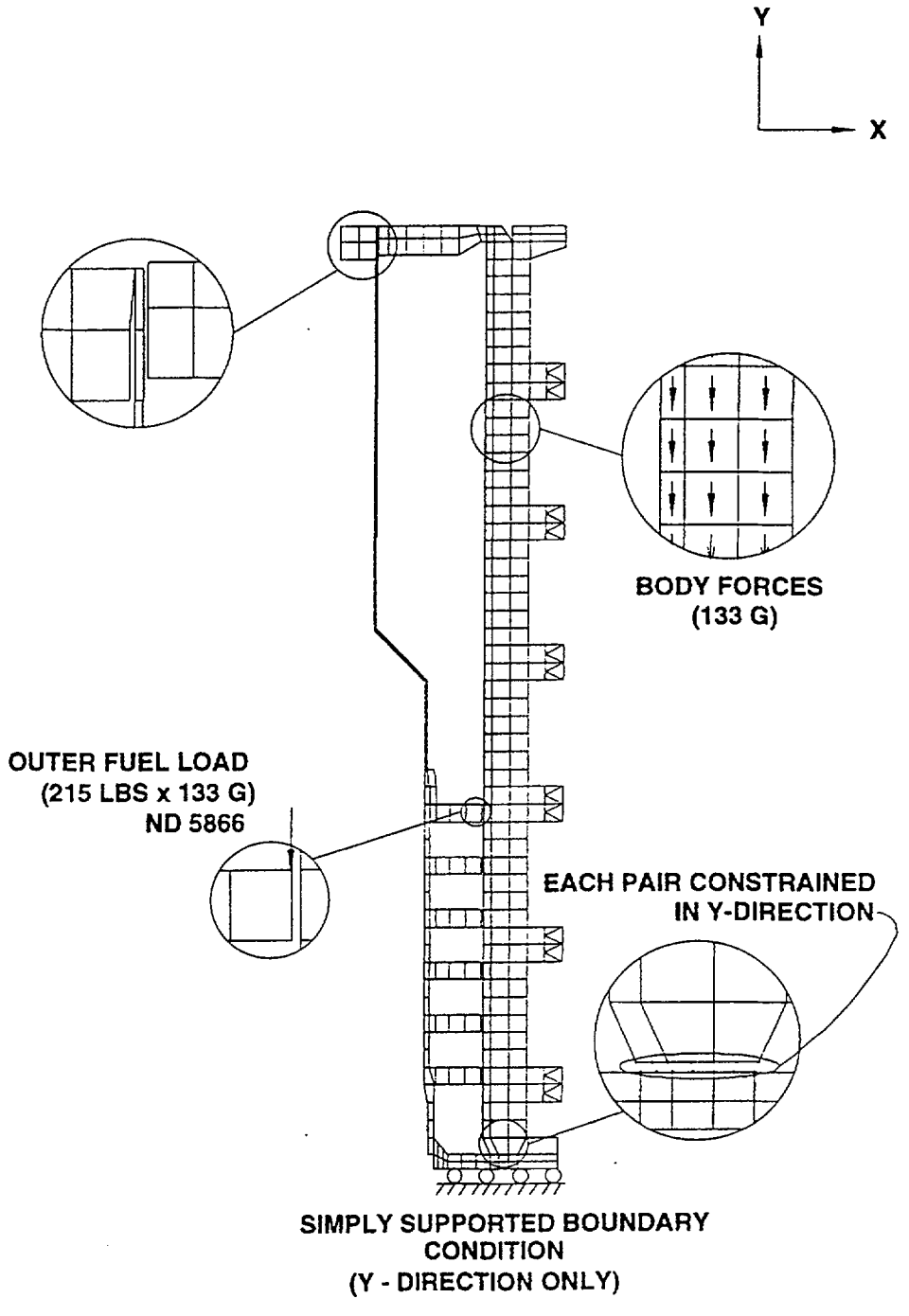

Figure 2.8.B. Accident Condition Head On Drop, FEM Model

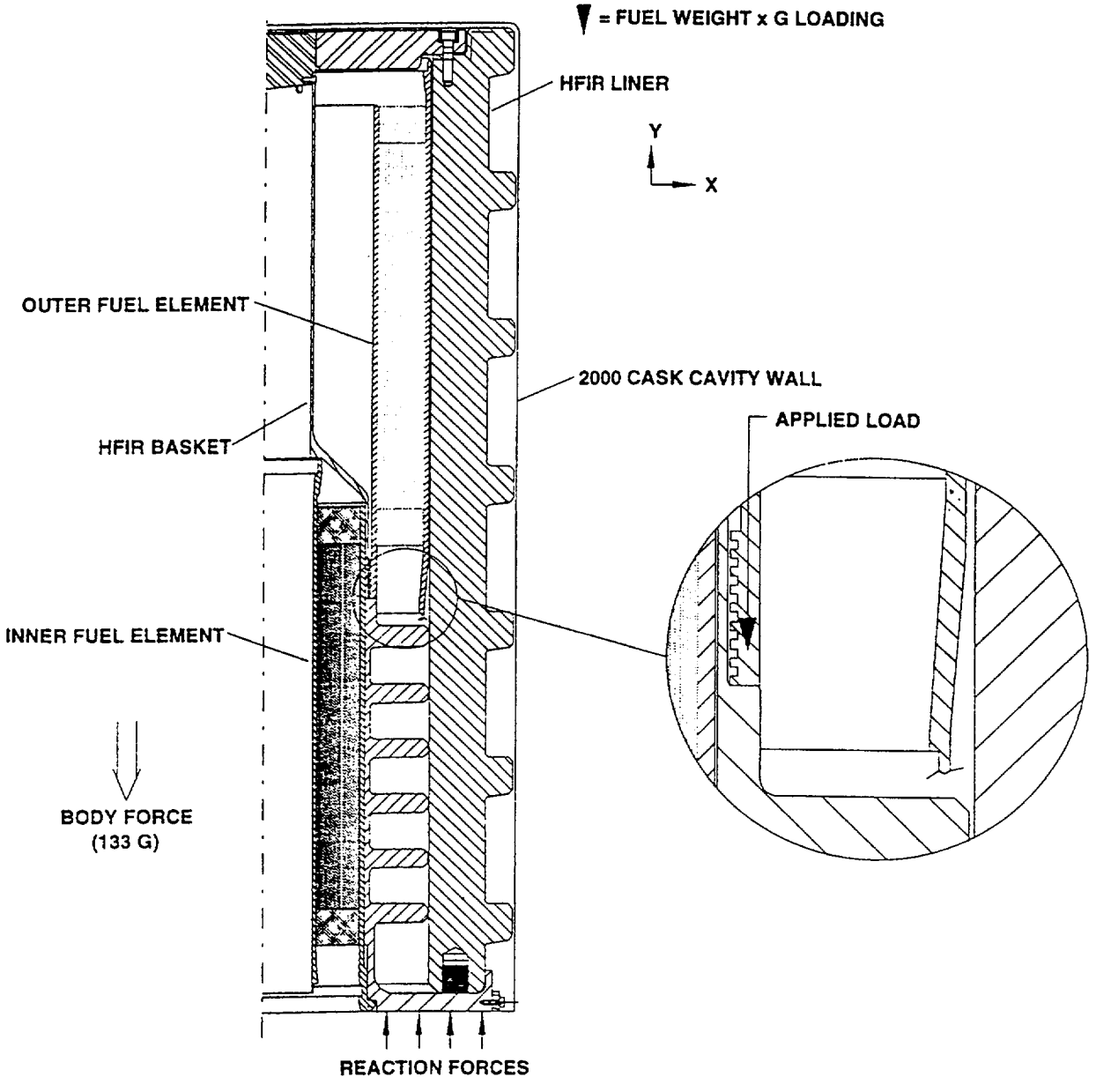

Figure 2.8.C. Accident Condition Head On Drop (Outer Fuel Load Applied at Step Near Basket Midsection)

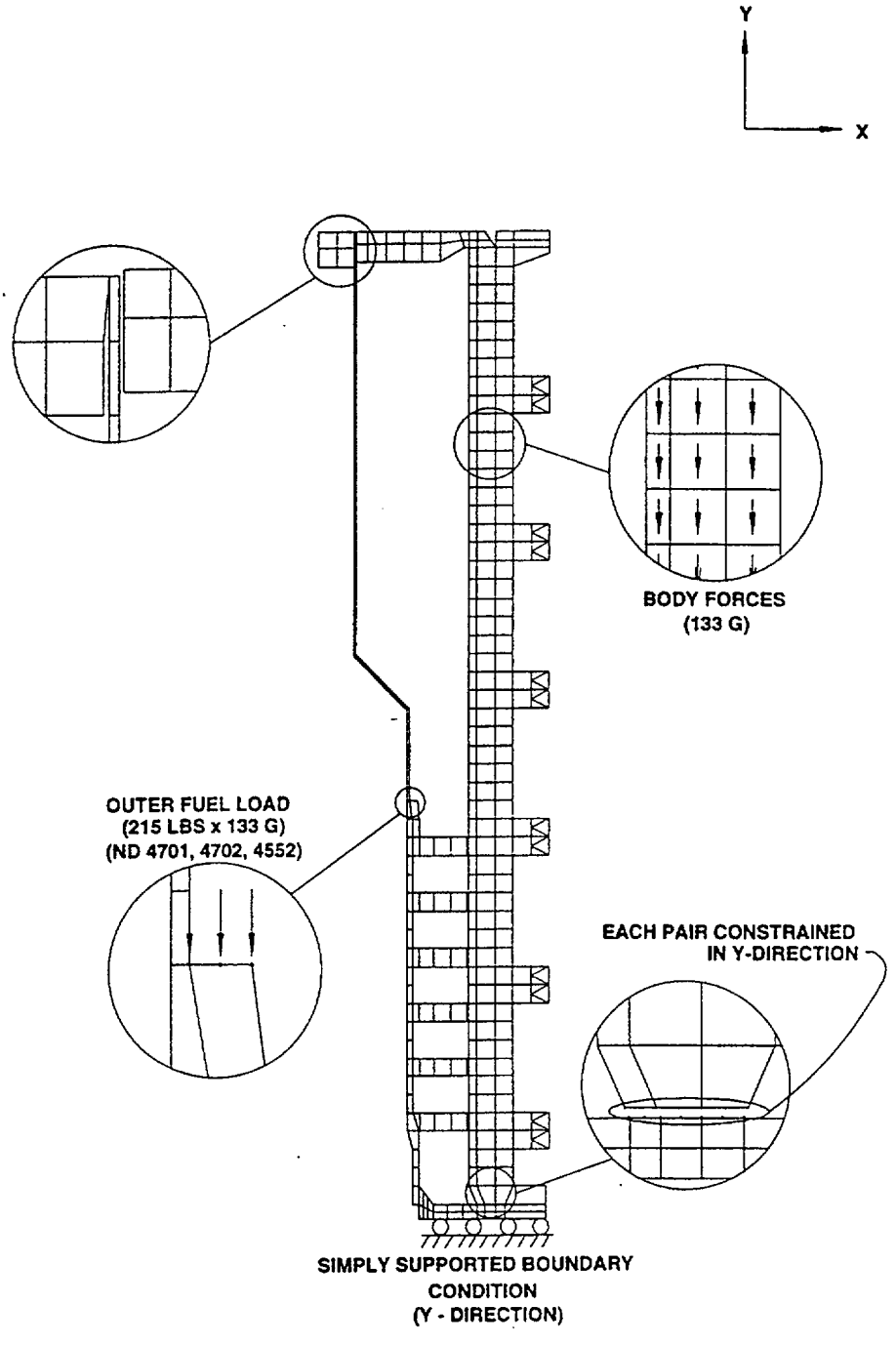

Figure 2.8.D. Accident Condition Head On Drop, FEM Model (Outer Fuel Load Applied at Step Near Basket Midsection)

ACCIDENT CONDITION

STRESS COMPONENTS	Pm	Pm+Pb	Shear (3)
ALLOWABLE CRITERIA	2.4Sm (1)	3.6Sm (2)	.42Su
ALLOWABLE VALUES (KSI)	38.9	58.3	27.1

LOADING CONDITION	MAX STRESS LOCATION	Component Pm	Allowable 2.4Sm	Component Pm+Pb	Allowable 3.6Sm
30 FOOT DROP ON TOP	Upper Basket				
	10062	1.09	38.9	2.98	58.30
	10063 (4)	3.15	38.9	3.65	58.30
	10064 (4)	2.07	38.9	2.49	58.30
	10065	1.18	38.9	1.92	58.30
	10200	2.72	38.9	3.37	58.30
	Basket				
	4202	1.78	38.9	1.81	58.30
	4222	2.53	38.9	4.14	58.30
	4400	2.05	38.9	3.10	58.30
	4500	4.03	38.9	7.34	58.30
	4509	5.02	38.9	7.80	58.30
	4814	7.85	38.9	9.13	58.30
	5500	4.58	38.9	6.80	58.30
	5600	5.45	38.9	7.50	58.30
	5601	5.45	38.9	9.32	58.30
	Liner				
	10590	2.61	38.9	4.32	58.30
	14061	1.44	38.9	2.07	58.30
	14100	1.41	38.9	3.30	58.30
	14101	1.53	38.9	2.41	58.30

Note 1: 2.4Sm was the lesser value when compared to .7Su.
Note 2: 3.6Sm was the lesser value when compared to Su.
Note 3: There were no elements in pure shear.
Note 4: The stress number was multiplied by 2.2 to account for a stress concentration in this area.

Table 2.16. Accident Condition Head On Drop (Outer Fuel Load Applied at Cooling Fin)

ACCIDENT CONDITION

STRESS COMPONENTS	Pm	Pm+Pb	Shear (3)
ALLOWABLE CRITERIA	2.4Sm (1)	3.6Sm (2)	.42Su
ALLOWABLE VALUES (KSI)	38.9	58.3	27.1

LOADING CONDITION	MAX STRESS LOCATION	Component Pm	Allowable 2.4Sm	Component Pm+Pb	Allowable 3.6Sm
30 FOOT DROP ON TOP	**Upper Basket**				
	10062	1.09	38.9	2.98	58.30
	10063 (4)	3.15	38.9	3.65	58.30
	10064 (4)	2.07	38.9	2.49	58.30
	10065	1.18	38.9	1.92	58.30
	10200	2.72	38.9	3.37	58.30
	Basket				
	4202	2.53	38.9	1.81	58.30
	4222	2.05	38.9	4.14	58.30
	4400	4.03	38.9	3.10	58.30
	4500	2.17	38.9	7.34	58.30
	4509	7.85	38.9	2.58	58.30
	4814	4.58	38.9	9.13	58.30
	5500	5.45	38.9	6.80	58.30
	5600	5.45	38.9	7.50	58.30
	5601	0.00	38.9	9.32	58.30
	Liner				
	10590	1.14	38.9	4.32	58.30
	14061	1.53	38.9	2.07	58.30
	14100	1.41	38.9	3.30	58.30
	14101	1.53	38.9	2.41	58.30

Note 1: 2.4Sm was the lesser value when compared to .7Su.
Note 2: 3.6Sm was the lesser value when compared to Su.
Note 3: There were no elements in pure shear.
Note 4: The stress numbers were multiplied by 2.2 to account for stress concentration factor in this area.

Table 2.16.A. Accident Condition Head On Drop (Outer Fuel Load Applied at Step Near Basket Midsection)

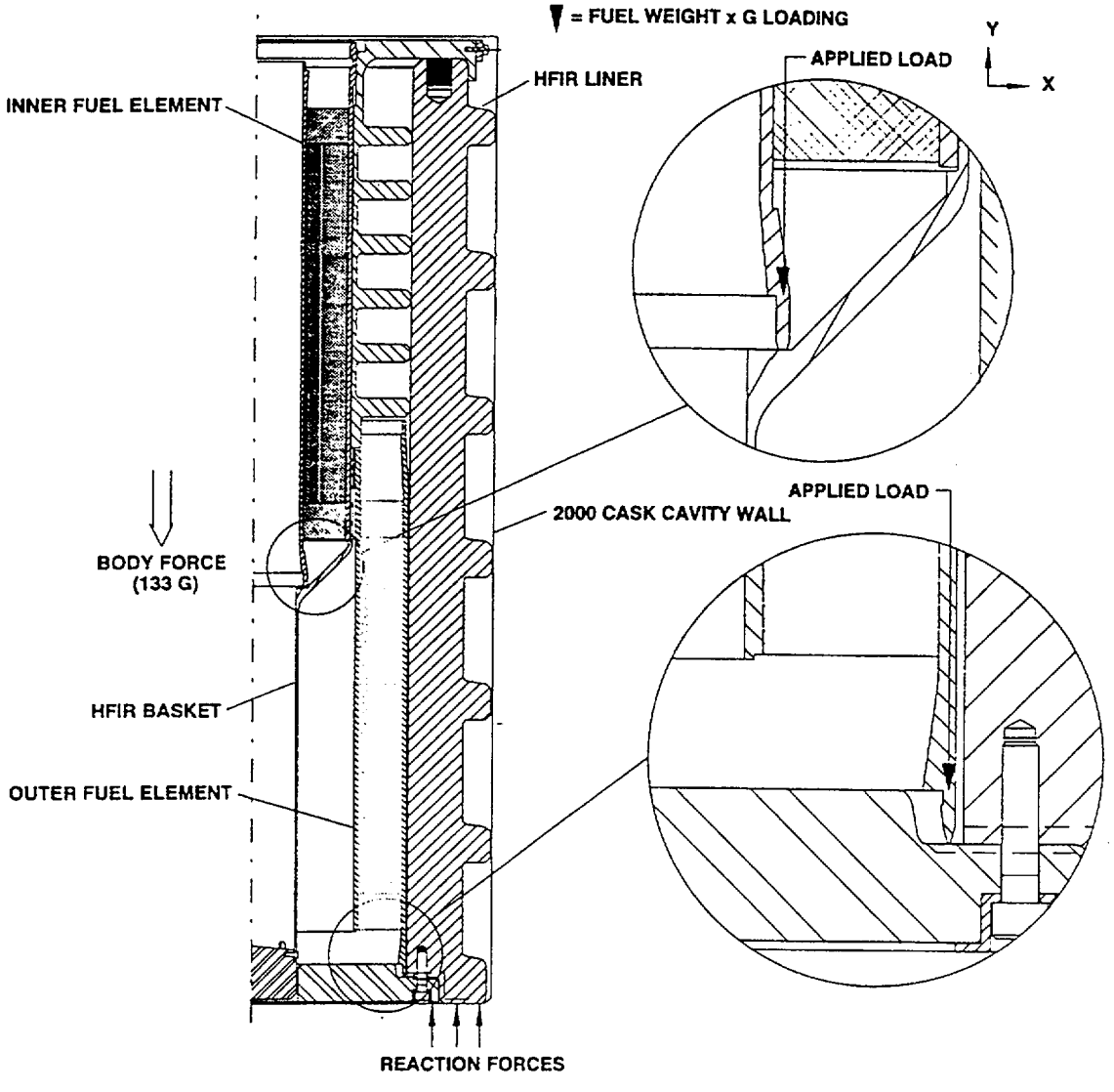

Figure 2.9.A. Accident Condition Bottom Drop (Inner Fuel Load Applied at Lower Funnel Section)

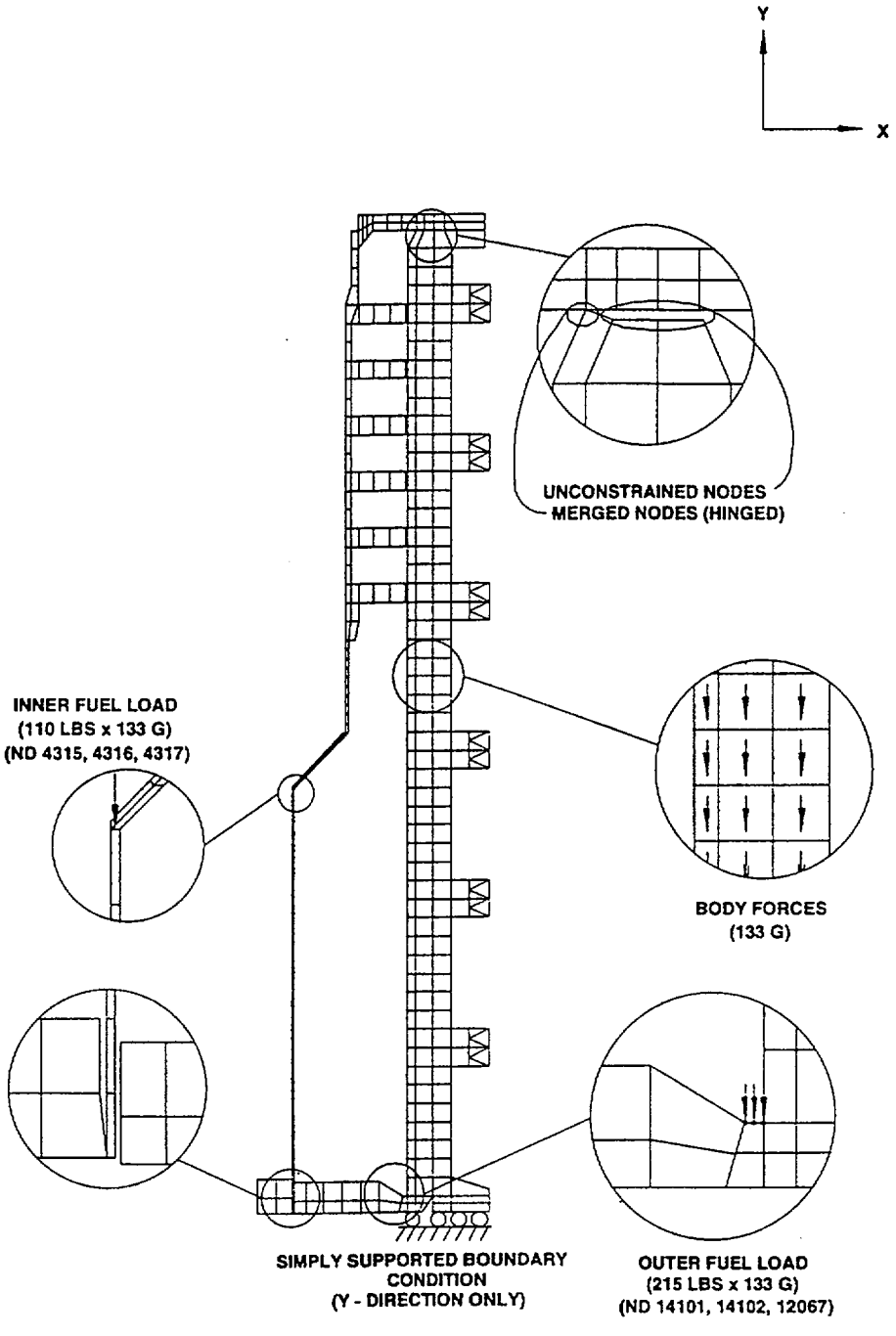

Figure 2.9.B. Accident Condition Bottom Drop, FEM Model (Inner Fuel Load Applied at Lower Funnel Section)

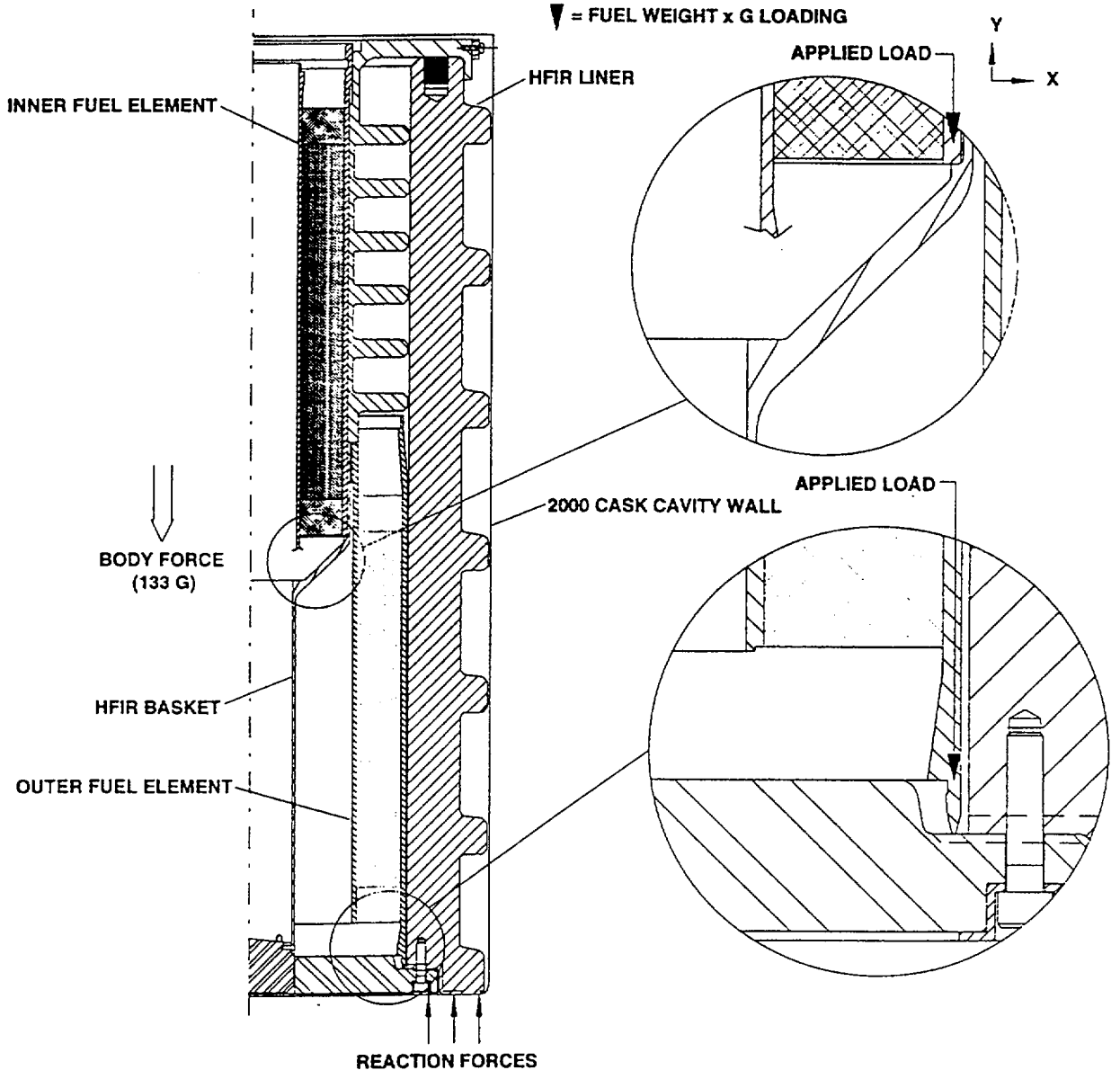

Figure 2.9.C. Accident Condition Bottom Drop (Inner Fuel Load Applied at Upper Funnel Section)

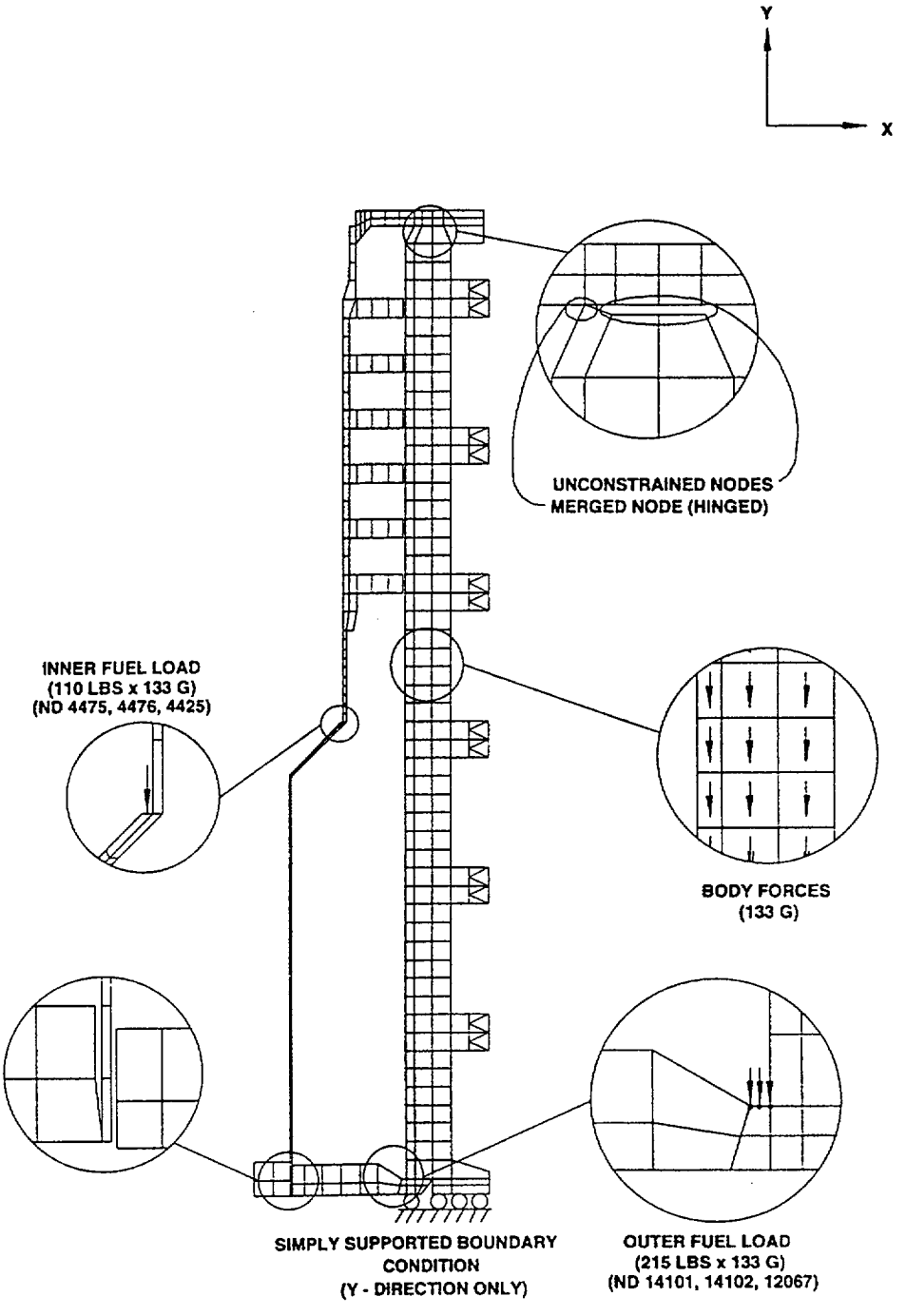

Figure 2.9.D. Accident Condition Bottom Drop, FEM Model (Inner Fuel Load Applied at Upper Funnel Section)

ACCIDENT CONDITION					
	STRESS COMPONENTS	Pm	Pm+Pb	Shear (3)	
	ALLOWABLE CRITERIA	2.4Sm (1)	3.6Sm (2)	.42Su	
	ALLOWABLE VALUES (KSI)	38.9	58.3	27.1	
LOADING CONDITION	MAX STRESS LOCATION	Component Pm	Allowable 2.4Sm	Component Pm+Pb	Allowable 3.6Sm
30 FOOT DROP ON BOTTOM	Basket Flange				
	10062	3.76	38.9	8.44	58.3
	10063 (4)	21.30	38.9	30.21	58.3
	10064 (4)	19.36	38.9	25.01	58.3
	10065	8.68	38.9	12.58	58.3
	10200	1.63	38.9	4.61	58.3
	Basket				
	4202	1.78	38.9	1.81	58.3
	4222	5.77	38.9	12.61	58.3
	4400	8.08	38.9	12.38	58.3
	4500	13.62	38.9	24.88	58.3
	4509	5.10	38.9	7.03	58.3
	4814	6.24	38.9	6.83	58.3
	5500	3.74	38.9	9.28	58.3
	5600	6.09	38.9	9.65	58.3
	5601	13.12	38.9	23.82	58.3
	Liner				
	10590	2.49	38.9	5.19	58.3
	14061	3.20	38.9	4.32	58.3
	14100	3.00	38.9	5.19	58.3
	14101	2.19	38.9	4.89	58.3

Note 1: 2.4Sm was the lesser value when compared to .7Su.
Note 2: 3.6Sm was the lesser value when compared to Su.
Note 3: There were no elements in pure shear.
Note 4: The stress numbers were multiplied by 2.2 to account for a stress concentration in this area.

Table 2.17. Accident Condition Bottom Drop – Case 1 (Inner Fuel Load Applied at Lower Funnel Area)

ACCIDENT CONDITION

STRESS COMPONENTS	Pm	Pm+Pb	Shear (3)
ALLOWABLE CRITERIA	2.4Sm (1)	3.6Sm (2)	.42Su
ALLOWABLE VALUES (KSI)	38.9	58.3	27.1

LOADING CONDITION	MAX STRESS LOCATION	Component Pm	Allowable 2.4Sm	Component Pm+Pb	Allowable 3.6Sm
30 FOOT DROP ON BOTTOM	**Basket Flange**				
	10062	3.76	38.9	8.44	58.3
	10063 (4)	21.30	38.9	30.21	58.3
	10064 (4)	19.36	38.9	25.01	58.3
	10065	8.68	38.9	12.58	58.3
	10200	1.63	38.9	4.61	58.3
	Basket				
	4202	1.78	38.9	1.81	58.3
	4222	2.53	38.9	3.94	58.3
	4400	2.04	38.9	2.95	58.3
	4500	8.77	38.9	14.83	58.3
	4509	5.11	38.9	7.01	58.3
	4814	6.24	38.9	6.83	58.3
	5500	3.74	38.9	9.29	58.3
	5600	6.09	38.9	9.65	58.3
	5601	13.12	38.9	23.82	58.3
	Liner				
	10590	2.49	38.9	5.19	58.3
	14061	3.20	38.9	4.32	58.3
	14100	3.00	38.9	5.19	58.3
	14101	2.19	38.9	4.89	58.3

Note 1: 2.4Sm was the lesser value when compared to .7Su.

Note 2: 3.6Sm was the lesser value when compared to Su.

Note 3: There were no elements in pure shear.

Note 4: The stress number was multiplied by 2.2 to account for a stress concentration factor in this area.

Table 2.17.A. Accident Condition Bottom Drop – Case 2 (Inner Fuel Load Applied at Upper Funnel Area)

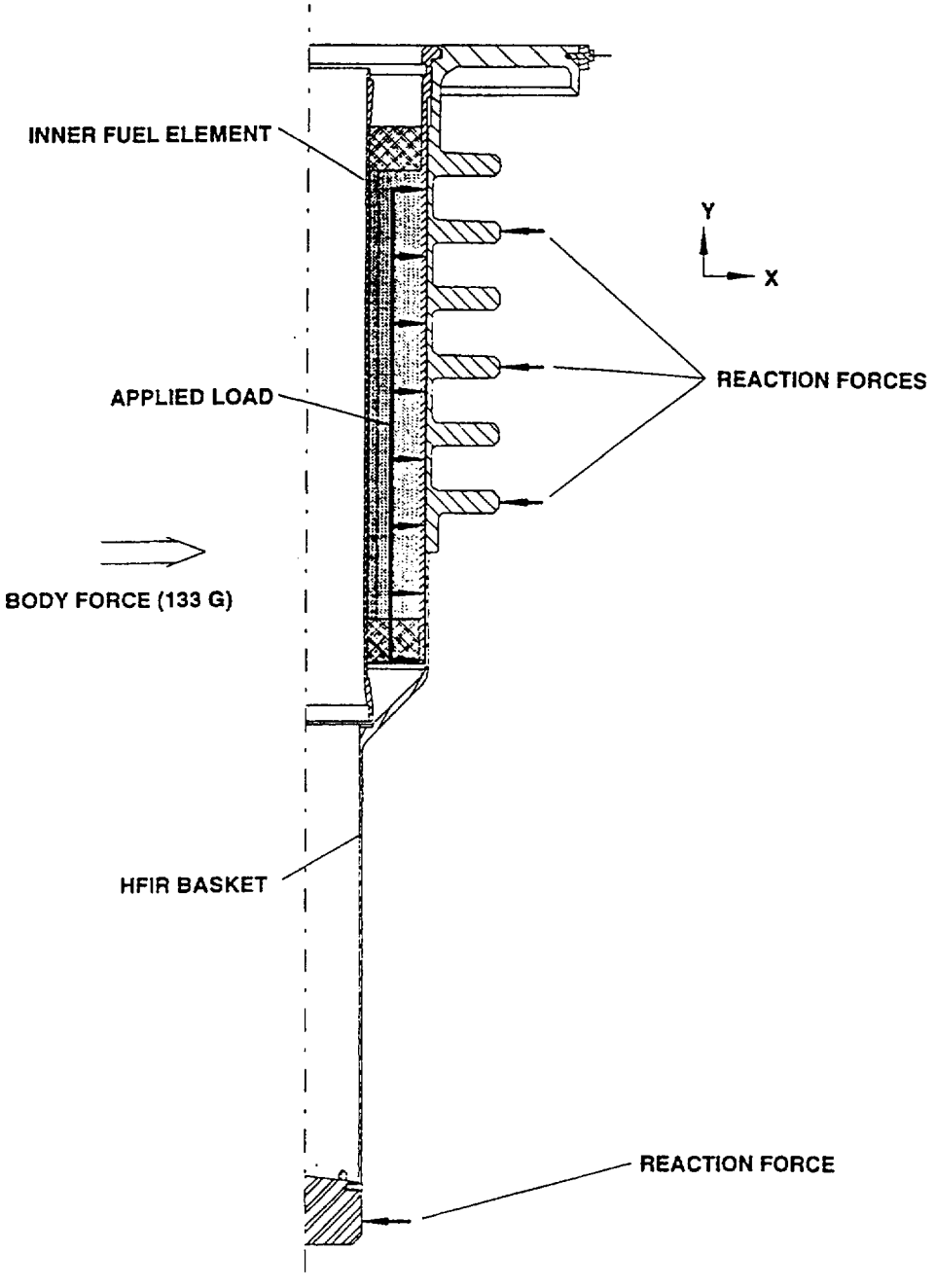

Figure 2.10.A. Accident Condition Side Drop

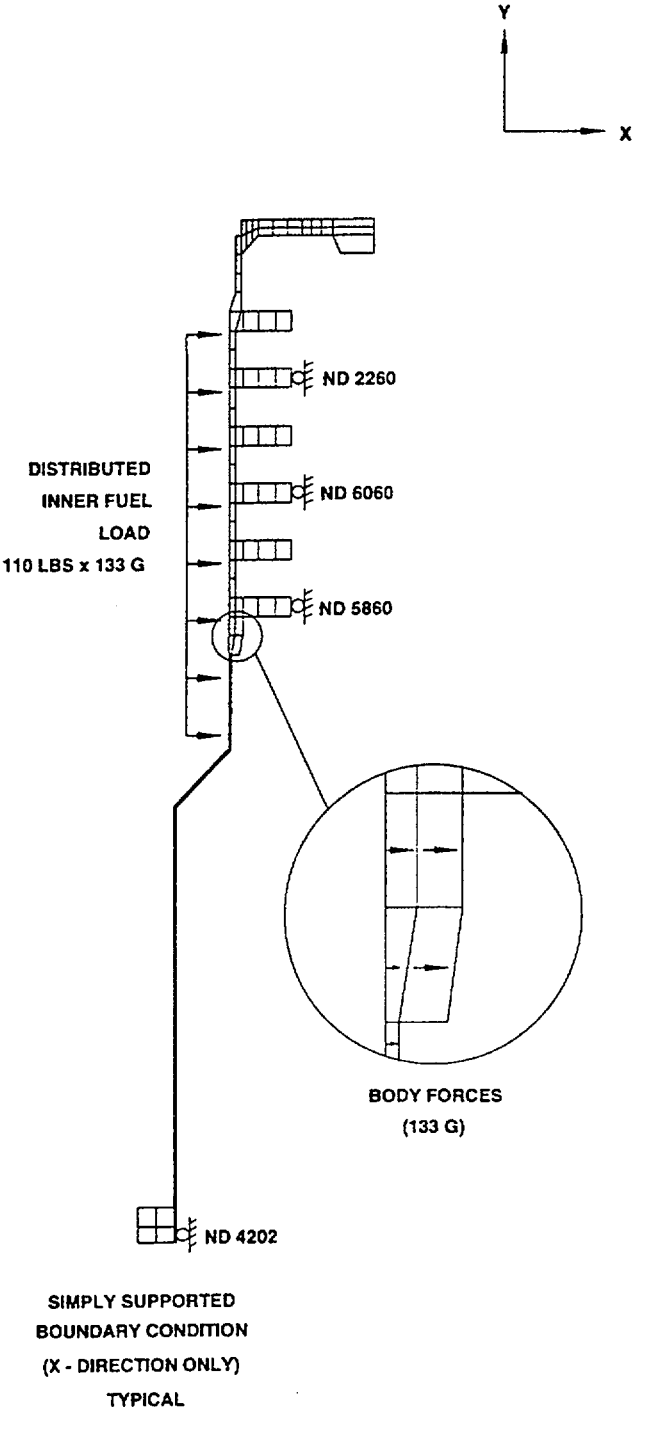

Figure 2.10.B. Accident Condition Side Drop, FEM Model

ACCIDENT CONDITION

STRESS COMPONENTS	Pm	Pm+Pb	Shear (3)
ALLOWABLE CRITERIA	2.4Sm (1)	3.6Sm (2)	.42Su
ALLOWABLE VALUES (KSI)	38.9	58.3	27.1

LOADING CONDITION	MAX STRESS LOCATION	Component Pm	Allowable 2.4Sm	Component Pm+Pb	Allowable 3.6Sm
30 FOOT DROP ON SIDE	**Basket Flange**				
	10062	1.18	38.9	2.21	58.3
	10063 (5)	1.76	38.9	3.52	58.3
	10064 (5)	2.33	38.9	3.83	58.3
	10065	1.70	38.9	2.98	58.3
	10200	1.29	38.9	4.01	58.3
	Basket				
	4202	2.03	38.9	2.96	58.3
	4222	1.77	38.9	1.97	58.3
	4400	0.72	38.9	1.12	58.3
	4404	3.00	38.9	4.94	58.3
	4500	6.76	38.9	8.72	58.3
	4504	6.01	38.9	7.47	58.3
	4509	9.49	38.9	11.40	58.3
	4814	12.94	38.9	13.78	58.3
	5500	5.61	38.9	6.75	58.3
	5600	5.95	38.9	6.74	58.3
	5601	4.92	38.9	6.24	58.3

Note 1: 2.4Sm was the lesser value when compared to .7Su.
Note 2: 3.6Sm was the lesser value when compared to Su.
Note 3: There were no elements in pure shear.
Note 4: Each stress value represents the maximum of all meridian angles.
Note 5: The stress number was multiplied by 2.2 to account for a stress concentration in this area.

Table 2.18. Accident Condition Side Drop

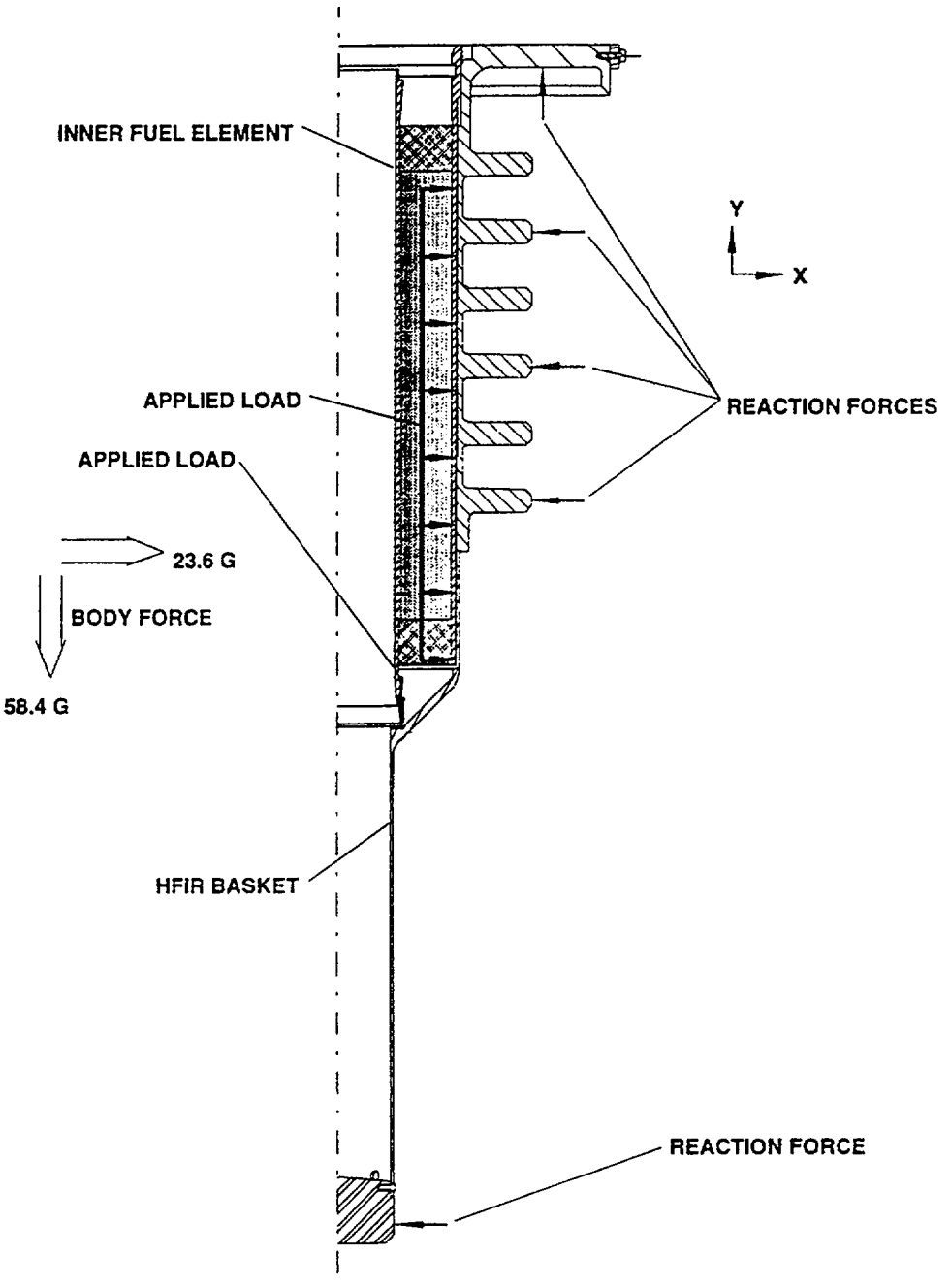

Figure 2.11.A. Accident Condition Cg Over Corner Drop (Inner Fuel Load Applied at Lower Funnel Section)

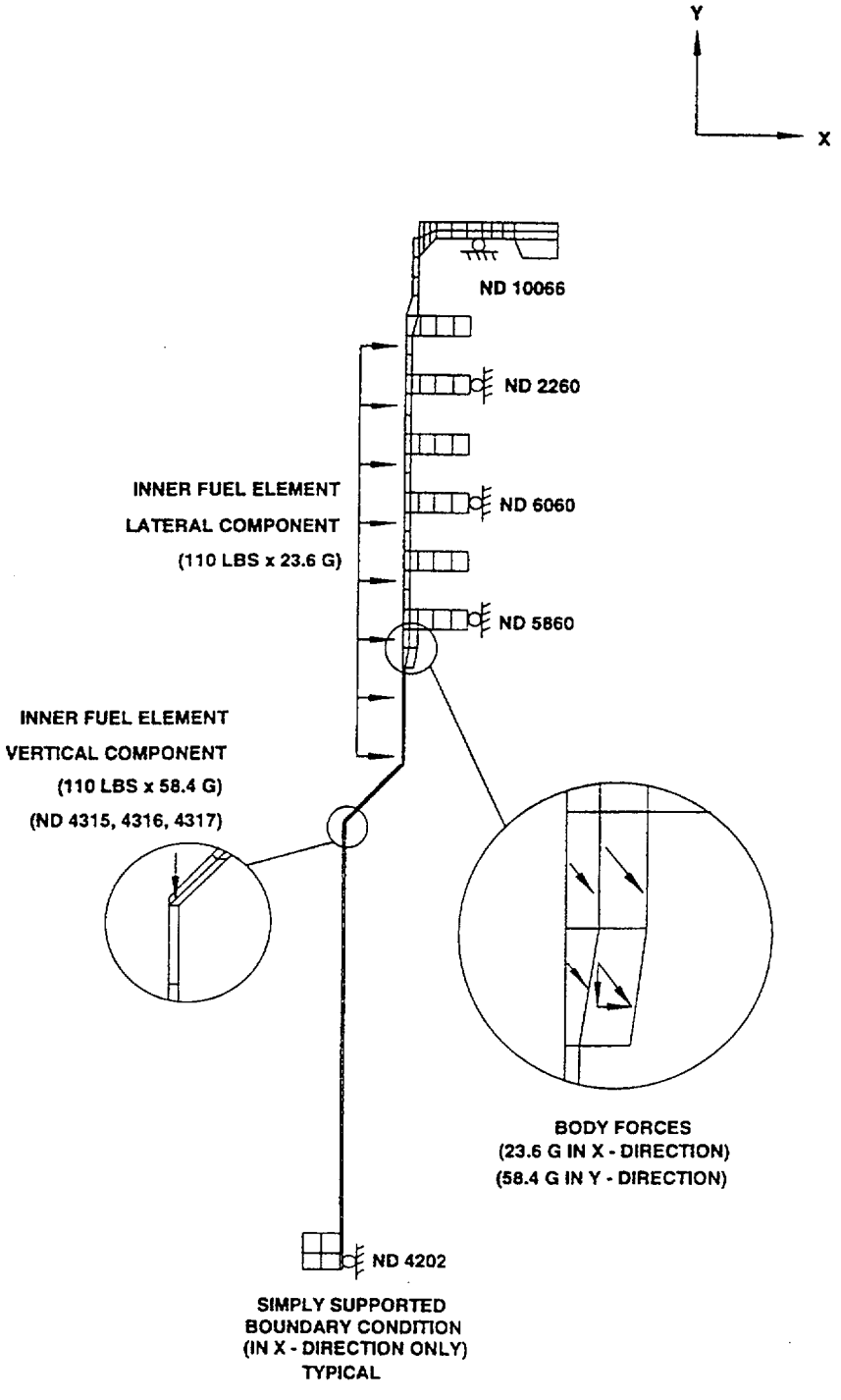

Figure 2.11.B. Accident Condition Cg Over Corner Drop – Case 2 (Inner Fuel Load Applied at Lower Funnel Section)

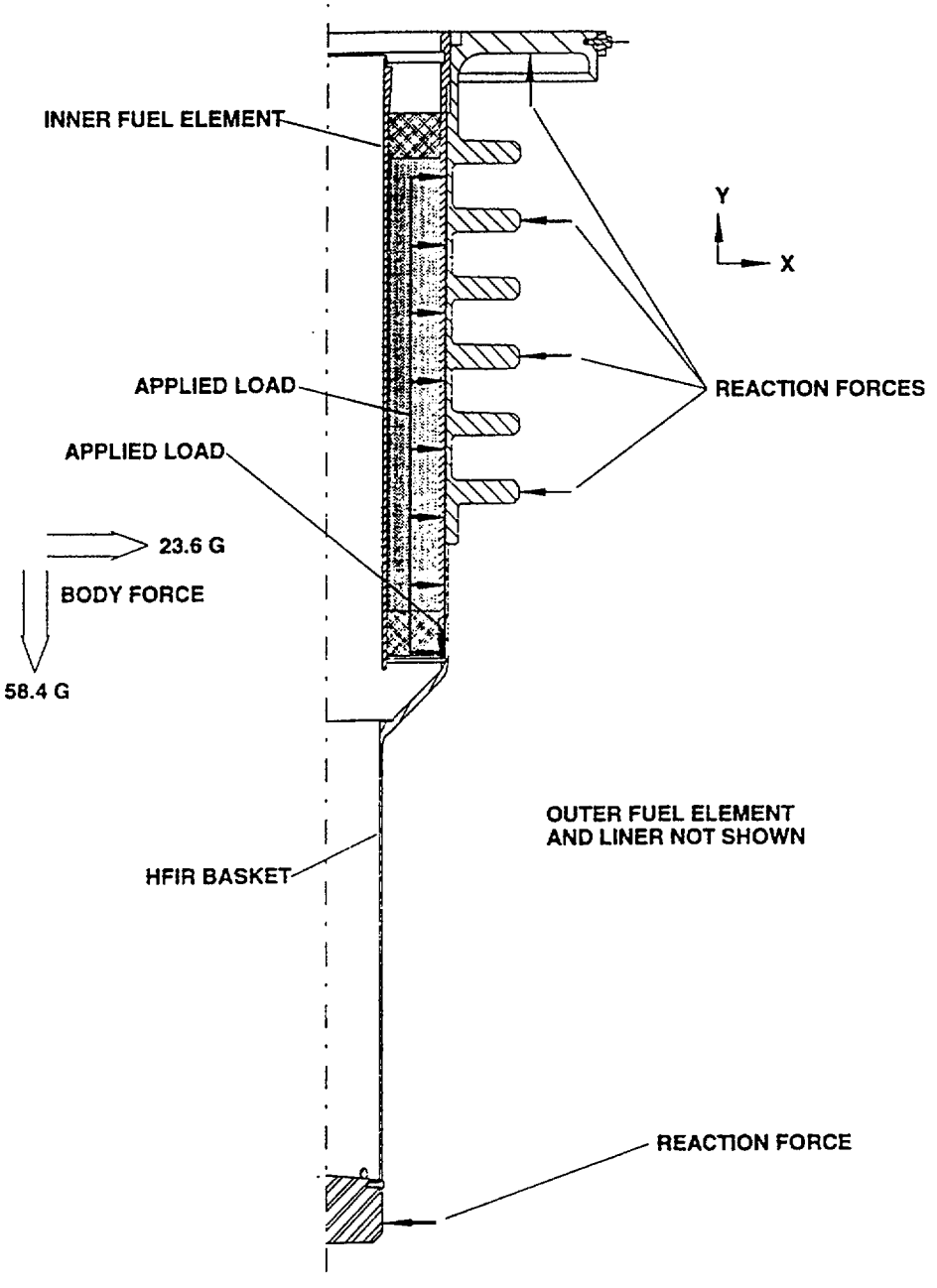

Figure 2.11.C. Accident Condition Cg Over Corner Drop (Inner Fuel Load Applied at Upper Funnel Section)

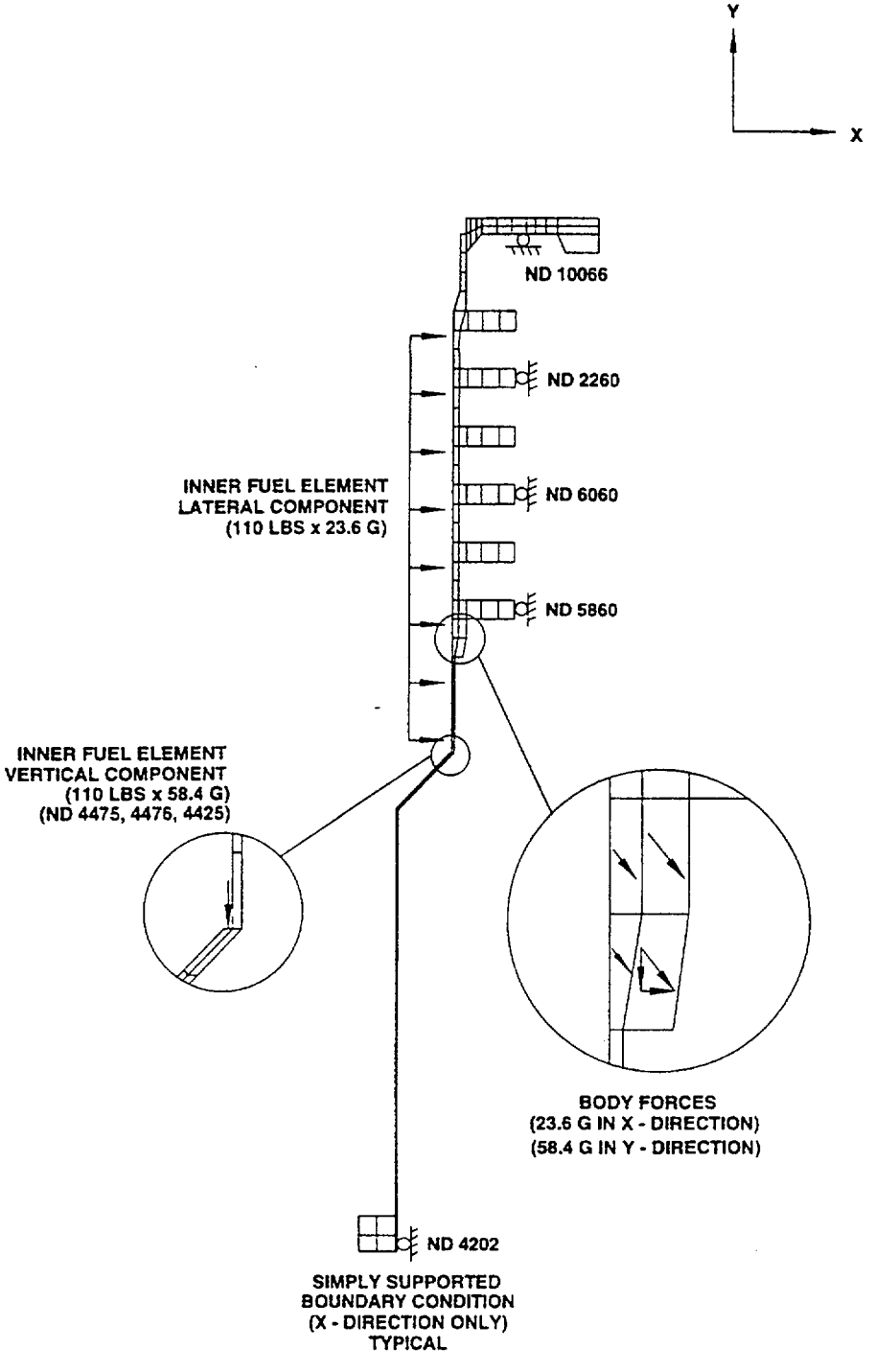

Figure 2.11.D. Accident Condition Cg Over Corner Drop, FEM Model (Inner Fuel Load Applied at Upper Funnel Section)

ACCIDENT CONDITION

STRESS COMPONENTS	Pm	Pm+Pb	Shear (3)
ALLOWABLE CRITERIA	2.4Sm (1)	3.6Sm (2)	.42Su
ALLOWABLE VALUES (KSI)	38.9	58.3	27.1

LOADING CONDITION	MAX STRESS LOCATION	Component Pm	Allowable 2.4Sm	Component Pm+Pb	Allowable 3.6Sm
	Basket Flange				
	10062	1.66	38.9	3.73	58.3
	10063 (4)	9.35	38.9	13.27	58.3
	10064 (4)	6.51	38.9	11.00	58.3
	10065	3.82	38.9	5.55	58.3
	10200	0.75	38.9	2.15	58.3
	Basket				
	4202	0.86	38.9	0.95	58.3
	4222	2.55	38.9	5.55	58.3
30 FOOT DROP	4400	3.55	38.9	5.44	58.3
Cg Over Corner	4404	4.82	38.9	6.41	58.3
	4500	6.10	38.9	11.04	58.3
	4504	2.45	38.9	2.83	58.3
	4509	2.80	38.9	3.69	58.3
	4814	3.58	38.9	3.87	58.3
	5500	1.92	38.9	4.25	58.3
	5600	2.88	38.9	4.40	58.3
	5601	5.83	38.9	10.52	58.3

Note 1: 2.4Sm was the lesser value when compared to .7Su.
Note 2: 3.6Sm was the lesser value when compared to Su.
Note 3: There were no elements in pure shear.
Note 4: The stress numbers are multiplied by 2.2 to account for a stress concentration in this area.

Table 2.19. Accident Condition Cg Over Corner – Case 1 (Inner Fuel Load Applied at Lower Funnel Area)

ACCIDENT CONDITION

STRESS COMPONENTS	Pm	Pm+Pb	Shear (3)
ALLOWABLE CRITERIA	2.4Sm (1)	3.6Sm (2)	.42Su
ALLOWABLE VALUES (KSI)	38.9	58.3	27.1

LOADING CONDITION	MAX STRESS LOCATION	Component Pm	Allowable 2.4Sm	Component Pm+Pb	Allowable 3.6Sm
	Basket Flange				
	10062	1.66	38.9	3.72	58.3
	10063 (4)	9.35	38.9	13.29	58.3
	10064 (4)	8.51	38.9	11.00	58.3
	10065	3.82	38.9	5.55	58.3
	10200	0.75	38.9	2.15	58.3
	Basket				
30 FOOT DROP	4202	0.86	38.9	0.95	58.3
Cg Over Corner	4222	1.15	38.9	1.77	58.3
	4400	0.90	38.9	1.31	58.3
	4404	2.71	38.9	3.38	58.3
	4500	4.03	38.9	6.74	58.3
	4504	2.46	38.9	2.74	58.3
	4509	2.80	38.9	3.69	58.3
	4814	3.58	38.9	3.87	58.3
	5500	1.92	38.9	4.25	58.3
	5600	2.88	38.9	4.40	58.3
	5601	5.83	38.9	10.52	58.3

Note 1: 2.4Sm was the lesser value when compared to .7Su.
Note 2: 3.6Sm was the lesser value when compared to Su.
Note 3: There were no elements in pure shear.
Note 4: The stress numbers were multiplied by 2.2 to account for a stress concentration factor in this area.

Table 2.19.A. Accident Condition Cg Over Corner – Case 2 (Inner Fuel Load Applied at Upper Funnel Area)

2.7.1.5 Oblique Drop. The oblique drop orientations are bounded by the end and side drop loading conditions and need not be evaluated as described in Section 2.7.1. Further discussion of oblique drops is provided in Section 2.7.1 .4 of Reference 2.3.

2.7.1.6 Summary of Results. The accident drop condition maximum stresses are summarized in Table 2.20. As can be seen from the table, all stresses are well within allowable limits. Therefore, the integrity of the HFIR fuel basket and liner assembly is maintained and remains fully functional for all accident drop conditions. To establish the accuracy of the finite element solution, the resulting stresses from the thirty foot bottom on condition are compared with close form solution. Detail and results of this comparison are given in Subsection 2. 11.4.

2.7.2 Puncture

Puncture conditions do not apply to the HFIR fuel basket and liner assembly and need not be specifically addressed. The effects of the basket assembly on the cask body puncture analysis is negligible. As discussed previously in Subsection 2.1.1, the basket loading on the cask body remains well within the currently licensed limits.

2.7.3 Thermal

The thermal evaluation of the HFIR fuel basket and liner assembly for the accident event is presented in Chapter 3.0. The structural evaluation of the resulting temperature distributions is presented in Section 2.6.1.

2.7.3.1 Summary of Pressures and Temperatures. The HFIR fuel basket and liner assembly is not a pressure boundary, therefore, pressure loadings need not be addressed in the structural analysis.

The drop event is postulated to occur prior to the postulated accident fire [2.1], therefore, applicable design temperatures for the drop analysis are those given in Table 2.5.

2.7.4 Immersion - Fissile Material

The criticality evaluation presented in Chapter 6.0 considers the effect of water in-leakage. Thus the requirements of 10CFR71 [2.1] Section 73(c)(4) are met.

2.7.5 Immersion - All Packages

A 21 psig external pressure due to immersion of the package in 50 feet of water as required by 10CFR71 [2.1] Section 73(c)(5) does not effect the HFIR fuel basket and liner assembly and need not be addressed.

2.7.6 Summary of Damage

The worst credible condition that brings the actual fuel regions of the inner and outer fuel elements closer is the 30 foot head on drop condition as shown in Figure 2.11.E. In this scenario, which was described as the second scenario in Paragraph 2.7.1.1, it is assumed that the outer aluminum shell of the outer fuel element has buckled allowing the inner shell of the element to impact against the basket. In this accident condition, the separation between the active fuel region of the outer fuel element and that of the inner fuel element is maintained at 1.177 inch, which meets the criticality criteria as presented in Table 6.6 in Chapter 6.

Table 2.20 presents the summary of maximum stresses in the HFIR fuel basket and liner assembly during the various accident conditions, which shows adequate margin of safety throughout. It is therefore concluded that the HFIR fuel basket and liner assembly meets the design criteria when subjected to the accident conditions as specified in 10CFR71.73 [2.1].

LOADING CONDITIONS	High Stress Element	Element Location	Stress Type	Stress (ksi) (1)	Allowable (ksi)	Margin of Safety
Accident Conditions						
30 foot head on drop (Load Applied at Cooling Fin)	5601	basket/flange thin section transition	Pm+Pb	10.44	58.3	4.58
30 foot head on drop (Load at Basket Mid Section)	5601	basket/flange thin section transition	Pm+Pb	10.44	58.3	4.58
30 foot bottom drop (Load Applied at Lower Funnel)	4500	transition funnel	Pm+Pb	27.87	58.3	1.09
30 foot bottom drop (Load Applied at Lower Funnel)	10063	basket flange (slot)	Pm	23.85	38.90	0.63
30 foot bottom drop (Load Applied at Upper Funnel)	5601	basket/flange thin section transition	Pm+Pb	26.68	58.3	1.19
30 foot bottom drop (Load Applied at Upper Funnel)	10063	basket flange (slot)	Pm	23.35	38.90	0.63
30 foot side drop	4814	basket/flange thin section transition	Pm+Pb	15.43	58.3	2.78
30 ft Cg over Corner drop (Load at Lower Funnel)	4500	transition funnel	Pm+Pb	12.37	58.3	3.71
30 ft Cg over Corner drop (Load at Lower Funnel)	10063	basket flange (slot)	Pm	10.47	38.90	2.71
30 ft Cg over Corner drop (Load at Upper Funnel)	5601	basket/flange thin section transition	Pm+Pb	11.78	58.3	3.95
30 ft Cg over Corner drop (Load at Upper Funnel)	10063	basket flange (slot)	Pm	10.47	38.90	2.71

(1) Resulting stresses increased by 12% to reflect basket weight increase.

Table 2.20. Summary of Results for Accident Conditions

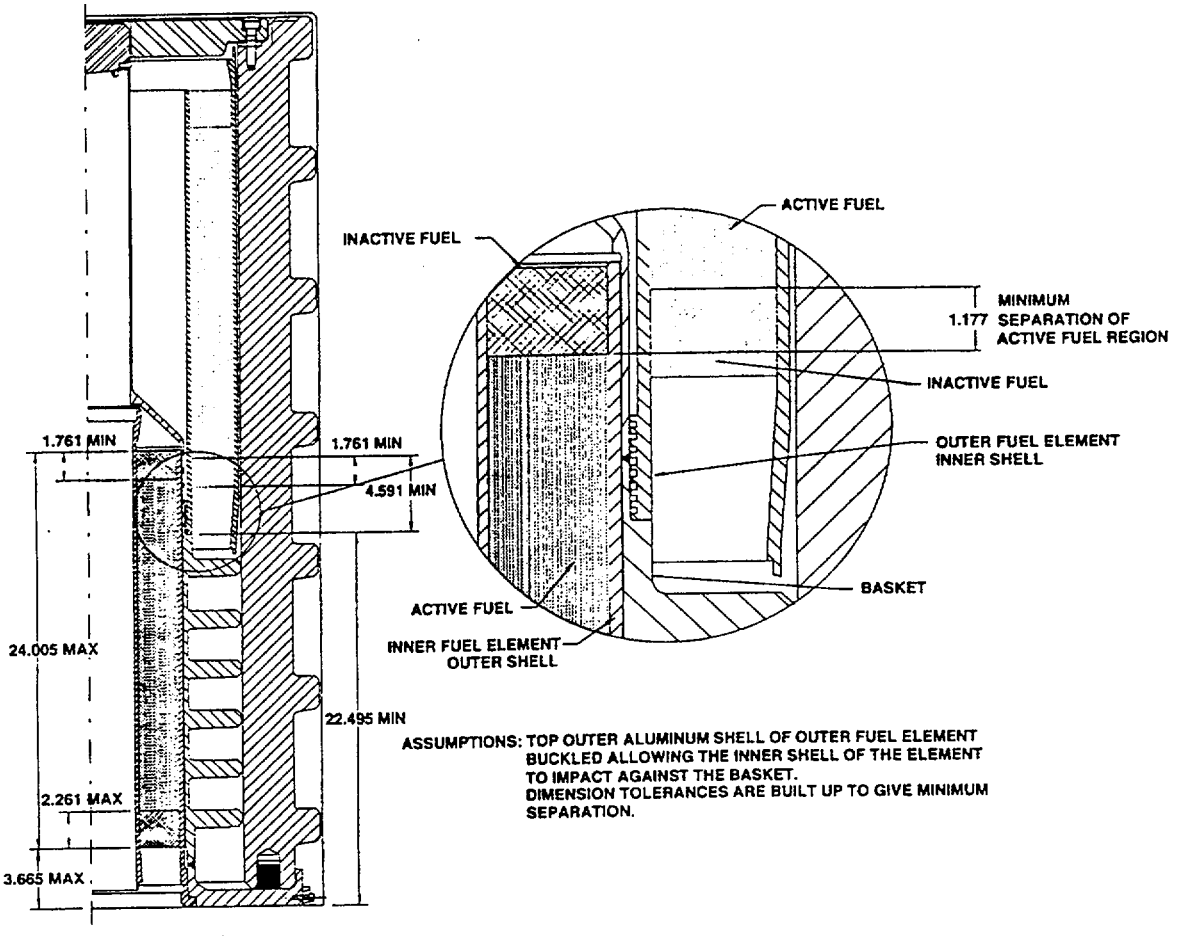

Figure 2.11.E. Worst Credible Accident Condition, 30 Foot Head On Drop

2.7.6.1 Buckling Analysis. Buckling of the HFIR basket is not a possible failure mechanism because of the load paths enforced by its design and that of the HFIR fuel liner. Except for the basket top flange, no other component of the basket and liner is under compressive forces for all loading conditions. For the basket top flange, both general and local instability modes are investigated below.

General Instability: A general instability can be developed by considering the basket's top flange and a portion of its cylinder to form an effective ring as shown below. According to Bruhn [2.12], page C7.11, the effective length of cylinder may be taken conservatively as 15 times the thickness of the cylinder, or approximately 4.0 inches.

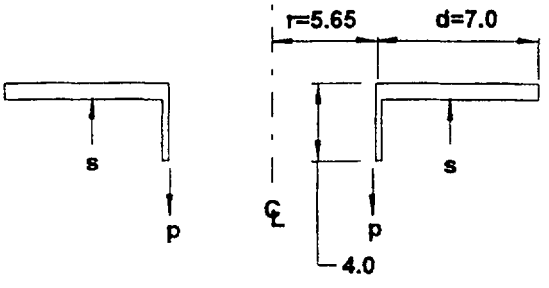

The ring is loaded by the distributed inertia loads, **p** and distributed reaction support loads, **s**. The unit for the distributed forces, **p** and **s** are lbs/in. The eccentricity of **p** and **s** produce a uniformly distributed moment loading **m** on the ring.

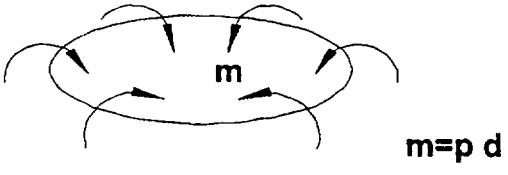

The net moment on any ring cross-section is $\mathbf{M} = \mathbf{m} \cdot \mathbf{r}$, where r is the ring radius, as shown below. Under the moment **M**, the ring flange is put in uniform compression. This compressive load is analogous to a ring under uniform compression.

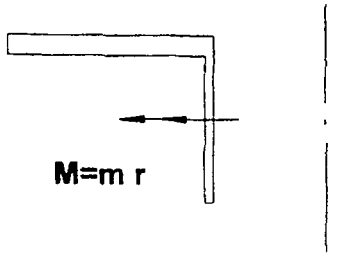

From Roark and Young [2.10], for a ring under uniform compression, the critical, or buckling load is

$$P_{cr} = \frac{3 \cdot E \cdot I}{r^3} \qquad \text{or} \qquad \sigma_{cr} = \frac{3 \cdot E \cdot I}{A \cdot r^2}$$

where P_{cr} = Critical uniform radial compression
σ_{cr} = Critical compressive stress
E = Elastic modulus of S.S. 304 = 27X106 psi at 200°F
I = Cross-sectional moment of inertia = 12.55 in4
A = Cross-sectional area = 8.55 in2
r = Mean radius of the ring = 6.5 in

The general buckling stress is calculated to be 2.8×10^6 psi, while the maximum stress in the top flange as given by the LIBRA finite element analysis is 14,000 psi, which shows that no buckling in this mode is likely.

Local Instability: A local instability mode can result from plate buckling of the top flange under compressive loading. From Bruhn [2.12], page C6.1, equation C6.1, the critical buckling stress for a long plate under compressive loading on short sides is calculated as

$$\sigma_{cr} = 0.388 \cdot E \cdot (t/b)^2$$

where E = Elastic Modulus of S.S. 304 = 27x106 psi
t = Thickness of the top flange = 1.0 inch
b = Width of the top flange = 7.0 inch

This equation gives the local buckling stress of 2.14x105 psi, which give a large margin when compared to the LIBRA prediction of 14,000 psi. Therefore it is concluded that the design of the basket and liner is adequate against buckling.

2.7.6.2 Plastic Collapse of Basket Top Flange. The top flange ring of the basket for the accident condition of 30 foot bottom drop is evaluated for plastic collapse analysis. The plastic collapse phenomenon is not likely since the compressive stress in the flange calculated from the LIBRA finite element analysis is 14,000 psi which is much smaller than the yield strength of S.S. 304 at 25,000 psi (at 200°F). Nevertheless, the plastic collapse loading is checked as suggested by J. Markowitz [2.13].

The top flange is modeled as a circular plate with the outer edge simply supported and subjected to a uniformly distributed vertical shear force along the inner edge of the flange where the rotation is prevented. The rotation of the inner edge of the flange is prevented because of the stiffness provided by the basket cylinder. The flange is assumed to be simply supported at the inner edge of the liner. This model is as shown in the following diagram.

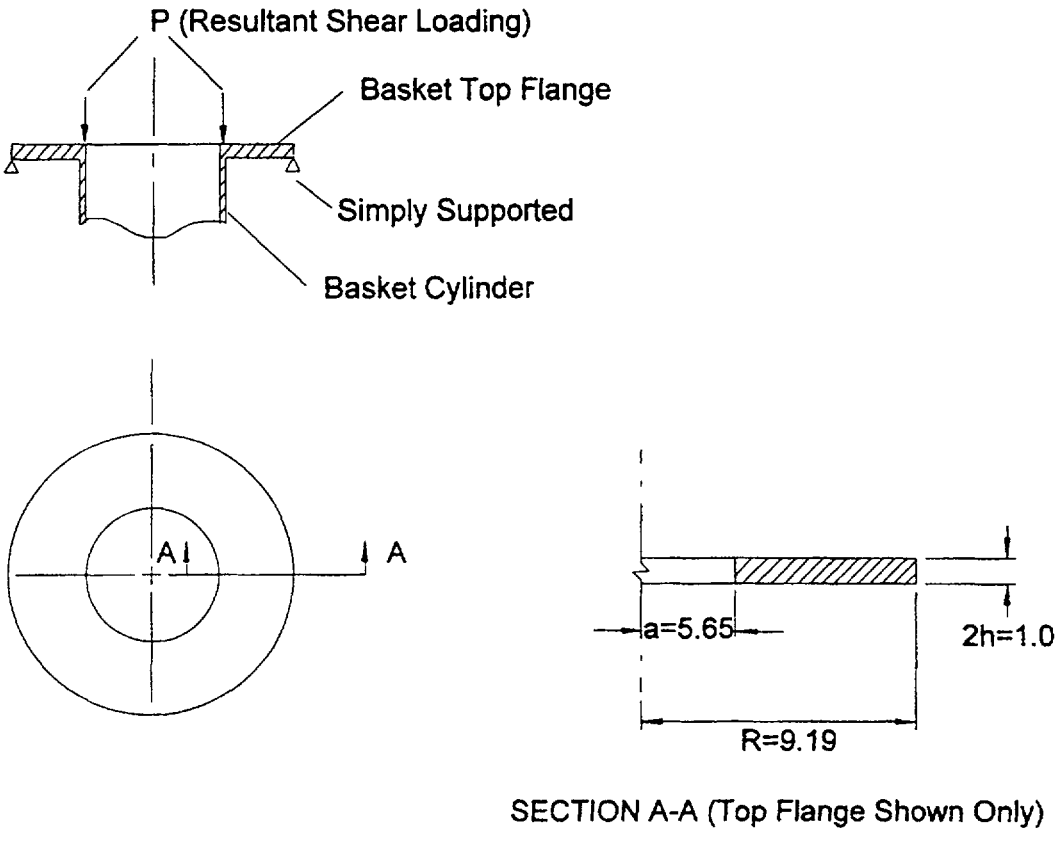

SECTION A-A (Top Flange Shown Only)

The shear force applied at the inner flange is from the combined weight loading of the basket and the inner fuel. According to J. Markowitz [2.13] the collapse loading P is calculated as

$$P = k \cdot \pi \cdot \sigma_\theta \cdot h^2$$

where P = Collapse Loading
k = 5.0, from Fig 10 of [2.13] for a/R=0.61 for isotropic material
where a = Inner radius of the top flange = 5.65 inch
R = Outer radius of the top flange = 9.19 inch
σ_θ = yield strength of S.S. 304 = 25,000 psi at 200F
h = 1/2 of the flange thickness = 0.5 inch

The critical loading calculated from the above equation is 98,000 lbs.

The actual shear loading during the 30 foot bottom drop condition is calculated as

$$\begin{aligned} P &= 133 \text{ G's} \cdot (\text{Weight of Basket} + \text{Weight of Inner Fuel}) \\ &= 133 \cdot (520 + 110) \\ &= 83{,}790 \text{ lbs} \end{aligned}$$

During the 30 foot bottom drop condition, the critical shear loading to cause the plastic collapse is 98,000 lbs, while the actual shear loading applied to the basket top flange is 83,790 lbs. In addition, the compressive stress in the top flange predicted by the finite element analysis is 14,000 psi which is significantly less than the yield strength of S.S. 304 of 25,000 psi (at 200°F). It is therefore concluded that the basket top flange is safe from plastic collapse.

2.7.6.3 Extreme of Total Stress Intensities. The extreme of the total stress intensity range must not exceed the value of 2(Sa) given for 10 cycles [2.6] per [2.2] paragraph c.7. This value turns out to be 1370 ksi which far exceeds the sum of the maximum stress intensities for the hypothetical accident condition and the normal condition. This sum is a bound on said extreme range. Therefore, the extreme of the total stress intensity range is much smaller than its permitted limit and poses no concern.

2.8 SPECIAL FORM

This Section does not apply to the HFIR fuel basket and liner.

2.9 FUEL RODS

The Model 2000 Package remains leak tight under all normal and accident conditions as demonstrated in the Package Safety Analysis Report [2.3]. Therefore the HFIR fuel cladding need not provide containment to the fuel material.

2.10 REFERENCES

2.1. Code of Federal Regulations, Title 10, Part 71, 1992.

2.2. U.S. NRC Regulatory Guide 7.6, "Design Criteria for the Structural Analysis of Shipping Cask Containment Vessels", Revision 1, March, 1978.

2.3. Safety Analysis Report, "G.E. Model 2000 Model 2000 Shipping Package", NEDO 31581, April, 1988.

2.4. ASME, Boiler and Pressure Vessel Code, Section III, Division I, Subsection NG, 1989.

2.5. U.S. NRC Regulatory Guide 7.8, "Load Combinations for the Structural Analysis of Shipping Casks", May, 1977.

2.6. ASME, Boiler and Pressure Vessel Code, Section III, Division I, Appendix I, 1989.

2.7. ASTM B 777, Class I, "Specification for Tungsten Base, High Density Metal", 1987.

2.8. Private communication with the Department of Meteorology at San Jose State University, San Jose, CA, 28 July 1993.

2.9. Peterson, R.E., Stress Concentration Factors, John Wiley and Sons.

2.10. Roark, R.J., and Young, W.C., Formulas for Stress and Strain, McGraw-Hill, 5th ea., 1975.

2.11. ASME, Boiler and Pressure Vessel Code, Section III, Division I, Appendix I, 1989.

2.12. Bruhn, E. F., Analysis and Design of Flight Vehicle Structures, Tri-State Offset Company, 1965

2.13. J. Markowitz, Plastic Analysis of Orthotropic Circular Plates, Proceedings of ASCE, vol. 90-251, 1964.

2.14. GE Drawing lO5E9520: Model 2000 Shipping Cask All S/N except S/N 2001.

2.15. Machinery's Handbook, 20th Edition, Industrial Press, p. 1169, 1975

2.16. J. E. Shigley and L. D. Mitchell, Mechanical Engineering Design, 4th Edition, McGraw-Hill Book Company, New York, 1983.

2.17. J. E. Shigley and C. R. Mischke, Mechanical Engineering Design, 5th Edition, McGraw-Hill Book Company, New York, 1989.

2.18. ASME, Boiler and Pressure Vessel Code, Section III, Subsection NB 3232.3.

2.19. ASME, Boiler and Pressure Vessel Code, Section III, Appendix I, Figure I-9.4.

2.20. ASME, Boiler and Pressure Vessel Code, Section III, Appendix I, Table I-1.3.

2.21. GE Drawing lO5E9523: HFIR Fuel Liner and Basket Certification Drawing.

2.11 APPENDIX

2.11.1 Thermal Stresses Due to a 40°F Temperature.

2.11.2 Stress Concentration Factors for Fatigue Evaluation.

2.11.3 Fatigue Cumulative Usage Factor.

2.11.4 Comparison of Closed Form Solutions With Finite Element Analysis Results.

2.11.5 Optional Lifting Ears

2.11.6 HFIR Basket Lifting Arrangement

APPENDIX 2.11.1

Thermal Stresses Due to a -40°F Temperature

The maximum stress found in Libra due to a -40°F temperature gradient is 4592 psi for the hoop stress component. This number is compared to the number we get from the following hand calculation. To verify that the stress given by Libra is correct, a hand calculation for stresses due to thermal expansion, using formulas found in Roark [2.10], is performed.

At -40°F, there will be a VT of 110° from normal conditions (70°F). Thus, the coefficients of thermal expansion for the two materials are:

$$\alpha \text{ (A-304 steel)} = 8.55 \times 10^{-6}$$

$$\alpha \text{ (90\% alloy tungsten)} = 5.40 \times 10^{-6}$$

Their respective deflections are:

$$\delta \text{ (A-304 steel)} = \alpha(\Delta T) = (8.55 \times 10^{-6})*(110) = 9.405 \times 10^{-4}$$

$$\delta \text{ (90\%alloy tungsten)} = \alpha\,(\Delta T) = (5.94 \times 10^{-6})*(110) = 5.940 \times 10^{-4}$$

Thus, the steel wants to deflect at a faster rate than the tungsten, causing stresses at their interface. The deflection difference of the two materials if they are allowed to deflect freely is 3.465×10^{-4}. However, this dimension is not allowed to deflect freely, due to the presence of the tungsten material, and thus, stresses occur. The stresses are calculated according to the following formulas, found in Roark [2.10], p. 458-461:

$$V_0 = 2D\lambda^3 y$$

$$D = \frac{Et^3}{12\left(1-\nu^2\right)}$$

$$\lambda = \left[\frac{3\left(1-\nu^2\right)}{R^2 t^2}\right]^{\frac{1}{4}}$$

where R = 2.375 in

t = .125 in

ν = .3

E=30x 106

$$\text{Max } \sigma = \frac{-2V_0\lambda R}{t} = 4387 \text{ psi}$$

Libra Output for element 4202, the element of highest thermal stress, is provided in the following set of stress data:

EL	PT	SIGMA_1	SIGMA_2	SIGMA_3	TAU
4202	1	-.10416E+04	-.49429E+04	.57257E+04	.53343E+04
4202	2	.43739E+04	.11809E+04	.89002E+04	.38597E+04
4202	3	.30477E+04	.84895E+03	.30354E+04	.10994E+04
4202	4	-.68180E+03	-.29541E+04	.70690E+03	.18305E+04
4202	AVE	.43800E+03	-.48021E+03	.45920E+04	.25361E+04

As seen, the maximum average stress for the hoop component, Sigma_3, is 4592 psi, compared to the 4376 psi calculated above. The % error for Libra compared to the hand calculation is:

$$\% \text{ error} = \frac{|4376 - 4592|}{4376} \text{ X } 100\% = 4.93\%$$

APPENDIX 2.11.2

Stress Concentration Factors for Fatigue Evaluation

The one-inch-thick fins that are positioned 3 inches on-center on the outer periphery of the top portion of the basket cause a mild rise in local stresses at their juncture with the thin wall cylindrical portion of the basket. This increase in local stress is applicable to the vertical component of normal stress.

Figure 2.12 shows a tension specimen with a symmetrical profile under load P. The wide shoulder with width "D" causes a rise in stresses at its juncture with the thinner part that has width "d". The stress concentration factors for this condition can be found in [2.9]. The top cylindrical portion of the basket with its fins forms a repetitive geometric pattern of varying cross sections that resembles one symmetrical half of that shown in Figure 2.12. The stress concentration factors for the basket are smaller than those for the geometry of Figure 2.12. However, the stress concentration factors for the geometry in Figure 2.12 will be used [2.9] leading to added conservatism.

For Element 4814, we can assume

r = 0.25 in. (min),

t = 0.25 in.,

W=3.31 in., and

L= 1.0 in.

resulting in the following ratios:

r/d=0.5

L/d = 2.0

d/D = 13.2

Using Figure 69 of Reference 2.9, the stress concentration factor is 1.47, however this will be rounded off to 1.5 for conservatism and simplicity. It will be pointed out that the stress concentration factors remain basically constant with increasing d/D ratios beyond 5.0; e.g., examining Figures 66 and 67 of [2.9] shows that for rid = 0.5, and L/d = 1.5 to 3.5, the stress concentration factor values are the same for the range of d/D = 7.0 to 8.5. Hence, for Element 4814, a value of 1.5 was used for the stress concentration factor.

For all elements other than Element 4814, for which a local stress concentration factor was applicable, the conservative value of 4.0 was used. For simplicity, no attempt was made to find the applicable stress concentration factor which under most circumstances would not exceed 2.2.

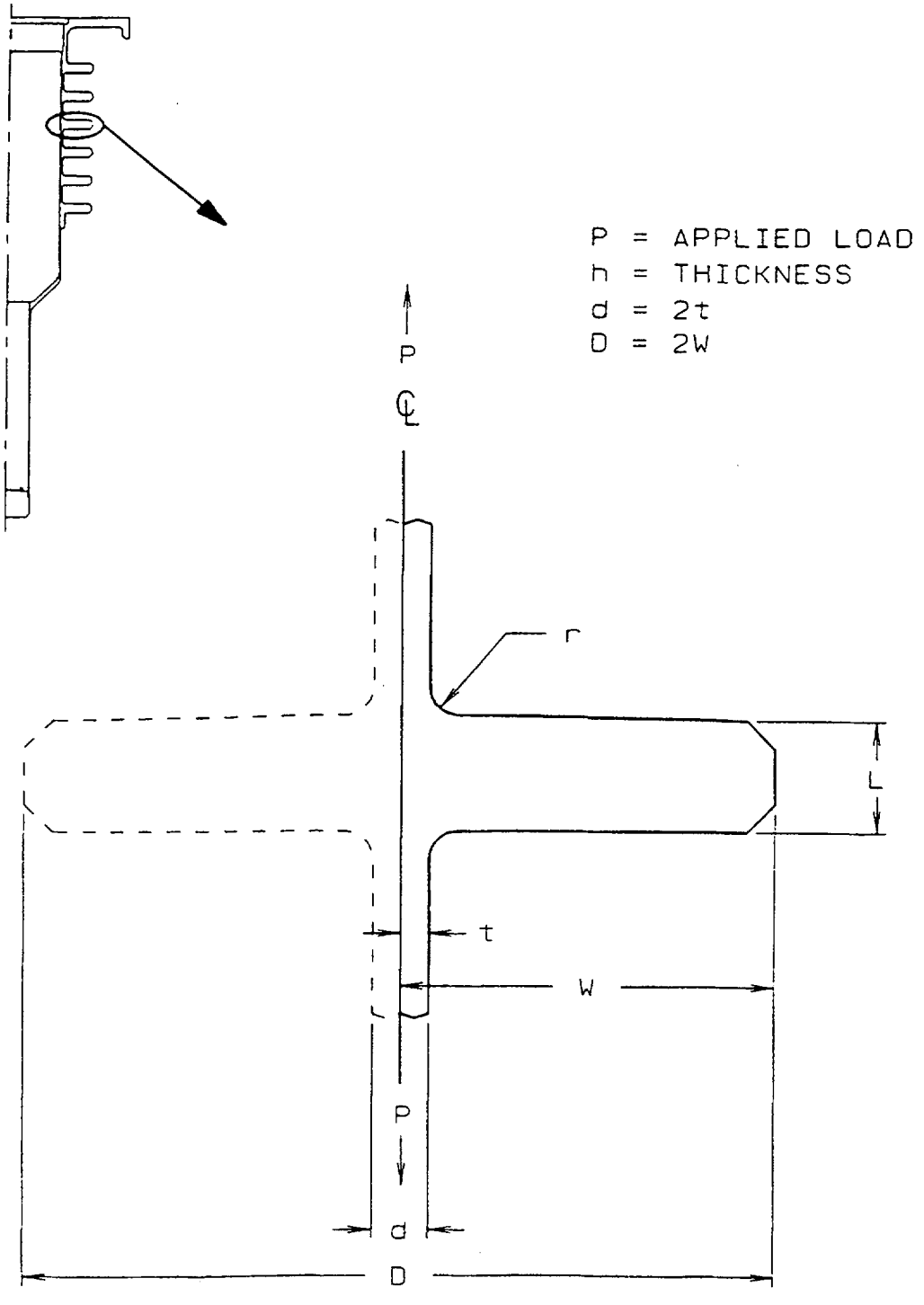

Figure 2.12. Geometry for Stress Concentration Factors in Basket Cylinder at Fin Juncture

APPENDIX 2.11.3

Fatigue Cumulative Usage Factor

The extremes of "normal condition" thermal stresses far exceed the stresses caused by the transportation shock and vibration alone as shown in Tables 2.7 and 2.8. In these tables, the last column on the right includes thermal stresses while the column next to it, just to the left of this column, excludes the thermal stresses.

For the steel used, the allowable value S_a =13.7 ksi for 10^{11} cycles (infinite life for all practical purposes) based on [2.6], Appendix I, Figure I-9.2.2, Curve C . Examination of the stress intensities in Tables 2.7 and 2.8 which include secondary and thermal effects ($P_m + P_b + Q$) indicates that if Element 4202 is excluded, $S_{alt} < S_a$, i.e., fatigue usage U = 0 and hence there would be no fatigue problem.

The thermally induced stresses of Element 4202 which have the highest magnitudes of all stresses in Tables 2.7 and 2.8, are cause by the difference between the coefficients of thermal expansion of the steel tubing and the tungsten plug near that element. The ASME code [2.6] excludes this type of thermally induced stress (see note 2 [2.6], Appendix I, Figure I-9.2.2) from analysis for fatigue.

Also, subsection NG of the ASME code [2.4] provides that under conditions specified in subparagraph NG-3222.4 under (d) (1) through (4) analysis for fatigue is not required. A review of the thermal profiles indicates that all of these conditions are met (after, of course, doing the required calculations which dictates less than 30 °F temp difference or range in this difference for any two points which are under the most restrictive condition at most 0.77 inches apart, we find that in our case this temperature difference is only on the order of 4° F). The condition specified under NG-3222.4 (d) (3), which is applicable to Element 4202 demands less than 428 degrees F range in temperature variation using $8.4x(10)^{-6}$ and $5.4x(10)^{-6}$ in/in/or for the average coefficients of thermal expansion of the steel and tungsten, respectively. This range in temperature variation turns out to be 250°F which is less than the 428 °F indicating no need to do fatigue analysis.

To eliminate the possibility of any concern, by any reviewer, about the thermal stresses in Element 4202, two options are at hand: (1) in the fabrication drawings, specify a connection between the tungsten plug and the steel tube that allows free relative radial expansion and contraction of these parts which will totally eliminate, for practical purposes, the thermal stresses in Element 4202; (2) show that if a fatigue analysis were to be performed, the maximum bound on the fatigue usage factor U would be less than 1.00.

Although option (1) above will be pursued, option (2) will be taken below to eliminate any possible concern.

2.11.3.1 Upper Bound on Fatigue Usage Factor

There are two basic classes of stress cycles applicable to the structure: 1) mechanical shock and vibration, and 2) thermal stress cycles. As mentioned above, the latter, (2), has a range that far exceeds that of the former, (1). The stress cycles of (1) occur at a rate which far exceeds the rate for (2); while the fundamental period of vibration is 0.00348 seconds the shortest period of a thermal cycle is on the order of 24 hours, yielding the ratio of ~$25x(10)^6$ for the cycling rate. This means that the cycling of (1) is about a mean stress level which is varying very slowly. For this reason, Curve C [2.6] of Appendix I, Figure I-9.2.2 is used for shock and vibration. However in most cases the thermal variation is far less than the full range experienced, a fact that can be used to advantage, if necessary, to demonstrate the extra conservatism used here but is ignored in favor of expediting the completion of this report.

The thermal stress cycles are broken down into four regimes with the following extra conservative attributes in a one year period:

1. for 1.5 months, the extremes of the "normal conditions" [2.2 and 2.5] thermal cycle are experienced every day; 45 of these cycles in total. Temperature varies between -20° F and 100°F. We can assume that this scenario covers the worst part of the worst possible winter;

2. for 1.5 months, 5/6th of the extremes of the "normal conditions" [2.2 and 2.5] thermal cycle are experienced every day; 45 of these cycles in total. Temperature varies between -0° F and 100°F. We can assume that this scenario covers the rest of the worst winter;

3. for 6 months, 2/3rd of the extremes of the "normal conditions" [2.2 and 2.5] thermal cycle are experienced every day; 183 of these cycles in total. Temperature varies between 20°F and 100°F. We can assume that this scenario covers the worst possible spring and fall;

4. for 3 months, 1/2 of the extremes of the "normal conditions" [2.2 and 2.5] thermal cycle are experienced every day; 92 of these cycles in total. Temperature varies between 40° F and 100°F. We can assume that this scenario covers the worst summer.

It should be noted that the record for the maximum temperature change in a 24 hour period ever since records have been kept is 100°F which happened in Montana [2.8].

For the sake of simplicity, in lieu of examining the cumulative damage ratios at several candidate points, the fatigue usage ratio from the highest stresses caused by shock and vibration and that from the highest stresses caused by thermal cycles will be used. This will be the most obvious way to convey the final conclusion. Note that these two categories of stresses will be at different locations.

For the transportation shock and vibration, the highest stress will be for Element 4404 to which the highly conservative stress concentration factor of 4 is applied.

$S_{alt,tr} = 4.60\ [28.3x(10)^3\ ksi / 27.7x(10)^3\ ksi]\ (2/2) = 4.80\ ksi$

From Curve C [2.6] of Appendix I, Figure I-9.2.2, S_a =13.7 ksi at $(10)^{11}$ cycles.

Assuming that on average, there are yearly 12 round trips of 10 hours duration each way and using the fundamental frequency of 287 Hz, the fatigue usage for 100 years of use is determined as follows:

N_{tr} = (287 cycles/sec)x(12x2xlOx3600 see of cycling/yr)x100 yrs = 248x$(10)^8$ total cycles

Even if $(10)^{13}$ allowable cycles were used (it should be noted that extrapolating Curve C [2.6] of Appendix I, Figure I-9.2.2, for 4.80 ksi, $(10)^{25}$ is a more proper number to use), for transportation shock and vibration cycles

$U_{tr} < 248x(10)^8 / (10)^{13} = +0.00$

For the thermal stress cycle the highest stress range will be for Element 4202. For regime (1) of the thermal stress cycle:

$S_{alt,thl}$ = [14.76+8.33+2(.158)][28.3x$(10)^3$ ksi / 27.7x$(10)^3$ ksi]/2 = 12.0 ksi

From Curve C [2.6] of Appendix I, Figure I-9.2.2, S_a =13.7 ksi at $(10)^{11}$ cycles; the fatigue usage is again

$U_{thl} <45 / (10)^{11} = 0.00$

It therefore follows that

$U_{th2} = 0.00$

$U_{th3} = 0.00$

$U_{th4} = 0.00$

and so for fatigue usage:

$U = U_{tr} + U_{thl} + U_{th2} + U_{th3} + U_{th4} < +0.00$

APPENDIX 2.11.4

Comparison of Closed Form Solutions with Finite Element Analysis Results

In this Appendix, the finite element analysis results from some of the drop conditions are In this Appendix, the finite element analysis results from some of the drop conditions are compared to hand calculations based on closed form solutions. This is done for regions at the top of the basket which show high stresses under the conditions of one foot drop, transportation shock and vibration, and the bottom-on drop from thirty feet. Referring to Figure 2.15, said critical regions are encompassed by Elements 4814 and 5601. Element 4814 also shows high stresses under the drop on top from thirty feet.

Below, selected components of finite element analysis stress from the LIBRA code outputs which are presented in Tables 2.23 through 2.23 are used. The values in these Tables are for the geometric constraint and loading configurations of the cases indicated. However, these values are for an acceleration magnitude of 1G. Therefore they need to be scaled by the appropriate number to get stresses for the actual loading; e.g., for a 1 foot drop on the bottom the numbers in Table 2.21 need to be multiplied by 69 to reflect the effect of a 69 G loading environment for this drop.

Stresses at the centroids or integration points of said elements are compared to hand calculations which use closed form solutions. The components of the finite element analysis stress, namely the x, y, and z components of normal stress presented in Tables 2.21 through 2.23 correspond to the global x, y, and z axes, respectively, at the centroids and integration points of said elements. For the cylindrical portion of the basket, these x, y, and z components are the radial, longitudinal, and hoop components, respectively; and are designated "SIG-1", "SIG-2", and "SIG-3" in these tables.

2.11.4.1 Comparisons for the Uppermost Cylindrical Portion of the Basket (Element 5601)

For vertical accelerations, the y-component (longitudinal) stress at this element is found from

$$\sigma_y = \frac{P}{A} \qquad \text{(A2.11.4.1)}$$

where

A = cross sectional area
P = net vertical force supported by this cross sectional area, and
$P = WG$ (A2.11.4.2)

and

G = magnitude of acceleration (in G's)
W = net weight supported by this cross sectional area.

Using finite element analysis results the average value of σy for this element (see "AVE" value rows under heading "SIG-2" in Tables 2.21 and 2.23) which represents the membrane longitudinal (y-component) normal stress at the center of this element is compared to hand calculations based on Equations A.2.11.4.1 and A.2.11.4.2. The results are shown, for the cases of 1 foot and 30 feet drops on bottom, in Table 2.24. As shown, these values show good comparison.

2.11.4.2 Comparisons for the Cylindrical Portion of the Basket Below the Highest Cooling Fin (Element 4814)

For vertical accelerations the y-component (longitudinal) stress at this element is found from Equation A2.11.4.1 as was done in subsection A2.11.4.1.

Using finite element analysis results, the average value of σy for this element (see "AVE" value rows under heading "SIG-2" in Tables 2.21 through 2.23), which represents the membrane longitudinal (y-component) normal stress at the center of this element, is compared to hand calculations based on Equations A.2.11.4.1 and A.2.11.4.2. The results are presented, for the cases of 1 foot and 30 feet drops on bottom and 1 foot drop on top, in Table 2.25. As shown, these values show good comparison for all of the three cases of loading shown.

Element 4814 is located at the upper end of a cylindrical section of the basket which as shown in Figure 2.13 can be thought of as a 2-inch-long cylinder being bordered at its top and bottom by cooling fins that prevent this cylindrical section from expanding or contracting in the radial direction at its top and bottom junctures with these fins. This geometric attribute will induce secondary shell bending stresses (Figure 2.14) which attenuate with increasing distance, in the longitudinal direction, away from the position of the radial constraints.

Hence, to also compare hand calculated secondary bending stresses of localized nature with finite element analysis results, the closed form solutions for displacements, moments, and stresses of thin walled cylinders subjected to a radial line load as shown in Figure 2.14, or a radial constraints see [2.10], (Table 30) are utilized.

The relationship between the magnitude of radial displacement and the radial line load is (see Table 30, Case 15 in [2.10]):

$$y = \frac{-p}{8D\lambda^3} e^{-\lambda x} (\cos \lambda x + \sin \lambda x) \qquad \text{(A2.11.4.3)}$$

where

$$D = \frac{Et^3}{12\left(1-\nu^2\right)} \qquad \text{(A2.11.4.4)}$$

$$\lambda = \left[\frac{3\left(1-\nu^2\right)}{Rt^2}\right]^{\frac{1}{4}} \qquad \text{(A2.11.4.5)}$$

and

y = radial displacement
p = magnitude of radial line load
x = position relative to (longitudinal distance from) the location of the line load
E= modulus of elasticity
t = wall thickness, for the cylinder
ν = Poisson's ratio
R= average radius = the average of the inner and outer radii, $(R_i + R_o)/2$.

The shell bending moment, per (on a) unit width, is given by (see Table 30, Case 15 in [2.10]):

$$M = \frac{p}{4\lambda} e^{-\lambda x}(\cos \lambda x + \sin \lambda x) \qquad \text{(A2.11.4.6)}$$

and the shell extreme fiber longitudinal bending stresses are:

$$\sigma_{l,b} = \frac{-6M}{t^2} = \frac{-3p}{2\lambda t^2} e^{-\lambda x}(\cos \lambda x + \sin \lambda x) \qquad \text{(A2.11.4.7)}$$

and the shell extreme fiber hoop bending stresses are:

$$_{h,b} = \nu\, \sigma_{l,.b} \qquad \text{(A2.11.4.8)}$$

These shell bending stresses are superimposed onto the membrane hoop and longitudinal stresses. The longitudinal membrane stress was given by Equation A2.11.4.1 (in this case, $\sigma_y = \sigma_{l,m}$), and the equation for the hoop membrane stress is

$$\sigma_{h,m} = yE/R \qquad \text{(A2.11.4.9)}$$

Referring to Figure 2.13, any axial tension in cylindrical wall would cause a longitudinal strain of

$$\varepsilon_{l,m} = \frac{\sigma_{l,m}}{E} = \frac{\sigma_y}{E} \qquad \text{(A2.11.4.10)}$$

which would lead to, due to the Poisson effect, a hoop strain of

$$\varepsilon_{h,m} = -\nu\ \varepsilon\sigma_{l,m} \qquad \text{(A2.11.4.11)}$$

and a resulting radial contraction of magnitude

$$\delta_r = R\ \varepsilon_{h,m} \qquad \text{(A2.11.4.12)}$$

However, the cooling fins provide radial restraint and prevent this radial contraction at their juncture with the cylinder, and therefore induce the shell bending and associated stresses.

The basis for using Equations A2.11.4.3 through A2.11.4.3.9 is the assumption that there is no shell longitudinal bending at the junctures of the cooling fins. This is for practical purposes a good assumption for the load cases discussed.

Because of the principle of superposition, the problem at hand is similar to accounting for the effects of two radial constraints which are two inches apart. However, we proceed by examining the effect of inducing a line load at x=0 while at x=I~2 inches there is a radial constraint (which is half of our problem). The solution to this problem is broken down into steps as follows: 1) find the solution for this loading; then find the displacement y(L) and rotation Ψ(L) at the location of the constraint as if this constraint was absent (using Equations A2.11.4.3 through A2.11.4.5); 2) because the constraint at x = 2 inches is present, the solution to an induced displacement and rotation at this constraint needs to be superimpose on the solution obtained in (1) to satisfy the boundary condition imposed by this constraint, hence, find the solution to inducing a displacement and rotation equal but opposite in sign to that found in (1) at the location of the constraint; 3) superimpose the solutions of (1) and (2) to obtain the final solution to the problem.

To demonstrate what the relative influence of these two solutions in (1) and (2) are, we proceed as follows: for our cylindrical shell of element 4814

R = 5.44 in.
t = 0.25 in.

If a line load of 1.456 lbs/in. causing a displacement of 3.22E-6 in. is imposed, we find by using Equations A2.11.4.3 through A2.11.4.3.7 that the ratio of displacements and longitudinal bending stresses at x=0 to those at x=2 in. are 0.02 and 0.15, respectively. It is obvious that if the solution of (2) is ignored the error on radial displacement y and longitudinal stress using only the solution of (1) shall be on the order of (.o2)2 = 0.0004, and $(0.15)^2$ = 0.02, respectively, in the vicinity of x=0 Hence only the solution of (1) is used.

It is also pointed out that the basket has, for the purpose of stress analysis by hand, a complicated geometry which can dictate a more complex problem definition for the assumed deformation phenomenon. For these more complex conditions, classical closed form solutions may not exist, dictating a hybrid approach using linear superposition of closed form solutions and systems of equations in a matrix form to deal with the necessary statically indeterminate problem at hand (which is more cumbersome than finite element analysis). This complexity depends not only on the geometry, but also on the nature of the loading. Hence, for the geometry at hand, loading conditions do play an important role. Some times, however, for the stresses of interest the loading conditions at hand enforce such a high complexity. The closed form solutions and approach presented here are simply a tool for getting reasonable approximations for the secondary stresses only for the specific loading conditions applied to in this subsection. They are not claimed to be a general procedure for accurately calculating these stresses (at the locations discussed) under any conditions of loading, nor should they be used as such. The cases selected here had to be from those specifically showing high stresses, and not from those which rendered conditions conducive to accurate hand calculations by available closed form solutions.

The following procedure is used for calculating the secondary stresses in this subsection: a) the longitudinal (axial) membrane stress is calculated using Equation A2.11.4.1; b) the applicable radial contraction or expansion due to the radial restraint of the cooling fins are calculated using Equations A2.11.4.10, through A2.11.4.12; c) the solution to applying the radial constraints calculated in (b) (using of course the solution of (1) from the discussion in the previous four paragraphs) at the junctures of the cylindrical shell with the top and bottom cooling fins (Figure 2.13) are found using Equations A2.11.4.3, through A2.11.4.9 and superimposed.

Referring to Figures 2.13 and 2.15, the primary and secondary stress components for Gauss points 3 and 4 of Element 4814 are calculated using Equations A2.11.4.3 through A2.11.4.3.9 and compared to the finite element analysis results.

These Gauss points are located vertically 0.211 in. below the bottom surface of the top cooling fin of Element 4814 which can be seen in Figures 2.13 and 2.15. Hence x = 0.211 in. is used in Equations A2.11.4.3, A2.11.4.6, and A2.11.4.3.7. These gauss points (3 and 4) are also located, radially, within the 0.25 in. thick cylindrical wall of the basket; specifically, (0.211)(0.25 in.)=0.05275 in. from the inner and outer surface of this cylindrical wall (see Figures 2.13, 2.15, and the design drawing of Appendix 1.3.2). Therefore, because the shell bending stresses vary linearly through the wall thickness, the stresses calculated by Equations A2.11.4.7 and A2.11.4.3 are scaled by the ratio

$$z = \frac{(0.5 - 0.211)}{0.5} = 0.578$$

before comparison with the finite element analysis results. Where 0.5 and 0.211 designate the relative distance (in fractions of the total shell thickness), respectively, of the centroid (neutral axis) of the shell, and the Gauss point locations, from the outer surface of the shell.

The comparison between the hand calculations and the finite element analysis results for the combined membrane and shell bending longitudinal stresses (ksi) arising from two different loading conditions, are presented in Table 2.26.

The comparison between the hand calculations and the finite element analysis results for the combined membrane and shell bending hoop stresses (ksi) for the one foot drop on top loading case are presented in Table 2.27.

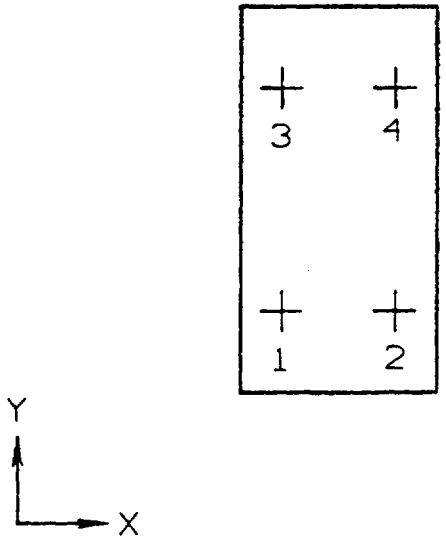

GAUSS POINTS

GAUSS POINTS FOR ELEMENT 4814

	1	.53728E+01 .53211E+02
	2	.55172E+01 .53211E+02
	3	.53728E+01 .53789E+02
COORDINATES:	4	.55172E+01 .53789E+02

GAUSS POINTS FOR ELEMENT 5601

	1	.55403E+01 .57211E+02
	2	.57597E+01 .57211E+02
	3	.55403E+01 .57789E+02
	4	.57597E+01 .57789E+02

EL	PT	SIG-1	SIG-2	TAU	SIG-3
4814	1	.18916E+01	.36786E+02	.31094E-01	.10350E+02
4814	2	.18738E+00	.30250E+02	-.11724E+01	.76042E+01
4814	3	-.11960E+01	.38626E+02	-.13246E+01	.61671E+01
4814	4	.22718E+00	.28674E+02	.15891E+01	.34265E+01
4814	AVE	.27760E+00	.33584E+02	-.21919E+00	.68869E+01

EL	PT	SIG-1	SIG-2	TAU	SIG-3
5601	1	-.19253E+01	-.32571E+01	.14208E+02	.75911E+02
5601	2	-.33544E+01	.52374E-02	.91834E+01	.87904E+02
5601	3	-.68606E+01	-.90337E+02	.10216E+02	.62332E+02
5601	4	.19990E+02	.13635E+03	.31063E+02	.13378E+03
5601	AVE	.19624E+01	.23783E+02	.16167E+02	.89981E+02

Table 2.21. LIBRA Finite Element Output for the 1-ft Drop on Bottom; 1G Loading

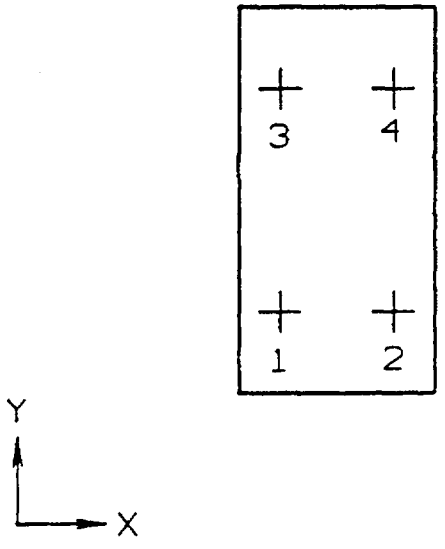

GAUSS POINTS

GAUSS POINTS FOR ELEMENT 4814

	1	.53728E+01	.53211E+02
	2	.55172E+01	.53211E+02
	3	.53728E+01	.53789E+02
COORDINATES:	4	.55172E+01	.53789E+02

EL	PT	SIG-1	SIG-2	TAU	SIG-3
4814	1	-.21417E+01	-.59493E+02	-.15668E+01	-.22376E+02
4814	2	.66067E+00	-.54759E+02	.92392E+00	-.19420E+02
4814	3	.33591E+01	-.48744E+02	.11919E+01	-.14789E+02
4814	4	-.41618E+01	-.65442E+02	-.58454E+01	-.21445E+02
4814	AVE	-.57093E+00	-.57110E+02	-.13241E+01	-.19508E+02

Table 2.22. LIBRA Finite Element Output for the 1-ft Drop on Top; 1G Loading

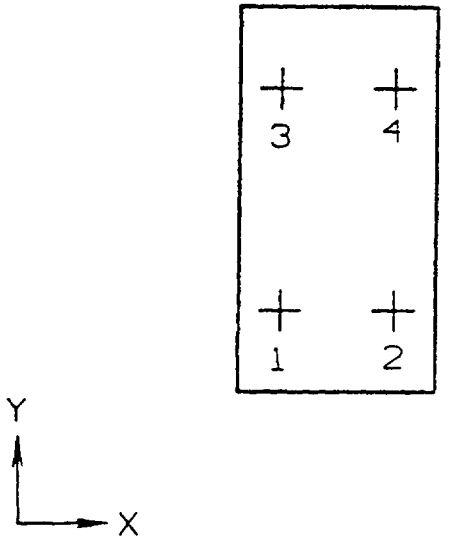

GAUSS POINTS

```
                GAUSS POINTS FOR ELEMENT 4814
                    1      .53728E+01      .53211E+02
                    2      .55172E+01      .53211E+02
                    3      .53728E+01      .53789E+02
COORDINATES:        4      .55172E+01      .53789E+02

                GAUSS POINTS FOR ELEMENT 5601
                    1      .55403E+01      .57211E+02
                    2      .57597E+01      .57211E+02
                    3      .55403E+01      .57789E+02
                    4      .57597E+01      .57789E+02
```

EL	PT	SIG-1	SIG-2	TAU	SIG-3
4814	1	.21428E+01	.48904E+02	.57596E+00	.15129E+02
4814	2	-.11258E+00	.42441E+02	-.11559E+01	.12080E+02
4814	3	-.20085E+01	.46435E+02	-.13782E+01	.95979E+01
4814	4	.15803E+01	.45061E+02	.31920E+01	.99186E+01
4814	AVE	.40049E+00	.45710E+02	.30846E+00	.11681E+02

EL	PT	SIG-1	SIG-2	TAU	SIG-3
5601	1	-.19494E+01	.45121E+01	.14417E+02	.75936E+02
5601	2	-.33269E+01	.60020E+02	.92658E+01	.87906E+02
5601	3	-.70162E+01	-.83433E+02	.10009E+02	.62655E+02
5601	4	.20452E+02	.14483E+03	.31610E+02	.13473E+03
5601	AVE	.20399E+01	.31482E+02	.16325E+02	.90307E+02

Table 2.23. LIBRA Finite Element Output for the 30-ft Drop on Bottom; 1G Loading

Table 2.24. Comparison of Longitudinal Membrane Stresses (ksi), EL 5601

	FEA	Hand Calc Eq A2.11.4.1	Difference
1 ft drop on bottom	1.64	1.73	-5%
30 ft drop on bottom	4.19	4.37	-4%

Table 2.25. Comparison of Longitudinal Membrane Stresses (ksi), EL 4814

	FEA	Hand Calc Eq A2.11.4.1	Difference
1 ft drop on bottom	2.32	2.31	0%
1 ft drop on top	3.94	3.94	0%
30 ft drop on bottom	6.08	6.07	0%

Table 2.26. Comparison of Combined Membrane and Local Shell Bending Longitudinal Stresses (ksi), EL4814

	FEA	Hand Calc Eq A2.11.4.3 thru A2.11.4.9	Difference
1 ft drop on top			
Near inner sfc	-3.36	-3.44	-2%
Near outer sfc	-4.52	-4.44	2%
30 ft drop on bottom			
Near inner sfc	6.18	6.85	-10%
Near outer sfc	5.99	5.29	13%

Table 2.27. Comparison of Combined Membrane and Local Shell Bending Hoop Stresses (ksi), EL4814

	FEA	Hand Calc Eq A2.11.4.3 thru A2.11.4.9	Difference
1 ft drop on top			
Near inner sfc	-1.02	-1.06	-4%
Near outer sfc	-1.48	-1.37	8%

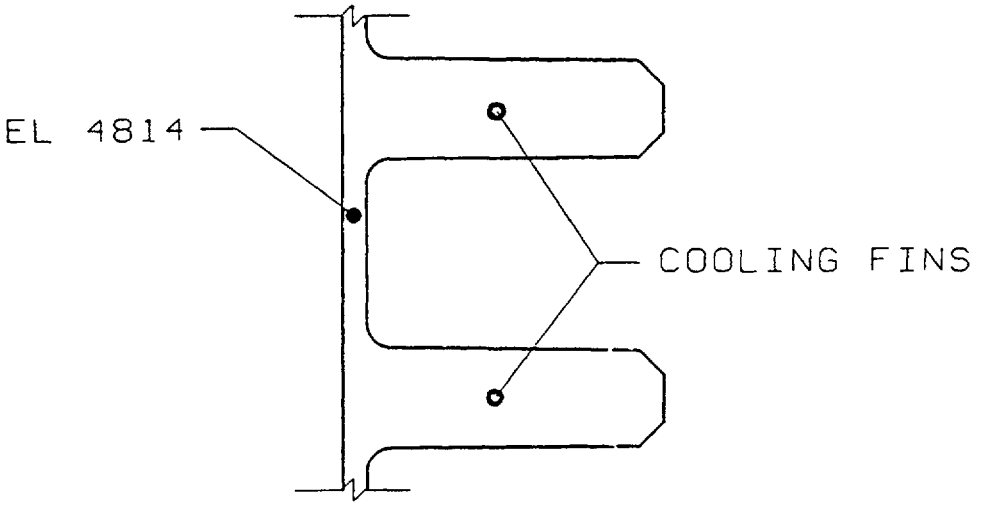

Figure 2.13. Highest Two Cooling Fins of the Basket and Position of Element 4814 on the Cylindrical Portion

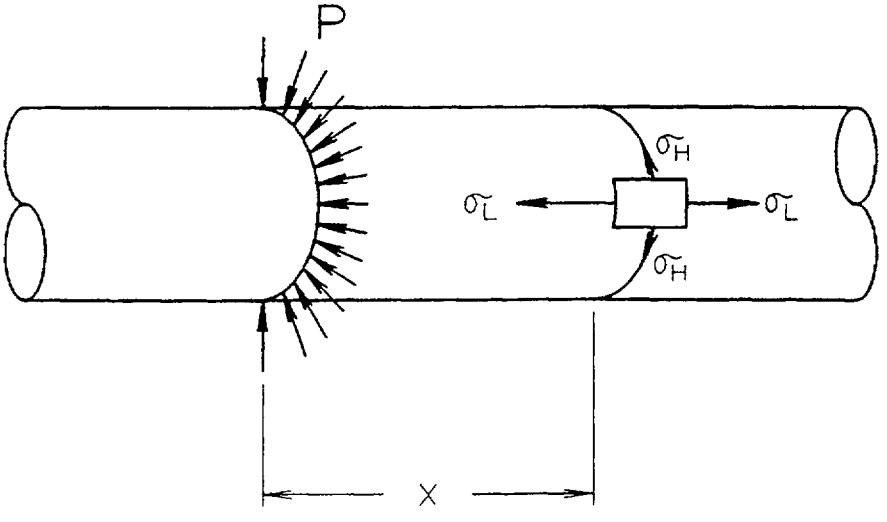

Figure 2.14. Secondary Shell Bending Stresses Arising from Radial Line Loading On a Thin Walled Cylinder

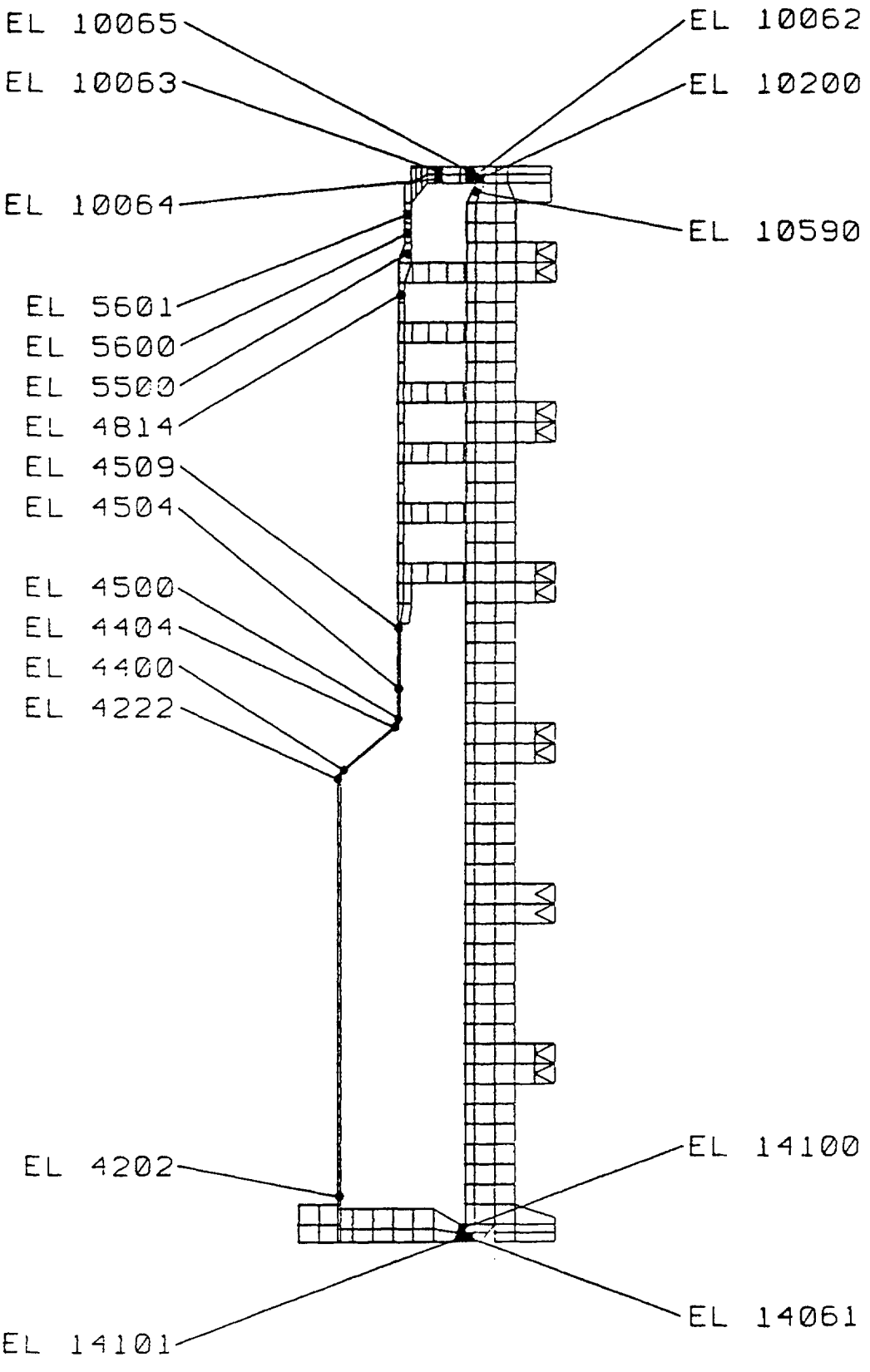

Figure 2.15. Elements of Highest Stress

APPENDIX 2.11.5

Optional Lifting Ear Analysis

This analysis demonstrates the structural integrity of the Optional Lifting Ears (hereinafter called Ears) on the Model 2000 Shielded Shipping Cask.

2.11.5.1 Design Criteria. The regulations require that lifting devices that are a structural part of the package shall be capable of supporting three tones the weight of the loaded package without generating stress in any material of the package in excess of its yield strength.

Material Properties are based on 218 °F, the maximum normal condition temperature. The Ears are fabricated from type 304 stainless steel forgings, ASME SA182. The cask outer shell is type 304 stainless steel, ASME SA240. The attaching screw material is ASTM A193-B6. Properties for these three materials [2.6] are summarized in Table 2.28.

Material Properties (at 218°F)	**Ear, SA182**	**Shell, SA240**	**Screw, A193-B6**
Elastic Modulus, E (x 10^6 psi)	27.5	27.5	28.7
Yield Strength, S_y (ksi)	24.6	24.6	85.0
Ultimate Strength, S_u (ksi)	70.1	70.1	110.0
Allowable Stresses (at 218°F)			
Normal Stress, σ_a (ksi)	24.6	24.6	85.0
Shear Stress, τ_a (ksi)	14.3	14.3	49.3

Table 2.28. Material Properties and Allowable Stresses

2.11.5.2 Load Analysis. The design rated load (W) is 23750 pounds. This includes the dead weight of the cask (body, lid, Ears) and the cask payload, including the optional liner.

The Ears are used in pairs for overhead crane lifts of the Model 2000 Cask [2.14]. The applied load (F) on each Ear is determined by dividing the weight of the cask and contents by the number of Ears, and multiplying the result by 3 (per Design Criteria). Figure 2.16 illustrates the loading condition.

$$F = \left(\frac{3W}{N} \right)$$

W= 23,750 lb

N= 2 Ears

F= 35,625 lb

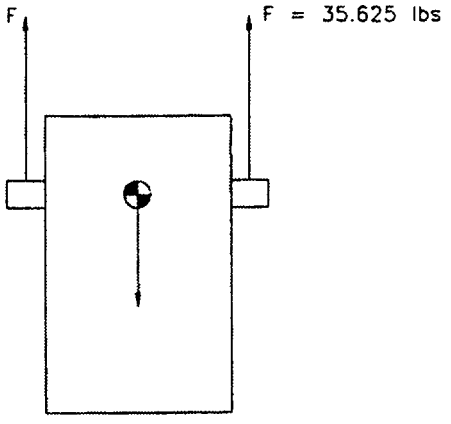

Figure 2.16. Loading Configuration

2.11.5.3 Ear Geometry. The Ear is a one-piece part machined from a SA182 type 304 stainless steel forging. The overhead crane lift hooks contact the Ear along the lower surface of the cylindrical section, as shown in Figure 2.17. Four attachment screws fasten the Ear to the cask outer shell. The screw heads are countersunk below the surface of the Ear's base, providing clearance for the crane hook to engage the Ear without interference. In order to use the existing cask mounting holes, four relief slots are machined in the cylindrical portion of the Ear.

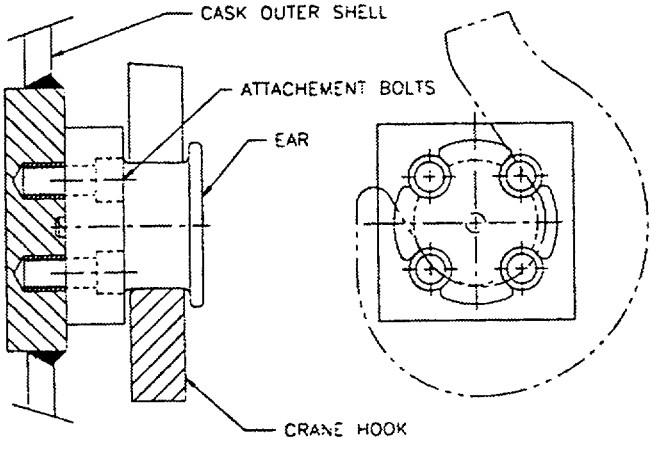

Figure 2.17. Ear Geometry

2.11.5.4 Design Evaluation. Several failure modes are investigated for the Ear design. These are:

A. Yielding of Ear
B. Bearing stress of crane hook on Ear
C. Yielding of attachment screw
D. Shearing of screw threads
E. Shearing of tapped hole threads
F. Yielding of cask outer shell

A. Yielding of Ear

The maximum Ear stresses are expected to be a combination of shear- and bending-stresses located at the point where the cylindrical portion of the Ear intersects the base portion. This point is indicated as "A" in Figure 2.18. As the screw slots in the Ear complicate the geometry with respect to the stress analysis, a conservative simplified geometry is examined as a substitute for the cylindrical section of the Ear. This simplified geometry is shown in Figure 2.19. The simplified geometry consists of a rectangular bar whose length is equal to the length of the cylindrical section of the Ear plus the countersink depth of the screw holes. The height and width of the bar are determined by the largest rectangle that fits in the cross-section of the cylindrical Ear section.

Section properties of the simplified geometry are as follows:

Area, A

$$A = BH \qquad \text{where} \quad B = 1.875$$
$$A = 8.183 \text{ in}^2 \qquad H = 4.364$$

Moment of Inertia, I

$$I = \frac{1}{12} BH^3$$
$$I = 12.99 \text{ in}^4$$

Outer Fiber Distance, C

$$C = \frac{H}{2}$$
$$C = 2.182 \text{ in.}$$

Calculate bending and shear stresses:

$$\tau = \frac{F}{A}$$
$$\tau = \frac{35625}{8.183} = 4354 \text{ psi}$$

Maximum Bending Moment, M = FL = 35625(2.31) = 82,294 in-lb

$$\sigma_B = \frac{MC}{I}$$

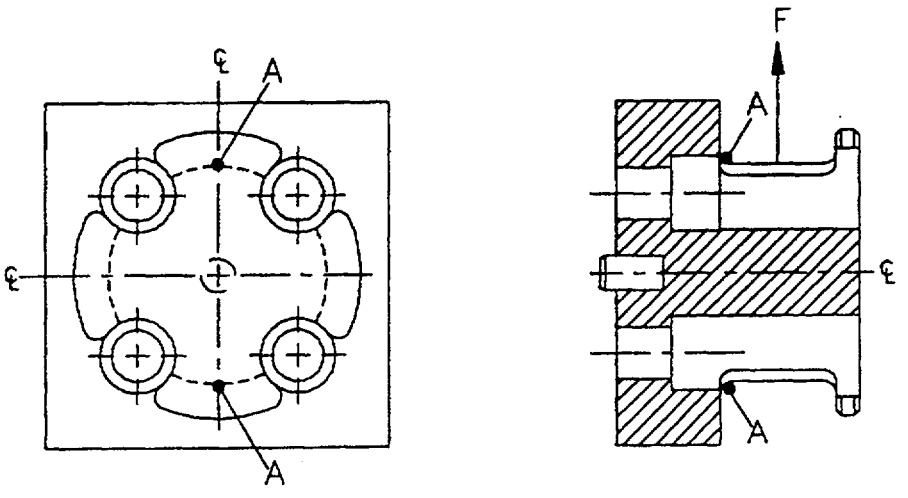

Figure 2.18. Location of Maximum Bending Stress, Actual Design

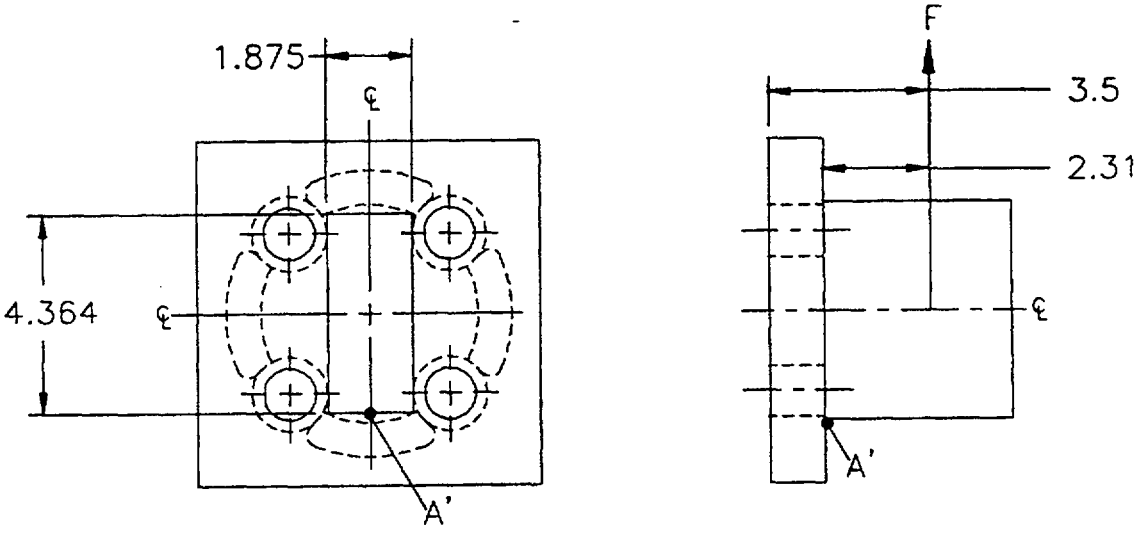

Figure 2.19. Location of Maximum Bending Stress, Simplified Design

$$\sigma_B = \frac{82{,}294(2.182)}{12.99} = 13{,}823\,\text{psi}$$

Using the shear and bending stresses, calculate the principal stresses at A', which is at least as great as the stress at A:

Tensile bending at A'

$$\sigma_{max,min} = \frac{\sigma_x + \sigma_y}{2} \pm \sqrt{\left(\frac{\sigma_x - \sigma_y}{2}\right)^2 + \tau_{xy}^{\ 2}} \qquad \tau_{xy} = \tau$$

$$\sigma_x = \sigma_B$$

$$\sigma_y = 0$$

$$\sigma_{max,min} = \frac{13{,}823}{2} \pm \sqrt{\left(\frac{13{,}823}{2}\right)^2 + 4354^2}$$

$$\sigma_{max,min} = 6911 \pm 8169\,\text{psi}$$

σ_{max} = **15,080 psi** **Allowable = 24,600 psi**

σ_{min} = −1258 psi

τ_{max} = **8169 psi** **Allowable = 14,300 psi**

Compressive bending at A'

$$\sigma_{max,min} = \frac{-13{,}823}{2} \pm \sqrt{\left(\frac{-13{,}823}{2}\right)^2 + 4354^2}$$

$$\sigma_{max,min} = -6911 \pm 8169\,\text{psi}$$

σ_{max} = 1258 psi

σ_{min} = **−15,080 psi** **Allowable = 24,000 psi**

B. Bearing stress of crane hook on Ear

The bearing stress is computed assuming the force is uniformly distributed over the projected contact area of the simplified beam. The stress is

$$\sigma = \frac{F}{A} \qquad A = tB$$

where t is the crane hook width (2.0 inch) and B is the beam width (1.875 inch).

$$\sigma = \frac{35{,}625}{(2)(1.875)} = \mathbf{9500\ psi} \qquad \mathbf{Allowable = 24{,}600\ psi}$$

C. Yielding of Attachment Screws

Bolt and thread section properties used in the following analyses for both internal and external threads are evaluated for a standard 1-8 UNC x 2-1/2 socket head cap screw. The tensile stress area A_t for a high strength screw with $\sigma_{ultimate} > 100$ ksi [2.15]:

$$A_t = \pi\left(\frac{E_{s,min}}{2} - \frac{0.16238}{n}\right)^2$$

where $E_{s,min}$ minimum pitch diameter = 0.9188 inch
n = number of threads per inch = 8

$$A_t = \pi\left(\frac{0.9188}{2} = \frac{0.16238}{8}\right)^2 = 0.606 in^2$$

The screw preload, F_i, should be between 60% and 80% of the proof load [2.16]. The proof load is 85% of the yield strength multiplied by the tensile stress area. Therefore, using 80% of the proof load, the preload is:

$$F_i = 0.80\left(0.85 S_y A_t\right) = 0.80(0.85)(85)(0.606) = 35.03 kip$$

The tightening torque for a lubricated bolt is:

$T = KF_id$ where T = torque
K = torque coefficient = 0.2
d = bolt nominal diameter = 1.0

T = 0.2(35,030)(1.0) = 7006 in – lb [583 ft – lb]

Note that a torque value of 600 ft-lb, which corresponds to a preload of 36,000 lb, is specified by the Model 200 certification drawing [2.14]. Consequently, further calculations will use 36,000 as the torque preload value:

$$F_i = \frac{(600 ft - lb)(12 in/lb)}{(0.2)(1.0 in)} = 36000 lb$$

The applied moment M produced by the lifting condition is:

M = 35,625(3.5) = 124,688 in-lb

The tensile stress σ_{tb} at the bottom of the contact area due to the applied moment is:

$$\sigma_{tb} = \frac{M^d / _2}{I} = \frac{6M}{bd^2}$$

where b and d are the base and height dimensions of the contact area. The tensile load on the screw, F_{tb} is the tributary area A_{tb} of each fastener multiplied by σ_{tb}:

$$F_{tb} = \sigma_{tb} A_{tb}$$

$$F_{tb} = \frac{6M}{bd^2} A_{tb}$$

A_{tb} for one screw is

$$A_{tb} = (7.5)(7.5)/4 = 14.06\,\text{in}^2/\text{screw}$$

Then

$$F_{tb} = \frac{6(124{,}700)(14.06)}{(7.5)(7.5)^2} = 24{,}940\,\text{lb}$$

Determine bearing stress between the Ear and cask due to the torque preload:

$$\sigma_{bi} = \frac{(\#\text{screws})(F_i)}{\text{contact area}} = \frac{4(36000)}{7.5^2}$$

$$\sigma_{bi} = 2560\ \text{psi}$$

The initial bearing pressure, σ_{tbi}, is assumed to be uniform over the contact area. Check that the bearing pressure is not be exceeded by the tensile stress, σ_{tb}.

$$\sigma_{tb} = \frac{F_{tb}}{A_{tb}} = \frac{24{,}940\,\text{lb}}{14.06\,\text{in}^2} = 1774\,\text{psi}$$

$$\sigma_{bi} > \sigma_{tb}$$

The actual stress state in the screws is a function of both the torque preload and the applied load, and depends on the relative stiffness of the screws and the joint members. Determine the screw stresses with consideration for the distribution of the applied load between the screw and the member [2.17]:

Calculation of Screw Spring Constant (k_b)

Major Dia.:	d	=	1.000 in
Length:	l	=	1.125 in
Major Dia. Area:	A_d	=	0.785 in^2
Tensile Stress Area:	A_t	=	0.606 in^2
Threaded Grip Length:	l_t	=	1.125 in
Un-Threaded Grip Length:	l_d	=	0
Modulus of Elasticity:	E	=	28.7×10^6 psi
Bolt Stiffness Constant:	k_b	=	$A_d A_t E/(A_d l_t + A_t l_d) = 1.546 \times 10^7$ lb/in

Calculation of Member Spring Constant (k_m)

Bolt Hole Dia.:	d_b	=	1.125 in
Modulus of Elasticity:	E	=	27.5×10^6 psi

Assume: Half-Apex Angle = 30°, Head Contact Dia. = 1.5 d

Member Stiffness Constant: $$k_m = \frac{0.577(\pi E d_b)}{2\ln\left((5)\frac{0.577l_t + 0.5d_b}{0.577l_t + 2.5d_b}\right)}$$

Calculation of Joint Constant (C)

Joint Constant: $$C = \left(\frac{k_b}{k_b + k_m}\right) = 0.236$$

Calculation of Screw Loading

Applied preload:	Fi	=	36.00 kip
Maximum Tensile Load:	F_{tb}	=	24.94 kip

Screw tensile stress: $$\sigma_b = \frac{CF_{tb}}{A_t} + \frac{F_i}{A_t} = \mathbf{69{,}120\ psi}$$

Screw shear stress: $$\tau_b = \frac{F}{(\#\text{screws})(A_t)}$$

$$t_b = \frac{35625}{(4)(0.606)} = \mathbf{14{,}700\ psi}$$

Principle screw stresses

$$\sigma_{max,min} = \left(\frac{\sigma_b}{2}\right) \pm \sqrt{\left(\frac{\sigma_b}{2}\right)^2 + \tau_b^2}$$

$$\sigma_{max,min} = \frac{69.12}{2} \pm \sqrt{\left(\frac{69.12}{2}\right)^2 + 14.7^2}$$

$$\sigma_{max,min} = 34,600 \pm 37,600 \text{ psi}$$

σ_{max} = **72,200 psi** **Allowable = 85,000 psi**

σ_{max} = **37,600 psi** **Allowable = 49,300 psi**

The interaction equation for the strength of a connection with bolt in combined shear and tension may be approximated by the elliptical relationship:

$$\left(\frac{\sigma_b}{\sigma_y}\right)^2 + \left(\frac{\tau_b}{0.6\sigma_y}\right)^2 \leq 1.0$$

$$\left(\frac{69.12}{85}\right)^2 + \left(\frac{14.70}{0.6(85)}\right)^2 \leq 1.0$$

$0.744 \leq 1.0$ $\therefore$ The selected screws are adequate.

Screw Fatigue Analysis

The maximum cyclic stress is due to a combination of the tensile stress and the shear stress. A fatigue strength reduction factor of 4.0 is to be used [2.18]. Since the fatigue curve [2.19] is based on a modulus of elasticity of 30E6 psi, the stress range is given by:

S = (72.2 ksi)(4.0)[30E6/28.73E6] = 301.6 ksi

To select the correct fatigue curve, the stress intensity value S_m must be determined [2.20]. For a temperature of 218°F, the value is 26.84 ksi.

By calculating the alternating stress S_a:

S_a = S/2 = 301.6/2 = 150.8 ksi

and using the fatigue curve for a maximum nominal stress ≤2.7 S_m, the fatigue limit is ≈450 cycles. Assuming an average of four lifts per usage and 12 usages per year, this gives a screw life of:

$$\text{screw life} = \frac{(450\,\text{cycles})}{(12\,\text{usages/year})(4\,\text{cycles/usage})} = 9.4\ \text{years}$$

D. Shearing of screw threads

The shear area of the external (A_s) threads:

$$A_s = \pi n L_e k_{n,max}\left[\frac{2}{2n} + 0.57735\left(E_{s,min} - k_{n,max}\right)\right]$$

where L_e = length of engagement = 1.680 inch

$k_{n,max}$ = Maximum internal thread diameter = 0.8795 in

$$A_s = \pi(8)(1.680)(0.8795)\left[\frac{1}{2(8)} + 0.57735(0.9188 - 0.8795)\right] = 3.163\,\text{in}^2$$

The shearing stress of screw threads is:

$$\tau = \frac{F_b}{A_s} = \frac{\sigma_b A_t}{A_s} = \frac{(69.12)(0.606)}{3.163} = \mathbf{13{,}243\ psi} \quad \mathbf{Allowable = 49{,}300\ psi}$$

E. Shearing of tapped hole threads

The shear area of the internal (A_n) threads:

$$A_n = \pi n L_e D_{s,min}\left[\frac{1}{2n} + 0.57735\left(D_{s,min} - E_{n,max}\right)\right]$$

where $D_{s,min}$ = Minimum external thread major diameter = 0.9848 in.

$E_{n,max}$ = Maximum internal thread pitch diameter = 0.9242 in.

$$A_n = \pi(8)(1.680)(0.9848)\left[\frac{1}{2(8)} + 0.57735(0.9848 - 0.9242)\right] = 4.054\,\text{in}^2$$

The shearing stress of tapped hole threads is:

$$\tau = \frac{F_b}{A_n} = \frac{\sigma_b A_t}{A_n} = \frac{(69.12)(0.606)}{4.054} = \textbf{10,332 psi} \quad \textbf{Allowable = 49,300 psi}$$

F. Yielding of cask outer shell

An analysis for yielding of the cask outer shell is not necessary for the Optional Ear, as the loading conditions the Ear applies to the cask is lower in magnitude than for the Standard Ear (Load Condition I, [2.3]). Specifically, since the design rated load is the same for both configurations, the only difference in the two Ears with respect to the applied cask loading is the moment arm length: For the Standard Ear it is 4.0 inches and the Optional Ear is 3.5 inches. Thus the Optional Ear applies a smaller moment to the cask, while the other loads remain the same.

APPENDIX 2.11.6

HFIR Basket Lifting Arrangement

The HFIR basket [2.21] provides for an alternate lift arrangement. Three sets of equally spaced slots and holes are machined on the basket's top flange, allowing the basket with the inner fuel element to be lifted. The following analyses are made in support of the design.

2.11.6.1 Slot Geometry

Each slot in the 1.0 inch thick Basket Top Flange is 0.62 inch wide by 1.91 inch. Each hole is 0.62 inches in diameter.

2.11.6.2 Top Flange Stresses

A theoretical stress concentration factor is estimated from Shigley [2.17, Figure A-15-2]:

$$K_t \approx 2.2 \text{ for } \frac{d}{h} = 0.62 \text{ and } \frac{d}{w} \approx 0.1 \quad \text{where} \quad d = 0.62$$

$$h = 1.0$$

$$w \approx 6.5$$

Elements 10062, 10063, 10064, 10065, and 10200 [Figure 2.3] represent the basket top flange, with the lifting slots located near elements 10063 and 10064.

Using a stress concentration factor of 2.2, the maximum stress under normal transport (Tables 2.12 through 2.14) and hypothetical accident conditions (Tables 2.16 through 2.19) remains within the allowable values for all basket flange elements.

3.0 THERMAL EVALUATION

The thermal analyses of the Model 2000 Transport Package with the HFIR fuel are described in this Chapter. The design basis fuel elements have a maximum burnup of 2300 MWD with sufficient cooling period for a total design basis heat load of 2048 Btu/hr. This corresponds to a maximum decay power of 600 watts.

The thermal analyses assume that the cask cavity is dry and has one atmosphere of helium, which is the normal shipping mode. These analyses demonstrate that the Model 2000 Transport Package with the HFIR fuel positioned in the basket and liner provides suitable heat dissipation to maintain the temperature distribution of the Package within the limits established in the Package's Safety Analysis Report [3.1]. All thermal conditions are analyzed using the finite element computer code LIBRA under normal and accident conditions with the exception of the cold environment (-20°F and -40°F). In these cases, it is assumed that a uniform temperature field exists throughout the Package. Subsection 3.6.1 of Reference [3.1] includes the qualification and verification program performed to support the use of the LIBRA Code. Subsection 3.7.1 of this report discusses the result of the thermal test done to verify the LIBRA model used in these analyses.

3.1 DISCUSSION

The principal design operating and performance characteristics of the Model 2000 Transport Package with the HFIR fuel are within the limits previously established. The performance of the Package components are not affected by the HFIR fuel basket and liner.

3.1.1 Thermal Design Criteria

The maximum fuel cladding temperature for the design basis of the HFIR fuel is 400°F. At this temperature, the mechanical material properties of the aluminum are significantly changed. However, the basket and liner designs provides additional structural support to the HFIR fuel under the regulatory-prescribed loadings during transport. The design pressure of the Model 2000 Cask is 30 psia. Temperature limits established in the Model 2000 Package SAR [3.1] are:

For the cask seal area	≤400°F
Within the lead regions	≤600°F
Cask cavity	≤600°F
Exterior Package surface	≤180°F (shade)

3.1.2 Design Bases Conditions

Temperature distributions in the Model 2000 Transport Package with the HFIR fuel are evaluated for the following thermal environments:

1. Normal Operating Condition
   a) 100°F ambient temperature with maximum decay heat
   b) -20°F ambient temperature
   c) -40°F ambient temperature

2. Thermal Fire Accident
   a) 30 minutes after start of fire
   b) Post fire steady-state

3.1.3 Results of Design Basis Thermal Analyses

The analytical results obtained from evaluating the design basis conditions for the HFIR fuel in the model 2000 package are summarized in Table 3.1. They are based on the use of the thermal analysis modules of the LIBRA Code. The design cases 1(b) and 1(c) in Subsection 3.1.2 are not included in the table, since the package is assumed to be at uniform ambient temperatures at these conditions.

Table 3.1. SUMMARY OF TEMPERATURES

Package Component	Design Basis Thermal Condition Temperatures (°F)			Component Criteria (°F)
	1.a	2.a	2.b[1]	
Cask Cavity Surface	221	223	281	T < 600
Lead Shield	220	223	282	T < 600
Cask Seal Area	214	218	269	T < 400
Cask Test Port	213	243	272	T < 400
Cask Drain Port	215	283	338	T < 400
Cask Vent Port	216	217	255	T < 400
Cask Outer Surface	215	262	335	NA
Overpack Inner Surface	195	792	792	N/A
Overpack Accessible Outer Surface	175	1338	1338	T < 180 for 1(a)
Inner Fuel Element	253	250	298	T < 400
Outer Fuel Element	253	252	296	T < 400
Basket	238	237	281	T < 400
Liner	243	243	288	T < 400

(1) Values given are maximum temperatures obtained for each component during the fire transient and cooling down period.

3.2 SUMMARY OF THERMAL PROPERTIES OF MATERIALS

The transport package model consists of seven materials whose thermal properties are listed in subsections 3.2.1 to 3.2.7. The curve fit functions which give the variation of the properties with temperature are also given. These property functions are used in the transient analysis to update the material properties as the temperature changes.

3.2.1 Lead

Temp (°F)	k (Btu/hr-ft-°F) [3.2]	Thermophysical Properties	
		Cp(Btu/lb-°F) [3.3]	ρ(lb/in.^{3}) [3.4]
68.0	—	0.0305	0.4097
80.3	20.3	—	
158.0	—	0.0310	
170.3	20.1		
248.0	—	0.0316	
260.3	19.5		
338.0	—	0.0320	
428.0	—	0.0325	
440.3	18.8		
500.0	—	0.0329	
608.0	—	0.0334	
620.3	18.0	—	

Conductivity, k (Btu/hr-in.-°F)

$$k(T) = 1.7263 - 3.6418 \times 10^{-4} T \qquad 68.0°F < T < 620.3°F$$

Specific Heat, Cp (Btu/lb-°F)

$$Cp(T) = 3.0177 \times 10^{-2} + 5.3924 \times 10^{-6} T \qquad 68.0°F < T < 620.3°F$$

Density, ρ (lb/in.^{3})

$$\rho(T) = 0.41 \qquad 68.0°F < T < 620.3°F$$

3.2.2 Stainless Steel (304 Type)

Thermophysical Properties[3.5]		
Temp (°F)	**k(Btu/hr-ft-°F)**	**α(ft^2/hr)**
70	8.6	0.151
100	8.7	0.152
200	9.3	0.156
300	9.8	0.160
400	10.4	0.165
500	10.9	0.170
600	11.3	0.174
700	11.8	0.179
800	12.2	0.184
900	12.7	0.189
1,000	13.2	0.194
1,100	13.6	0.198
1,200	14.0	0.203
1,300	14.5	0.208
1,400	14.9	0.212
1,500	15.3	0.216

Conductivity, k (Btu/hr-in.-°F)

$$k(T) = 7.0287 \times 10^{-1} + 3.8987 \times 10^{-4}\, T \qquad 70°F < T < 1500°F$$

Thermal Diffusivity, α (in.^{2}/hr)

$$\alpha(T) = 21.110 + 6.7346 \times 10^{-3}\, T \qquad 70°F < T < 1500°F$$

Density, ρ (lb/in.^{3})

$$\rho(T) = 0.29 \qquad 70°F < T < 1000°F$$

Specific Heat, Cp (Btu/lb-°F)

$$Cp(T) = k(T)/\alpha(T)(\rho) = k(T)/(6.1219 + 1.953 \times 10^{-3}\, T) \qquad 70°F < T < 1000°F$$

3.2.3 Air

Temp (°F)	Thermophysical Properties[3.6]					
	ρ (lb/ft^3)	Cp (Btu/lb-°F)	μx10^{-5} (lb/ft-sec)	k(Btu/hr-ft-°F)	Pr	gβρ^2/μ^2
32	0.081	0.200	1.165	0.0140	0.76	3.16 x 10^6
100	0.071	0.240	1.285	0.0154	0.72	1.76
200	0.060	0.241	1.440	0.0174	0.72	0.850
300	0.052	0.243	1.610	0.0193	0.71	0.444
400	0.046	0.245	1.750	0.0212	0.689	0.258
500	0.0412	0.247	1.890	0.0231	0.683	0.159
600	0.0373	0.250	2.000	0.0250	0.685	0.106
700	0.0341	0.253	2.140	0.0268	0.690	70.4 x 10^3
800	0.0314	0.256	2.250	0.0286	0.697	49.8
900	0.0291	0.259	2.360	0.0303	0.705	36.0
1,000	0.0271	0.262	2.470	0.0319	0.713	26.5
1,500	0.0202	0.276	3.000	0.0400	0.739	7.45
2,000	0.0161	0.286	3.450	0.0471	0.753	2.84

Conductivity, k (Btu/hr-in.-°F)

$$k(T) = 1.1138 \times 10^{-3} + 1.6988 \times 10^{-6}\, T - 1.4993 \times 10^{-10}\, T^2 \qquad 32°F < T < 2000°F$$

Prandtl Number, Pr

$$Pr(T) = 0.72 \qquad 32°F < T < 200°F$$

$$Pr(T) = 0.603 + 1.3017 \times 10^{-3}\, T - 4.450 \times 10^{-6}\, T^2 + 4.3333 \times 10^{-9}\, T^3$$

$$200°F < T < 500°F$$

$$Pr(T) = 0.7793 - 4.6950 \times 10^{-4}\, T + 7.474 \times 10^{-7}\, T^2 - 4.2962 \times 10^{-10}\, T^3 + 8.5365 \times 10^{-19}\, T^4$$

$$500°F < T < 2000°F$$

Parameter, $g\beta\rho^2/\mu^2$ (1/°F-in.^{3})

$$g\beta\rho^2/\mu^2\,(T) = 2.4306 \times 10^3 - 21.484\,T + 8.8318 \times 10^{-2}\,T^2 - 1.4682 \times 10^{-4}\,T^3$$

$0°F < T < 200°F$

$$g\beta\rho^2/\mu^2\,(T) = 1.6610 \times 10^3 - 9.2850\,T + 2.1356 \times 10^{-2}\,T^2 - 2.268 \times 10^{-5}\,T^3 + 9.1329 \times 10^{-9}\,T^4$$

$200°F < T < 800°F$

$$g\beta\rho^2/\mu^2\,(T) = 1.8475 \times 10^2 - 3.2975 \times 10^{-1}\,T + 2.0129 \times 10^{-4}\,T^2 - 4.1096 \times 10^{-8}\,T^3$$

$800°F < T < 2000°F$

Specific Heat, Cp (Btu/lb-°F)

$$Cp(T) = 0.2386 + 8.8082 \times 10^{-6}\,T + 2.1375 \times 10^{-8}\,T^2 - 6.9784 \times 10^{-12}\,T^3$$

$100°F < T < 2000°F$

Density, ρ(lb/in.^{3})

$$\rho(T) = 5.787 \times 10^{-4}/(11.6125 + 2.527 \times 10^{-2}\,T) \qquad 32°F < T < 2000°F$$

3.2.4 Aluminum

HFIR Fuel Element Aluminum (Type 6061) Material

	Thermophysical Properties[3.7]		
Temp (°F)	**k (Btu/hr-in-°F)**	**Cp(Btu/lb-°F)**	**ρ(lb/in.^{3})**
0	—	0.195	
32	9.75	—	
77	—	—	0.0978
140	—	0.21	
212	9.92	—	
480	—	0.25	
572	11.08	—	
800	—	0.29	
932	12.29	—	

Thermal Conductivity (Btu/hr-in-°F)

$$k(T) = 9.74795 - 6.804 \times 10^{-5} T + 4.12 \times 10^{-6} T^2 + 1.143 \times 10^{-10} T^3$$

$$32°F < T < 932°F$$

Specific heat, Cp(Btu/lb-°F)

$$Cp(T) = 1.95 \times 10^{-1} + 1.11875 \times 10^{-4} T \qquad 0°F < T < 800°F$$

Density, ρ (lb/in^3)

$$\rho(T) = 0.098 \qquad 77°F < T < 600°F$$

3.2.5 Tungsten Alloy

The thermophysical properties of Tungsten Alloy [3.9] are considered constant throughout the analyses with the following values:

$k = 8.0$ Btu/hr-in-°F

$Cp = 0.0318$ Btu/lb-°F

$\rho = 0.70$ lb/in^3

3.2.6 Helium

	Thermophysical Properties[3.6]				
Temp (°F)	ρ(lb/ft^3)	Cp(Btu/ lb-°F)	k(Btu/ hr-ft-°F)	Pr	$g\beta\rho^2/\mu^2$ (1/°F-ft^3)
0	0.012	1.24	0.078	0.670	77800
200	0.0085	1.24	0.097	0.686	15600
400	0.0064	1.24	0.115	0.700	4840
600	0.0052	1.24	0.129	0.715	2010
800	0.0044	1.24	0.138	0.730	932

Thermal Conductivity (Btu/hr-in-°F)

$$k(T) = 0.00675 + 7.042E^{-6}T \qquad 0°F < T < 800°F$$

Prandtl Number, Pr

$$Pr(T) = 0.67040 + 0.00007 T \qquad 0°F < T < 800°F$$

Parameter, $g\beta\rho^2/\mu^2$ (1/°F-in.^{3})

$$g\beta\rho^2/\mu^2 = 45.0 - 3.2 \times 10^{-1} T + 9.4 \times 10^{-4} T^4 - 1.2 \times 10^{-6} T^3 + 5.7 \times 10^{-10} T^4$$

$0°F < T < 800°F$

Specific heat, Cp (Btu/lb-°F)

$Cp = 1.242$ $0°F < T < 800°F$

Density, ρ (lb/in^3)

$\rho(T) = 1/1728\ (0.0119/(1+0.002168T))$ $0°F < T < 800°F$

3.2.7 Fuel Material (Al + Fuel Meat + Helium Composite) [3.8]

Specific Heat, Cp(Btu/lb-°F)

	Cp(Btu/lb-°F)	
Temp °F	**Inner Element**	**Outer Element**
80	0.374	0.274
440	0.431	0.316
980	0.514	0.376
1205	0.563	0.411

Conductivity, k (Btu/hr-in-°F)

Inner Element

$k = 2.30$

Outer Element

$k = 2.96$

Density, ρ (lb/in^3)

Inner Element

$\rho = .0985$

Outer Element

$\rho = .0745$

Specific Heat, Cp (Btu/lb-°F)

Inner Element

$$Cp(T) = .35910 + 0.00016\ T \qquad 80°F < T < 1205°F$$

Outer Element

$$Cp(T) = 0.26348 + 0.00012\ T \qquad 80°F < T < 1205°F$$

3.3 TECHNICAL SPECIFICATIONS OF COMPONENTS

The HFIR fuel basket and liner contains Type 304 stainless steel and tungsten alloy material with a transition temperature of 2600°F [3.9] and 6150°F [3.9] respectively. The maximum design fuel element temperature for the HFIR fuel is 400°F.

The temperature resulting from 10CFR71 [3.10] normal and accident conditions fall well within the design critieria limit as shown in Table 3.1 in the Subsection 3.1.3. The technical specifications of the Model 2000 Transport Package [3.1] are not affected by the HFIR fuel basket and liner.

3.4 THERMAL EVALUATION FOR NORMAL CONDITIONS OF TRANSPORT

This Section presents the thermal analyses of the Model 2000 Transport Package with the HFIR fuel including its basket and liner for the normal conditions of transport. The thermal conditions considered are those specified in 10CFR71 [3.10] applicable to the basket and liner design as summarized in Subsection 3.1.2. The Model 2000 Transport Package is mounted on the truck in its normal position (vertical orientation) and is subjected to natural convection and radiation heat transfer on the Package surface.

The cask cavity is gas-filled (helium). Heat dissipation is by radiation and conduction from the fuel to the basket and liner, by conduction throughout these structures, by conduction and radiation to the cask cavity wall, conduction through the cask body, convection across the gap between the cask and overpack, convection and conduction across overpack wall, and a combination of natural convection and radiation from the overpack exterior to the environment. The analytical model used in thermal evaluation during normal conditions of transport is described in Section 3.4.1.

3.4.1 Analytical Model

The model closely represents the actual transport package with the exception of the overpack toroid shells. Figure 3.1 shows the finite element model. The toroidal shells are not included in the model because they will collapse during the free-drop event, and their omission in the evaluation of normal condition is conservative.

The finite element model of the basket and liner with HFIR fuel elements inside a Model 2000 type transport package used for the thermal analyses consists of 5324 nodes and 3597 elements, as is shown in Figure 3.1. The helium and air spaces are not shown in the figure for clarity. The model represents the Model 2000 cask, the overpack structure, the basket, the liner and HFIR fuel elements. Because an axisymmetric solution is used, only a cross section of the package need be modeled. The model consists of various axisymmetrie elements; two-node conduction elements, two-node boundary elements, three-node triangular elements, and four- and eight-node quadrilateral elements. Each element is characterized by one of a total of 71 different material property sets. These many property sets allow a detailed representation of the seven materials (steel, lead, aluminum, air, uranium, tungsten and helium) within the model. Several material property sets represent the same material but at different temperatures. This is because of their locations within the model. Helium and air are also represented by various property sets to account not only for temperature variation but also for different heat transfer modes. The mode of heat transfer across a helium and air space varies if the helium or air space is enclosed or open and also if it is horizontally or vertically oriented.

3.4.1.1 Cask and Overpack. The bulk of the cask is lead. The cask cavity and surface are lined with a 304 stainless steel cladding, 1.0 inch in thickness. This cladding is modeled with one-element thickness, eight-node quadrilateral elements. An air gap exists between the cask lead and the outer cladding. This air gap forms due to shrinkage of the lead relative to the stainless steel during the manufacturing process. The air gap is modeled by two-node conduction elements with conduction and radiation properties. The cask sits inside the overpack on a 4-inch-thick aluminum honeycomb material pad. A plate, 0.5 in. thick, separates the bottom of the cask from the honeycomb pad. The plate is represented by one element while the honeycomb pad is represented by four elements in thickness.

Between the vertical cask surface and the inner overpack shell is an air space. This vertical air space is modeled by four-node conduction elements, one element in thickness. Air space followed by honeycomb material pad exists between the top cask surface and the overpack inner top plate. This region is represented with four-node conduction elements with four- and six-element thickness for the horizontal air space and the honeycomb pad. The overpack consists of two concentric 0.5-inch-thick, type 304 stainless steel cylindrical shells separated by an air space. Eight equally spaced 3-in. OD tubes vertically separate these shells, and two 7.25-in. OD tubes horizontally separate them at both ends. The overpack is modeled by one-element thickness on the steel and three-element thickness on the vertical air space. The top and bottom horizontal air spaces are represented by seven-element thickness. The presence of these tubes in the air spaces enhances the heat conduction across the air space. The model accounts for this effect by increasing the conductivity in the air space proportionally to the volume ratio of steel to the total space volume. The boundary elements manifest the convective and radiative interfaces between the overpack outer surface and the regulatory environments, as well as the solar heat flux.

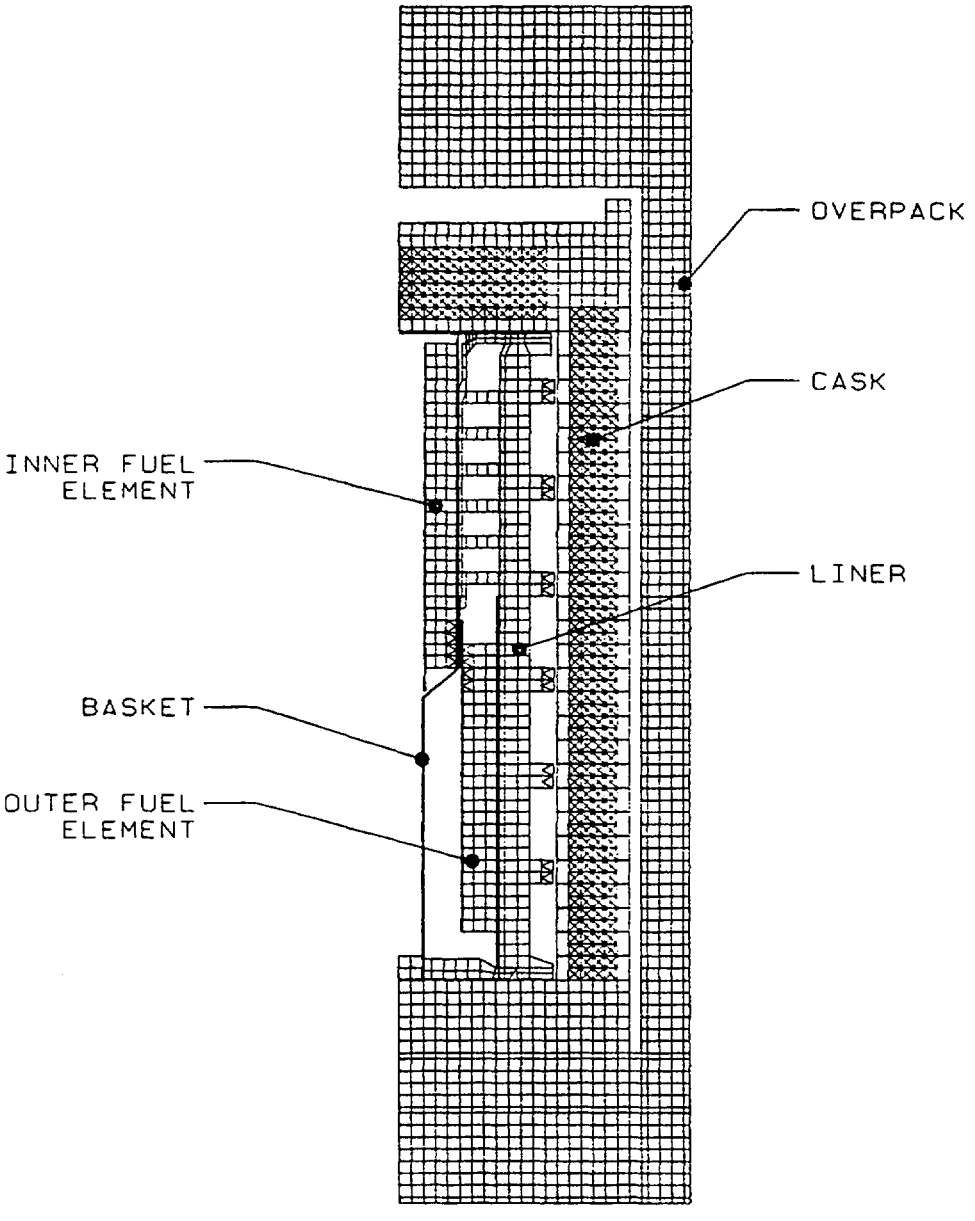

NUMBER OF ELEMENTS: 3,597 NUMBER OF NODES: 5,324

Figure 3.1. Thermal Finite Element Model

3.4.1.2 Basket and Liner with Fuel Elements. The content of the package consists of inner fuel element, outer fuel element, basket and liner. The liner and the cask wall are separated by helium space except at the base, where a portion of the liner base makes a full contact with the cask surface. The helium space between the cask cavity surface and the liner cooling fin is modeled with four node quadrilateral elements, one element thick, capable of conduction and radiation. The gap between cask cavity surface and the liner body is modeled with triangular and four noded quadrilateral elements, three to four elements thick, also capable of conduction and radiation. The rest of the helium spaces between the cask surface and the content, including the liner base and the basket top areas, are modeled with both triangular and four node quadrilateral elements which are capable of heat transfer by conduction, convection and radiation.

The stainless steel liner and basket are modeled with four and eight node quadrilateral elements and triangular elements. The narrow section of the basket which is sandwiched by both fuel elements is 0.125 inch thick, and is modeled with eight node quadrilateral element, one element thick.

All helium gaps between components in the content are modeled with triangular and four node quadrilateral elements; between the inner fuel element and the basket, between the outer element and the basket, between the outer fuel element to the liner, and between the basket cooling ring and the liner. Since the helium spaces between the basket and the fuel elements are narrow, ranging from 0.020 inch to 0.17 inch, they are modeled with one element thick, capable of radiation and conduction, but no convection. Temperature gradients across these gaps are not expected to be high, which is confirmed later with the temperature distribution on the model. Similarly, the helium spaces between the basket ribs to the liner and the outer element to the liner inner surface are modeled with one element thick, capable of conduction and radiation. It turns out that conduction is the dominant mode of heat transfer for all helium gaps in the model.

The aluminum cladding of the inner and outer fuel elements are modeled with four node quadrilateral elements and triangular elements, one element thick. Both fuel elements are modeled also with four node and triangular elements. The material properties of the fuel are adjusted for the inhomogeniety of the fuel, which consists of aluminum, uranium and air. The decay heat generated from both elements, 166 W from the inner fuel and 434 W from the outer fuel, are uniformly distributed within the respective area of the fuels. Heat input used in the model is dicussed further in Paragraph 3.4.1.3.

3.4.1.3 Heat Input. The maximum heat load allowable for the Model 2000 Transport Package is 600 watts. The total decay heat is divided between the inner and outer elements by the ratio of their respective U-235 contents. The inner element generates a decay heat of 166 watts and the outer element the remaining decay heat of 434 watts.

For axisymmetric elements, LIBRA requires the heat input to the model to be in the form of heat flux i.e., total heat divided by the elements area. The heat in each fuel element is assumed to be uniformly distributed throughout the element body. The heat flux values used in the finite element model are calculated as follows:

$$q_{inner} = \frac{\text{Heat Loading}}{\text{Model Area}}$$

$$= \frac{166\ (\text{Watts}) \times (3.413\ \text{BTU/hr} - \text{Watts})}{20\ (\text{inch}) \times (5.29 - 2.71)\ (\text{inch})}$$

$$= 10.98\ \text{BTU/hr-in}^2$$

$$q_{outer} = \frac{\text{Heat Loading}}{\text{Model Area}}$$

$$= \frac{434\ (\text{Watts}) \times (3.413\ \text{BTU/hr} - \text{Watts})}{20\ (\text{inch}) \times (8.317 - 5.867)\ (\text{inch})}$$

$$= 30.20\ \text{BTU/hr-in}^2$$

3.4.1.4 Enclosed Air and Helium Space Property Sets. The enclosed air spaces are represented by five property sets, and the enclosed helium spaces by twelve property sets. When the convective heat transfer becomes the dominant mode, heat transfer via conduction is negligible. The criteria for selecting the heat transfer mode is discussed below.

For convective heat transfer in an enclosed vertical space, Gebhart [3.11] gives the following:

$$Nu = 0.18 \cdot \sqrt[4]{Gr(H/s)}^{-\frac{1}{9}} \qquad 2 \cdot 10^4 < Gr < 2 \cdot 10^5$$

$$Nu = 0.065 \cdot \sqrt[3]{Gr(H/s)}^{-\frac{1}{9}} \qquad 2 \cdot 10^5 < Gr < 11 \cdot 10^6$$

where: Nu = Nusselt Number
Gr = Grashof Number based on s
s = distance across enclosed space
H = height of enclosed space

For Gr less than 2,000 the process is simple conduction, i.e., Nu = 1.0. The Grashof Number is defined here as

$$Gr = \frac{\rho^2 g \beta s^3 \Delta T}{\mu^2}$$

where: ρ = density, lb/ft^3
g = acceleration of gravity (32.1 ft/sec^2)
β = coefficient of the thermal expansion (°F)
ΔT = temperature difference across enclosure (°F)
μ = viscosity (lb/ft-sec)

The relationship between Nu and Gr given above applies strictly to an air and helium space enclosed between plates. In general, a curved surface may be considered flat without significant error, if according to Gebhart [3.12]

$$\frac{D}{L} \geq \frac{35}{\sqrt[4]{Gr_L}}$$

where: D = diameter
L = height
Gr_L = Grashof Number based on height

For our problem, values for the property sets 24 and 32 (enclosed vertical air spaces) are:

Set No.	D	L	Gr_L	$D/L \leq \frac{35}{\sqrt[4]{Gr_L}}$
24	39.50	72.0	439.0	0.549< 2.432
32	44.50	82.0	8,500	0.543 < 3.642

From the values shown above, this correlation should be adequate for this geometry.

The convective heat transfer in an enclosed horizontal space depends on the temperature of the upper and lower plates. If the upper plate temperature is higher than the lower plate, the process is simple conduction; therefore

$$Nu = 1.0$$

If vice versa, lower plate warmer, then

$Nu = 1.0$ $\quad Gr < 2 \cdot 10^4$

$Nu = 0.195\sqrt[4]{Gr}$ $\quad 2 \cdot 10^4 < Gr < 4 \cdot 10^5$

$Nu = 0.068\sqrt[4]{Gr}$ $\quad 4 \cdot 10^5 < Gr$

These relations are given in Gebhart [3.13]. Properties are evaluated at the average of the two surface temperatures.

Once Nu is known, convective heat transfer coefficient, h_c, can be found by the following expression for both vertical and horizontal air and helium spaces:

$$h_C = \frac{Nu \cdot k}{s}$$

where: k = thermal conductivity of air (Btu/hr-in.-°F)
s = as before, distance across the space (in.)

For radiative heat transfer,

$$h_r = F\sigma (T_1^2 + T_2^2) \cdot (T_1 + T_2)$$

where: T_1, T_2 = temperatures on either side of the space (°R)
σ = 1.1944×10^{11} (Btu/hr-in.^{2} -°R^4)
F = gray body shape factor

The gray body shape factor, F, is defined as:

$$F = \frac{1}{\left(\frac{1}{e_1 - 1}\right) + \frac{A_1}{A_2}\left(\frac{1}{e_2} - 1\right) + \frac{1}{F_{12}}}$$

where: A_1 = area of smaller surface
A_2 = area of larger surface
e_1, e_2 = emissivities
F_{12} = shape factor

The shape factor, F_{12}, is purely a function of the geometry of the system. When body A_1 is completely enclosed by body A_2 and A_1 cannot see itself, $F_{12} = 1.0$ [3.14].

As an example, for oxidized 304 SS, $e_1 = e_2 = 0.52$ [3.9] and assuming $A_1 = A_2$,

$$F_{12} = 0.351$$

for all enclosed air space material sets.

The finite element model represents air and helium spaces with conductive elements. The conversions from h to k are as follows:

$$k = h \cdot s$$

As before, s is the distance across the space.

In general, the effective conductivity across the air and helium space, k_e, is due to conduction plus radiation. However, a convective mode may arise depending upon the Gr and/or the plates' temperatures as discussed before. Therefore, the makeup of k_e may be as follows:

$$k_e = k+h_r \cdot s, \text{ or}$$

$$k_e = (h_c + h_r) \cdot s$$

In the perpendicular direction, along the space, the effective conductivity, k_e, is assumed to be pure conduction.

$$k_e = k$$

The vertical air space between the inner and outer shells of the overpack structure, material set 32, contains eight evenly spaced tubes. These tubes are used as energy absorbing devices and spacers. The effect of these tubes as heat transfer mechanisms is neglected. This is based on the low value 0.03 of the ratio of total tube area to total air area.

3.4.1.5 Boundary Property Sets. There are three material property sets, numbers 39 through 41, surrounding the model. These sets link the model with the external environment. Each set contains the film coefficient, ambient temperature and solar heat flux value.

Property set 40 covers the vertical outside wall of the model, while sets 39 and 41 are along the bottom and top horizontal surfaces, respectively. For convection from a large diameter cylinder [3.15].

$$Nu = 0.59 \sqrt[4]{Ra} \qquad 10^4 < Ra < 10^8$$

$$Nu = 0.13 \sqrt[3]{Ra} \qquad 10^8 < Ra$$

where the Rayleigh number, Ra, is defined as

$$Ra = Gr \cdot Pr$$

and the Gr is based upon L dimensions instead of s in the enclosed space condition in section 3.4.1.2. The fluid properties are determined at the average temperature between the wall (T_o) and film (T_f) temperatures.

For horizontal surfaces, the following relations apply [3.16]:

If the surface warmer than the surrounding medium is facing upward or the cooler surface is facing downward, then:

$$Nu = 0.54\ (GrPr)^{1/4} \qquad 10^5 < Gr \leq 2 \cdot 10^7$$

$$Nu = 0.14\ (GrPr)^{1/3} \qquad 2 \cdot 10^7 < Gr \leq 3 \cdot 10^{10}$$

However, for the warmer side facing downward and the cooler side facing upward,

$$Nu = 0.27\ (GrPr)^{1/4} \qquad 3 \cdot 10^5 < Gr < 3 \cdot 10^{10}$$

Here, also, the fluid properties are determined at the average temperature, $0.5(T_o + T_f)$; and the L dimension is replaced by 0.9 D, where D is the diameter of the disk.

After Nu is determined, the convective heat transfer coefficient is calculated using the equation below. In this equation, s represents the cylinder length L for material set 40 and 0.9 D for the other sets.

$$h_c = \frac{Nu \cdot k}{s}$$

In addition to convection, the cask surface interacts radiatively with its surroundings. The radiative heat transfer coefficient, h_r, is calculated using the equations given in Paragraph 3.4.1.2. Regulatory environments place the transport package in an outside environment. Therefore, in evaluating the equation for the gray body shape factor, it was assumed that:

(1) A_1 is negligible compared with A_2, and

(2) $F_{12} = 1$.

The film coefficient, h (Btu/hr-in.^{2}-°F) is

$$h = h_c + h_r$$

The overpack structure of the transport package is basically cylindrical but does contain a toroidal shell at both ends. These shells substantially mitigate the effects of the thermal environment. However, their effects are local in relation to the cask structure because of the transport package geometry. The distance from the cask structure to the outside environment is shorter in the radial direction than through the toroidal shell. Therefore, the cask structure would not be affected by the surroundings of the toroidal shells. For this reason, the model does not account for their effects. These areas are treated in the model as an extension of the top and bottom horizontal plates and the vertical cylindrical wall. The only credit taken for their presence is during the solar load calculations. The solar input over the toroid shell area is calculated based on fraction of curve and horizontal surfaces to the total surface of the model.

3.4.1.6 Solar Heat Load. The solar load is represented in the model by the quantity "q", rate of heat transfer per unit area. The value of q is calculated as follows:

For flat surface transported horizontally,

Solar Load Value = 2,950 Btu per ft^2 per 12 hours [3.7.14]

$$q_f = \frac{2{,}950\,\text{Btu}}{(144\ \text{in}^2)12\,\text{hr}} = 1.707\ \frac{\text{Btu}}{\text{hr}-\text{in}^2}$$

For curved surface:

Solar Load Value = 1,475 Btu per ft^2 per 12 hours [3.7.14]

$$q_c = \frac{1475\,\text{Btu}}{(144\ \text{in}^2)12\,\text{hr}} = .853\ \frac{\text{Btu}}{\text{hr}-\text{in}^2}$$

Overpack outside shell, material set 40:

$$q_{(40)} = (q_c)\left(\frac{\text{actual overpack cylindrical shell height}}{\text{model overpack cylindrical shell height}}\right)$$

$$= .854\left(\frac{82.5}{99.38}\right) = .709\ \text{Btu / hr - in.}^2$$

Overpack top surface, material set 41:

$$q_{(41)} = q_f\left(\frac{\text{flat surface area}}{\text{total model area}}\right) q_c\left(\frac{\text{curve surface area}}{\text{total model area}}\right)$$

$$= 1.707\left(\frac{471.43}{1847.45}\right) + .854\left(\frac{1376.02}{1847.45}\right)$$

$$= 1.074\ \text{Btu/hr-in}^2$$

3.4.1.7 Fire Effect. Fire effect is introduced to the model by a thermal radiation environment of 1,475°F for 30 minutes with an emmissivity coefficient of 0.9 and a transport package surface absorption coefficient of 0.8 [3.8]. After the fire, the cask is cooled naturally for a total period of 3 hours in ambient air at 100°F. To search for the maximum temperatures of the content (basket, liner and fuel elements), the model is monitored for a total of 35 hours. The maximum temperature of the elements is reached at around 13 hours.

During the fire the gray body shape factor, F, is given by:

$$F = \frac{1}{\frac{1}{e_1} + \frac{1}{e_2} - 1} = \frac{1}{\frac{1}{0.8} + \frac{1}{0.9} - 1}$$

and the radiation coefficient is calculated by the equation given in Paragraph 3.4.1.2.

3.4.1.8 Overpack Outer Shell Elements Property Set. The overpack outer shell is represented in the model by three material property sets, sets 34 through 38. The model does not account for any effect given by the toroidal shells because they are smashed during the 30-foot free-drop event. The free-drop event precedes the fire event.

3.4.1.9 Aluminum-Air Conglomerate Property Sets (Honeycomb Material). Property sets 26 and 28 represent the honeycomb pad installed at the bottom and top of the cask structure. The material is made of corrugated aluminum foil 0.002 in. gauge with a cell width of 0.125 in. The density of the material is listed by the manufacturer as 8.1 pcf nominal. Based on these data, the thermal properties were calculated as follows:

Pad Volume, Vp

$$Vp = \pi R^2 H$$

where: R = pad radius
H = pad height

For property set 20

$$Vp = \pi(20.0)^2(4) = 5{,}026.55 \text{in.}^3$$

Its weight,

$$Wt = Vp \cdot \rho = 5{,}026.55\ (8.1)/1{,}728$$
$$= 23.56 \text{ lbs.}$$

Next, the air and aluminum volume fractions are determined by solving the following equations,

$$Wt = \rho_{Al} \cdot V_{Al} + \rho_{Air} V_{air}$$

$$VP = V_{Al} + V_{Air}$$

$V_{Al} = 241.64$ in.^{3} and $V_{Air} = 4{,}784.91$ in.^{3}

Therefore,

$$\frac{V_{Al}}{V_P} = 0.048 \text{ and } \frac{V_{Air}}{V_P} = 0.952$$

$$k_x = \frac{V_{Al}}{V_P} \cdot k_{Al} + \frac{V_{Air}}{V_P} \cdot k_{Air}$$

$$= 0.048 \cdot k_{Al} + \cdot 0.952\, k_{Air}$$

$$k_y = \frac{b_1}{L} \cdot k_{Al} + \frac{b_2}{L} \cdot k_{Air}$$

$$= 0.0679 \cdot k_{Al} + 0.9321 \cdot k_{Air}$$

where

b_1 = Aluminum foil thickness

b_2 = Air space thicknes

L = Honeycomb pad thickness

$$C_p = \frac{V_{Al}}{V_P} \cdot C_{P_{Al}} + \frac{V_{Air}}{V_P} \cdot C_{P_{Air}}$$
$$= 0.048 \cdot C_{P_{Al}} + 0.952 \cdot C_{P_{Air}}$$

$$\rho = 0.048\rho_{Al} + 0.952\rho_{Air}$$

3.4.1.10 Fuel Elements Property Sets (Al/Fuel Meats/Al/Helium Composite) [3.8]. Property sets 59 and 60 represent the outer fuel element and inner fuel element, respectively. The fuel element consists of array of fuel plates arranged in a radial direciton with 0.05 inch helium gaps between them. Each fuel plate consists of 0.03 inch fuel meats sandwiched between 0.01 inch aluminum clads. The effective material property of the fuel element can be calculated by considering a composite material of 0.01 inch Al, 0.03 inch of fuel meat, 0.01 inch of Al and 0.005 inch of helium as suggested in HFIR System RELAP5 Input Model, Reference [3.8].

The thermal conductivity is calculated as

$$k_{eff} = a \cdot \frac{\sum_i (k_i \cdot t_i)}{\sum_i t_i}$$

where a = 0.5092 for inner element
= 0.6970 for outer element
k_{eff} = Thermal conductivty (Btu/hr-in-°F)
t_i = Thickness of each component of the composite
k_i = Thermal conductivity of each component of the composite

And for effective density,

$$\rho_{eff} = \frac{1}{a} \cdot \frac{\sum_i (\rho_i \cdot t_i)}{\sum_i t_i}$$

where a = 0.5092 for inner element
= 0.6970 for outer element
ρ_{eff} = Density (lb/in^3)
t_i = Thickness of each component of the composite
ρ_i = Density of each component of the composite

Similarly, for specific heat,

$$c_{Peff} = \frac{1}{a} \cdot \frac{\sum_i (C_{p_i} \cdot \rho_i \cdot t_i)}{\sum_i \rho_i \cdot t_i}$$

where a = 0.5092 for inner element
= 0.6970 for outer element
c_{Peff} = Specific Heat (Btu/lb-°F)
t_i = Thickness of each component of the composite
ρ_i = Density of each component of the composite
c_{p_i} = Specific heat of each component of the composite

3.4.2 Maximum Temperatures

Under the normal conditions of transport, the maximum temperature distribution in the Model 2000 Transportation Package occurs when the ambient temperature is 100°, with maximum decay heat and the maximum solar load. Figures 3.2 through 3.7 present temperature values at several locations on the thermal model under normal conditions. Some of the elements within the thermal model on these figures have been erased for clarity. These figures also include values which are maximum.

3.4.3 Minimum Temperatures

The minimum temperature distribution is a result of an ambient temperature of -40°F. It is assumed that there is no heating effect from decay heat or solar radiation; therefore, the transport package is assigned a minimum temperature of -40°F throughout.

3.4.4 Maximum Internal Pressures

The cask cavity is initially filled with dry helium to 15 psia at ambient temperature (70°F). Under the normal conditions of transport, the maximum temperature of the helium inside the cavity occurs near the fuel element. Although the average temperature of the helium is quite less, the worst case fuel surface temperature of 253°F is used as the helium temperature to calculate the maximum internal pressure.

Using the ideal gas law, the temperature and pressure relationship is, for a constant volume,

$$\frac{P_1}{T_1} = \frac{P_2}{T_2}$$

where P_1 and T_1 = Presssure and Temperature at initial state, respectively
P_2 and T_2 = Pressrue and Temperature at steady state, respectively

Therefore the maximum internal pressure during normal transportation is calculated as

$$P2 = (15\,\text{psia}) \cdot \left(\frac{253 + 460}{70 + 460} \right) = 20.2\,\text{psia}$$

3.4.5 Evaluation of Package Performance for Normal Conditions of Transport

Temperature values throughout the package components associated with normal conditions of transport are all within the allowable limits for the respective materials (see Table 3.1). The design pressure of 30 psia is a higher value than the pressure value corresponding to the maximum cavity (helium) temperature of 253°F.

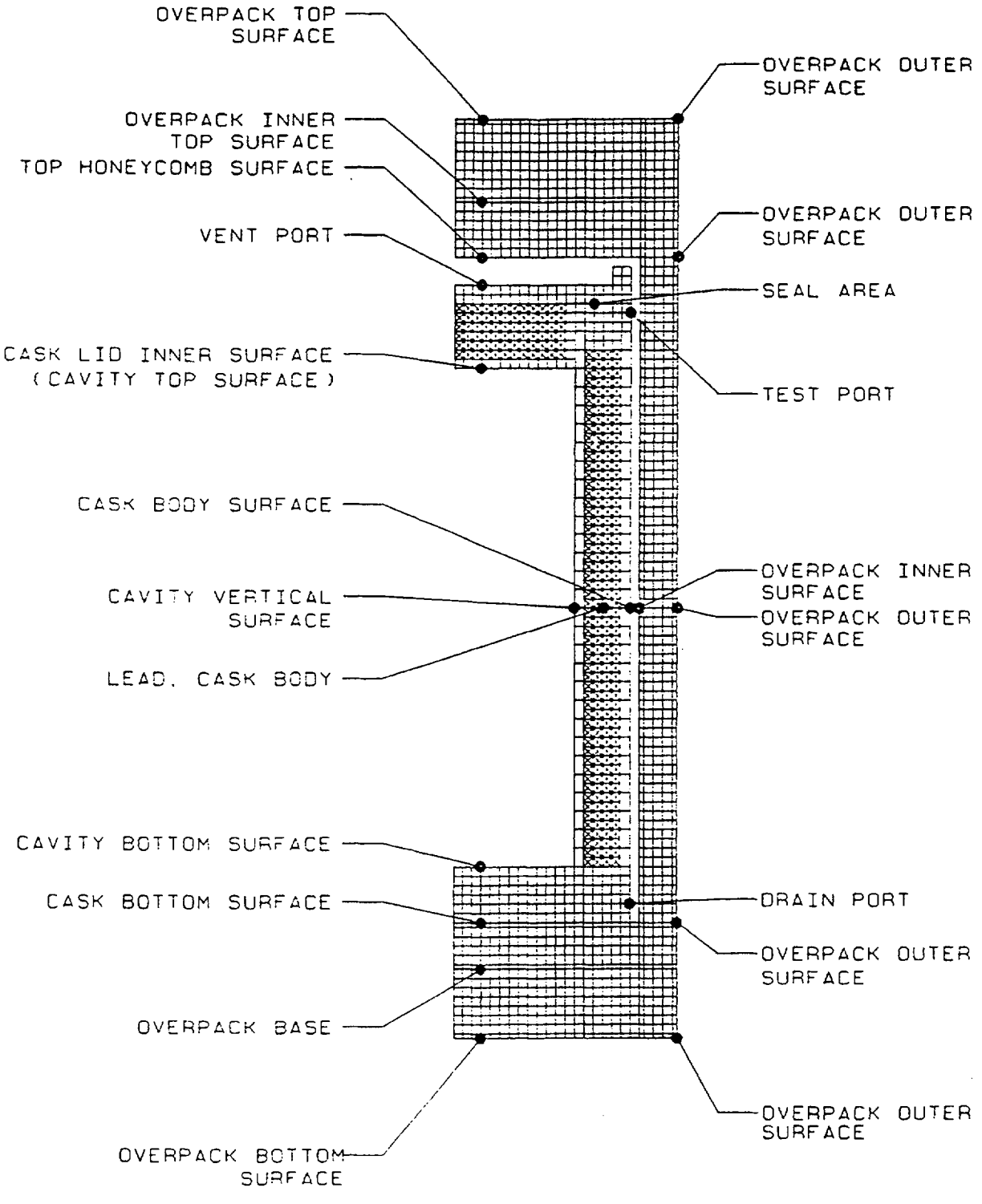

Figure 3.2. Key Plot of Temperature Locations – Cask and Overpack

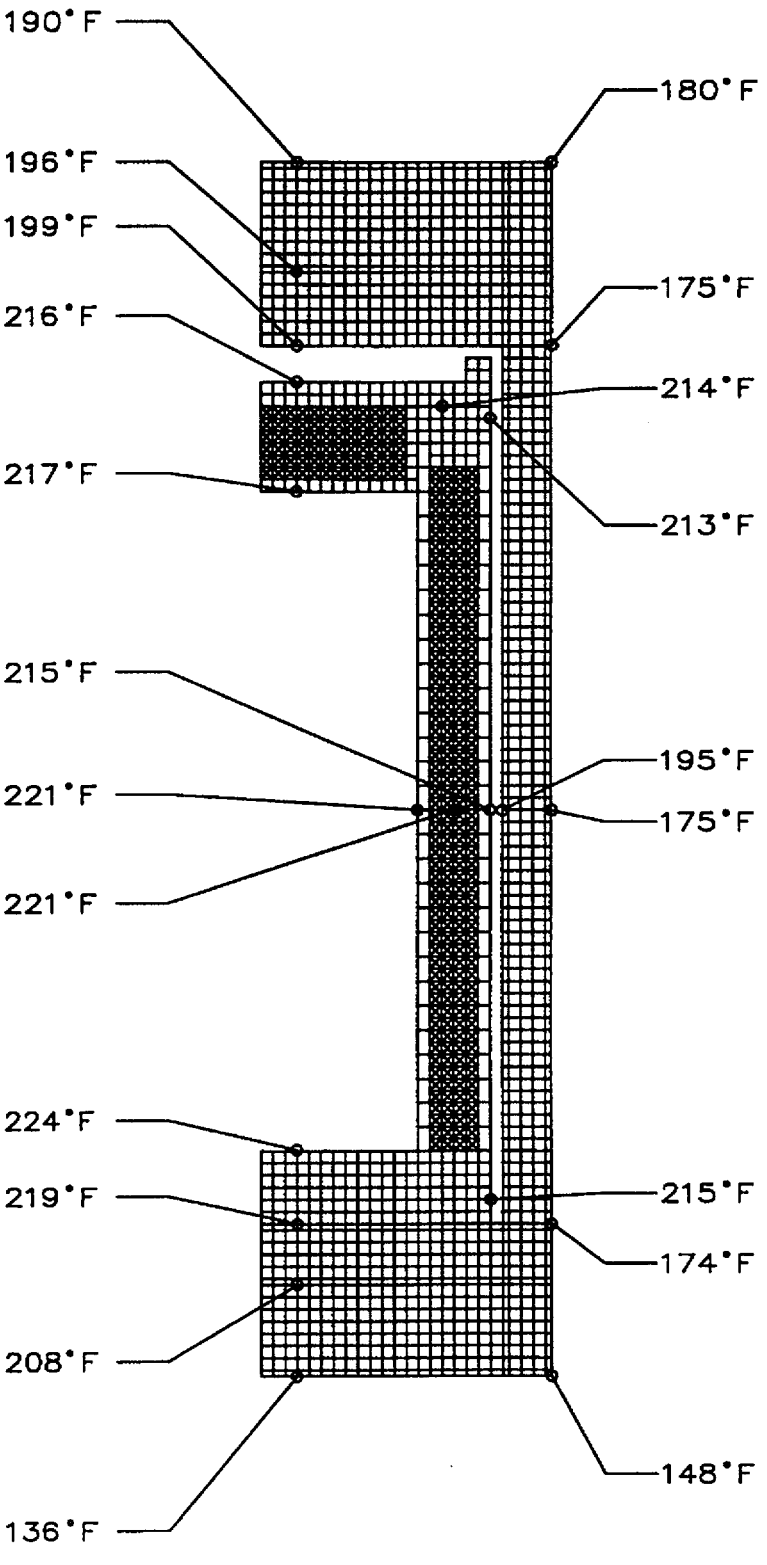

Figure 3.3. Steady-State Thermal Analysis – Cask and Overpack 100°F Ambient With Maximum Decay Heat and Maximum Isolation

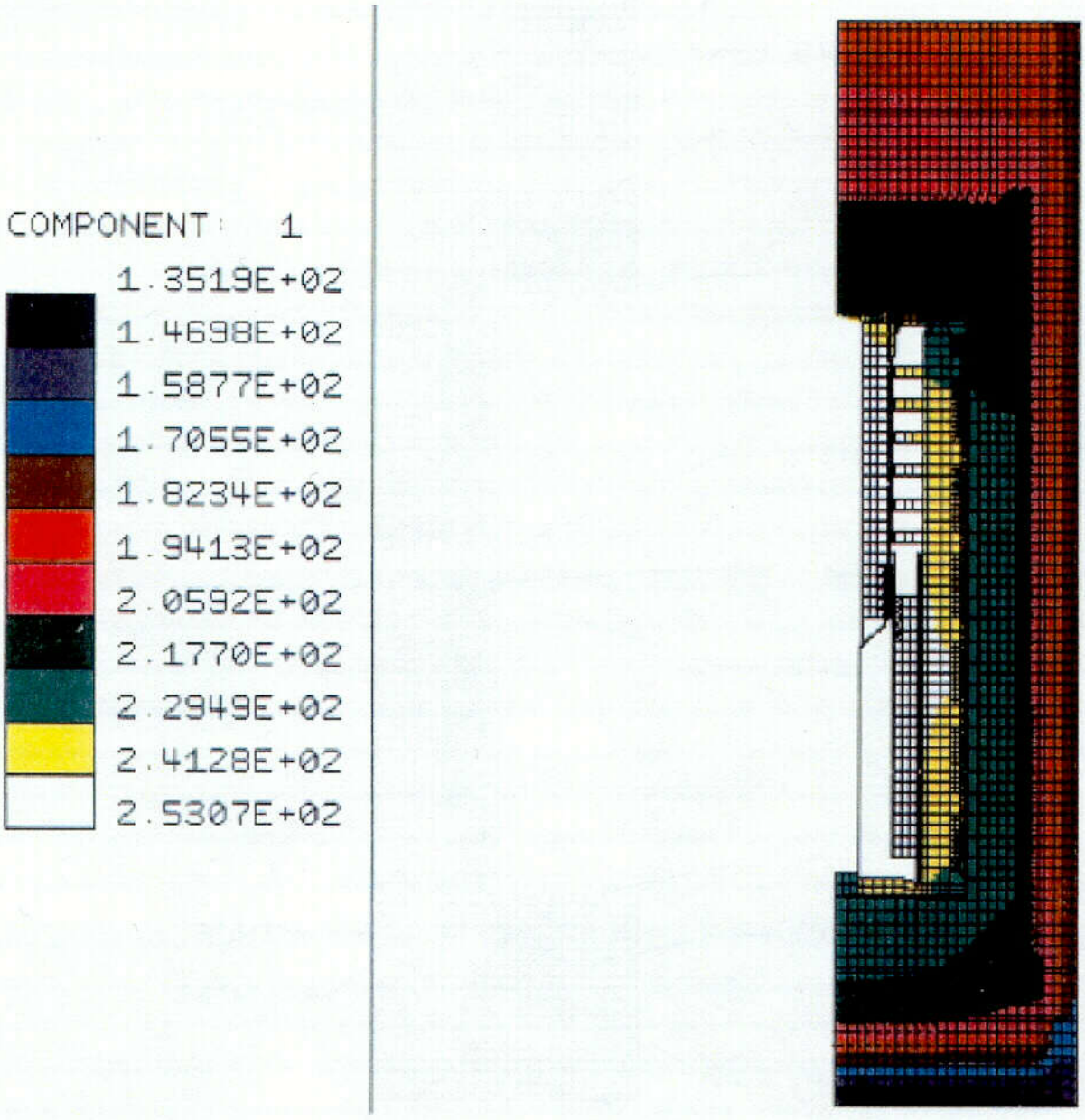

Figure 3.4. Steady-State Thermal Analysis – Contour Plot
100°F Ambient With Maximum Decay Heat and Maximum Insolation

C01

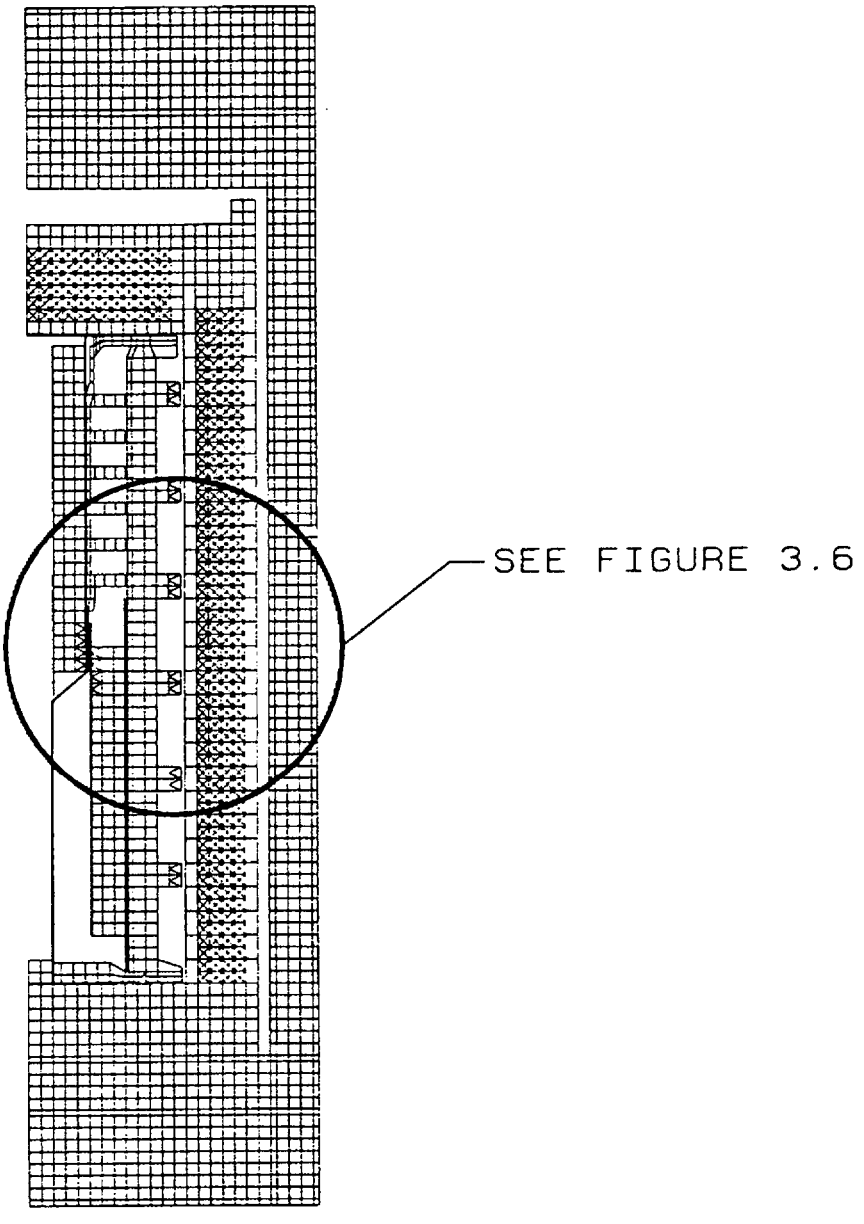

Figure 3.5. Steady-State Thermal Analysis – Basket and Liner w/Fuel Elements 100°F Ambient With Maximum Decay Heat and Maximum Insolation

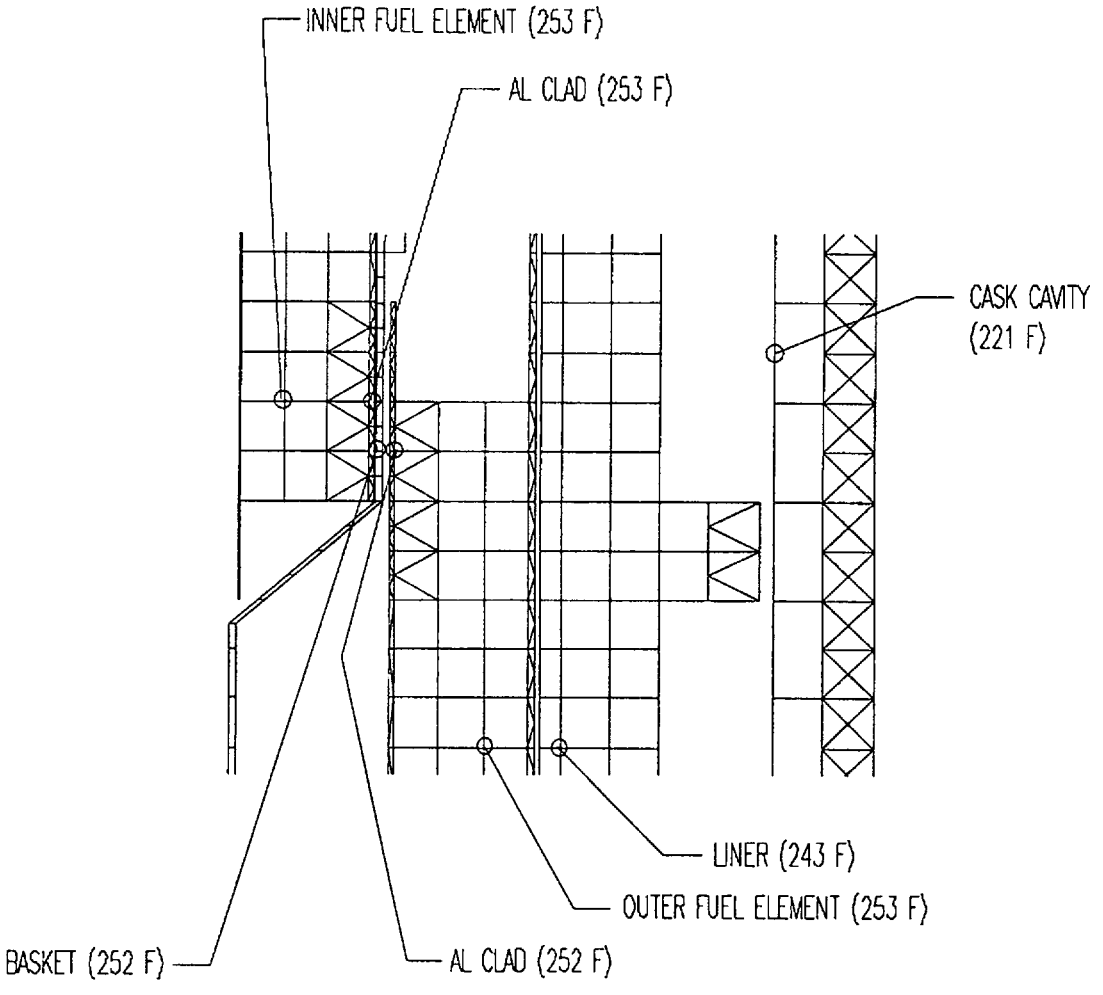

Figure 3.6. Steady-State Thermal Analysis – Temperature Plot 100°F Ambient With Maximum Decay Heat and Maximum Insolation

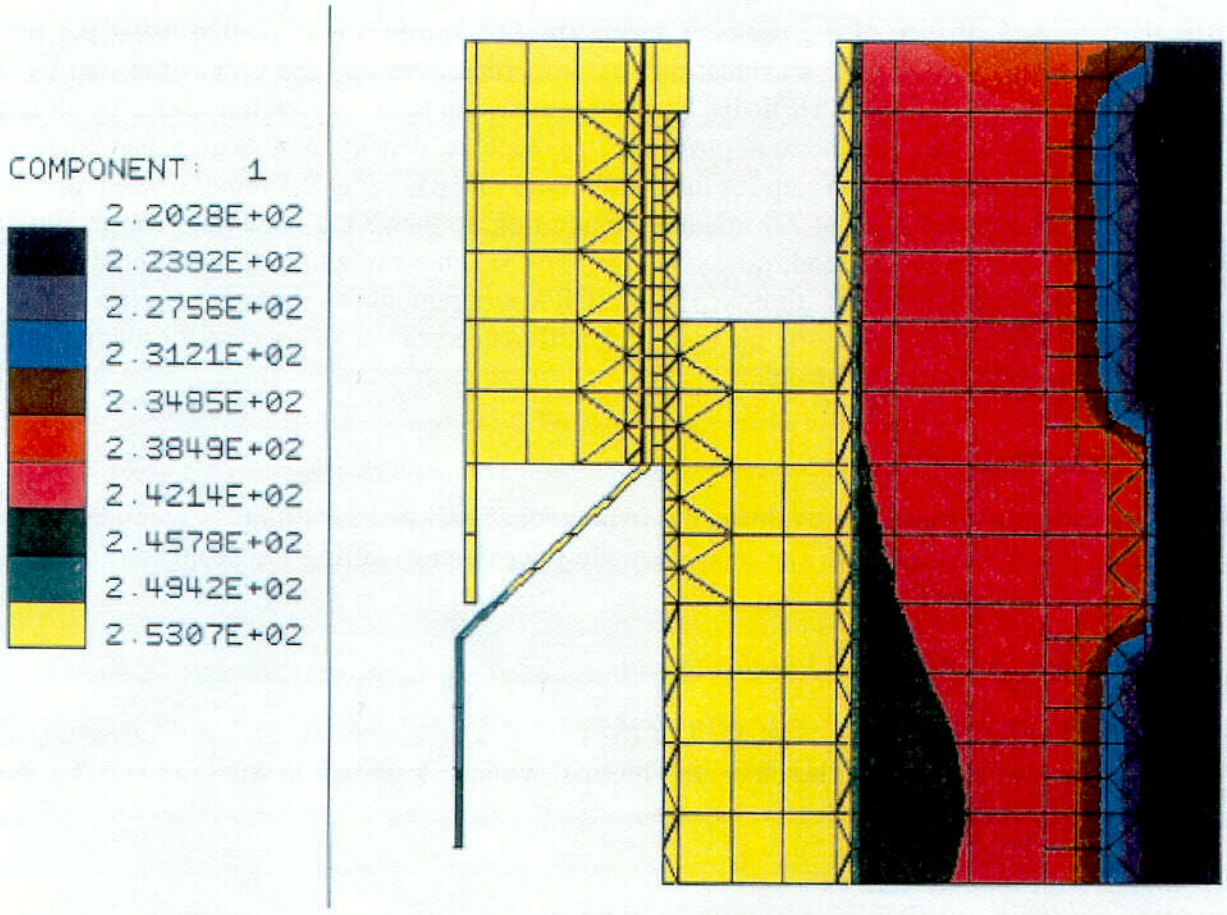

Figure 3.7. Steady-State Thermal Analysis – Contour Plot 100°F Ambient With Maximum Decay Heat and Maximum Insolation

C02

3.5 HYPOTHETICAL ACCIDENT THERMAL EVALUATION

After a free drop through 30 feet and a free drop through four feet onto a cylindrical punch, the package should be exposed to a fire transient. This thermal test consists of exposure of the whole package for not less than 30 minutes to a radiation environment of 800°C (1,475°F) with an emissivity coefficient of at least 0.9. The surface absorptivity of the package is taken as 0.8, and a convective heat input based on still ambient air at 800°C (1,475°F) is applied. The transient is then continued until maximum temperature values within the cask are obtained [3.18].

The thermal performance of the package during the fire transient is evaluated using the finite element program LIBRA. In this evaluation, the properties were updated every time step by the user-originated subroutine CPHFIR.F. This subroutine contains expressions relating element properties to temperature. Thermal properties as well as density and heat capacitance are updated periodically. The time step for the 0 - 0.5 hour range is set at 0.5 minute, while the time step for 0.5 - 3.0 hours is set at 2.5 minutes. In addition, to locate the maximum temperature of the content beyond 3 hour period, time steps for 3.0 - 33.0 hour is set at 1 hour. (The maximum temperature was peaked near 12th hour.) The LIBRA program allows the user to select the time marching scheme. In this analysis, the backward difference scheme is selected for mathematical stability of the finite element model.

3.5.1 Analytical Model

The analytical model used to evaluate the hypothetical accident condition is identical to that described in Subsection 3.4.1. The model accounts for damage during the accidental condition by not including the toroidal shells.

3.5.2 Package Conditions and Environment

During the drop events the toroidal shell of the overpack structure will collapse, absorbing the kinetic energy of the event. Therefore, the thermal models described in Subsection 3.3.1 does not include the toroidal shells.

3.5.3 Package Temperatures

Temperature values at several locations within the model are given in Figures 3.8 through 3.18 for time steps for 0 to 3.0 hours during the fire transient. In addition, the maximum temperature values of content at 12 hours are also presented in Figures 3.19 through 3.20. Temperature versus time plot is given in Figures 3.21 and 3.22.

3.5.4 Maximum Internal Pressures

The maximum internal pressure is reached at the maximum cavity temperature, which occurs around thirteen hours after the fire. The helium temperature of 298°F is used to calculate the maximum internal temperature using the same methodology as discussed in Subsection 3.5.3.

The maximum internal pressure is calculated as

$$P = (15 \text{ psia}) \cdot \left(\frac{298 + 460}{70 + 460} \right) = 21.5 \text{ psia}$$

3.5.5 Evaluation of Package Performance for the Hypothetical Accident

The temperature values obtained within the model during the fire transient are presented in Subsection 3.5.3. The temperatures evaluated are below the thermal design criteria of the material for each component. The highest lead temperature noted is 282°F. This temperature is way below the melting point of lead. The maximum temperature of any elastomeric component is 338°F. This temperature is given around the cask drain port O-ring. The elastomeric material employed is capable of performing up to 400°F (see Subsection 4.4.1 of Reference [3.1]). The maximum temperature of the fuel element is 298°F which is well below the design temperature of 400°F.

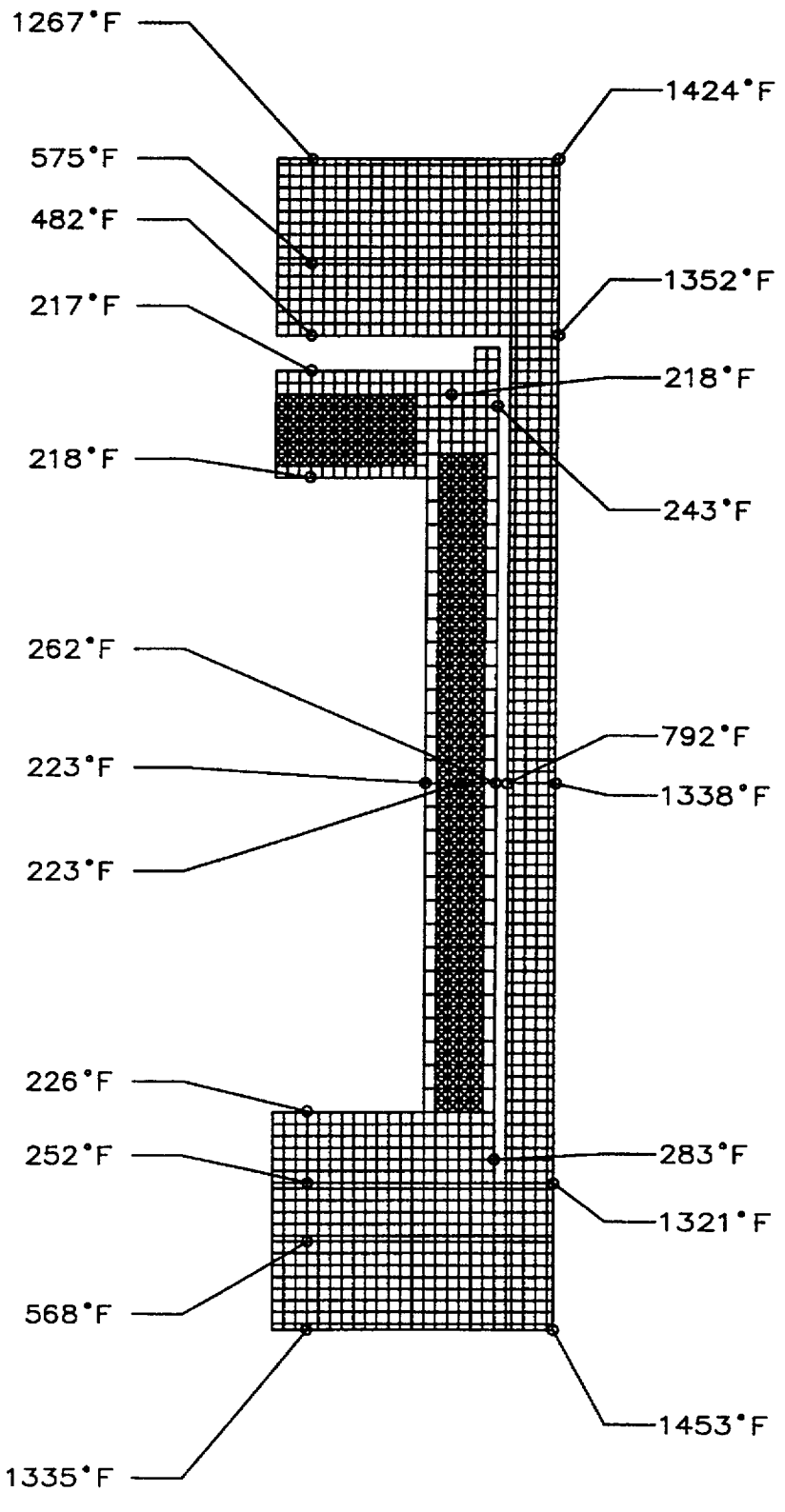

Figure 3.8. Transient Thermal Analysis – Fire Accident 100°F Ambient With Maximum Decay Heat, Time: 0.5 Hr

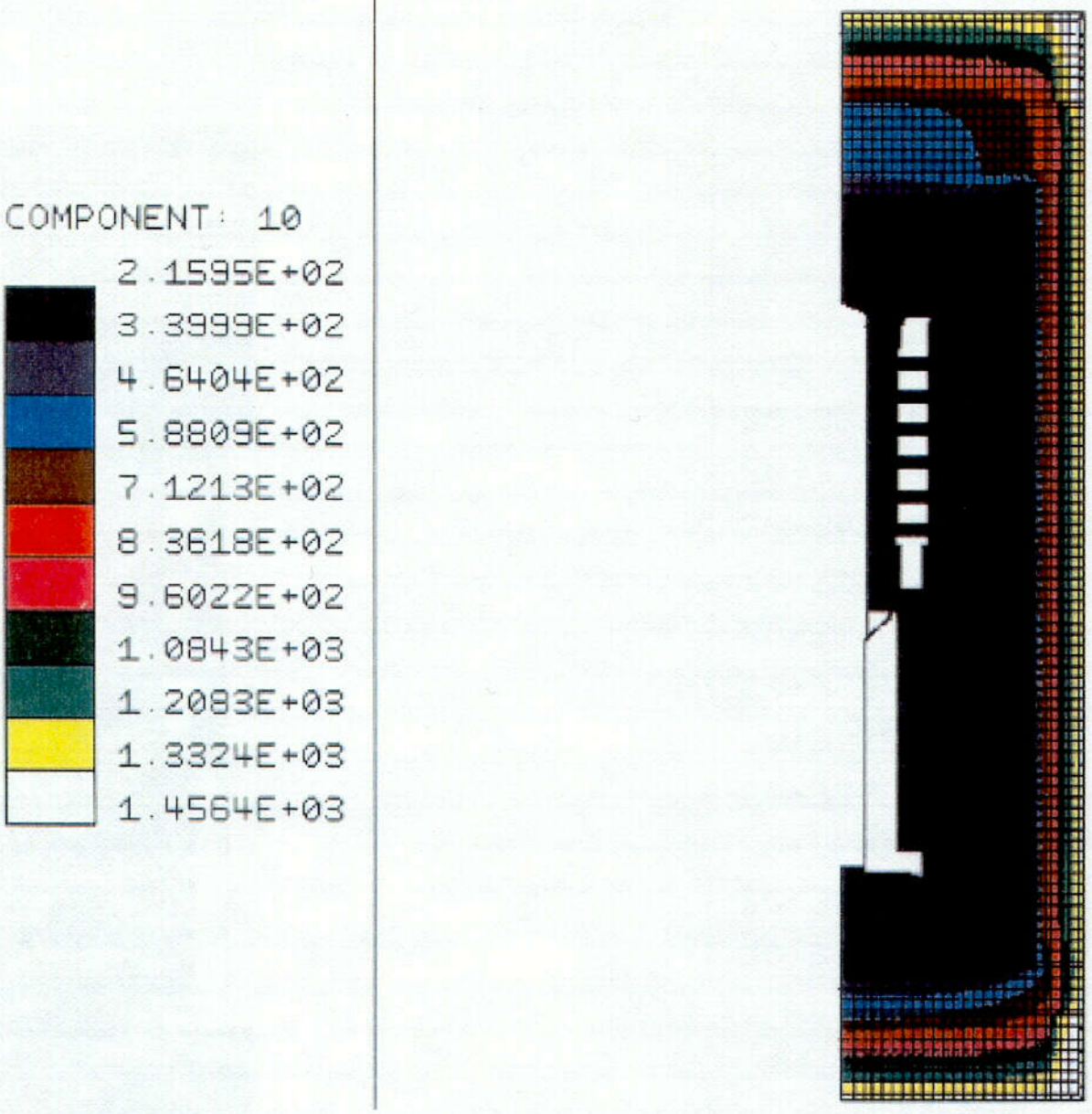

Figure 3.9. Transient Thermal Analysis – Contour Plot
100°F Ambient With Maximum Decay Heat, Time: 0.5 Hr

C03

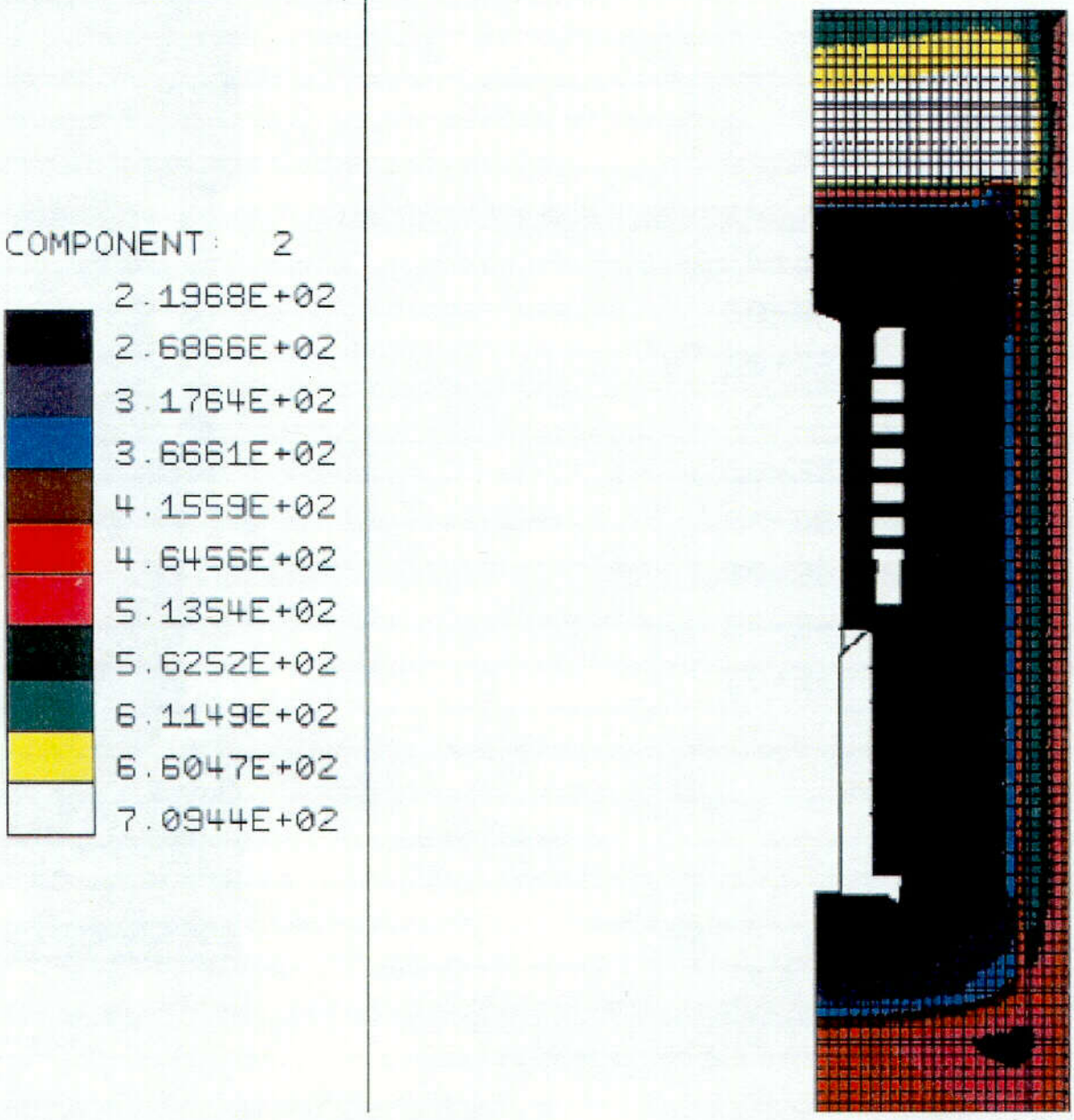

Figure 3.10. Transient Thermal Analysis – Contour Plot
100°F Ambient With Maximum Decay Heat and Maximum Insolation, Time: 1.0 Hr

C04

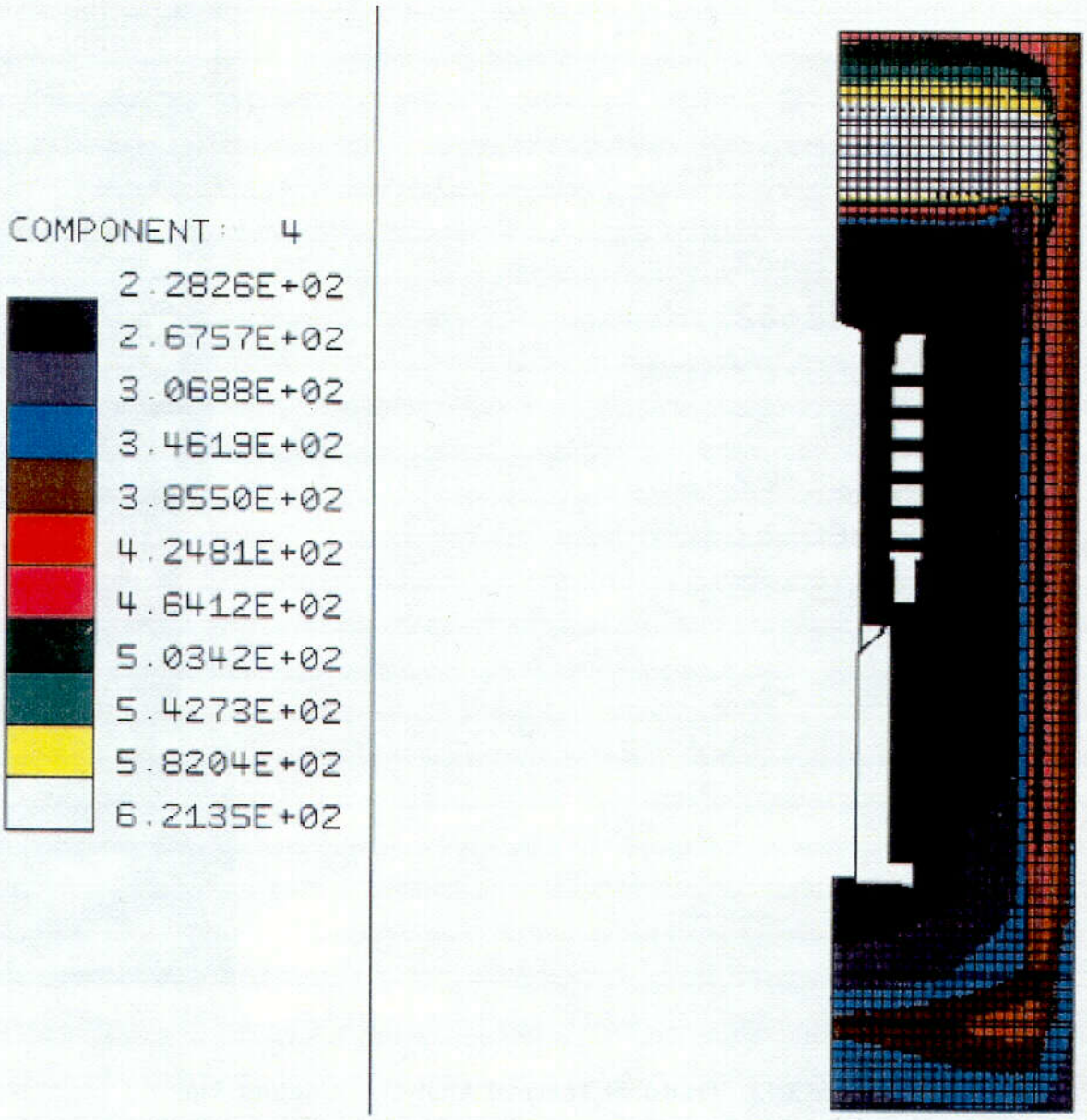

Figure 3.11. Transient Thermal Analysis – Contour Plot
100°F Ambient With Maximum Decay Heat and Maximum Insolation, Time: 1.5 Hr

C05

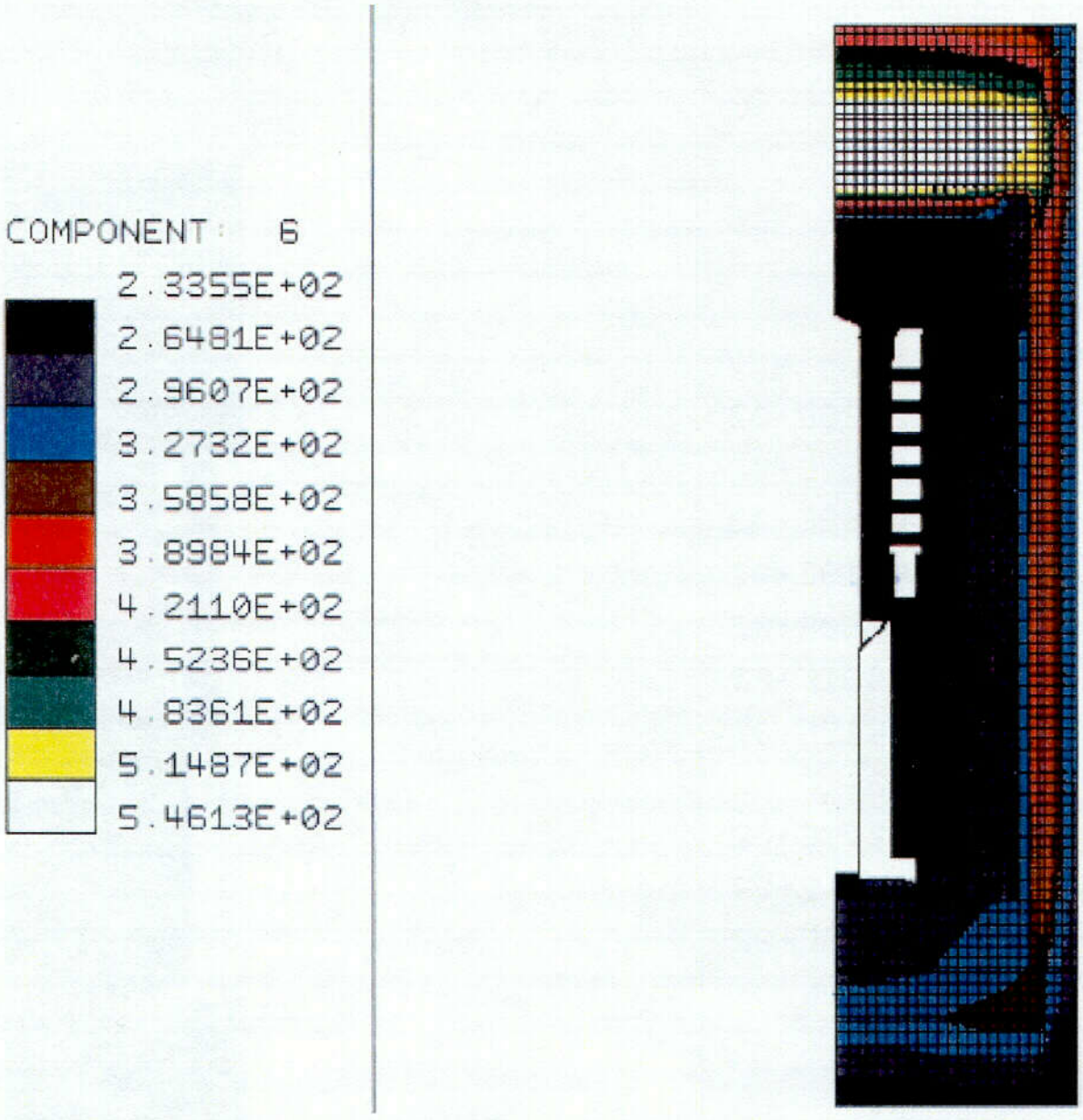

Figure 3.12. Transient Thermal Analysis – Contour Plot
100°F Ambient With Maximum Decay Heat and Maximum Insolation, Time: 2.0 Hr

C06

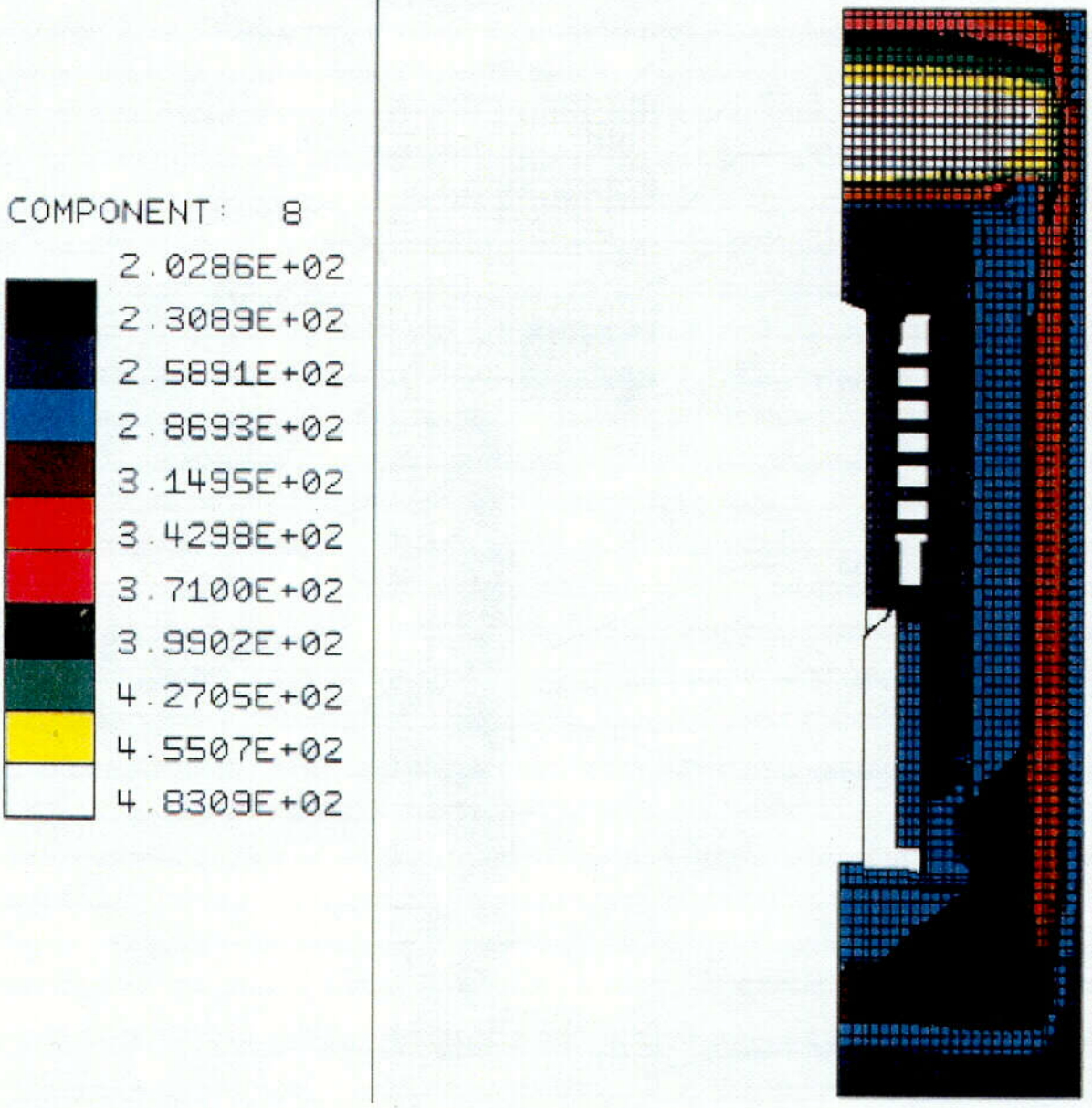

Figure 3.13. Transient Thermal Analysis – Contour Plot
100°F Ambient With Maximum Decay Heat and Maximum Insolation, Time: 2.5 Hr

C07

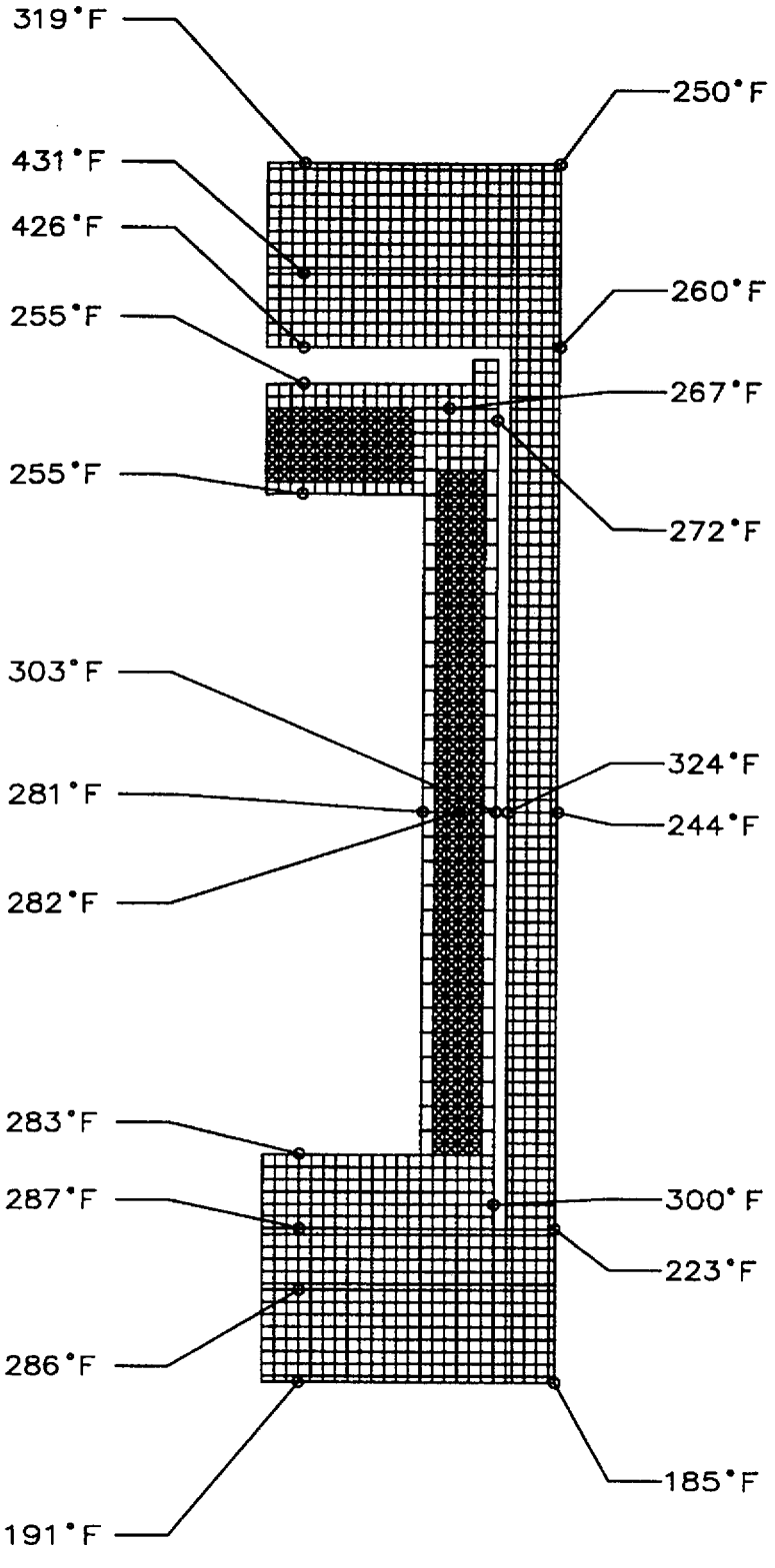

Figure 3.14. Transient Thermal Analysis – Temperature Plot
100°F Ambient With Maximum Decay Heat and Maximum Insolation, Time: 3.0 Hr

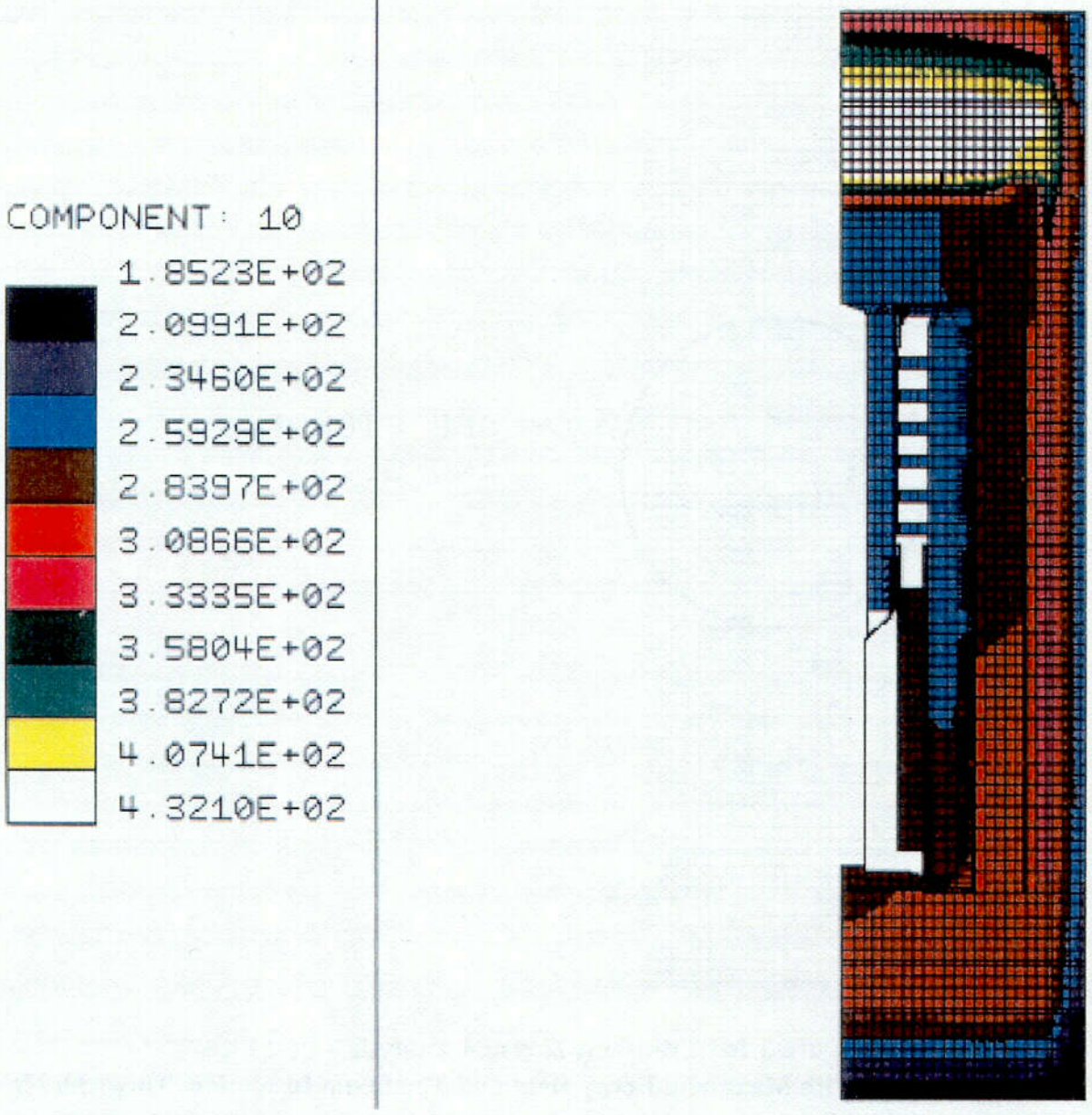

Figure 3.15. Transient Thermal Analysis – Contour Plot
100°F Ambient With Maximum Decay Heat and Maximum Insolation, Time: 3.0 Hr

C08

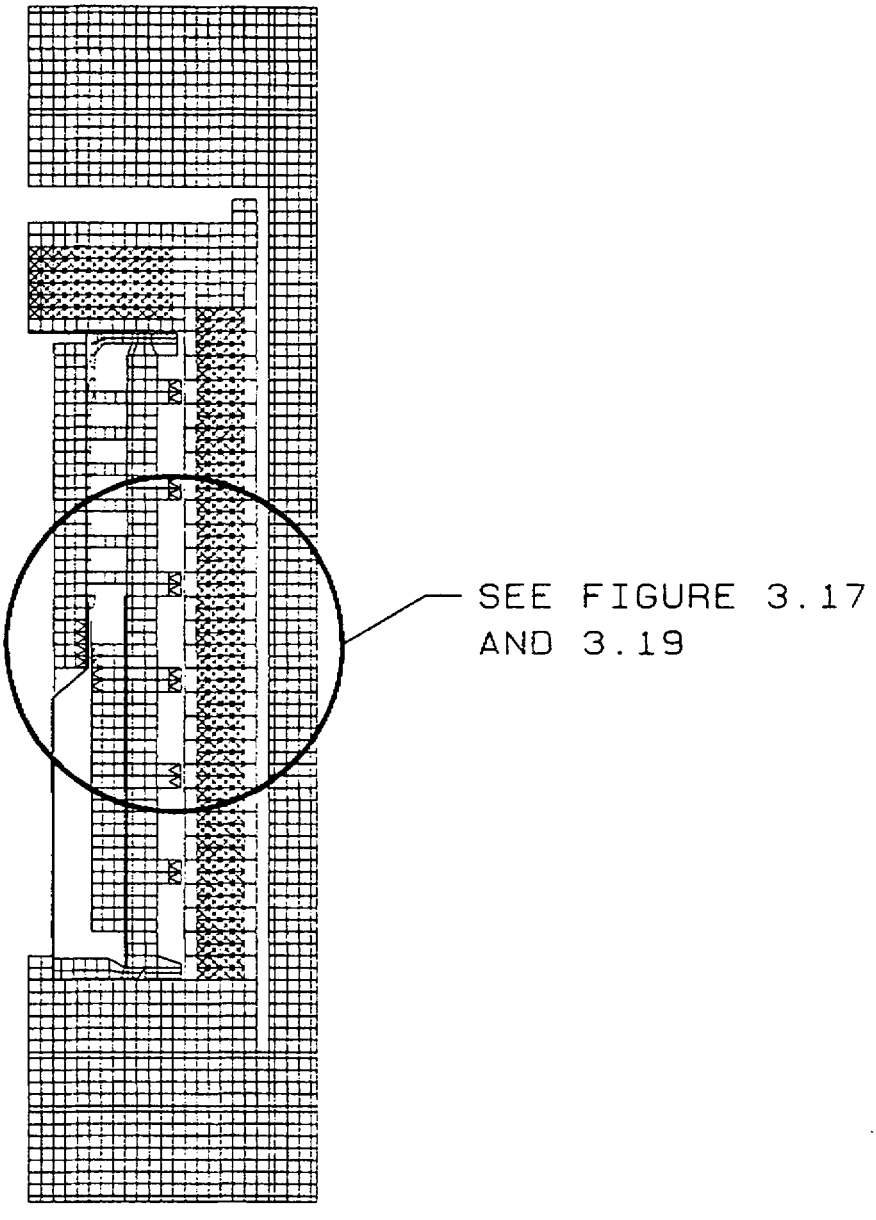

Figure 3.16. Transient Thermal Analysis – Post Fire
100°F Ambient With Maximum Decay Heat and Maximum Insolation, Time: 3.0 Hr

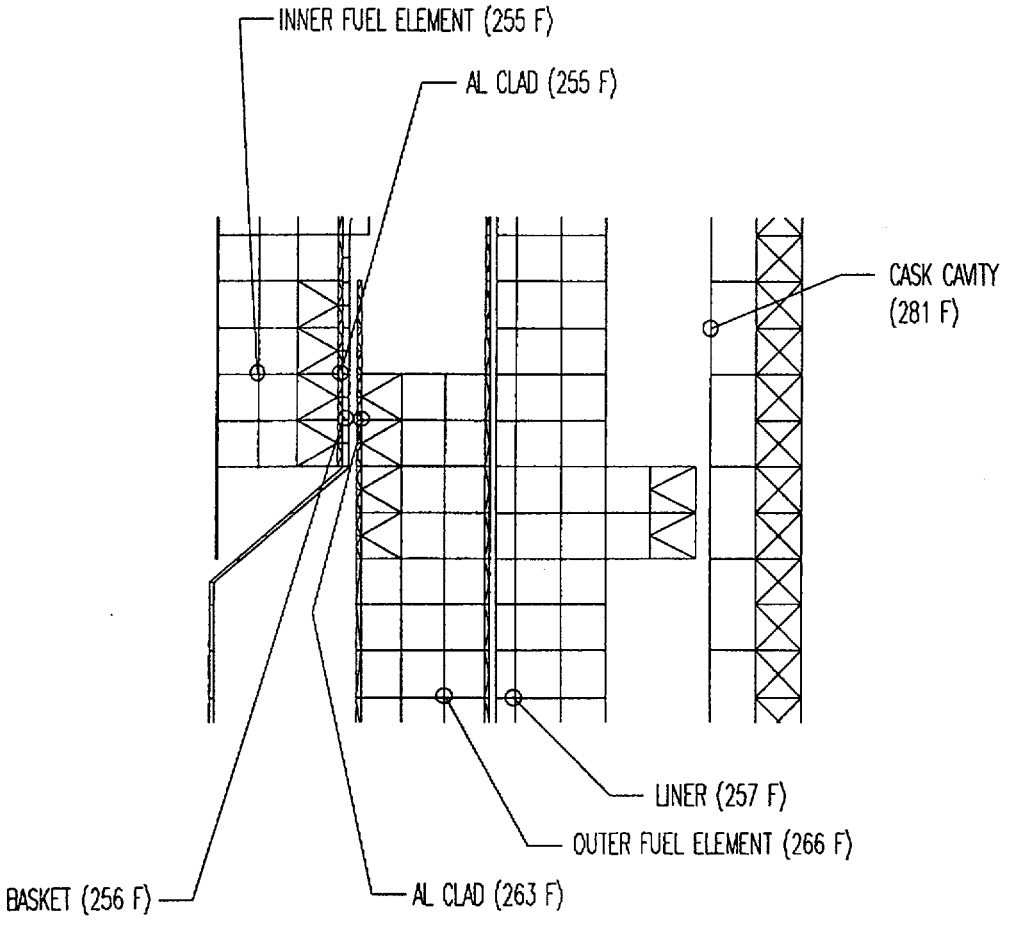

Figure 3.17. Transient Thermal Analysis – Temperature Plot
100°F Ambient With Maximum Decay Heat and Maximum Insolation, Time: 3.0 Hr

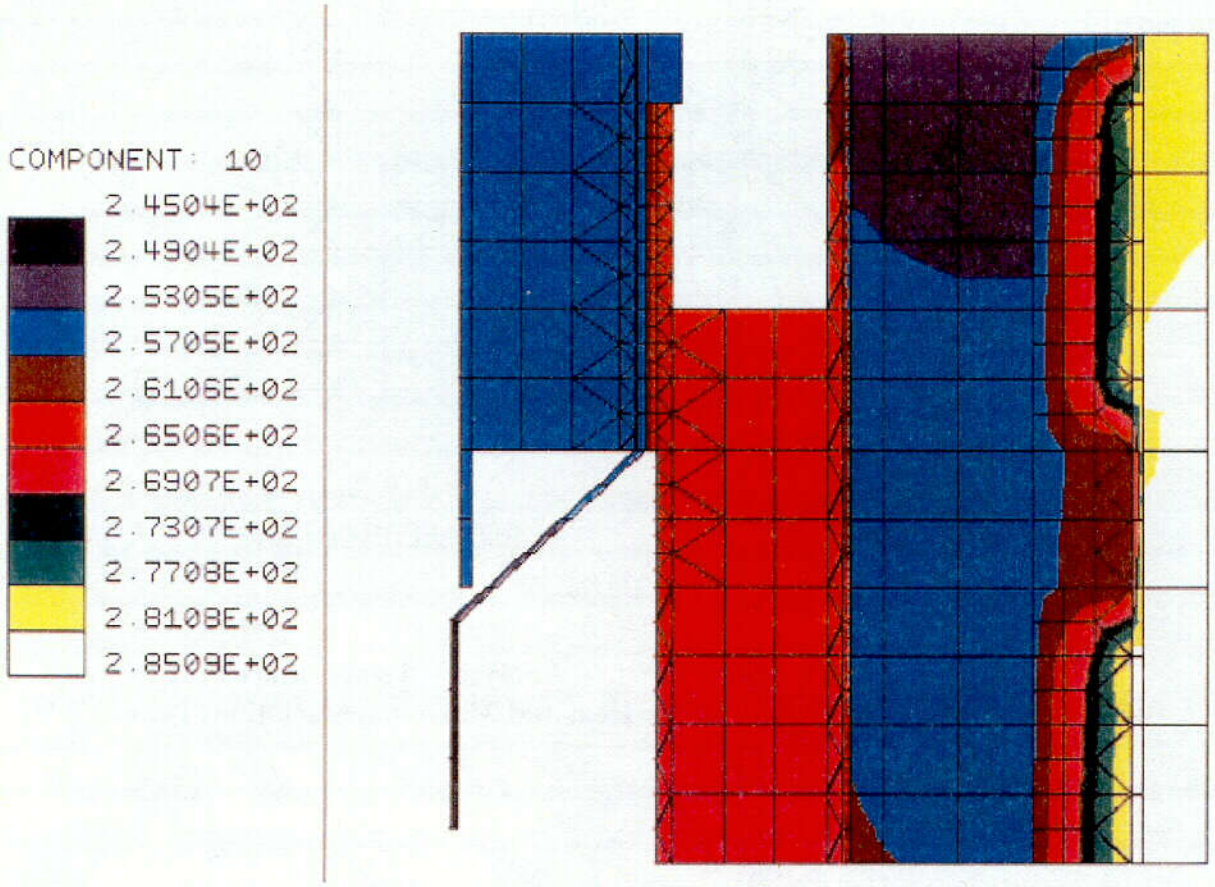

Figure 3.18. Transient Thermal Analysis – Contour Plot
100°F Ambient With Maximum Decay Heat and Maximum Insolation, Time: 3.0 Hr

C09

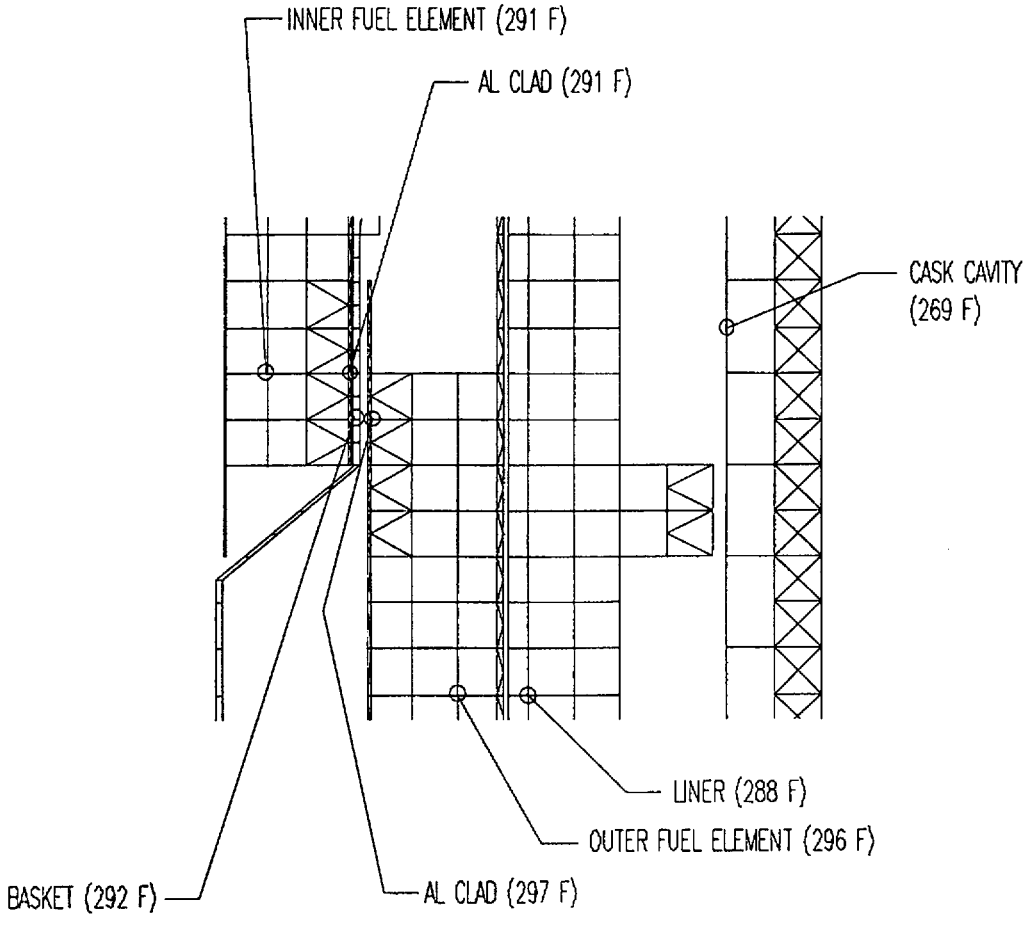

Figure 3.19. Transient Thermal Analysis – Temperature Plot
100°F Ambient With Maximum Decay Heat and Maximum Insolation, Time: 12.0 Hr

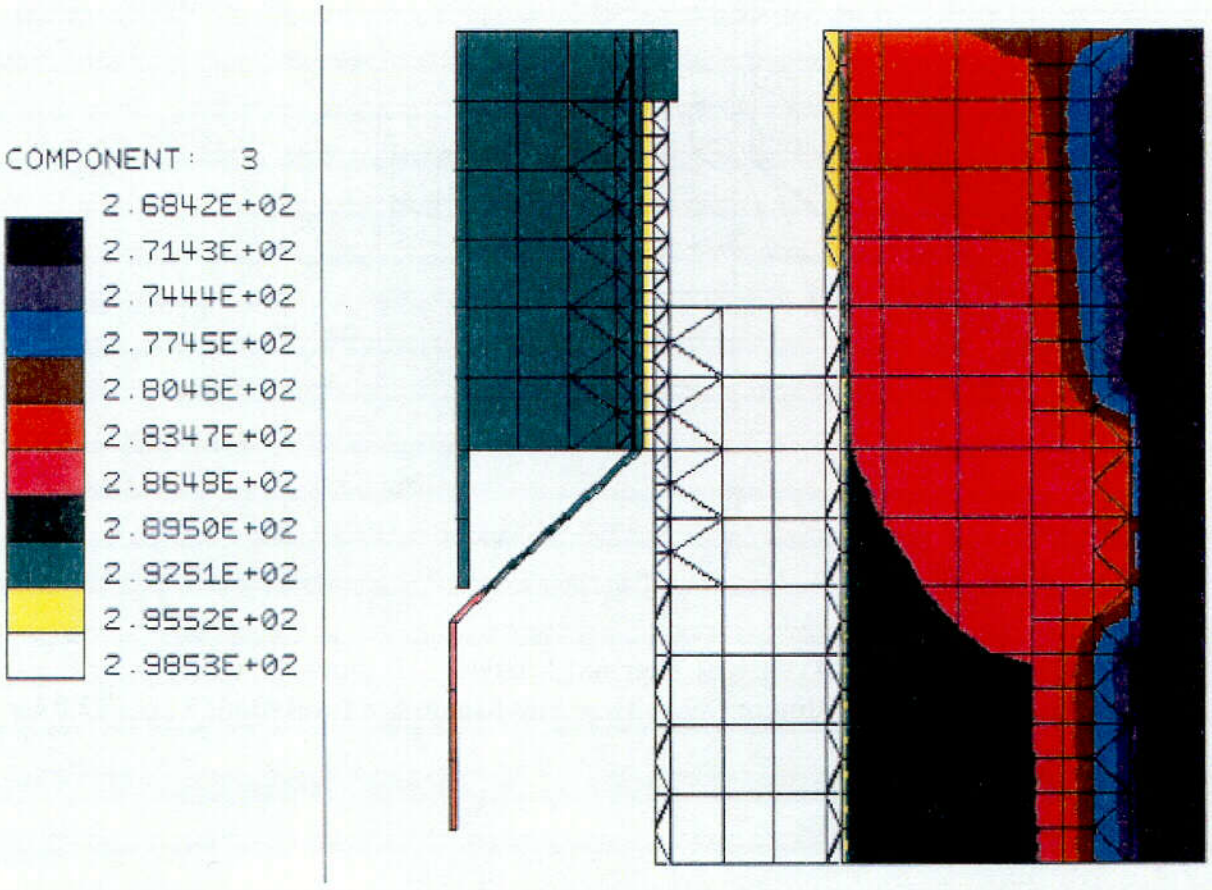

Figure 3.20. Transient Thermal Analysis – Contour Plot
100°F Ambient With Maximum Decay Heat and Maximum Insolation, Time: 12.0 Hr

C10

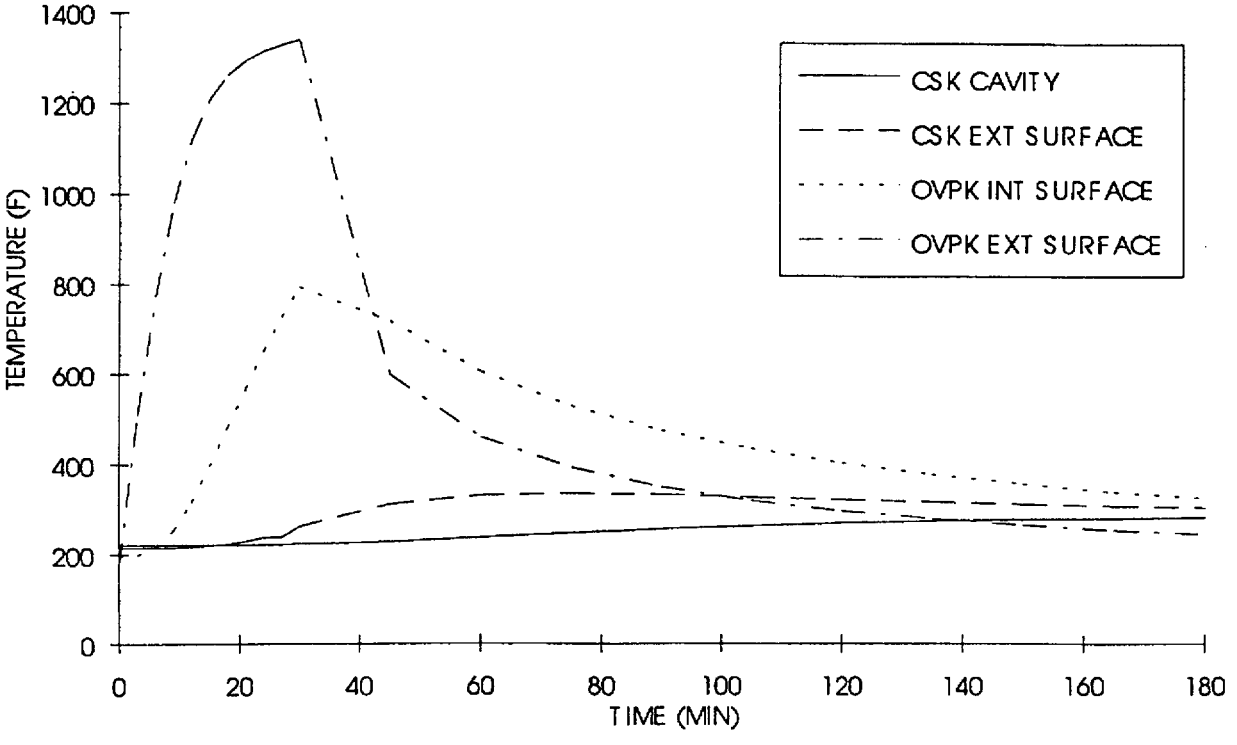

Figure 3.21. Temperature vs. Time, Fire Accident Transient – Overpack and Cask

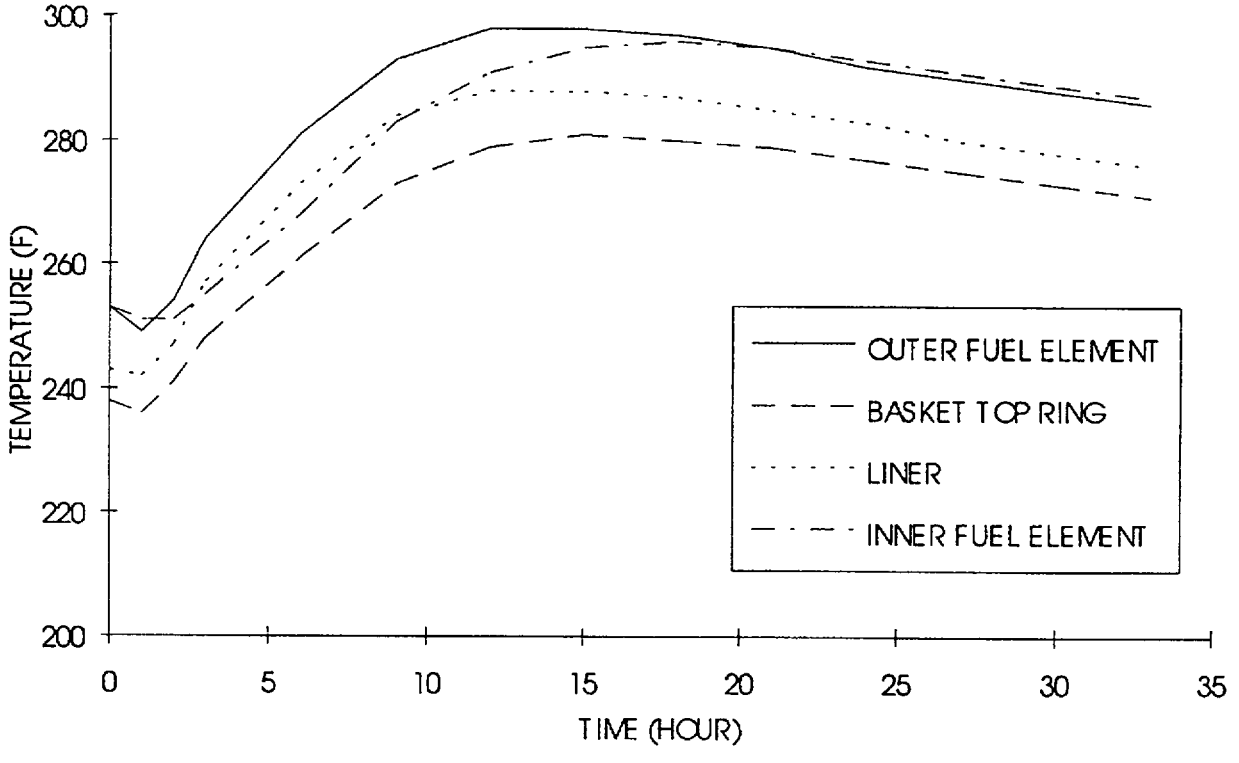

Figure 3.22. Temperature vs. Time, Fire Accident Transient – Fuel, Basket and Liner

3.6 REFERENCES

3.1. Safety Analysis Report, "G.E. Model 2000 Shipping Package", NEDO - 31581 April, 1988.

3.2. Touloukian, Y. S., Thermophysical Properties of Matter, Purdue University, 1970, Vol. 1, p. 191.

3.3. Ibid, Vol. 4, p. 115.

3.4. Heat Transfer Data Book, D. A. Kaminski, Ed.; General Electric Company, New York, 1981, Sct. G515.29, p. 5.

3.5. ASME, Boiler and Pressure Vessel Code, Section III, Division I, Appendix I, 1980.

3.6. Kreith, F., Principles of Heat Transfer, International Textbook Company, Pennsylvania, 2nd Ed., 1969, Table A-3.

3.7. Ibid, Table A-1.

3.8. Morris & Wendel, "HFIR System RELAP5 Input Model", Oak Ridge National Laboratory, ORNL/TM-11647, January, 1993.

3.9. Heat Transfer Data Book, D. A. Kaminski, Ed.; General Electric Company, New York, 1981, Sct. G515.5, p. 13.

3.10. USNRC Rules and Regulation, 10CFR71, "Packaging and Transportation of Radioactive Material", November, 1992.

3.11. Gebhart, B., Heat Transfer, McGraw-Hill Book Company, New York, 2nd Ed., 1971, p. 377.

3.12. Ibid, p. 355.

3.13. Ibid, p. 376.

3.14. Kreith, F., Principles of Heat Transfer, International Textbook Company, Pennsylvania, 2nd Ed., 1969, Table 5-2.

3.15. Gebhart, B., Heat Transfer, McGraw-Hill Book Company, New York, 2nd Ed., 1971, p. 371.

3.16. Kreith, F., Principles of Heat Transfer, International Textbook Company, 3.7.14. Pennsylvania, 2nd Ed., 1969, p. 340.

3.17. V. Quan and R. Pomares, "Thermal Test - GE Model 2000 Transport Package", May, 1993, Draft Report.

3.18. USNRC, Regulatory Guide 7.8, "Load Combinations for the Structural Analysis of Shipping Cask", May 1977.

3.7 APPENDIX

3.7.1 Thermal Test on GE Model 2000 Transport Package [3.17]

A thermal testing is done on a GE Model 2000 Transport Package to evaluate the performance of the thermal analytical model used in the analysis. The testing is done at ambient condition with 600 watts heat input in the cask cavity to simulate the maximum decay heat.

The LIBRA finite element model used for this evaluation is the same model except that the contents (fuel, basket and liner) are not included. Heat loading of 600 watts is uniformly distributed in the cask internal walls. At various points the casks are monitored for over forty hours continuously. Tested data and the LIBRA predictions of cavity wall temperature vs. time are plotted in Figure 3.23, which displays excellent correlation between test and analysis results. This physical test verifies the adequacy and accuracy of the LIBRA finite element thermal analysis model.

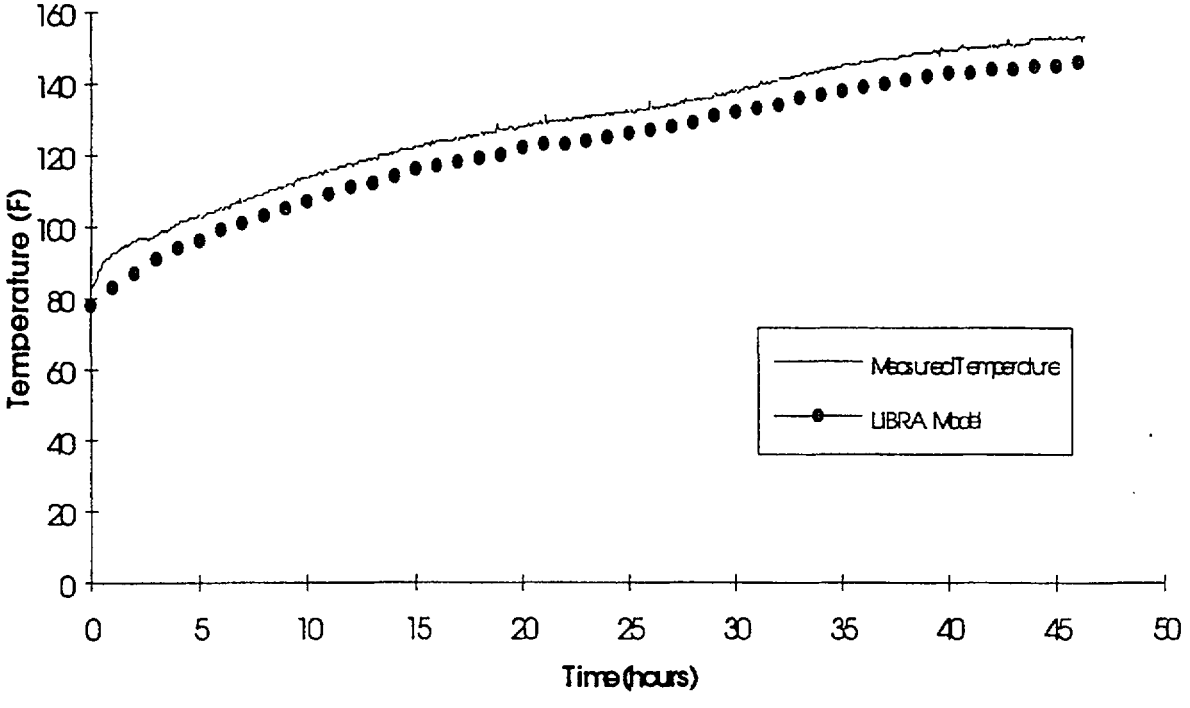

Figure 3.23. Cavity Wall Temperature – Thermal Test vs. LIBRA Model Model 2000 Transport Package with 600 Watts Heat

4.0 CONTAINMENT

The containment evaluation of the Model 2000 Transport Package is provided in Chapter 4.0 of the Package Safety Analyses Report (SAR), NEDO-31581, April 1988. It was demonstrated that the Package remains leak tight under all normal and specified hypothetical accident conditions. The use of the HFIR fuel basket and liner has no physical effect on the cask containment boundary. The HFIR fuel fission gas inventory for a burn up of 2300 MWD's and approximate 2 years cooling period is 26.34 gm Kr, 404.4 gm Xe, and 17.0 gm I. If these gases are released in the Model 2000 cask cavity which has 14.7 psia He pressure at a temperature of 300°F, the total pressure will be then 27.5 psia. This pressure of 27.5 psia is less than the design pressure of 30 psia. It should be noted that the fission gas is contained within the matrix of the metal fuel alloy. A fuel temperature exceeding 800°F would have to be achieved before the fission gas could be released. The maximum fuel temperature criteria is less than 400°F and the evaluation in Chapter 3.0 has shown a temperature of 294°F at the end of the Fire condition. Therefore, the Model 2000 design pressure is a conservative design basis for the shipment of the HFIR fuel, although assuming the release of the fission gas from the fuel matrix alloy, which is an unlikely event.

5.0 SHIELDING EVALUATION

The shielding analysis of the Model 2000 Package with the HFIR fuel basket and liner is described in this chapter. The Model 2000 Package contains one HFIR spent fuel assembly. The design basis fuel assembly has a maximum bump of 2300 megawatt days and an initial U-235 enrichment of 93% by weight. The fuel assembly has an asssumed minimum 2 years cooling time after discharge from the reactor.

The Model 2000 Package with the HFIR fuel basket and liner is shown in the following sections to provide adequate shielding to ensure compliance with the external dose rate requirements specified in 10CFR Part 71.47, 10CFR Part 71.51 [5.1], and 49CFR Part 173.441 [5.2] for the fuel parameters stated above.

5.1 DISCUSSION AND RESULTS

The Model 2000 Transport Package is designed for transporting irradiated fuel, hardware, and waste. In view of the above, there is no single specific source term. This evaluation is made specifically to consider shipments of irradiated fuel, cores from the HFIR reactor. The purpose of the shielding is to maintain the dose rates from the loaded container within DOT transportation limits. Calculations have been made to demonstrate that the normal and accident condition dose rates with the HFIR core fission product radionuclide load will not exceed the regulatory limits.

Theoretical analyses of the Model 2000 Transport Package shielding capabilities were performed for the HFIR spent fuel assembly. A shielding model was set up for an irradiated uranium fuel load. The uranium mass and operating conditions used for the analyzed case were 9,500 grams of U-235 at 93% enrichment operated at 100 MW for 23 days. The fission product inventory and gamma dose rate calculations for irradiated fuel were made with two Radiation Shielding Information Center (RSIC) provided computer codes, RIBD and ISOSHLD. RIBD generates the fission product inventory from irradiated fuel, and ISOSHLD is a point kernel, general purpose shielding analysis code. The neutron dose rates from HFIR cores are insignificant due to the fuel enrichment, composition and relatively short irradiation times.

The gamma source used in the irradiated fuel analysis consisted of the fission product inventory from 9,500 grams of U-235, in 93% enriched uranium, irradiated for 23 days at 100 MW and cooled for two years. The total beta and gamma decay heat from this source as calculated by RIBD was 595 watts, slightly below the 600-watt package limit.

The neutron dose rate was considered nil in this evaluation.

The 2000 Series Cask uses poured lead and stainless steel as the primary shielding media. The stainless steel structural shells of the overpack and distances to the outer surfaces of the overpack serve to further attenuate the radiation from the contents. The liner used for supporting the core sections also provides additional shielding in the stainless steel wall and tungsten alloy base.

The nominal thicknesses of shielding materials and distances, as determined from the fabrication drawings, were used in the shielding analysis. A cylindrical source geometry was used in the normal and accident cases, taking credit for self-shielding by the source material.

The summary of the maximum calculated dose rates from an irradiated fuel load is given in Table 5.1.

	Package Surface			1 Meter from Surface of Package			2 Meters from Side of Vehicle (Exclusive use)	Cab of Vehicle
	Side	Top	Bottom	Side	Top	Bottom		
Normal Conditions								
Gamma	66.7	14.2	34.1	13.4	5.7	12.1	3.6	0.9
Neutron								
Total	66.7	14.2	34.1	13.4	5.7	12.1	3.6	0.9
49 CFR part 173.441 Limit	200	200	200	—	—	—	10	2
Hypothetical Accident Conditions								
Gamma	66.7	14.2	34.1	13.4	5.7	12.1	—	—
Neutron								
Total	66.7	14.2	34.1	13.4	5.7	12.1	—	—
10 CFR Part 71 Limit	—	—	—	1000	1000	1000	—	—

Table 5.1. Summary of Maximum Dose Rates (mr/hr), From a Fuel Source

5.2 SOURCE SPECIFICATIONS

The fuel source consists of the radiation emitted by the decay of up to some 450 fission product isotopes calculated by computer code RIBD. The gamma photons are segregated into 25 energy groups for dose rate calculations. It is recognized that high-burnup low-enriched oxide fuel has a finite neutron emission rate from both spontaneous fissioning nuclides and alpha-neutron reactions with light elements (oxygen). However, the HFIR U_3O_8-Aluminum dispersion fuel is highly enriched in U-235 and experiences short (23-day) irradiation times which do not produce significant TRU to produce the neutron emission by alpha bombardment of oxygen atoms. This lack of a neutron dose rate from highly enriched fuel has been verified by years of experience with the fuel from the GETR and can be further demonstrated by calculations with codes such as ORIGEN.

The RIBD Code accounts for isotope decay and progeny buildup which results from the fission process during power production and the cooling following shutdown. The source is assumed to be uniformly distributed throughout two annular uranium volumes. The normal condition source is located at the centerline of the cask cavity, and since source deformation cannot be tolerated, the hypothetical accident condition source is assumed to be the same as the normal condition. The evaluations in Chapter 2 demonstrate the lack of damage to or degradation of the cask shielding and internal structures.

5.2.1 Gamma Sources

The sum of the fission products used as the cylindrical sources, after two years of decay, is 1.647E5 curies. Of this total fission product activity, the gamma source activity is 1.059E15 photons per second. The tabular list of the gamma photon source and the average energy of each group is shown below.

The RIBD Code uses an isotope library which contains the major decay modes, fission yields, and abundances in the calculation of a particular fission product source. The total photon data base resulting from the RIBD calculations is sorted into the 25 energy groups by a computer routine.

Details of these processes can be found in the code descriptions (References 5.3 and 5.4).

Of the 25 energy groups generated for ISOSHLD, only 22 groups contain a significant number of photons after two years of decay.

90-DAY DECAY, FISSION PRODUCT GAMMA SOURCE

Group	Total Group Production Rate (photons/sec)	Group Average Energy (MeV)
1	0.	1.500E-02
2	8.035E 10	2.500E-02
3	3.459E 11	3.500E-02
4	5.238E 09	4.500E-02
5	4.268E 09	5.500E-02
6	1.300E 09	6.500E-02
7	2.333E-19	7.500E-02
8	3.127E 13	8.500E-02
9	6.499E 08	9.500E-02
10	1.685E 14	1.500E-01
11	5.529E 11	2.500E-01
12	1.104E 11	3.500E-01
13	1.501E 14	4.750E-01
14	6.003E 14	6.500E-01
15	7.410E 13	8.250E-01
16	1.079E 13	1.000E 00
17	4.691E 12	1.225E 00
18	6.848E 12	1.475E 00
19	7.871E 10	1.700E 00
20	6.161E-01	1.900E 00

90-DAY DECAY, FISSION PRODUCT GAMMA SOURCE (Continued)

Group	Total Group Production Rate (photons/sec)	Group Average Energy (MeV)
21	1.057E 13	2.100E 00
22	6.349E 11	2.300E 00
23	2.947E-02	2.500E 00
24	0.	2.700E 00
25	1.080E-03	3.000E 00
TOTAL	**1.059E 15**	

5.2.2 Neutron Source

Neutron emissions from irradiated fuel are dependent on the fuel composition and burnup. The neutron dose rates from highly enriched uranium fuel is a small fraction of the neutron dose rate from low ennched power reactor fuel, the reason being that the amount of both oxygen and U-238 is lower in highly enriched aluminum-uranium plate-type fuel. These are the basic components required to produce neutrons from high burnup power reactor fuel. The U-238 is required for high-energy alpha-emitting transuranic nuclides which create neutrons by (α, n) reactions with oxygen in the oxide fuel. The low neutron output from HFIR-type highly enriched fuel can be verified by computer calculations with codes such as ORIGEN. Therefore, ignoring the neutron dose from the HFIR core is a justified assumption.

5.3 MODEL SPECIFICATION

5.3.1 Description of the Radial and Axial Shielding Configuration

A cutaway sketch of the package showing the normal and accident condition source and dose rate points is presented in Figure 5.1.

The simplified geometry used for the computer analysis (i.e., a cylindrical source shielded by iron, tungsten and lead) is shown in Figure 5.2. Iron is used in place of the stainless steel shells because it is one of the standard materials available in the ISOSHLD library, and there is no significant difference in attenuation properties.

FIGURE WITHHELD UNDER 10 CFR 2.390

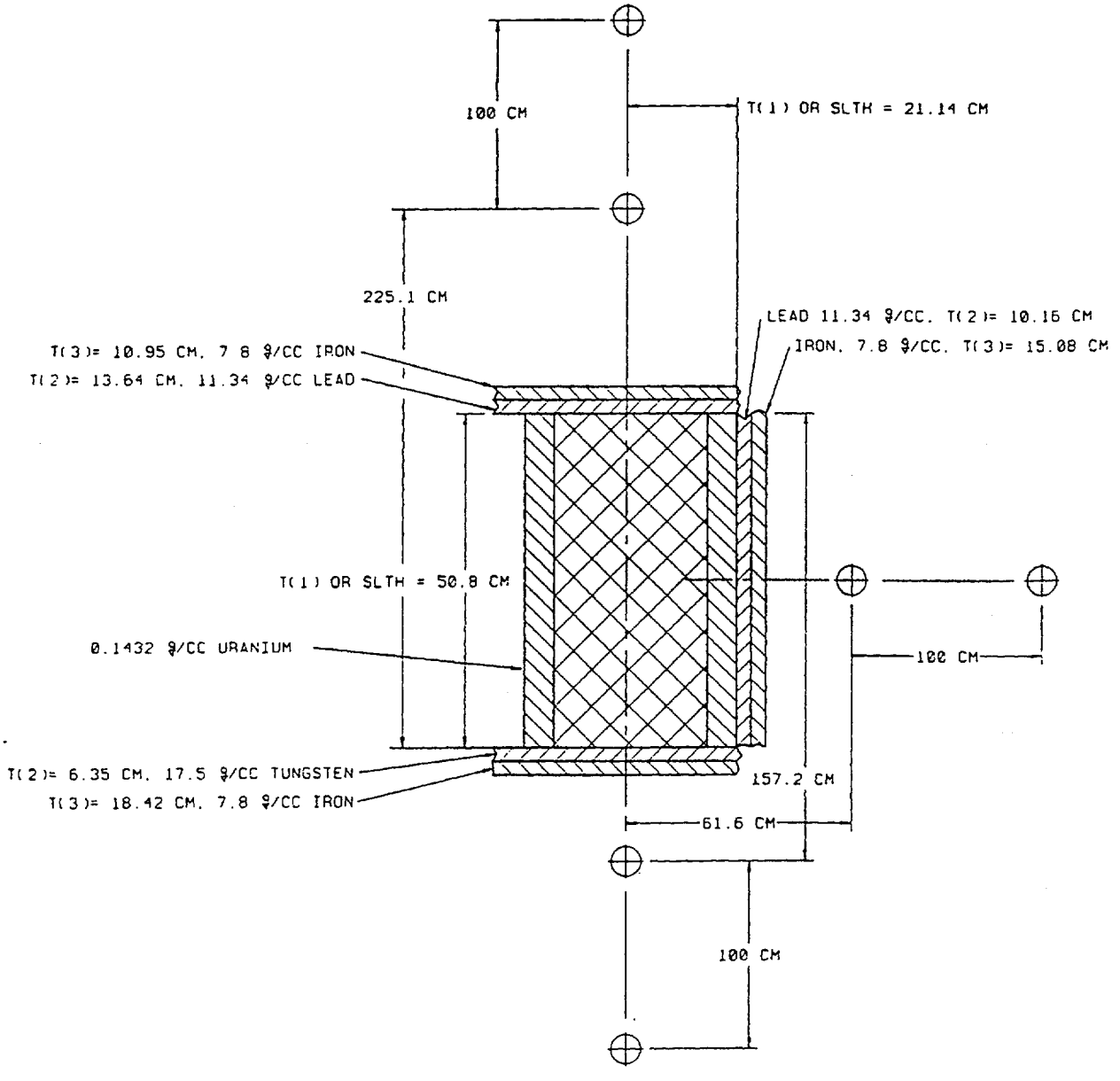

Figure 5.2. Source and Shield Models for ISOSHLD Core Input (Outer Core Case)

The stacked core components (inner core and outer core) were modeled in multiple evaluations. The outer core was first set up as a cylinder with the outside diameter of the outer core fuel. This cylinder contained a proportionately higher fraction of the total core activity to account for the "to-be-subtracted" center cylinder. Next, a model representing the "to-be-subtracted" center cylinder was run. This model likewise had a proportionate amount of the total core activity. The net dose rate from the outer core annulus was the difference between the first cylinder dose rates and the center cylinder dose rates. The side dose rates were calculated at three elevations: equivalent to the mid-plane of the outer core, the plane separating the two core elements, and at the mid-plane of the inner core. The same procedure was repeated for the inner core, and the dose rates Dom the evaluations were summed to give the total dose rates at the three elevations from the two core components. Similar subtraction and summing evaluations were done for the end case evaluations.

No reductions in the nominal shield thickness were made for localized penetrations or variations, such as drain lines or bolt holes. The justification for this decision is that only a small fraction of the source radiation would penetrate directly through shield depletions. Practically, any maximum dose rate from streaming or localized source concentration will be detected during the mandatory radiation surveys on loaded containers before shipment. The dose rates must comply with the appropriate transport limits.

There is no difference between the normal condition evaluation and the accident condition evaluation. In both evaluations, the distance from the centerline of the cylindrical source to the side dose points was equivalent to placing the source at the centerline of the cask cavity. No shield thickness changes were made for any of the evaluations.

5.3.2 Shield Regional Densities

The material densities used for the shielding analyses were:

Uranium in the fuel volume	0.1432 g/cc
Lead in the liner and cask	11.34 g/cc
Iron in the liner, cask and overpack	7.8 g/cc
Tungsten in Hevimet base plate	17.5 g/cc

5.4 SHIELDING EVALUATION

5.4.1 Fuel Source

The basic method of determining the estimated dose rates at the surface, one meter, two meters from the vehicle, and 21 feet (cab of vehicle) from the source in the Model 2000 transport container is outlined as follows.

1. The isotopic source was selected to be a mixture of the fission products which result from the 23-day irradiation of U-235 fuel followed by two years of cooling (decay). The operating power of the fuel was 100 MW.

2. The selected fuel operating and decay conditions were used as the input to the RIBD computer code portion of the combined RIBD and ISOSHLD codes. All of the fission products calculated by RIBD were used as source input to the ISOSHLD portion of the combined codes. The specific RIBD input parameters used are:

   Fuel operating power= 100 MW
   Operating time = 23 days
   Decay time after shutdown = 2 years
   Average thermal neutron flux = 1.0 v 10^{15} n/cm^2-s
   U-235 absorption cross section = 492 barns
   U-235 fission cross section = 416 barns
   U-238 absorption cross section = 2.71 barns
   U-235 weight = 9,500 grams
   Total U weight = 10,215 grams
   U-239 production rate= 0.093 g U-239/MWd

3. The normal condition geometry for the outer core consisted of a 20-in.-long x 16.64-in.-diameter cylindrical source centered in the cask shielded by a 4-in. slab of lead plus a 6-in. slab of iron at the side, a 5.37-in. slab of lead plus a 4.31-in. slab of iron at the top, and a 2.125-in. slab of tungsten plus a 7.25-in. slab of iron at the bottom. The input to ISOSHLD to express the relative geometry of a cylindrical source, slab shields, and the dose point requires differential thickness to define the point source elements, the thickness of the shields, the distance from the dose point to the center or end of the cylinder, and the dimensions of the cylinder.

The RIBD input values for the outer core model are:

	All Cases	Top Case	Bottom Case	Side Case
Source radius =	21.14 cm			
Source length =	0.80 cm			
Tungsten thickness =			5.398 cm	
Iron thickness =	—	10.95 cm	18.42 cm	15.08 cm
Lead thickness =	—	13.64 cm	0.00 cm	10.16 cm
Buildup shield =	—	Lead	Tungsten	Lead
Number of source division angles =		20	20	20 x 20
Source length or radius divisions =	—	2.54 cm	2.54 cm	1.057 cm
Distance to surface =	—	225.10 cm	156.21 cm	61.600 cm
Distance to one meter =	—	325.10 cm	256.21 cm	161.600 cm
Distance to two meters from vehicle =	—			321.9 cm
Distance to cab of truck =	—	—	—	639.4 cm

The RIBD-ISOSHLD computer program was selected for the shielding analysis because it is a public domain code (i.e., it is distributed by the RSIC for unrestricted use), and reasonable accuracy is possible with the standard isotope, attenuation, and buildup libraries included in the code. The results from the ISOSHLD evaluation could be reasonably duplicated by standard hand calculations, barring human error.

The gamma flux-to-dose rate conversion factors as a function of energy are given below.

Flux-to-Dose Rate Average Energy (MeV)	Conversion Factor (R/hr per MeV/cm^2-sec)
1.500E-02	8.230E-05
2.500E-02	1.730E-05
3.500E-02	6.349E-06
4.500E-02	3.280E-06
5.500E-02	2.289E-06
6.500E-02	1.891E-06
7.500E-02	1.714E-06
8.500E-02	1.618E-06
9.500E-02	1.603E-06
1.500E-01	1.728E-06
2.500E-01	1.960E-06
3.500E-01	2.060E-06
4.750E-01	2.039E-06
6.500E-01	2.080E-06
8.250E-01	2.000E-06
1.000E 00	1.930E-06
1.225E 00	1.841E-06
1.475E 00	1.761E-06
1.700E 00	1.710E-06
1.900E 00	1.660E-06
2.100E 00	1.600E-06
2.300E 00	1.540E-06
2.500E 00	1.520E-06
2.700E 00	1.480E-06
3.000E 00	1.430E-06

4. The summed gamma dose rates were compared with the regulatory dose rate limits, i.e., 200 mRem/hr at the surface, 2 mRem/hr in the vehicle cab, and 10 mRem/hr at two meters from the vehicle for exclusive use; and 1,000 mRem/hr at one meter for the accident case.

5.5 REFERENCES

5.1 Code of Federal Regulations, Title 10, Part 71, 1992.

5.2 Code of Federal Regulations, Title 49, Part 173, 1992.

5.3. RIBD, Radioisotope Buildup and Decay Code and Library, CCC-137.

5.4. ISOSHLD, Kernel Integration Code – General Purpose Isotope Shielding Analysis, CCC-79.

PAGE LEFT BLANK

5.6 APPENDIX

5.6.1 RIBD Input and Selected Summary Tables of Activities, Grams, Gram Atoms, and Decay Power

5.6.2 RIBD Generated Gamma Source Term Groups and Distribution of Activity in Various Core Components Used in ISOSHLD Models

5.6.3 ISOSHLD Input and Output for the Analysis of the Dose Rates at the Side of the Package From the Outer Core Plus the "Subtracted Center"

5.6.4 ISOSHLD Input and Output for the Analysis of the Dose Rates at the Side of the Package From the "subtracted Center" of the Outer Core

5.6.5 ISOSHLD Input and Output for the Analysis of the Dose Rates at the Top and Bottom of the Package from the Outer Core Plus the "Subtracted Center"

5.6.6 ISOSHLD Input and Output for the Analysis of the Dose Rates at the Top and Bottom of the "ackage From the "Subtracted" Center of the Outer Core

5.6.7 Summary Tabulation of the Calculated Dose Rates From the Various ISOSHLD Models of the Outer and Inner Core Components

APPENDIX 5.6.1

RIBD INPUT AND SELECTED SUMMARY TABLES OF ACTIVITIES, GRAMS, GRAM ATOMS, AND DECAY POWER

```
$$ ASIS,ROUT(1U),TAB(:,8,16,79),KEYWORD(BMM)
$:IDENT:V151,BMM,WW16,X4455
$:OPTION:FORTRAN
$:SELECT:ISHLD01
$:LIMITS:100,44K,,30K
$:REMOTE:05,1U
$:DATA:1*
   MODEL = 4
450  RIED LIBRARY CURRENT THRU JAN 74 (E.J. MORGAN JAN 74)
GE2000 HIGH FUEL, 100 MW 23 D              9.32BE-02          01
 1.0000E 02 2.3000E 01 9.777E-01 4.92 E 02 0.000E 00 0 0
 6.312E7 7.100E7 7.889E7 8.678E7 9.467E7 1.026E8 1.105E8 1.183E8 1.262E8
999999
```

CASE I.D. GE2000 HIFER FUEL. 100 MW 23 D WRITTEN BY SUBROUTINE FROG. PETE'S VERSION OF RIBD

CONVERSION RATIO G(U-239)/PIWD	0.093
SCRAM REACTIVITY. MILLI-K	0.
PROMPT NEUTRON LIFE, MSEC	0.
NUMBER OF EXTRA DECAY CARDS	0
OUTPUT OPTION REOUESTEO	1
FUEL POWER, MEGAWATTS	1.0000E 02
TIME AT THIS POWER. DAYS	2.3000E 01
EXPOSURE (FLUX*SIGMA25*TIME)	9.7770E-01
U-235 ABSORPTION CROSS-SECT.	4.9200E 02
PU239 FISSIONS/U235 FISSIONS	0.
NUMBER OF EXTRA IRRAD. CARDS	0

```
 EXP UNDERFLO     AT LOCATION              056561
 EXP UNDERFLO     AT LOCATION              057147
 EXP UNDERFLO     AT LOCATION              056561
 EXP UNOERFLO     AT LOCATION              057147
 EXP UNDERFLO     AT LOCATION              056566
 EXP UNDERFLO     AT LOCATION              056706
 EXP UNUERFLO     AT LOCATION              056706
 EXP UNDERFLO     AT LOCATION              036706
 EXP UNDERFLO     AT LOCATION              056706
 EXP UNDERFLO     AT LOCATION              056706
 EXP UNDERFLO     AT LOCATION              056706
 EXP UNDERFLO     AT LOCATION              056706
 EXP UNDERFLO     AT LOCATION              056706
 EXP UNDERFLO     AT LOCATION              056706
 EXP UNOERFLO     AT LOCATION              056706
 EXP UNDERFLO     AT LOCATION              056706
 EXP UNDERFLO     AT LOCATION              056706
 EXP UNDERFLO     AT LOCATION              056706
 EXP UNDERFLO     AT LOCATION              056706
 EXP UNDERFLO     AT LOCATION              056561
 EXP UNDERFLO     AT LOCATION              057147
 EXP UNDERFLO     AT LOCATION              056566
 EXP UNDERFLO     AT LOCATION              056561
 EXP UNDERFLO     AT LOCATION              057147
 EXP UNOERFLO     AT LOCATION              057316
**THIS IS THE LAST TIME THE ABOVE MESSAGE WILL APPEAR
```

DECAY POINTS – SECONDS

6.312E 07	7.100E 07	7.889E 07	8.678E 07	9.467E 07	1.026E 08	1.105E 08	1.183E 08	I.262E 08

GE2000 HIFER FUEL 100 MW 23 0 ACTIVITY AFTER SHUTDOWN - CU. W 2300.0 PIWO IN 23.0 DAYS. SUMMARY

ELEMENT SHUTDOWN		2.0 YRS.	2.3 YRS.	2.5 YRS	2.8 YRS .	3.0 YRS.	3.3 YRS.	3.5 YRS.	3.8 YRS.	4.0YRS.
30 ZN	9.488E01	0.	0.	0.	0.	0.	0.	0.	0.	0.
31 GA	6.499E 02	0.	0.	0.	0.	0.	0.	0.	0.	0.
32 GE	9.675E 03	0.	0.	0.	0.	0.	0.	0.	0.	0.
33 AS	3.283E 05	0.	0.	0.	0.	0.	0.	0.	0.	0.
34 SE	2697E 06	1.344E-02	I.344E-02	I.344E-02	I.344E-02	1.344E-02	I.344E-02	I.344E-02	I.344E-02	I.344E-02
35 BR	6.886E 06	0.	0.	0.	0.	0.	0.	0.	0.	0.
36 KR	1.860E 07	7.582E 02	7.461E 02	7.341E 02	7.224E 02	7.109E 02	6.994E 02	6.882E 02	6.774E 02	6.665E 02
37 RB	2.764E 07	9.317E-10	3.170E-11	1.074E-12	3.639E-14	1.233E-15	4.107E-17	1.386E-18	4.879E-20	I.646E -21
38 SR	2.443E 07	5.773E 03	5.704E 03	5.659E 03	5.621E 03	5.585E 03	5.550E 03	5.516E 03	5.482E 03	5.448E 03
39 Y	2.630E 07	5.900E 03	5.151E 03	5.676E 03	5.628E 03	5.589E 03	5.553E 03	5.518E 03	5.484E 03	5.450E 03
40 ZR	8.771E 06	4.690E 02	1.775E 02	6.716E 01	2.550E 01	9.763E 00	3.803E 00	1.569E 00	7.325E-01	4.106E-01
41 NB	2.553E 07	1.026E 03	3.881E 02	1.466E 02	5.540E 01	2.094E 01	7.864E 00	2.990E 00	1.159E 00	4.555E-01
42 MO	1.956E 07	0.	0.	0.	0.	0.	0.	0.	0.	0.
43 IC	2.209E 07	1.054E 00	1.054E 00	1.054E 00	1.054E 00	1.054E 00	1.054E 00	1.054E 00	1.054E 00	1.054E 00
44 RU	4.659E 06	1.716E 04	1.443E 04	1.213E 04	1.020E 04	8.577E 03	7.205E 03	6.057E 03	5.102E 03	4.289E 03
45 RH	6.165E 06	1.716E 04	1.443E 04	1.213E 04	1.020E 04	8.577E 03	7.205E 03	6.057E 03	5.102E 03	4.289E 03
46 PD	1.712E 06	1.351E-04	1.351E-04	1.351E-04	1.352E-04	1.351E-04	1.351E-04	1.351E-04	1.351E-04	1.351E-04
47 AG	1.134E 06	7.133E 00	5.594E 00	4.385E 00	3.437E 00	2.695E 00	2.110E 00	1.653E 00	1.300E 00	1.019E 00
4* CD	2.533E 04	3.452E-03	2.594E-03	2.374E-03	2.302E-03	2.263E-03	2.233E-03	2.205E-03	2.176E-03	2.151E-03
49 IN	3.687E 04	5.601E-11	1.582E-11	4.460E-12	1.258E-12	3.546E-13	9.936E-14	2.797E-14	8.002E-15	2.253E-15
50 SN	2.357E 06	9.324E 00	7.723E 00	6.541E 00	5.661E 00	4.998E 00	4.492E 00	4.105E 00	3.810E 00	3.576E 00
51 SB	1.700E 07	3.302E 02	3.097E 02	2.905E 02	2.724E 02	2.555E 02	2.395E 02	2.246E 02	2.108E 02	1.976E 02
52 TE	2.100E 07	2.120E 02	1.517E 02	1.164E 02	9.503E 01	8.136E 01	7.205E 01	6.525E 01	5.998E 01	5.555E 01
53 I	3.413E 01	2.261E-03	2.261E-03	2.261E-03	2.261E-03	2.261E-03	2.261E-03	2.261E-03	2.261E-03	2.261E-03
54 XE	2.929E 07	2.281E-14	1.175E-16	6.017E-19	3.080E-21	1.577E-23	7.859E-26	3.996E-28	0.	0.
55 CS	2.990E 07	8.198E 03	8.096E 03	7.999E 03	7.906E 03	7.817E 03	7.732E 03	7.651E 03	7.574E 03	7.500E 03
56 BA	2.618E 07	6.853E 03	6.814E 03	6.775E 03	6.736E 03	6.697E 03	6.658E 03	6.620E 03	6.582E 03	6544E 03
57 LA	2.129E 07	2.655E-11	1.901E-13	1.354E-15	9.635E-18	6.858E-20	4.761E-22	3.368E-24	2.536E-26	0.
58 CE	1.423E 07	4.082E 04	3.270E 04	2.619E 04	2.097E 04	1.680E 04	1.344E 04	1.076E 04	8.636E 03	6.914E 03
59 PR	1.166E 07	4.082E 04	3.270E 04	2.619E 04	2.097E 04	1.680E 04	1.344E 04	1.076E 04	8.636E 03	6.914E 03
60 NO	3.260E 06	2.413E-14	8.114E-17	2.708E-19	9.040E-22	3.017E-24	9.784E-27	0.	0.	0.
61 PM	2.407E 06	1.900E 04	1.779E 04	1.665E 04	1.558E 04	1.456E 04	1.364E 04	1.227E 04	1.196E 04	1.119E 04
62 SM	6.903E 05	3.241E 01	3.241E 01	3.235E 01	9.228E 01	3.222E 01	3.216E 01	3.210E 01	3.204E 01	3.197E 01
63 LU	1.763E 05	1.601E 02	1.511E 02	1.430E 02	1.354E 02	1.286E 02	1.222E 02	1.164E 02	1.112E 02	1.063E 02
64 GD	1.595E 04	5.902E 00	4.964E 00	4.173E 00	3.509E 00	2.950E 00	2.478E 00	2.063E 00	1.755E 00	1.475E 00
65 TB	4.960E 03	5937E 00	4.979E 00	4.180E 00	3.512E 00	2.952E 00	2.479E 00	2.084E 00	1.756E 00	1.476E 00
66 DY	4.716E 02	0.	0.	0.	0.	0.	0.	0.	0.	0.
67 NO	4.941E 01	0.	0.	0.	0.	0.	0.	0.	.	0.
68 ER	4.549E-03	0.	0.	0.	0.	0.	0.	0.	0.	0.
TOTAL	4.102E 08	1.647E 05	1.404E 05	1.209E 05	1.052E 05	9.227E 04	8.161E 04	7.284E 04	6.566E 04	5.961E 04

GE2000 HIFER FUEL. 100 MW 23 0 2300.0 MWD IN 23.0 DAYS SUMMARY

CONCENTRATION AFTER SHUTDOWN- GRAMS

ELEMENT	SHUTDOWN	2.0 YRS.	2.3 YRS.	2.5 YRS.	2.8 YRS.	3.0 YRS.	3.3 YRS.	3.5 YRS.	3.8 YRS.	4.0 YRS.
30 ZN	6.817E-05	0.	0.	0.	0.	0.	0.	0.	0.	0.
31 CA	2.432E-05	0.	0.	0.	0.	0.	0.	0.	0.	0.
32 GE	1.321E-02	1.256E-02	1. 256E-02	1.256E-02	1.256E-02	1.256E-02	1.256E-02	1.256E-02	1.256E-02	1.256E-02
33 AS	7.350E-03	3.923E-03	3.923E-03	3.923E-03	3.923E-03	3.923E-03	3.923E-03	3.923E-03	3.923E-03	3.923E-03
34 SE	7.746E-01	7.767E-01	7.767E-01	7.767E-01	7.767E-01	7.767E-01	7.767E-01	7.767E-01	7.767E-01	7.767E-01
35 BR	7.373E-01	7.079E-01	7.079E-01	7.079E-01	7.767E-01	7.079E-01	7.079E-01	7.079E-01	7.079E-01	7.079E-01
36 KR	2.684E 01	2.634E 01	2.631E 01	2.627E 01	2.624E 01	2.622E 01	2.619E 01	2.616E 01	2.613E 01	2.610E 01
37 RB	2.612E 01	2.645E 01	2.648E 01	2.651E 01	2.654E 01	2.637E 01	2.660E 01	2.663E 01	2.666E 01	2.665E 01
38 SR	9.819E 01	6.646E 01	6.621E 01	6.596E 01	6.572E 01	6.547E 01	6.523E 01	6.499E 01	6.475E 01	6.451E 01
39 Y	4.366E 01	3.374E 01	3.374E 01	3.374E 01	3.374E 01	3.374E 01	3.374E 01	3.374E 01	3.374E 01	3.374E 01
40 ZR	2.756E 02	2.615E 02	2.617E 02	2.620E 02	2.622E 02	2.625E 02	2.627E 02	2.630E 02	2.632E 02	2.634E 02
41 NB	6.140E 00	2.597E-02	9.885E-03	3.799E-03	1.506E-03	6.458E-04	3.260E-04	2.122E-04	1.756E-04	1.675E-04
42 MO	1.955E 02	2.470E 02	2.470E 02	2.470E 02	2.470E 02	2.470E 02	2.470E 02	2.470E 02	2.470E 02	2.470E 02
43 TC	6.613E 01	7.676E 01	7.676E 01	7.675E 01	7.675E 01	7.675E 01	7.675E 01	7.675E 01	7.675E 01	7.675E 01
44 RU	1.983E 02	1.476E 01	1.467E 02	1.461E 02	1.455E 02	1.450E 02	1.446E 02	1.443E 02	1.440E 02	1.437E 02
45 RH	6.928E 00	4.150E 01	4.150E 01	4.150E 01	4.150E 01	4.150E 01	4.150E 01	4.150E 01	4.150E 01	4.150E 01
46 PD	3.139E 01	4.729E 01	4.810E 01	4.878E 01	4.935E 01	4.983E 01	5.024E 01	5.058E 01	5.086E 01	5.110E 01
47 AG	5.842E 00	5.626E 00	5.626E 00	5.626E 00	5.626E 00	5.625E 00	5.625E 00	5.625E 00	5.625E 00	5.625E 00
48 CD	1.736E 00	2.337E 00	2.338E 00	2.338E 00	2.338E 00	2.338E 00	2.338E 00	2.338E 00	2.338E 00	2.338E 00
49 IN	6.450E-02	7.972E-02	7.972E-02	7.972E-02	7.972E-02	7.972E-02	7.972E-02	7.972E-02	7.972E-02	7.972E-02
50 SN	2.808E 00	2.498E 00	2.498E 00	2.498E 00	2.498E 00	2.498E 00	2.498E 00	2.498E 00	2.498E 00	2.498E 00
51 SB	1.966E 00	7.394E-01	7.203E-01	7.023E-01	6.854E-01	6.696E-01	6.548E-01	6.409E-01	6.280E-01	6.158E-01
52 TE	5.201E 01	3.358E 01	3.360E 01	3.361E 01	3.363E 01	3.365E 01	3.366E 01	3.367E 01	3.369E 01	3.370E 01
53 I	3.786E 01	1.700E 01	1.701E 01	1.701E 01	1.701E 01	1.701E 01	1.701E 01	1.701E 01	1.701E 01	1.701E 01
54 XE	3.963E 02	4.044E 02	4.044E 02	4.044E 02	4.044E 02	4.044E 02	4.044E 02	4.044E 02	4.044E 02	4.044E 02
55 CS	1.444E 02	1.719E 02	1.713E 02	1.708E 02	1.703E 02	1.697E 02	1.692E 02	1.687E 02	1.682E 02	1.677E 02
56 BA	1.336E 02	9.032E 01	9.086E 01	9.140E 01	9.192E 01	9.245E 01	9.296E 01	9.347E 01	9.397E 01	9.447E 01
57 LA	9.163E 01	8.450E 01	8.450E 01	8.450E 01	8.450E 01	8.450E 01	8.450E 01	8.450E 01	8.450E 01	8.450E 01
58 CE	2.650E 02	1.832E 02	1.806E 02	1.786E 02	1.770E 02	1.756E 02	1.746E 02	1.737E 02	1.731E 02	1.725E 02
59 PR	6.347E 01	8.447E 01	8.447E 01	8.447E 01	8.447E 01	8.447E 01	8.447E 01	8.447E 01	8.447E 01	8.447E 01
60 ND	1.977E 02	2.944E 02	2.970E 02	2.990E 02	3.007E 02	3.020E 02	3.031E 02	3.039E 02	3.046E 02	3.051E 02
61 PM	1.953E 01	2.045E 01	1.914E 01	1.791E 01	1.677E 01	1.569E 01	1.468E 01	1.374E 01	1.287E 01	1.204E 01
62 SM	3.560E 01	5.316E 01	5.447E 01	5.569E 01	5.584E 01	5.791E 01	5.892E 01	5.986E 01	6.073E 01	6.155E 01
63 EU	6.731E 00	5.811E 00	5.802E 00	5.793E 00	5.785E 00	5.778E 00	5.771E 00	5.764E 00	5.758E 00	5.752E 00
64 GD	1.589E 00	3.680E 00	3.692E 00	3.702E 00	3.712E 00	3.722E 00	3.731E 00	3.740E 00	3.748E 00	3.756E 00
65 TB	1.664E-01	1.337E-01	1.337E-01	1.337E-01	1.337E-01	1.337E-01	1.337E-01	1.337E-01	1.337E-01	1.337E-01
66 DY	7.471E-02	1.256E-01	1.260E-01	1.264E-01	1.267E-01	1.269E-01	1.272E-01	1.273E-01	1.275E-01	1.276E-01
67 HO	2.214E-03	2.171E-03	2.171E-03	2.171E-03	2.171E-03	2.171E-03	2.171E-03	2.171E-03	2.171E-03	2.171E-03
68 ER	3.885E-04	6.313E-04	6.313E-04	6.313E-04	6.313E-04	6.313E-04	6.313E-04	6.313E-04	6.313E-04	6.313E-04
TOTAL	2.434E 03	2.434E 03	2.434E 03	2.434E 03	2.434E 03	2.434E 03	2.434E 03	2.434E 03	2.434E 03	2.434E 03

GE2000 HIFER 100 MW 23 D 2300.0 MWD IN 23.0 DAYS SUMMARY

CONCENTRATION AFTER SHUTDOWN - GRAM ATOMS

ELEMENT	SHUTDOWN	2.0 YRS	2.3 YRS.	2.5 YRS.	2.8 YRS.	3.0 YRS.	3.3 YRS.	3.5 YRS.	3.6 Tits.	4.0 YRS.
30 ZN	9.468E-07	0.	0.	0.	0.	0.	0.	0.	0.	0.
31 GA	3.366E-07	0.	0.	0.	0.	0.	0.	0.	0.	0.
32 GE	1.747E-04	1.665E -04	1.665E-04	1.665E-04	1.665E-04	1.665E-0,	1.665E-04	1.665E-04	1.665E -04	1.665E-04
33 AS	9.674E-05	5.231E-05	5.231E-05	5.231E-05	5.231E-05	5.231E-05	5.231E-05	5.231E-05	5.231E-05	3.231E-05
34 SE	9.767E-03	9.796E-03	9.796E-03	9.796E-03	9.796E-03	9.796E-03	9.796E-03	9.796E-03	9.796E-03	9.796E-03
35 BR	9.092E-03	1.739E-03	6.739E-03	1.739E-03	1.739E-03	1.739E-03	6.739E-03	6.739E-03	1.739E-03	1.739E-03
36 KR	3.157E-01	3.096E-01	3.095E-01	3.091E-01	3.016E-01	3.064E-01	3.061E-01	3.077E-01	3.074E-01	3.071E-01
37 RR	3.023E-01	3.062E-01	3.066E-01	3.070E-01	3.073E-01	3.077E-01	3.060E-01	3.063E-01	3.067E-01	3.090E-01
38 SR	1.101E 00	7.451E-01	7.423E-01	7.395E-01	7.361E-01	7.341E-01	7.314E-01	7.267E-01	7.260E-01	7.234E-01
39 Y	4.126E-01	3.791E-01	3.791E-01	3.791E-01	3.791E-01	3.791E-01	3.791E-01	3.791E-01	3.791E-01	3.791E-Ol
40 ZR	2.931E 00	2.102E 00	2.105E 00	2.101E 00	2.110E 00	2.113E 00	2.116E 00	2.116E 00	2.121E 00	2.124E 00
41 NB	6.456E-02	2.734E-04	1.041E-04	4.001E -05	1.516E-05	6.124E-06	3.,61E-06	2.265E-06	1.112E-06	1.799E-06
42 MO	1.916E 00	2.532E 00	2.532E 00	2.533E 00	2.533E 00	2.533E 00	2.533E 00	2.533E 00	2.533E 00	2.533E 00
43 TC	6.563E-01	7.636E-01	7.636E-01	7.636E-01	7.636E-01	7.636E-01	7.636E-01	7.636E-01	7.636E-01	7.636E-01
44 RU	1.932E 00	1.444E 00	1.436E 00	1.430E 00	1.424E 00	1.420E 00	1.416E 00	1.413E 00	1.410E 00	1.406E 00
45 RH	6.713E-02	4.029E-01	4.029E-01	4.029E-01	4.029E-01	4.029E-01	4.029E-01	4.029E-01	4.029E-01	4.029E-01
46 PO	2.949E-01	4.451E-01	4.527E-01	4.591E-01	4.645E-Ol	4.690E-01	4.729E-01	4.761E-01	4.711E-01	4.110E-01
47 AG	5.350E-02	5.162E-02	5.162E-02	5.161E-02	5.161E-02	5.161E-02	5.161E-02	5.161E-02	5.161E-02	5.161E-02
48 CO	1.553E-02	2.095E-02	2.095E-02	2.096E-02	2.096E-02	2.096E-02	2.096E-02	2.096E-02	2.096E-02	2.096E-02
49 IN	5.606E-04	6.932E-04	6.932E-04	6.932E-04	6.932E-04	6.932E-04	6.932E-04	6.932E-04	6.932E-04	6.932E-04
50 SN	2.259E-02	2.012E-02	2.011E-02	2.011E-02	2.011E-02	2.011E -02	2.011E-02	2.011E-02	2.011E-02	2.010E-02
51 SB	1.561E-02	6.011E-03	5.156E-03	5.715E-03	5.560E-03	5.453E-03	5.334E-03	5.223E-03	5.121E-03	5.023E-03
52 TE	3.995E-01	2.592E-01	2.593E-01	2.594E-01	2.596E-01	2.597E-01	2.596E-01	2.599E-01	2.600E-01	2.601E-Ol
53 I	2.697E-01	1.323E-01	1.323E-01	1.323E-01	1.323E-01	1.323E-01	1.323E-01	1.323E-01	1.323E-01	1.323E-01
54 XE	2.941E 00	3.012E 00	3.012E 00	3.012E 00	3.012E 00	3.012E 00	3.012E 00	3.012E 00	3.012E 00	3.012E 00
55 CS	1.066E 00	1.273E 00	1.269E 00	1.265E 00	1.261E 00	1.256E 00	1.254E 00	1.250E 00	1.246E 00	1.243E 00
56 BA	9.629E-01	6.549E-01	6.569E-01	6.626E-01	6.666E-01	6.704E-01	6.742E-01	6.760E-01	6.616E-01	6.653E-01
57 LA	6.566E-01	6.079E-01	6.079E-01	6.079E-01	6.079E-01	6.079E-01	6.079E-01	6.079E-01	6.079E-01	6.079E-01
58 CE	1.665E 00	1.291E 00	1.210E 00	1.266E 00	1.254E 00	1.245E 00	1.236E 00	1.232E 00	1.227E 00	1.224E 00
59 PR	4.455E-01	5.991E-01	5.991E-01	5.991E-01	5.991E-01	5.991E-01	5.991E-01	5.991E-01	5.991E-01	5.991E-01
60 ND	1.356E 00	2.033E 00	2.051E 00	2.065E 00	2.076E 00	2.015E 00	2.093E 00	2.096E 00	2.103E 00	2.107E 00
61 PM	1.324E-01	1.391E-01	1.302E-01	1.219E-01	1.141E-01	1.067E-01	9.967E-02	9.347E-02	1.754E-02	1.193E-02
62 SM	2.356E-01	3.549E-01	3.636E-01	3.721E-Ol	3.799E-01	3.172E-01	3.941E-01	4.004E-01	4.063E-01	4.119E-01
63 EU	4.371E-02	3.796E-02	3.790E-02	3.714E-02	3.779E-02	3.774E-02	3.770E-02	3.765E-02	3.762E-02	3.756E-02
64 GD	1.012E-02	2.353E-02	2.360E-02	2.367E-02	2.374E-02	2.310E-02	2.316E-02	2.392E-02	2.397E-02	2.402E-02
65 TB	1.043E-03	1.412E-04	1.412E-04	1.412E-04	1.411E-04	1.411E-04	1.411E-04	1.411E-04	6.411E-04	1.411E-04
66 DY	4.626E-04	7.715E-04	7.112E-04	7.134E-04	7.153E-04	7.161E-04	7.161E-04	7.192E-04	7.902E-04	7.909E-04
67 HO	1.341E-OS	1.316E-05	1.316E-05	1.316E-05	1.316E-05	1.316E-05	1.316E-05	1.316E-05	1.316E-05	1.316E-05
61 ER	2.340E-06	3.103E-06	3.103E-06	3.103E-06	3.103E-06	3.103E-06	3.603E-06	3.103E-06	3.103E-06	3.103E-06
TOTAL	2.067E 01	2.067E 01	2.067E 01	2.067E 01	2.067E 01	2.067E 01	2.067E 01	2.067E 01	2.067E 01	2.067E 01
POISON	44.7	53.5	53.5	53.6	53.6	53.7	53.7	53.6	53.8	53.1

TOTAL BARNS/TOTAL FISSIONS - EXCLUDING XE 135. SM 149, AND SM 151

GE2000 HIFER FUEL, 100 M11 23 0 BETA POWER AFTER SHUTDOWN - MW 2300.0 MWD IN 23.0 DAYS. SUMMARY

ELEMENT	SHUTDOWN	2.0 YRS.	2.3 YRS.	2.5 YRS.	2.1 YRS.	3.0 YRS.	3.3 YRS.	3.5 YRS.	3.8 YRS.	4.0 YRS.
30 ZN	4.602E-07	0.	0.	0.	0.	0.	0.	0.	0.	0.
31 GA	7.134E-06	0.	0.	0.	0.	0.	0.	0.	0.	0.
32 GE	2.633E-05	0.	0.	0.	0.	0.	0.	0.	0.	0.
33 AS	2.756E-03	0.	0.	0.	0.	0.	0.	0.	0.	0.
34 SE	4.358E-02	3.116E-12	3.156E-12	3.116E-12	3.116E-12	3.116E-12	3.116E-12	3.116E-12	3.116E-12	3.116[-12
35 BR	9.101E-02	0.	0.	0.	0.	0.	0.	0.	0.	0.
36 KR	2.447E-01	1.124E-06	1.106E-06	1.011E-06	1.070E-06	1.053E-06	1.036E-06	1.020E-06	1.004E-06	9.177E-07
37 RB	4.704E-01	3.645E-18	1.240E-19	4.202E-21	1.424E-22	4.124E-24	1.607E-25	5.420E-27	1.909E-21	6.440E-30
38 SR	2.931E-01	6.951E-06	6.794E-06	6.711E-06	6.666E-06	6.622E-06	6.510E-06	6.539E-06	6.499E-06	6.459E-06
39 Y	2.593E-01	3.253E-05	3.192E-05	3.159E-05	3.134E-05	3.114E-05	3.094E-05	3.074E-05	3.055E-05	3.037E-05
40 ZR	4.635E-02	3.335E-07	1.261E-07	4.764E-07	1.100E-01	6.110E-09	2.571E-09	9.117E-10	3.167E-10	1.576E-10
41 NB	2.046E-01	2.519E-07	9.797E-OS	3.701E-01	1.391E-01	5.279E-09	1.954E-09	7.412E-10	2.157E-10	1.071E-10
42 M0	6.295E-02	0.	0.	0.	0.	0.	0.	0.	0.	0.
43 TC	1.247E-01	5.250E-10	5.250E-10	5.250E-10	5.250E-10	5.250E-10	5.250E-10	5.250E-10	5.250E-10	5.250E-10
44 RU	9.970E-03	1.018E-06	1.556E-07	7.192E-07	6.047E-07	5.014E-07	4.271E-07	3.590E-07	3.024E-07	2.542E-07
45 RH	2.513E-02	1.424E-04	1.19•[-04	1.007E-04	1.465E-05	7.181E-05	5.979E-05	5.026E-05	4.234E-05	3.559E-05
46 PD	2.429E-03	1.121E-14	1.121E-14	1.121E-14	1.121E-14	1.121E-14	1.121E-14	1.121E-14	1.121E-14	1.121E-14
47 AC	1.534E-03	3.130E-09	3.003E-09	2.354E-09	1.146E-09	1.447E-09	1.133E-09	8.878E-10	6.979E-10	5.469E-10
48 CD	1.093E-04	6.429E-12	3.391E-12	2.671E-12	2.419E-12	2.422E-12	2.314E-12	2.353E-12	2.324E-12	2.295E-12
49 IN	1.126E-04	1.293E-19	3.652E-20	1.030E-20	2.904E-21	1.117E-22	2.294E-22	6.458E-23	1.147E-23	5.201E-24
50 SN	5.221E-02	5.723E-09	4.495E-09	3.746E-09	3.217E-09	3.004E-09	2.125E-09	2.711E-09	2.636E-09	2.514E-09
51 SB	2.247E-01	1.111E-07	1.764E-07	1.654E-07	1.552E-07	1.455E-07	1.364E-07	1.210E-07	1.201E-07	1.126E-07
52 TE	8.461E-02	8.337E-01	4.563E-01	2.497E-01	1.366E-01	7.471E-09	4.010E-09	2.231E-09	1.229E-09	6.723E-10
53 I	2.199E-01	6.700E-13	6.700E-13	6.700E-13	6.700E-13	6.700E-13	6.700E-13	6.700E-13	6.700E-13	6.700E-13
54 XE	2.251E-01	0.	0.	0.	0.	0.	0.	0.	0.	0.
55 CS	3.170E-01	9.541E-06	9.434E-0d	9.332E-06	9.234E-06	9.140E-06	9.049E-06	1.962E-06	1.110E-06	8.799E-06
56 BA	1.496E-01	4.103E-20	2.939E-22	2.092E-24	1.489E-26	1.060E-28	7.351E-31	5.205E-33	3.920E-35	0.
57 LA	1.605E-01	7.553E-20	5.410E-22	3.151E-24	2.741E-26	1.951E-28	1.355E-30	9.512E-33	7.217E-36	0.
58 CE	4.177E-02	1.936E-05	1.551[-05	1.242E-05	9.945E-06	7.964E-06	6.371E-06	5.101E-06	4.095E-06	3.279E-06
59 PR	6.693E-02	2.952E-04	2.365[-04	1.194E-04	1.517E-04	1.215E-04	9.716E-05	7.779E-05	6.245E-06	5.000E-05
60 ND	7.930E-03	3.290E23	1.106E-25	3.692E-21	1.232E-30	4.114E-33	1.334E-35	0.	0.	0.
61 PM	6.341E-03	6.645E-06	6.220[-06	5.122E-06	5.449E-06	5.099E-06	4.771E-06	4.465E-06	4.112E-06	3.914E-06
62 SM	1.227E-03	3.657E-09	3.650E-09	3.643E-09	3.636E-09	3.629E-09	3.622E-09	3.615E-09	3.601E-09	3.601E-09
63 EU	7.165E-04	1.014E-07	1.052[-07	1.023E-07	9.951E-01	9.703E-08	9.463E-01	9.239E-01	9.031E-01	1.133E-01
64 GD	3.559E-05	1.119E-01	1.000[-01	1.411E-09	7.072E-09	5.946E-09	4.995E-09	4.199E-09	3.537E-09	2.973E-09
65 TB	5.953E-06	5.113E-01	4.946E-01	4.157E-01	9.495E-01	2.939E-08	2.469E-01	2.075E-01	1.741E-01	1.469E-01
66 DY	6.449E-07	0.	0.	0.	0.	0.	0.	0.	0.	0.
67 H0	1.962E-07	0.		0.	0.	0.	0.	0.	0.	0. 0.
61 ER	0.	0.		0.	0.	0.	0.	0.	0.	0. 0.
92 U 239	1.750E-02	0.		0.	0.	0.	0.	0.	0.	0. 0.
93 NP239	3.911E-03	0.		0.	0.	0.	0.	0.	0.	0. 0.
TOTAL	3.561E 00	5.151E-04	4.217E-04	3.512E-04	3.010E-04	2.545E-04	2.164E-04	1.155E-04	1.606E-04	1.399E-04
NOBLES	4.708E-01	1.124E-06	1.106E-06	1.088E-06	1.070E-06	1.053E-06	1.036E-06	1.020E-06	1.004E-06	9.177E-07
HALOGENS	3.179E-01	6.700E-13	6.700E-13	6.700E-13	6.700E-13	6.700E-13	6.700E-13	6.700E-13	6.700E-13	6.700E-13
VOLATILES	1.296E 00	9.119E-06	9.656E-06	9.522E-06	9.402E-06	9.293E-06	9.190E-06	9.092E-06	9.001E-06	1.912E-06
OTHERS	1.477E 00	5.049E-04	4.179E-04	3.476E-04	2.905E-04	2.441E-04	2.062E-04	1.754E-04	1.505E-04	1.300E-04
TOTAL LESS NOBLES	3.091E 00	5.147E-04	4.276E-04	3.571E-04	2.999E-04	2.534E-04	2.154E-04	1.145E-04	1.596E-04	1.319E-04

SUBTOTALS

GE2000 HIFER FU(0 MW 23 D 2300.0 MWD IN 23.0 DAYS 1MARY

GAMMA POWER AFTER SHUTDOWN - MW

ELEMENT	SHUTDOWN	2.0 YRS.	2.3 YRS.	2.5 YRS.	2.8 YRS.	3.0 YRS.	3.3 YRS.	3.5 YRS.	3.1 YRS.	4.0 YRS.
30 ZN	4.669E-07	0.	0.	0.	0.	0.	0.	0.	0.	0.
31 GA'	5.530E-06	0.	0.	0.	0.	0.	0.	0.	0.	0.
32 GE	2.373E-05	0.	0.	0.	0.	0.	0.	0.	0.	0.
33 AS	7.247E-03	0.	0.	0.	0.	0.	0.	0.	0.	0.
34 SE	8.036E-04	0.	0.	0.	0.	0.	0.	0.	0.	0.
35 BR	4.292E-02	0.	0.	0.	0.	0.	0.	0.	0.	0.
36 KR	1.204E-01	1.798E-08	1.769E-01	1.741E-01	1.713E-08	1.685E-00	1.658E-08	1.632E-08	1.606E-08	1.510E-08
37 RB	1.410E-01	5.357E-19	1.823E-20	6.176E-22	2.093E-23	7.090E-25	2.361E-26	7.966E-28	2.805E-29	9.464E-31
38 SR	6.540E-02	5.659E-11	1.678E-11	4.968E-12	1.471E-12	4.354E-13	1.281E-13	3.786E-14	1.137E-14	3.360E-15
39 Y	6.453E-02	1.434E-08	1.154E-08	1.054E-08	1.016E-08	9.991E-09	9.892E-09	9.118E-09	9.754E-09	9.692E-09
40 ZR	1.137E-02	2.023E-06	7.649E-07	2.889E-07	1.091E-07	4.120E-08	1.548E-01	5.139E-09	2.230E-09	8.410E-10
41 NB	1.035E-01	4.590E-06	1.737E-06	6.561E-07	2.478E-07	9.358E-08	3.517E-08	1.327E-08	5.070E-09	1.915E-09
42 MO	1.061E-01	0.	0.	0.	0.	0.	0.	0.	0.	0.
43 IC	8.199E-02	0.	0.	0.	0.	0.	0.	0.	0.	0.
44 RU	1.425E-02	1.026E-08	2.113E-09	4.342E-10	8.922E-I1	1.133E-11	3.737E-12	7.663E-13	1.603E-13	3.288E-14
45 RH	2.720E-02	2.258E-05	1.899E-05	1.597E-05	1.342E-05	1.129E-05	9.481E-06	7.970E-06	6.714E-06	5.644E-06
46 PO	1.048E-03	0.	0.	0.	0.	0.	0.	0.	0.	0.
47 AG	7.940E-04	1.129E-07	8.850E-08	6.938E-08	5.439E-08	4.263E-08	3.338E-08	2.616E-08	2.056E-01	1.612E-08
48 CD	7.523E-05	2.341E-13	5.701E-14	1.624E-14	6.151E-15	4.658E-15	4.115E-15	3.954E-15	3.181E-15	3.127E-15
49 IN	1.821E-04	3.220E-20	9.095E-21	2.564E-21	7.231E-22	2.039E-22	5.712E-23	1.608E-23	4.601E-24	1.295E-24
50 SN	1.050E-03	3.137E-09	2.458E-09	1.938E-09	1.540E-09	1.234E-09	9.971E-10	1.149E-10	6.755E-10	5.659E-10
51 SB	2.326E-02	6.126E-07	7.622E-07	7.148E-07	6.704E-07	6.287E-07	5.894E-07	3.528E-07	5.118E-07	4.165E-07
52 TE	5.574E-02	1.115E-07	9.164E-08	7.186E-08	7.008E-01	6.360E-08	5.846E-01	5.419E-08	5.051E-08	4.717E-08
53 I	3.088E-01	5.360E-13	5.360E-13	5.360E-13	5.360E-13	5.360E-13	5.360E-13	5.360E-13	5.360E-13	5.360E-13
54 XE	6.114E-02	2.217E-23	1.143E-25	5.849E-28	2.994E-30	1.533E-32	7.640E-35	3.185E-37	0.	0.
55 CS	8.967E-02	7.041E-06	6.490E-06	5.976E-06	5.502E-06	5.066E-06	4.663E-06	4.293E-06	3.956E-06	3.642E-06
56 BA	2.272E-02	2.689E-05	2.674E-05	2.658E-05	2.643E-05	2.628E-05	2.613E-05	2.597E-05	2.583E-05	2.568E-05
57 LA	1.111E-01	3.883E-19	2.712E-21	1.980E-23	1.409E-25	1.003E-27	6.965E-30	4.927E-32	3.711E-34	0.
58 CE	1.639E-02	7.259E-06	5.815E-06	4.657E-06	3.729E-06	2.987E-06	2.389E-06	1.913E-06	1.536E-06	1.229E-06
59 PR	2.546E-02	7.501E-06	6.009E-06	4.112E-06	3.854E-06	3.086E-06	2.469E-06	1.977E-06	1.587E-06	1.271E-06
60 ND	7.580E-03	2.104E-23	9.427E-26	3.146E-21	1.050E-30	3.505E-33	1.137E-35	0.	0.	0.
61 PM	6.971E-03	3.611E-11	7.742E-12	1.653E-12	3,531E-13	7.541E-14	1.598E-14	3.406E-IS	7.403E-16	1.578E-16
62 SM	4.082E-04	7.699E-11	7.684E-11	7.669E-11	7.654E-11	7.640E-11	7.625E-11	7.610E-11	7.596E-11	7.511E-11
63 EU	9.740E-04	6.051E-07	3.962E-07	5.870E-07	5.781E-07	5.696E-07	5.613E-07	5.533E-07	5.457E-07	5.313E-07
64 GD	1.683E-05	3.499E-01	2.942E-08	2.474E-08	2.080E-01	1.749E-01	1.469E-08	1.235E-01	1.040E-08	8.745E-09
65 TB	1.517E-06	2.333E-10	9.813E-11	4.123E-11	1.733E-11	7.280E-12	3.045E-12	1.278E-12	5.424E-13	2.276E-13
66 DY	1.995E-07	0.	0.	0.	0.	0.	0.	0.	0.	0.
67 HO	1.634E-08	0.	0.	0.	0.	0.	0.	0.	0.	0.
68 ER	5.608E-12	0.	0.	0.	0.	0.	0.	0.	0.	0.
92 U 239	3.201E-09	0.	0.	0.	0.	0.	0.	0.	0.	0.
93 NP239	1.750E-02	0.	0.	0.	0.	0.	0.	0.	0.	0.
NOBLES	1.815E-01	1.798E-08	1.769E-08	1.741E-08	1.713E-08	1.685E-08	1.658E-08	1.632E-08	1.606E-08	1.580E-08
HALOGENS	3.517E-01	5.360E-13	5.360E-13	5.360E-13	5.360E-13	8.360E-13	5.360E-13	3.360E-13	5.360E-13	5.360E-13
VOLATILES	4.231E-01	7.972E-06	7.344E-06	6.770E-06	6.243E-06	5.758E-06	5.310E-06	4.900E-06	4.525E-06	4.176E-06
OTHERS	5.907E-01	7.163E-03	6.078E-05	5.366E-05	4.846E-05	4.441E-05	4.114E-05	3.846E-05	3.626E-03	3.440E-05
TOTAL LESS NOBLES	1.366E 00	7.960E-OS	6.813E-05	6.043E-05	5.470E-05	5.017E-05	4.645E-05	4.336E-05	4.071E-05	3.857E-05

SUBTOTALS -

APPENDIX 5.6.2

RIBD GENERATED GAMMA SOURCE TERM GROUPS AND DISTRIBUTION OF ACTIVITY IN VARIOUS CORE COMPONENTS USED IN ISOSHLD MODELS

CALCULATED SOURCE TERMS OF HFIR CORE COMPONENTS FOR SOSHLD INPUT

TOTAL CORE MASS AND OPERATING PARAMETERS :

OPERATING POWER :	100	MW
OPERATING TIME :	23	DAYS
DECAY TIME :	2	YEARS
TOTAL CORE U-235 MASS :	9500	GRAMS
INNER CORE U-235 MASS :	2630	GRAMS
OUTER CORE U-235 MASS :	6870	GRAMS
INNER/TOTAL MASS RATIO :	0.27684	
OUTER/TOTAL MASS RATIO :	0.72315	
U-235 ABSORPTION CROSS-SECTION :	492	BARNS
U-235 FISSION CROSS-SECTION :	577	BARNS
THERMAL FLUX :	1.0E+15	N/CM^3/S
INNER CORE OD:	10.09	INCHES
INNER CORE ID :	5.446	INCHES
OUTER CORE OD:	16.644	INCHES
OUTER CORE ID :	11.411	INCHES
CORE LENGTH :	20	INCHES
INNER TOTAL VOLUME :	26206.1	CUBIC CENTIMETERS
INNER NEGATIVE VOLUME :	7634.42	CUBIC CENTIMETERS
OUTER TOTAL VOLUME :	71307.7	CUBIC CENTIMETERS
OUTER NEGATIVE VOLUME :	33517.2	CUBIC CENTIMETERS

TOTAL CORE SOURCE (FROM RIBD OUTPUT AT 2 YEARS DECAY):

	PH/SEC		MeV	
SOURCE (1,1)=	8.04E+10 ,	SOURCE (2,1) =	0.025 ,
SOURCE (1,2) =	3.48E+11 ,	SOURCE (2,2) =	0.035 ,
SOURCE (1,3) =	5.24E+09 ,	SOURCE (2,3) =	0.045 ,
SOURCE (1,4) =	4.27E+09 ,	SOURCE (2,4) =	0.055 ,
SOURCE (1,5) =	1.30E+19 ,	SOURCE (2,5) =	0.065,
SOURCE (1,6) =	3.13E+13 ,	SOURCE (2,6) =	0.085 ,
SOURCE (1,7) =	6.50E+08 ,	SOURCE (2,7) =	0.095 ,
SOURCE (1,8) =	1.69E+14 ,	SOURCE (2,8) =	0.150 ,
SOURCE (1,9) =	5.53E+11,	SOURCE (2,9) =	0.250 ,
SOURCE (1,10) =	1.10E+11,	SOURCE (2,10)	0.350 ,
SOURCE (1,11) =	1.50E+14 ,	SOURCE (2,11)	0.475 ,
SOURCE (1,12) =	6.00E+14 ,	SOURCE (2,12)	0.650 ,
SOURCE (1,13) =	7.41E+13 ,	S0 URCE (2,13)	0.825 ,
SOURCE (1,14) =	1.08E+13 ,	S0 URCE (2,14)	1.000 ,
SOURCE (1,15) =	4.69E+12 ,	SOURCE (2,15)	1.225 ,
SOURCE (1,16) =	6.85E+12 ,	SOURCE (2,16)	1.475 ,
SOURCE (1,17) =	7.87E+10,	SOURCE (2,17)	1.700 ,
SOURCE (1,18) =	6.16E-01 ,	SOURCE (2,18)	1.900 ,
SOURCE (1,19) =	1.06E+13 ,	SOURCE (2,19)	2.100 ,
SOURCE (1,20) =	6.35E+11 ,	SOURCE (2,20)	2.300 ,
SOURCE (1,21) =	2.95E-02 ,	SOURCE (2,21)	2.500 ,
SOURCE (1,22) =	1.08E-03 ,	SOURCE (2,22)	3.000 .

OUTER CORE SOURCE :

FRACT. TOTAL= 0.723

SOURCE (1,1) = 5.81E+10,
SOURCE (1,2) = 2.51E+11,
SOURCE (1,3) = 3.75E+09 ,
SOURCE (1,4) = 3.09E+19 ,
SOURCE (1,5) = 9.40E+05,
SOURCE (1,6) = 2.26E+13 ,
SOURCE (1,7) = 4.70E+08,
SOURCE (1,8) = 1.22E+14,
SOURCE (1,9) = 4.00E+11,
SOURCE (1,10) = 7.98E+10,
SOURCE (1,11) = 1.09E+14,
SOURCE (1,12)= 4.34E+14,
SOURCE (1,13) = 5.36E+13,
SOURCE (1,14) = 7.80E+12,
SOURCE (1,15) = 3.39E+12,
SOURCE (1,16) = 4.95E+12,
SOURCE (1,17) = 5.69E+10,
SOURCE (1,18) = 4.46E-01,
SOURCE (1,19) = 7.64E+12,
SOURCE (1,21) = 4.59E+11,
SOURCE (1,21) = 2.13E-02,
SOURCE (1,22) = 7.81E-04 ,

SOURCE (2,1) = 0.025,
SOURCE (2,2) = 0.035,
SOURCE (2,3) = 0.045,
SOURCE (2,4) = 0.055,
SOURCE (2,5) = 0.065,
SOURCE (2,6) = 0.085,
SOURCE (2,7) = 0.095,
SOURCE (2,8) = 0.150,
SOURCE (2,9) = 0.250,
SOURCE (2,10) 0.350,
S0 URCE (2,11) 0.475,
SOURCE (2,12) 0.650,
SOURCE (2,13) 0.825,
SOURCE (2,14) 1.000,
SOURCE (2,15) 1.225,
SOURCE (2,16) 1.475,
SOURCE (2,17) 1.700,
SOURCE (2,18) 1.900,
SOURCE (2,19) 2.100,
SOURCE (2,20) 2.300,
SOURCE (2,21) 2.500,
SOURCE (2,22) 3.000,

INNER CORE SOURCE:

FRACT. TOTAL = 0.277

SOURCE (1,1) = 2.22E+10,
SOURCE (1,2) = 9.58E+10,
SOURCE (1,3) = 1.45E+09,
SOURCE (1,4) = 1.18E+09,
SOURCE (1,5) = 3.60E+08,
SOURCE (1,6) = 8.66E+12,
SOURCE (1,7) = 1.80E+08,
SOURCE (1,8) = 4.66E+13,
SOURCE (1,9) = 1.53E+11,
SOURCE (1,10) = 3.06E+10,
SOURCE (1,11) = 4.16E+13,
SOURCE (1,12) = 1.66E+14,
SOURCE (1,13) = 2.05E+13,
SOURCE (1,14) = 2.99E+12 ,
SOURCE (1,15) = 1.30E+12 ,
S0 URCE (1,16) = 1.90E+12 ,
SOURCE (1,17) = 2.18E+10,
SOURCE (1,18) = 1.71E-01,
SOURCE (1,19) = 2.93E+12,
S0 URCE (1,20) = 1,76E+11,
SOURCE (1,21) = 8.16E-03,
SOURCE (1,22) = 2.99E-04,

SOURCE (2,1) = 0.025,
SOURCE (2,2) = 0.035 ,
SOURCE (2,3) = 0.045 ,
SOURCE (2,4) = 0.055,
SOURCE (2,5) = 0.065,
SOURCE (2,6) = 0.085,
SOURCE (2,7) = 0.095,
SOURCE (2,8)- 0.150,
SOURCE (2,9) = 0.250,
SOURCE (2.11) 0.350,
S0 URCE (2,11) 0.475,
S0 U9 CE (2,12) 0.650,
SOURCE (2,13) 0.825,
SOURCE (2,14) 1.000,
SOURCE (2,15) 1.225,
SOURCE (2,16) 1.475,
SOURCE (2,17) 1.700,
SOURCE (2,18) 1.900,
SOURCE (2,19) 2.100,
SOURCE (2,20) 2.300,
SOURCE (2,21) 2.500,
SOURCE (2,22) 3.000,

OUTER CORE + SUBTRACTED CENTER

FRACT. TOTAL = 1.365

SOURCE (1,1) = 1.10E+11,
SOURCE (1,2) = 4.72E+11,
SOURCE (1,3) = 7.15E+09,
SOURCE (1,4) = 5.82E+09,
SOURCE (1,5) = 1.77E+05,
SOURCE (1,6) = 4.27E+13,
SOURCE (1,7) = 8.87E+08,
SOURCE (1,8) = 2.30E+14,
SOURCE (1,9)= 7.54E+11,
SOURCE (1,10) = 1.51E+11,
SOURCE (1,11) = 2.05E+14,
SOURCE (1,12) = 8.19E+14,
SOURCE (1,13)= 1.01E+14,
SOURCE (1,14) = 1.47E+13,
SOURCE (1,15) = 6.40E+12,
SOURCE (1,16) = 9.34E+12,
SOURCE (1,17) = 1.07E+11,
SOURCE (1,18) = 8.41E -01,
SOURCE (1,19) = 1.44E+13,
SOURCE (1,20) = 8.66E+11,
SOURCE (1,21)= 4.02E -02,
SOURCE (1,22)= 1.47E-03,

SOURCE (2,1) = 0.025,
SOURCE (2,2) = 0.035,
SOURCE (2,3) = 0.045,
SOURCE (2,4) = 0.055,
SOURCE (2,5) = 0.065,
SOURCE (2,6) = 0.085,
SOURCE (2,7) = 0.095,
SOURCE (2,8) = 0.150,
SOURCE (2,9) = 0.250,
SOURCE (2,10) = 0.350,
SOURCE (2,11) 0.475,
SOURCE (2,12) 0.650,
SOURCE (2,13) 0.825,
SOURCE (2,14) 1.000,
SOURCE (2,15) 1.225,
SOURCE (2,16) 1.475,
SOURCE (2,17) 1.700,
SOURCE (2,18) 1.900,
SOURCE (2,19) 2.100,
SOURCE (2,20) 2.300,
SOURCE (2,21) 2.500,
SOURCE (2,22)= 3.000,

INNER CORE + SUBTRACTED CENTER:

FRACT. TOTAL = 1.391

SOURCE (1,1) = 3.14E+10 ,
SOURCE (1,2) = 1.35E+11 ,
SOURCE (1,3) = 2.05E+09 ,
SOURCE (1,4) = 1.67E+09 ,
SOURCE (1,5) = 5.08E+08 ,
SOURCE (1,6) = 1.22E+13 ,
SOURCE (1,7)= 2.54E+08 ,
SOURCE (1,8) = 6.58E+13 ,
SOURCE (1,9) = 2.16E+11 ,
SOURCE (1,10) = 4.31E+10,
SOURCE (1,11) = 5.86E+13 ,
SOURCE (1,12) = 2.35E+14,
SOURCE (1,13) = 2.89E+13 ,
SOURCE (1,14) = 4.22E+12 ,
SOURCE (1,15) = 1.83E+12 ,
SOURCE (1,16) = 2.68E+12 ,
SOURCE (1,17) = 3.07E+10,
SOURCE (1,18) = 2.41E -01,
SOURCE (1,19) = 4.13E+12 ,
SOURCE (1,20) = 2.48E+11 ,
SOURCE (1,21) = 1.15E -02 ,
SOURCE (1,22) = 4.22E -04 ,

SOURCE (2,1) = 0.025 ,
SOURCE (2,2) = 0.035 ,
SOURCE (2,3) = 0.045 ,
SOURCE (2,4) = 0.055 ,
SOURCE (2,5) = 0.065,
SOURCE (2,6) = 0.085 ,
SOURCE (2,7) = 0.095 ,
SOURCE (2,8) = 0.150,
SOURCE (2,9) = 0.250,
SOURCE (2,10) = 0.350 ,
SOURCE (2,11) = 0.475 ,
SOURCE (2,12) = 0.650,
SOURCE (2,13) = 0.825 ,
SOURCE (2,14) = 1.000,
SOURCE (2,15) = 1.225,
SOURCE (2,16) = 1.475,
SOURCE (2,17) = 1.700 ,
SOURCE (2,18) = 1.900 ,
SOURCE (2,19) = 2.100 ,
SOURCE (2,20) = 2.300 ,
SOURCE (2,21) = 2.500,
SOURCE (2,22) = 3.000, ,

OUTER CORE SUBTRACTED CENTER:

		FRACT. TOTAL =	0.641		
SOURCE (1,1) =	5.15E+10,	SOURCE (2,1) =	0.025,		
SOURCE (1,2) =	2.22E+11,	SOURCE (2,2) =	0.035,		
SOURCE (1,3) =	3.36E+09,	SOURCE (2,3) =	0.045,		
SOURCE (1,4) =	2.74E+09,	SOURCE (2,4) =	0.055,		
SOURCE (1,5) =	8.34E+08,	SOURCE(2,5)=	0.065,		
SOURCE (1,6) =	2.01E+13,	SOURCE (2,6) =	0.085,		
SOURCE (1,7) =	4.17E+08,	SOURCE (2,7) =	0.095,		
SOURCE (1,8) =	1.08E+14,	SOURCE (2,8) =	0.150,		
SOURCE (1,9) =	3.55E+11,	SOURCE (2,9) =	0.250,		
SOURCE (1,10) =	7.05E+10,	SOURCE (2,10)	0.350,		
SOURCE (1,11) =	9.63E+13,	SOURCE (2,11)	0.475,		
SOURCE (1,12) =	3 .85E+14	SOURCE (2 ,12)	0.650,		
SOURCE (1,13) =	4.75E+13,	SOURCE (2,13)	0.825,		
SOURCE (1,14) =	6.92E+12,	SOURCE (2,14)	1.000,		
SOURCE (1,15) =	3.01E+12,	SOURCE (2,15)	1.225,		
SOURCE (1,16)	4.39E+12,	SOURCE (2,16)	1.475,		
SOURCE (1,17) =	5.05E+10,	SOURCE (2,17)	1.700,		
SOURCE (1,18) =	3.95E -01,	SOURCE (2,18)	1.900,		
SOURCE (1,19) =	6.78E+12,	SOURCE (2,19)	2.100,		
SOURCE (1,20) =	4.07E+11,	SOURCE (2,20)	2.300,		
SOURCE (1,21) =	1.89E -02,	SOURCE (2,21)	2.500,		
SOURCE (1,22) =	6.93E -04 ,	SOURCE (2,22)	3 .000,		

INNER CORE SUBTRACTED CENTERR:

		FRACT. TOTAL	0.114		
SOURCE (1,1) =	9.14E+09,	SOURCE (2,1) =	0.025,		
SOURCE (1,2) =	3.94E+10,	SOURCE (2,2) =	0.035,		
SOURCE (1,3) =	5.96E+08,	SOURCE (2,4) =	0.045,		
SOURCE (1,4) =	4.86E+08,	SOURCE (2,4) =	0.055,		
SOURCE (1,5) =	1.48E+08,	SOURCE(2,5) =	0.065,		
SOURCE (1,6)=	3.56E+12,	SOURCE (2,6) =	0.085,		
SOURCE (1,7) =	7.40E+07,	SOURCE (2,7) =	0.095,		
SOURCE (1,8) =	1.92E+13,	SOURCE (2,8) =	0.150,		
SOURCE (1,9) =	6.29E+10,	SOURCE (2,9) =	0.250,		
SOURCE (1,10) =	1.26E+10,	SOURCE (2,10)	0.350,		
SOURCE (1,11) =	1.71E+13,	SOURCE (2,11)	0.475,		
SOURCE (1,12) =	6.83E+13,	SOURCE (2,12)	0.650,		
SOURCE (1,13) =	8.43E+12,	SOURCE (2,13)	0.825,		
SOURCE (1,14) =	1.23E+12,	SOURCE (2,14)	1.000,		
SOURCE (1,15) =	5.34E+11,	SOURCE (2,15)	1.225,		
SOURCE (1,16) =	7.79E+11,	SOURCE (2,16)	1,475,		
SOURCE (1,17) =	8.96E+09,	SOURCE (2,17)	1.700,		
SOURCE (1,18) =	7.01E -02,	SOURCE (2,18)	1.900,		
SOURCE (1,19) =	1.20E+12,	SOURCE (2,19)	2.100,		
SOURCE (1,20) =	7.23E+10,	SOURCE (2,20)	2.300,		
SOURCE (1,21) =	3.35E -03,	SOURCE (2,21)	2.500,		
SOURCE (1,22) =	1.23E -04,	SOURCE (2,22)	3.000,		

APPENDIX 5.6.3

ISOSHLD INPUT AND OUTPUT FOR THE ANALYSIS OF THE DOSE RATES AT THE SIDE OF THE PACKAGE FROM THE OUTER CORE PLUS THE "SUBTRACTED CENTER"

```
$$ ABIS,ROUT(10),TAB(:,6,16,79),KEYWORD(BMM)
$:IDENT:V151,BMM,WW16,X4455
$:OPTION:FORTRAN
$:SELECT:ISHLD01
$:LIMITS:100,44K,,30K
$:REMOTE:06.10
$:DATA:1*
   MODE = 3
2 YR HIFER OUTER CYLINDER IN 2000, CORE+SUBTRCTD, MIDSIDE SURFACE, 3" Fe
 $INPUT NEXT = 3, IGEOM = 7, X = 61.6, SLTH = 50.8, NTHETA = 20,
 NPSI = 20, DELR = 1.057, Y = 25.4, JBUF = 2,
 T(1) = 21.138, T(2) = 10.16, T(3) = 15.08, ISPEC = 1, NSHLD = 3,
 SOURCE(1,1)=  1.10E+11, SOURCE(2,1)= 0.025,
 SOURCE(1,2)=  4.72E+11, SOURCE(2,2)= 0.035,
 SOURCE(1,3)=  7.15E+09, SOURCE(2,3)= 0.045,
 SOURCE(1,4)=  5.62E+09, SOURCE(2,4)= 0.055,
 SOURCE(1,5)=  1.77E+09, SOURCE(2,5)= 0.065,
 SOURCE(1,6)=  4.27E+13, SOURCE(2,6)= 0.085,
 SOURCE(1,7)=  8.87E+06, SOURCE(2,7)= 0.095,
 SOURCE(1,8)=  2.30E+14, SOURCE(2,8)= 0.150,
 SOURCE(1,9)=  7.54E+11, SOURCE(2,9)= 0.250,
 SOURCE(1,10)= 1.51E+11, SOURCE(2,10)= 0.350,
 SOURCE(1,11)= 2.03E+14, SOURCE(2,11)= 0.475,
 SOURCE(1,12)= 6.15E+14, SOURCE(2,12)= 0.650,
 SOURCE(1,13)= 1.01E+14, SOURCE(2,13)= 0.825,
 SOURCE(1,14)= 1.47E+13, SOURCE(2,14)= 1.000,
 SOURCE(1,15)= 6.40E+12, SOURCE(2,15)= 1.225,
 SOURCE(1,16)= 9.34E+12, SOURCE(2,16)= 1.475,
 SOURCE(1,17)= 1.07E+11, SOURCE(2,17)= 1.700,
 SOURCE(1,18)= 6.41E-01, SOURCE(2,18)= 1.900,
 SOURCE(1,19)= 1.44E+13, SOURCE(2,19)= 2.100,
 SOURCE(1,20)= 8.60E+11, SOURCE(2,20)= 2.300,
 SOURCE(1,21)= 4.02E-02, SOURCE(2,21)= 2.500,
 SOURCE(1,22)= 1.47E-03, SOURCE(2,22)= 3.000 $
 IRAN    15 1.43IE-01
 LEAD    14            1.134E 01
 IRON     6                        7.800E 00                                  1
2 YR HIFER FUEL CYLINDER, CORE+SUBT. IN 2000 CASK, 1 m. FROM MIDSIDE
 $INPUT NEXT = 4, X = 161.6 $
2 YR HIFER FUEL CYLINDER, CORE+SUBT. IN 2000 CASK, SIDE OF TRUCK
 $INPUT NEXT = 4, X = 121.92 $
2 YR HIFER FUEL CYLINDER, CORE+SUBT. IN 2000 CASK, 2 m. FROM TRUCK
 $INPUT NEXT = 4, X = 321.92 $
2 YR HIFER FUEL CYLINDER, CORE+SUBT. IN 2000 CASK, IN CAB OF TRUCK
 $INPUT NEXT = 4, X = 639.4 $
OUTER CYLINDER, CORE+SUBT. IN 2000, TOPSIDE, JACKET SURFACE
 $INPUT NEXT = 4, Y = 50.8, X = 61.6 $
OUTER CYLINDER, CORE+SUBT. IN 2000 CASK, TOPSIDE, 1 m. FROM JACKET
 $INPUT NEXT = 4, X = 161.6 $
OUTER CYLINDER, CORE+SUBT. IN 2000 CASK, TOPSIDE, TRUCK SIDE SURFACE
 $INPUT NEXT = 4, X = 121.92 $
OUTER CYLINDER, CORE+SUBT. IN 2000 CASK, TOPSIDE, 2 m. FROM TRUCK
 $INPUT NEXT = 4, X = 321.92 $
OUTER CYLINDER, CORE+SUBT. IN 2000 CASK, TOPSIDE, IN CAB OF TRUCK
 $INPUT NEXT = 4, X = 639.4 $
OUTER CYLINDER, CORE+SUBT. IN 2000, MID-INNER, JACKET SURFACE
 $INPUT NEXT = 4, Y = 76.2, X = 61.6 $
OUTER CYLINDER, CORE+SUBT. IN 2000 CASK, MID-INNER, 1 m. FROM JACKET
 $INPUT NEXT = 4, X = 161.6 $
OUTER CYLINDER, CORE+SUBT. IN 2000 CASK, MID-INNER, TRUCK SIDE SURFACE
 $INPUT NEXT = 4, Y = 121.92 $
OUTER CYLINDER, CORE+SUBT. IN 2000 CASK, MID-INNER, 2 m. FROM TRUCK
 $INPUT NEXT = 4, X = 321.92 $
OUTER CYLINDER, CORE+SUBT. IN 2000 CASK, MID-INNER, IN CAB OF TRUCK
 $INPUT NEXT = 4, X = 639.4 $
DUMMY TITLE CARD
 $INPUT NEXT = 6 $
$:ENDDECK
```

GAMMA ATTENUATION CALCULATION 2 YR HIFER OUTER CYLINDER 2000, CORE•SURTRCTD. MIDSIDE SURFACE, 3" FE

CYLINDRICAL SOURCE CYLINDRICAL SHIELDS DIST TO DETECTOR 6.1602 01 CM. LENGTH 5.080E 01CM. VOL.=7.131E 04CC

INTEGRATION SPECS NTHETA = 21 NPSI = 21 DELR =0.1057E 01

TAYLOR BUILDUP DATA FOR SHIELD 2 WITH EFFECTIVE ATOMIC NUMBER OF 82.0 USED

SHIELD THICKNESS 2.111E 01 1.016E 01 1.508E 01

GROUP	GROUP PRODUCTION RATE PHOTONS	GROUP AVERAGE ENERGY MEV	ENERGY FLUX AT DOSE POINT MEV/CMS/SEC	DOSE RATE AT DOSE POINT ROENTGENS/HOUR
1	1.100E 11	2.500E-02	8.771E-35	1.517E-39
2	4.720E 11	3.500E-02	5.493E-34	3.488E-39
3	7.150E 09	1.500E-02	1.114E-35	0.
1	5.820E 09	5.500E-02	1.143E-35	0.
5	1.770E 09	6.500E-02	4.207E-36	0.
6	4.270E 13	8.500E-02	1.389E-31	2.246E-37
7	8.870E 08	9.500E-02	3.297E-36	0.
1	2.300E 14	1.500E-01	9.507E-30	1.643E-35
9	7.540E 11	2.500E-01	2.910E-30	5.703E-36
10	1.510E 11	3.500E-01	6.700E-16	1.380E-21
11	2.050E 14	4.750E-01	3.635E-05	7.415E-11
12	8.190E 14	6.500E-01	5.275E-01	1.097E-06
13	1.010E 14	8.250E -0I	4.801E 01	9.608E-05
11	1.470E 13	1.000E 00	1.020E 02	1.968E-04
15	6.400E 12	1.225E 00	4.885E 02	8.988E-04
16	9.340E 12	1.475E 00	4.093E 03	7.204E-03
17	1.070E 11	1.700E 00	1.286E 02	2.200E-04
18	8.4I0E -01	1.900E 00	2.361E-09	3.918E-15
19	1.440E 13	2.100E 00	6.706E 04	1.073E-01
20	8.660E 11	2.300E 00	6.803E 03	1.048E-02
21	4.020E-02	2.500E 00	3.932E-10	5.977E-16
22	1.470E-03	3.000E 00	2.439E-11	3.488E-17
TOTAL	1.445E 15		7.872E 04	1.261E-01

SH.. ..J COMPOSITION	GR/CC	1	2	3	4	5
URANIUM	1.432E-01	0.	0.	0.	0.	
LEAD		0.	1.134E 01	0.	0.	0.
IRON		0.	0.	7.800E 00	0.	0.

MASS ABSORPTION COEFFICIENTS (LAST REGION IS AIR)

7.312E 00	5.415E 02	9.576E 01	6.036E-04	0.	0.
3.308E 00	1.928E 02	4.434E 01	3.233E-04	0.	0.
1.582E 00	9.202E 01	2.055E 01	2.505E-04	0.	0.
8.964E-01	5.262E 01	1.135E 01	2.219E-04	0.	0.
5.878E-01	3.489E 01	7.574E 00	2.073E-04	0.	0.
2.847E-01	2.507E 01	3.918E 00	1.891E-04	0.	0.
2.152E-01	2.853E 01	3.111E 00	1.831E-04	0.	0.
3.030E-01	1.564E 01	1.591E 00	1.591E-04	0.	0.
1.027E-01	6.339E 00	1.069E 00	1.360E-04	0.	0.
5.556E-02	3.476E 00	7.784E-01	1.211E-04	0.	0.
3.258E-02	2.013E 00	6.825E-01	1.092E-04	0.	0.
1.962E-02	1.452E 00	5.616E-01	1.032E-04	0.	0.
1.425E-02	9.923E-01	4.969E-01	8.291E-05	0.	0.
1.167E-02	8.233E-01	4.586E-01	7.575E-05	0.	0.
9.594E-03	7.008E-01	4.001E-01	6.835E-05	0.	0.
8.019E-03	6.056E-01	3.666E-01	6.143E-05	0.	0.
7.375E-03	5.534E-01	3.479E-01	5.702E-05	0.	0.
6.917E-03	5.250E-01	3.237E-01	5.368E-05	0.	0.
6.616E-03	5.024E-01	3.136E-01	5.070E-05	0.	0.
6.444E-03	4.854E-01	2.972E-01	4.855E-05	0.	0.
6.315E-03	4.751E-01	2.948E-01	4.617E-05	0.	0.
6.186E-03	4.661E-01	2.769E-01	4.044E-05	0.	0.
0.	0.	0.	0.	0.	0.
0.	0.	0.	0.	0.	0.
0.	0.	0.	0.	0.	0.

EXP UNDERFLO AT LOCATION 003335
EXP UNDERFLO AT LOCATION 005335
EXP UNDERFLO At LOCATION 005335
EXP UNDERFLO AT LOCATION 005335
EXP UNDERFLO AT LOCATION 005335
EXP UNDERFLO AT LOCATION 003335
EXP UNDERFLO AT LOCATION 005335
EXP UNDERFLO At LOCATION 005335
EXP UNDERFLO AT LOCATION 005335
EXP UNDERFLO AT LOCATION 005335
EXP UNDERFLO AT LOCATION 005335
EXP UNDERFLO AT LOCATION 003335
EXP UNDERFLO AT LOCATION 005335
EXP UNDERFLO AT LOCATION 005335
EXP UNDERFLO At LOCATION 003335
EXP UNDERFLO AT LOCATION 003335
EXP UNDERFLO AT LOCATION 003335
EXP UNDERFLO AT LOCATION 005335
EXP UNDERFLO AT LOCATION 003335
EXP UNDERFLO At LOCATION 005335
EXP UNDERFLO At LOCATION 003335
EXP UNDERFLO AT LOCATION 005335
EXP UNDERFLO AT LOCATION 003335
EXP UNDERFLO AT LOCATION 005335
EXP UNDERFLO AT LOCATION 005335
EXP UNDERFLO AT LOCATION 005335

**THIS IS THE LAST TIME THE ABOVE MESSAGE HILL APPEAR*

GAMMA ATTENUATION CALCULATION 2 YR HIFER FUEL CYLINDER. CORE+SUBT. IN 2000 CASK. 1 M. FROM MIDSIDE

CYLINDRICAL SOURCE CYLINDRICAL SHIELDS DIST TO DETECTOR 1.616E 02 CM. LENGTH 5.060E 01 CM. VOL. = 7.131E 04CC

INTEGRATION SPECS NTHETA = 21 NPSI= 21 DELR= 0.1057E 01

TAYLOR BUILDUP DATA FOR SHIELD 2 WITH EFFECTIVE ATOMIC NUMBER OF 82.0 USED

SHIELD THICKNESS 2.114E 01 1.016E 01 1.508E 01

GROUP	GROUP PRODUCTION RATE PHOTONS	GROUP AVERAGE ENERGY MEV	ENERGY FLUX AT DOSE POINT MEV/CMS/SEC	DOSE RATE AT DOSE POINT ROENTGENS/HOUR
1	1.100E 11	2.500E-02	1.276E-35	0.
2	4.720E 11	3.500E-02	7.994E-35	0.
3	7.150E 09	4.500E-02	1.624E-36	0.
4	5.820E 09	5.500E-02	1.661E-36	0.
5	1.770E 09	6.500E-02	6.123E-37	0.
6	4.270E 13	8.500E-02	2.022E-32	3.269E-38
7	8.870E 08	9.500E-02	4.798E-37	0.
8	2.300E 14	1.500E-01	1.298E-30	2.243E-36
9	7.540E 11	2.500E-01	9.728E-31	1.907E-36
10	1.510E 11	3.500E-01	1.920E-16	3.956E-22
11	2.050E 14	4.750E-01	9.016E-06	1.839E-11
12	8.190E 14	6.500E-01	1.195E-01	2.486E-07
13	1.010E 14	8.250E-01	1.003E 01	2.007E-05
14	1.470E 13	1.000E 00	2.053E 01	3.963E-05
15	6.400E 12	1.225E 00	9.466E 01	1.742E-04
16	9.340E 12	1.475E 00	7.715E 02	1.358E-03
17	1.070E 11	1.700E 00	2.386E 01	4.080E-05
18	8.410E-01	1.900E 00	4.316E-10	7.165E-16
19	1.440E 13	2.100E 00	1.216E 04	1.946E-02
20	8.660E 11	2.300E 00	1.222E 03	1.883E-03
21	4.020E-02	2.500E 00	7.048E-11	1.071E-16
22	1.470E-03	3.000E 00	4.312E-12	6.209E-18
TOTAL	1.445E 15		1.430E 04	2.297E-02

GAMMA ATTENUATION CALCULATION 2 YR HIFER FUEL CYLINDER, CORE +SUBT. IN 2000 CASK, SIDE OF TRUCK

CYLINDRICAL SOURCE CYLINDRICAL SHIELDS DIST TO DETECTOR 1.219E 02 CM. LENGTH 5.080E 01 CM. VOL. = 7.131E 04CC
INTEGRATION SPECS NTHETA • 21 NPSI • 21 DELR = 0.1057E 01

TAYLOR BUILDUP DATA FOR SHIELD 2 WITH EFFECTIVE ATOMIC NUMBER OF 82.0 USED

SHIELD THICKNESS 2.114E 01 1.016E 01 1.508E 01

GROUP	GROUP PRODUCTION RATE PHOTONS	GROUP AVERAGE ENERGY MEV	ENERGY FLUX AT DOSE POINT MEV/CMS/SEC	DOSE RATE At DOSE POINT ROENTGENS/HOUR
1	1.100E 11	2.500E-02	2.243E-35	0.
2	1.720E 11	3.500E-02	1.405E-34	0.
3	7.150E 09	4.500E-02	2.848E-36	0.
4	5.820E 09	5.500E-02	2.923E-36	0.
3	1.770E 09	6.500E-02	1.076E-36	0.
6	4.270E 13	8.500E-02	3.552E-32	5.743E-38
7	8.870E 01	9.500E-02	8.430E-37	0.
8	2.300E 14	1.500E-OI	2.297E-30	3.970E-36
9	7.540E 11	2.500E-01	1.422E-30	2.787E-36
10	1.510E 11	3.500E-01	2.987E-16	6.153E-22
11	2.050E 11	4.750E-01	1.458E-05	2.974E-11
12	8.190E 11	6.500E-01	1.969E-01	4,096E-07
13	1.010E 11	8.250E-01	1.678E 01	3.356E-05
14	1.470E 13	1.000E 00	3.454E 01	6. 666E-05
15	6.400E 12	1.225E 00	1.602E 02	2.948E-04
16	9.340E 12	1.475E 00	1.311E 03	2.308E-03
17	1.070E 11	1.700E 00	4.061E 01	6.950E-05
18	8.410E-01	1.900E 00	7.368E-10	1,223E-15
19	1.440E 13	2.100E 00	2.078E 01	3.325E-02
20	8.660E 11	2.300E 00	2.092E 03	3.222E-03
21	4.020E-02	2.500E 00	1.207E-10	1.834E-16
22	1.470E-03	3.000E 00	7.439E-12	1.064E-17
TOTAL	1.445E 15		2.444E 04	3.925E-02

GAMMA ATTENUATION CALCULATION 2 YR HIFER FUEL CYLINDER, CORE + SUBT. IN 2000 CASK. 2 M. FROM TRUCK

CYLINDRICAL SOURCE CYLINDRICAL SHIELDS DIST TO DETECTOR 3.219E 02 CM. LENGTH 5.080E 01 CM. VOL. = 7.131E 04CC

INTEGRATION SPECS NTHETA = 21 NPSI = 21 DELR = 0.1057E 01

TAYLOR BUILDUP DATA FOR SHIELD 2 WITH EFFECTIVE ATOMIC NUMBER OF 82.0 USED

SHIELD THICKNESS 2.114E 01 1.016E 01 1.508E 01

GROUP	GROUP PRODUCTION RATE PHOTONS	GROUP AVERAGE ENERGY MEV	ENERGY FLUX AT DOSE POINT MEV/CMS/SEC	DOSE RATE AT DOSE POINT ROENTGENS/HOUR
1	1.100E 11	2.500E-02	3.216E-36	0
2	4.720E 11	3.500E-02	2.014E-35	0.
3	7.150E 09	4.500E-02	4.084E-37	0.
4	5.820E 09	5.500E-02	4.192E-37	0.
5	1.770E 09	6.500E-02	1.543E-37	0.
6	4.270E 13	8.500E-02	5.094E-33	8.236E-39
7	8.870E 08	9.500E-02	1.209E-37	0.
8	2.300E 14	1.500E-01	3.251E-31	5.617E-37
9	7.540E 11	2.500E-01	2.967E-31	5.815E-37
10	1.510E 11	3.500E-01	5.397E-17	1.112E-22
11	2.050E 14	4.750E-01	2.432E-06	4.962E-12
12	8.190E 14	6.500E-01	3.167E-02	6.587E-08
13	1.010E 14	8.250E-01	2.626E 00	5.251E-06
14	1.470E 13	1.000E 00	5.345E 00	1.032E-05
15	6.400E 12	1.225E 00	2.452E 01	4.512E-05
16	9.340E 12	1.475E 00	1.993E 02	3.507E-04
17	1.070E 11	1.700E 00	6.150E 00	1.052E-05
18	8.410E-01	1.900E 00	1.111E-10	1.844E-16
19	1.440E 13	2.100E 00	3.128E 03	5.004E-03
20	8.660E 11	2.300E 00	3.141E 02	4.837E-04
21	4.020E-02	2.500E 00	1.811E-11	2.753E-17
22	1.470E-03	3.000E 00	1.116E-12	1.595E-18
TOTAL	1.445E 15		3.680E 03	5.910E-03

GAMMA ATTENUATION CALCULATION 2 YR HIFER FUEL CYLINDER, CONE + SUBT. IN 2000 CASK. IN CAB OF TRUCK

CYLINDRICAL SOURCE CYLINDRICAL SHIELDS DIST TO DETECTOR 6.394E .02 CM. LENGTH 5.080E 01 CM. VOL. = 7.131E 04CC 0

INTEGRATION SPECS NTHETA= 21 NPSI= 21 DELR= 0.1057E 01

TAYLOR BUILDUP DATA FOR SHIELD 2 WITH EFFECTIVE ATOMIC NUMBER OF 82.0 USED

SHIELD THICKNESS 2.114E 01 1.016E 01 1.508E 01

GROUP	GROUP PRODUCTION RATE PHOTONS	GROUP AVERAGE ENERGY MEV	ENERGY FLUX AT DOSE POINT MEV/CMS/SEC	DOSE RATE AT DOSE POINT ROENTGENS/HOUR
1	1.100E 11	2.500E-02	8.185E-37	0.
2	1.720E 11	3.500E-02	5.126E-36	0.
3	7.150E 09	4.500E-02	1.039E-37	0.
4	5.820E 09	5.500E-02	1.067E-37	0.
5	1.770E 09	6.500E-02	3.926E-31	0.
6	4.270E 13	8.500E-02	1.296E-33	2.096E-39
7	8.870E 01	9.500E-02	3.076E-31	0.
8	2.300E 14	1.500E-01	8.262E-32	1.428E-37
9	7.540E 11	2.500E-01	7.544E-32	1.479E-37
10	1.510E 11	3.500E-01	1.355E-17	2.790E-23
11	2.050E 14	4.750E-01	6.082E-07	1.241E-12
12	8.190E 11	6.500E-01	7.912E-03	1.646E-01
13	1.010E 14	8.250E-01	6.583E-01	1.317E-06
14	1.470E 13	1.000E 00	1.342E 00	2.589E-06
15	6.400E 12	1.225E 00	6.163E 00	1.134E-05
16	9.340E 12	1.475E 00	5.015E 01	8.827E-05
17	1.070E 11	1.700E 00	1.550E 00	2.650E-06
18	8.410E-01	1.900E 00	2.801E-11	4.650E-17
19	1.440E 13	2.100E 00	7.892E 02	1.263E-03
20	8.660E 11	2.300E 00	7.929E 01	1.221E-04
21	4.020E-02	2.500E 00	4.575E-12	6.954E-11
22	1.470E-03	3.000E 00	2.822E-13	4.035E-19
TOTAL	1.445E 15		9.284E 02	1.491E-03

GAMMA ATTENUATION CALCULATION OUTER CYLINDER, CORE + SUBT. 2000, TOPSIDE. JACKET SURFACE

CYLINDRICAL SOURCE CYLINDRICAL SHIELDS DIST TO DETECTOR 6.160E 01 CM. LENGTH 5.060E 01 CM. VOL. = 7.131E 04CC

INTEGRATION SPECS NTHETA = 21 NPSI= 21 DELR •0.1057E 01

TAYLOR BUILDUP DATA FOR SHIELD 2 WITH EFFECTIVE ATOMIC NUMBER OF 82.0 USED

SHIELD THICKNESS 2.114E 01 1.016E 01 1.501E 01

GROUP	GROUP PRODUCTION RATE PHOTONS	GROUP AVERAGE ENERGY MEV	ENERGY FLUX AT DOSE POINT MEV/CMS/SEC	DOSE RATE AT DOSE POINT ROENTGENS/HOUR
1	1.100E 11	2.500E-02	7.708E-35	0.
2	4.720E 11	3.500E-02	4.828E-34	3.066E-39
3	7.150E 09	4.500E-02	9.787E-36	0.
4	5.820E 09	5.500E-02	1.005E-35	0.
5	1.770E 09	6.500E-02	3.697E-36	0.
6	4.270E 13	8.500E-02	1.221E-31	1.974E-37
7	8.870E 01	9.500E-02	2.897E-36	0.
8	2.300E 14	1.500E-01	9.981E-30	1.725E-35
9	7.540E 11	2.500E-01	1.519E-30	2.977E-36
10	1.510E 11	3.500E-01	3.452E-16	7.112E-22
11	2.050E 11	4.750E-01	1.895E-03	3.865E-11
12	8.190E 14	6.500E-01	2.809E-01	5.843E-07
13	1.010E 14	8.250E-01	2.641E 01	5.282E-05
14	1.470E 13	1.000E 00	5.719E 01	1.104E-04
15	6.400E 12	1.225E 00	2.810E 02	5.170E-04
16	9.340E 12	1.475E 00	2.406E 03	4.235E-03
17	1.070E 11	1.700E 00	7.668E 01	1.311E-04
18	8.410E-01	1.900E 00	1.426E-09	2.367E-15
19	1.440E 13	2.100E 00	4.083E 04	6.534E-02
20	8.660E 11	2.300E 00	4.180E 03	6.438E-03
21	4.020E-02	2.500E 00	2.423E-10	3.683E-16
22	1.470E-03	3.000E 00	1.514E-11	2.165E-17
TOTAL	1.445E 15		4.786E 04	7.682E-02

GAMMA ATTENUATION CALCULATION OUTER CYLINDER. CORE + SUBT. 2000 CASK. TOPSIDE. 1 M. FROM JACKET

CYLINDRICAL SOURCE CYLINDRICAL SHIELDS DIST TO DETECTOR 1.610E 02 CM. LENGTH 5.080E 01 CM. VOL. = 7.131E 04CC

INTEGRATION SPECS NTHETA= 21 NPSI= 21 DELR .0.1057E 01

TAYLOR BUILDUP DATA FOR SHIELD 2 WITH EFFECTIVE ATOMIC NUMBER OF 82.0 USED

SHIELD THICKNESS 2.114E 01 1.016E 01 1.508E 01

GROUP	GROUP PRODUCTION RATE PHOTONS	GROUP AVERAGE ENERGY MEV	ENERGY FLUX AT DOSE POINT MEV/CMS/SEC	DOSE RATE AT DOSE POINT ROENTGENS/HOUR
1	1.100E 11	2.500E-02	1.258E-35	0.
2	4.720E 11	3.500E-02	7.878E-35	0.
3	7.150E 09	4.500E-02	1.597E-36	0.
4	5.820E 09	5.500E-02	1.640E-36	0.
5	1.770E 09	6.500E-02	6.034E-37	0.
6	4.270E 13	8.500E-02	1.992E-32	3.221E-31
7	8.870E 08	9.500E-02	4.728E-37	0.
8	2.300E 14	1.500E-01	1.314E-30	2.270E-36
9	7.540E 11	2.500E-01	5.631E-31	1.104E-36
10	1.510E 11	3.500E-01	1.267E-16	2.609E-02
11	2.050E 14	4.750E-01	6.615E-06	1.350E-11
12	8.190E 14	6.500E-01	9.316E-02	1.938E-07
13	1.010E 14	8.250E-01	8.227E 00	1.645E-05
14	1.470E 13	1.000E 00	1.720E 01	3.320E-05
15	6.400E 12	1.225E 00	8.105E 01	1.491E-01
16	9.340E 12	1.475E 00	6.709E 02	1.181E-03
17	1.070E 11	1.700E 00	2.093E 01	3.578E-05
18	8.410E-01	1.900E 00	3.815E-10	6.333E-16
19	1.440E 13	2.100E 00	1.080E 04	1.727E-02
20	8.660E 11	2.300E 00	1.090E 03	1.679E-03
21	4.020E-02	2.500E 00	6.296E-11	9.570E-17
22	1.470E-03	3.000E 00	3.893E-12	5.567E-18
TOTAL	1.455E15		1.268E 04	2.037E-02

GAMMA ATTENUATION CALCULATION OUTER CYLINDER, CORE + SUBT. ... 2000 CASK. TOPSIDE, TRUCK SIDE SURFACE
CYLINDRICAL SOURCE CYLINDRICAL SHIELDS DIST TO DETECTOR 1.219E 02 CM. LENGTH 5.010E 01 CM. VOL. = 7.131E 04CC

INTEGRATION SPECS NTHETA= 21 NPSI= 21 DELR= 0.1057E 01

TAYLOR BUILDUP DATA FOR SHIELD 2 WITH EFFECTIVE ATOMIC NUMBER OF 82.0 USED

SHIELD THICKNESS 2.114E 01 1.016E 01 1.501E 01

GROUP	GROUP PRODUCTION RATE PHOTONS	GROUP AVERAGE ENERGY MEV	ENERGY FLUX AT DOSE POINT MEV/CMS/SEC	DOSE RATE AT DOSE POINT ROENTGENS/HOUR
1	1.100E 11	2.500E-02	2.174E-35	0.
2	4.720E 11	3.500E-02	1.362E-34	0.
3	7.150E 09	4.500E-02	2.760E-36	0.
4	5.820E 09	5.500E-02	2.834E-36	0.
5	1.770E 09	6.500E-02	1.043E-36	0.
6	4.270E 13	8.500E-02	3.443E-32	5.668E-38
7	8.870E 01	9.500E-02	8.172E-37	0.
8	2.300E 14	1.500E-01	2.333E-30	4.031E-36
9	7.540E 11	2.500E-01	7.536E-31	1.477E-36
10	1.510E 11	3.500E-01	1.724E-16	3.551E-22
11	2.050E 14	4.750E-01	9.318E-06	1.901E-11
12	8.190E 14	6.500E-01	1.350E-01	2.808E-07
13	1.010E 14	8.250E-0I	1.227E 01	2.454E-05
14	1.470E 13	1.000E 00	2.601E 01	5.020E-05
15	6.400E 12	1.225E 00	1.244E 02	2.289E-04
16	9.340E 12	1.475E 00	1.041E 03	1.833E-03
17	1.070E 11	1.700E 00	3.269E 01	5.590E-05
18	8.410E-01	1.900E 00	5.994E-10	9.950E-16
19	1.440E 13	2.100E 00	1.702E 04	2.723E-02
20	8.660E 11	2.300E 00	1.725E 03	2.657E-03
21	4.020E-02	2.500E 00	9.973E-11	1.516E-16
22	1.470E-03	3.000E 00	6.183E-12	8.842E-18
TOTAL	1.445E 15		1.998E 04	3.208E-02

GAMMA ATTENUATION CALCULATION OUTER CYLINDER, CORE + SUBT 2000 CASK. TOPSIDE. 2 M. FROM TRUCK

CYLINDRICAL SOURCECYLINDRICAL SHIELDS OIST TO DETECTOR 3.21?E 02 CM. LENGTH 5.080E 01 CM. VOL. = 7.131E 04CC

INTEGRATION SPECS NTHETA= 21 NPSI= 21 DELR .0.1057E 01

TAYLOR BUILDUP DATA FOR SHIELD 2 WITH EFFECTIVE ATOMIC NUMBER OF 02.0 USED

SHIELD THICKNESS 2.114E 01 1.016E 01 1.501E 01

GROUP	GROUP PRODUCTION RATE PHOTONS	GROUP AVERAGE ENERGY MEV	ENERGY FLUX AT DOSE POINT MEV/CMS/SEC	DOSE RATE AT DOSE POINT ROENTGENS/HOUR
1	1.100E 11	2.500E-02	3.225E-36	0.
2	4.720E 11	3.500E-02	2.020E-35	0.
3	7.150E 09	4.500E-02	4.094E-37	0.
4	5.820E 09	5.500E-02	4.204E-37	0.
5	1.770E 09	6.550E-02	1.547E-37	0.
6	4.270E 13	8.500E-02	5.107E-33	8.258E-39
7	8.870E 08	9.500E-02	1.212E-37	0.
8	2.300E 14	1.500E-01	3.282E-31	5.670E-37
9	7.540E 11	2.500E-01	2.382E-31	4.669E-37
10	1.510E 11	3.500E-01	4.716E-17	9.716E-23
11	2.050E 14	4.750E-01	2.226E-06	4.541E-12
12	8.190E 14	6.500E-01	2.962E-02	6.162E-08
13	1.010E 14	8.250E-01	2.498E 00	4.996E-06
14	1.470E 13	1.000E 00	5.120E 00	9.882E-06
15	6.400E 12	1.225E 00	2.365E 01	4.351E-05
16	9.340E 12	1.475E 00	1.930E 02	3.397E-04
17	1.070E 11	1.700E 00	5.973E 00	1.021E-05
18	8.410E-01	1.900E 00	1.081E-10	1.795E-16
19	1.440E 13	2.100E 00	3.048E 03	4.878E-03
20	8.660E 11	2.300E 00	3.066E 02	4.721E-04
21	4.020E-02	2.500E 00	1.768E-11	2.688E-17
22	1.470E-03	3.000E 00	1.090E-12	1.559E-11
TOTAL	1.445E 15		3.585E 03	5.758E-03

GAMMA ATTENUATION CALCULATION OUTER CYLINDER. CORE + SUBT. 000 CASK TOPSIDE, IN CAB OF TRUCK

CYLINDRICAL SOURCE CYLINDRICAL SHIELDS DIST TO DETECTOR 6.394E 02 CM. LENGTH 5.080E 01 CM VOL. = 7.131E 04CC

INTEGRATION SPECS NTHETA= 21 NPSI= 21 DELR= 0.1057E 01

TAYLOR BUILDUP DATA FOR SHIELD 2 WITH EFFECTIVE ATOMIC NUMBER OF 82.0 USED

SHIELD THICKNESS 2.114E 01 1.016E 01 1.501E 01

GROUP	GROUP PRODUCTION RATE PHOTONS	GROUP AVERAGE ENERGY MEV	ENERGY FLUX AT DOSE POINT MEV/CMS/SEC	DOSE RATE AT DOSE POINT ROENTGENS/HOUR
1	1.100E 11	2.500E-02	8.243E-37	0.
2	4.720E 11	3.500E-02	5.163E-36	0.
3	7.150E 09	4.500E-02	1.047E-37	0.
4	5.820E 09	5.500E-02	1.074E-37	0.
5	1.770E 09	6.500E-02	3.954E-38	0.
6	4.270E 13	8.500E-02	1.305E-33	2.111E-39
7	8.870E 01	9.500E-02	3.098E-31	0.
8	2.300E 14	1.500E-01	8.334E-32	1.440E-37
9	7.540E 11	2.500E-01	7.137E-32	1.399E-37
10	1.510E 11	3.500E-01	1.314E-17	2.708E-23
11	2.050E 14	4.750E-01	5.978E-07	1.220E-12
12	8.190E 14	6.500E-01	7.823E-03	1.627E-08
13	1.010E 14	8.250E-01	6.539E-01	1.308E-06
14	1.470E 13	1.000E 00	1.335E 00	2.577E-06
15	6.400E 12	1.225E 00	6.144E 00	1.130E-05
16	9.340E 12	1.475E 00	5.006E 01	8.810E-05
17	1.070E 11	1.700E 00	1.548E 00	2.647E-06
18	8.410E-01	1.900E 00	2.799E-11	4.647E-17
19	1.440E 13	2.100E 00	7.890E 02	1.262E-03
20	8.660E 11	2.300E 00	7.930E 01	1.221E-04
21	4.020E-02	2.500E 00	4.575E-12	6.955E-11
22	1.470E-03	3.000E 00	2.823E-13	4.037E-19
TOTAL	1.445E 15		9.280E 02	1.490E-03

GAMMA ATTENUATION CALCULATION OUTER CYLINDER, CORE + SUB. 2000, MID-INNER. JACKET SURFACE

CYLINRICAL SOURCE CYLINDRICAL SHIELDS DIST TO DETECTOR 6.160E. 01 CM. LENGTH 5.010E 01 CM. VOL. = 7.131E 04CC

INTEGRATION SPECS NTHETA = 21 NPSI = 21 DELR = 0.1057E 01

TAYLOR BUILDUP DATA FOR SHIELD 2 WITH EFFECTIVE ATOMIC NUMBER OF 82.0 USED

SHIELD THICKNESS 2.114E 01 1.016E 01 1.508E 01

GROUP	GROUP PRODUCTION RATE PHOTONS	GROUP AVERAGE ENERGY MEV	ENERGY FLUX AT DOSE POINT MEV/CMS/SEC	DOSE RATE AT DOSE POINT ROENTGENS/HOUR
1	1.100E 11	2.500E-02	7.701E-35	0.
2	4.720E 11	3.500E-02	4.121E-34	3.066E-39
3	7.150E 09	4.500E-02	9.717E-36	0.
4	5.820E 09	5.500E-02	1.003E-33	0.
5	1.770E 09	6.300E-02	3.697E-36	0.
6	4.270E 13	8.500E-02	1.221E-31	1.971E-37
7	8.870E 09	9.500E-02	2.997E-36	0.
8	2.300E 14	1.500E-01	9.911E-30	1.725E-95
9	7.540E 11	2.500E-01	1.519E-30	2.977E-36
10	1.510E 11	3.500E-01	3.452E-16	7.112E-22
11	2.050E 14	4.750E-01	1.895E-05	3.865E-11
12	8.190E 14	6.500E-01	2.009E-01	5.843E-07
13	1.010E 14	8.250E-01	2.611E 01	5.282E-05
14	1.470E 13	1.000E 00	5.719E 01	1.104E-04
15	6.400E 12	1.225E 00	2.110E 02	5.170E•04
16	9.340E 12	1.475E 00	2.406E 03	4.235E-03
17	1.070E 11	1.700E 00	7.661E 01	1.311E-01
18	8.410E-01	1.900E 00	1.426E-09	2.367E-15
19	1.440E 13	2.100E 00	1.013E 04	6.534E-02
20	8.660E 11	2.300E 00	1.110E 03	6.438E-03
21	4.020E-02	2.500E 00	2.423E-10	3.683E-16
22	1.470E-03	3.000E 00	1.514E-11	2.165E-17
TOTAL	1.445E 15		4.786E 04	7.682E-02

GAMMA . ATTENUATION CALCULATION OUTER CYLINDER, CORE + SUBT. 0000 CASK, MID-INNER, 1 M. FROM JACKET

CYLINDRICAL SOURCE CYLINDRICAL SHIELDS DIST TO DETECTOR 1.616E 02 CM. LENGTH 5.080E 01 CM. VOL. = 7.131E 04CC

INTEGRATION SPECS NTHETA • 21 NPSI = 21 DELR = 0.1057E 01

TAYLOR BUILDUP DATA FOR SHIELD 2 WITH EFFECTIVE ATOMIC NUMBER OF 82.0 USED

SHIELD THICKNESS 2.114E 01 1.016E 01 1.508E 01

GROUP	GROUP PRODUCTION RATE PHOTONS	GROUP AVERAGE ENERGY MEV	ENERGY FLUX AT DOSE POINT MEV/CMS/SEC	DOSE RATE AT DOSE POINT ROENTGENS/HOUR
1	1.100E 11	2.500E-02	1.258E-33	0.
2	4.720E 11	3.500E-02	7.878E-33	0.
3	7.150E 09	4.500E-02	1.597E-36	0.
4	5.820E 09	5.500E-02	1.640E-36	0.
5	1.770E 09	6.500E-02	6.034E-37	0.
6	4.270E 13	8.500E•02	1.992E-32	3.221E-38
7	8.870E 09	9.500E-02	4.728E-37	0.
8	2.300E 14	1.500E-01	1.314E-30	2.270E-36
9	7.540E 11	2.500E-01	5.631E-31	1.104E-36
10	1.510E 11	3.500E-01	1.267E-16	2.609E-22
11	2.050E 14	4.750E-01	6.615E-06	1.350E-11
12	8.190E 14	6.500E-01	9.316E-02	1.938E-07
13	1.010E 14	8.250E-01	8.227E 00	1.645E-05
14	1.470E 13	1.000E 00	1.720E 01	3.320E-05
15	6.400E 12	1.225E 00	8.105E 01	1.491E-01
16	9.3101E 12	1.475E 00	6.709E 02	1.181E-03
17	1.070E 11	1.700E 00	2.093E 01	3.578E-05
18	8.410E-01	1.900E 00	3.815E-10	6.333E-16
19	1.440E 13	2.100E 00	1.080E 04	1.727E-02
20	8.660E 11	2.300E 00	1.090E 03	1.679E-03
21	4.020E-02	2.500E 00	6.296E-11	9.570E-17
22	1.470E-03	3.000E 00	3.893E-12	5.567E-18
TOTAL	1.445E 15		1.268E 04	2.037E-02

GAMMA ATTENUATION CALCULATION OUTER CYLINDER, CORE +SUBT. 2000 CASK, MID-INNER, TRUCK SIDE SURFACE

CYLINDRICAL SOURCE CYLINDRICAL SHIELDS DIST TO DETECTOR 1.21?E 02 r2 CM.LENGTH 5.080E 01 CM. VOL. = 7.131E 04CC
INTEGRATION SPECS NTHETA . 21 NPSI • 21 DELR= 0.1057E 01

TAYLOR BUILDUP DATA FOR SHIELD 2 WITH EFFECTIVE ATOMIC NUMBER OF 82.0 USED

SHIELD THICKNESS 2.114E 01 1.016E 01 1.508E 01

GROUP	GROUP PRODUCTION RATE PHOTONS	GROUP AVERAGE ENERGY MEV	ENERGY FLUX AT DOSE POINT MEV/CMS/SEC	DOSE RATE AT DOSE POINT ROENTGENS/HOUR
1	1.100E 11	2.300E-02	2.174E-35	0.
2	4.720E 11	3.500E-02	1.362E-34	0.
3	7.150E 09	4.300E-02	2.760E-36	0.
4	5.820E 09	5.500£-02	2.831E-36	0.
5	1.770E 09	6.500E-02	1.043E-36	0.
6	4.270E 13	8.500E-02	3.443E-32	5.568E-38
7	8.870E 08	9.500E-02	8.172E-37	0.
8	2.300E 14	1.500E-01	2.333E-30	4.031E-35
9	7.540E 11	2.500E-01	7.536E-31	1.477E-36
10	1.510E 11	3.500E-0I	1.724E-16	3.551E-22
11	2.050E 14	4.750E-01	9.318E-06	1.901E-11
12	8.190E 14	6.500E-01	1.350E-01	2.808E-07
13	1.010E 11	8.250E-01	1.227E 01	2.454E-05
14	1.470E 13	1.000E 00	2.601E 01	5.020E-03
15	6.100E 12	1.225E 00	1.244E 02	2.289E-04
16	9.340E 12	1.475E 00	1.041E 03	1.833E-03
17	1.070E 11	1.700E 00	3.269E 01	5.590E-05
18	8.410E-01	1.900E 00	5.994E-10	9.950E-16
19	1.440E 13	2.100E 00	1.702E 01	2.723E-02
20	8.660E 11	2.300E 00	1.725E 03	2.657E-03
21	4.020E-02	2.500E 00	9.973E-11	1.516E-16
22	1.470E-03	3.000E 00	6.183E-12	8.842E-11
TOTAL	1.445E 15		1.998E 04	3.208E-02

GAMMA ATTENUATION CALCULATION OUTER CYLINDER. CORE + SUBT. 2000 CASK. MID-INNER. 2 M. FROM TRUCK

CYLINDRICAL SOURCE CYLINDRICAL SHIELDS DIST TO DETECTOR 3.219E 02 CM.....LENGTH 5.080E 01 CM. VOL. = 7.131E 04CC

INTEGRATION SPECS NTHETA • 21 NPSI • 21 DELR= 0.1057E 01

TAYLOR BUILDUP DATA FOR SHIELD 2 WITH EFFECTIVE ATOMIC NUMBER OF 12.0 USED

SHIELD THICKNESS 2.114E 01 1.016E 01 1.508E 01

GROUP	GROUP PRODUCTION RATE PHOTONS	GROUP AVERAGE ENERGY MEV	ENERGY FLUX AT DOSE POINT MEV/CMS/SEC	DOSE RATE AT DOSE POINT ROENTGENS/HOUR
1	1.100E 11	2.500E-02	3.225E-36	0.
2	4.720E 11	3.500E-02	2.020E-35	0.
3	7.150E 09	4.300E-02	4.094E-37	0.
4	5.820E 09	5.500E-02	4.204E-37	0.
5	1.770E 09	6.500E-02	1.547E-37	0.
6	4.270E 13	8.500E-02	5.107E-33	1.238E-39
7	8.870E 08	9.500E-02	1.212E-37	0.
8	2.300E 14	1.500E-01	3.282E-31	5.670E-37
9	7.540E 11	2.500E-01	2.382E-31	4.669E-37
10	1.510E 11	3.500E-01	4.716E-17	9.716E-23
11	2.050E 14	4.750E-01	2.226E-06	4.541E-12
12	8.190E 14	6.500E-01	2.962E-02	6.162E-01
13	1.010E 14	8.250E-01	2.498E 00	4.996E-06
14	1.470E 13	1.000E 00	5.120E 00	9.882E-06
15	6.400E 12	1.225E 00	2.365E 01	4.351E-05
16	9.340E 12	1.475E 00	1.930E 02	3.397E-04
17	1.070E 11	1.700E 00	5.973E 00	1.021E-05
18	8.410E-01	1.900E 00	1.081E-10	1.795E-16
19	1.440E 13	2.100E 00	3.048E 03	4.878E-03
20	8.660E 11	2.300E 00	3.066E 02	4.721E-04
21	4.020E-02	2.500E 00	1.768E-11	2.688E-17
22	1.470E-03	3.000E 00	1.090E-12	1.559E-18
TOTAL	1.445E 15		3.585E 03	5.758E-03

GAMMA ATTENUATION CALCULATION OUTER CYLINDER, CORE + OBT. IN 2000 CASK, MID-INNER, IN CAB OF TRUCK

CYLINDRICAL SOURCE CYLINDRICAL SHIELDS DIST TO DETECTOR 6.3??E 02 CM. LENGTH 5.080E 01 CM. VOL. = 7.131E 04CC

INTEGRATION SPECS NTHETA = 21 NPSI = 21 DELR = 0.1057E 01

TAYLOR BUILDUP DATA FOR SHIELD 2 WITH EFFECTIVE ATOMIC NUMBER OF 82.0 USED

SHIELD THICKNESS 2.114E 01 1.016E 01 1.501E 01

GROUP	GROUP PRODUCTION RATE PHOTONS	GROUP AVERAGE ENERGY MEV	ENERGY FLUX AT DOSE POINT MEV/CMS/SEC	DOSE RATE At DOSE POINT ROENTGENS/HOUR
1	1.100E 11	2.500E-02	8.243E-37	0.
2	4.720E 11	3.500E-02	5.163E-36	0.
3	7.150E 09	4.500E-02	1.047E-37	0.
4	5.820E 09	5.500E-02	1.074E-37	0.
5	1.770E 09	6.500E-02	3.954E-38	0.
6	4.270E 13	8.500E-02	1.305E-33	2.111E-39
7	8.870E 08	9.500E-02	3.098E-38	0.
8	2.300E 14	1.500E-01	8.331E-32	1.440E-37
9	7.540E 11	2.500E-01	7.137E-32	1.399E-37
10	1.510E 11	3.500E-01	1.314E-17	2.708E-23
11	2.050E 14	4.750E-01	5.978E-07	1.220E-12
12	8.190E 14	6.500E-01	7.823E-03	1.627E-08
13	1.010E 14	8.250E-01	6.539E-01	1.308E-06
14	1.470E 13	1.000E 00	1.335E 00	2.577E-06
15	6.400E 12	1.225E 00	6.144E 00	1.130E-05
16	9.340E 12	1.475E 00	5.006E 01	8.810E-05
17	1.070E 11	1.700E 00	1.548E 00	2.647E-06
18	8.410E-01	1.900E 00	2.799E-11	4.647E-17
19	1.440E 13	2.100E 00	7.890E 02	1.262E-09
20	8.660E 11	2.300E 00	7.930E 01	1.221E-04
21	4.020E-02	2.500E 00	4.575E-12	6.955E-11
22	1.470E-03	3.000E 00	2.823E-13	4.037E-19
TOTAL	1.445E 15		9.280E 02	1.490E-03

APPENDIX 5.6.4

ISOSHLD INPUT AND OUTPUT FOR THE ANALYSIS OF THE DOSE RATES AT THE SIDE OF THE PACKAGE FROM THE "SUBTRACTED CENTER" OF THE OUTER CORE

```
$$ ASIS,ROUT(1U),TAP(:,8,16,79),KEYWORD(BMM)
$:IDENT:V151,BMM,WW1B,X4455
$:OPTION:FORTRAN
$:SELECT:ISHLD01
$:LIMITS:150,44K,,30K
$:REMOTE:00,1U
$:DATA:1*
   MODE = 3
2 YR HIFER OUTER CORE, SUBTRACTED CYLINDER IN 2000, MIDSIDE SURFACE
 $INPUT NEXT = 3, IGEOM = 7, X = 61.6, SLTH = 50.8, NTHETA = 20,
 NPS1 = 20, Y = 25.4, ISPEC = 1, DELR = 0.725, JBUF = 3, NSHLD = 4,
 T(1) = 14.492, T(2) = 6.646, T(3) = 10.16, T(4) = 15.08,
 SOURCE(1,1)=  5.15E+10, SOURCE(2,1)= 0.025,
 SOURCE(1,2)=  2.22E+11, SOURCE(2,2)= 0.035,
 SOURCE(1,3)=  3.30E+09, SOURCE(2,3)= 0.045,
 SOURCE(1,4)=  2.74E+09, SOURCE(2,4)= 0.055,
 SOURCE(1,5)=  8.34E+08, SOURCE(2,5)= 0.065,
 SOURCE(1,6)=  2.01E+13, SOURCE(2,6)= 0.085,
 SOURCE(1,7)=  4.17E+08, SOURCE(2,7)= 0.095,
 SOURCE(1,8)=  1.09E+14, SOURCE(2,8)= 0.150,
 SOURCE(1,9)=  3.55E+11, SOURCE(2,9)= 0.250,
 SOURCE(1,10)= 7.08E+10, SOURCE(2,10)=  0.350,
 SOURCE(1,11)= 9.63E+13, SOURCE(2,11)=  0.475,
 SOURCE(1,12)= 3.85E+14, SOURCE(2,12)=  0.650,
 SOURCE(1,13)= 4.75E+13, SOURCE(2,13)=  0.825,
 SOURCE(1,14)= 6.92E+12, SOURCE(2,14)=  1.000,
 SOURCE(1,15)= 3.01E+12, SOURCE(2,15)=  1.225,
 SOURCE(1,16)= 4.39E+12, SOURCE(2,16)=  1.475,
 SOURCE(1,17)= 5.05E+10, SOURCE(2,17)=  1.700,
 SOURCE(1,18)= 3.95E-01, SOURCE(2,18)=  1.900,
 SOURCE(1,19)= 6.78E+12, SOURCE(2,19)=  2.100,
 SOURCE(1,20)= 4.07E+11, SOURCE(2,20)=  2.300,
 SOURCE(1,21)= 1.89E-07, SOURCE(2,21)=  2.500,
 SOURCE(1,22)= 6.93E-04, SOURCE(2,22)=  3.000 $
 UFAM   15 1.432E-01 1.432E-01
 LEAD   14                    1.134E 01
 IFOL    6                                7.800E 00                    1
HIFER OUTER CORE SUBTRACTED CYLINDER IN 2000 CASK, 1 m. FROM MIDSIDE
 $INPUT NEXT = 4, X = 161.6 $
HIFER OUTER CORE SUBTRACTED CYLINDER IN 2000 CASK, 2 m. FROM MIDSIDE
 $INPUT NEXT = 4, X = 261.6 $
HIFER OUTER CORE SUBTRACTED CYLINDER IN 2000 CASK, SIDE OF TRUCK
 $INPUT NEXT = 4, X = 121.92 $
HIFER OUTER CORE SUBTRACTED CYLINDER IN 2000 CASK, 2 m. FROM TRUCK
 $INPUT NEXT = 4, X = 321.92 $
HIFER OUTER CORE FUEL CORE, SUBTRACTED CYL. IN 2000 CASK, IN TRUCK CAB
 $INPUT NEXT = 4, X = 639.4 $
OUTER CORE, SUBTRACTED CYL. IN 2000, TOPSIDE, JACKET SURFACE
 $INPUT NEXT = 4, Y = 50.8, X = 61.6 $
OUTER CORE, SUBTRACTED CYL. IN 2000 CASK, TOPSIDE, 1 m. FROM JACKET
 $INPUT NEXT = 4, X = 161.6 $
OUTER CORE, SUBTRACTED CYL. IN 2000 CASK, TOPSIDE, TRUCK SIDE SURFACE
 $INPUT NEXT = 4, X = 121.92 $
OUTER CORE, SUBTRACTED CYL. IN 2000 CASK, TOPSIDE, 2 m. FROM TRUCK
 $INPUT NEXT = 4, X = 321.92 $
OUTER CORE, SUBTRACTED CYL. IN 2000 CASK, TOPSIDE, IN CAB OF TRUCK
 $INPUT NEXT = 4, X = 639.4 $
OUTER CORE, SUBTRACTED CYL. IN 2000, MID-INNER, JACKET SURFACE
 $INPUT NEXT = 4, Y = 76.2, X = 61.6 $
OUTER CORE, SUBTRACTED CYL. IN 2000 CASK, MID-INNER, 1 m. FROM JACKET
 $INPUT NEXT = 4, X = 161.6 $
OUTER CORE, SUBTRACTED CYL. IN 2000 CASK, MID-INNER, TRUCK SIDE SURFACE
 $INPUT NEXT = 4, X = 121.92 $
OUTER CORE, SUBTRACTED CYL. IN 2000 CASK, MID-INNER, 2 m. FROM TRUCK
 $INPUT NEXT = 4, X = 321.92 $
OUTER CORE, SUBTRACTED CYL. IN 2000 CASK, MID-INNER, IN CAB OF TRUCK
 $INPUT NEXT = 4, X = 639.4 $
[illegible] CORE
 $[illegible] NEXT = 0 $
$:END:DOE
```

SHIELD COMPOSITION GR/CC	1	2	3	4	5	
URANIUM	1.432E-01	1.432E-01	0.	0.	0.	
LEAD	0.	0.	1.134E 01	0.	0.	
IRON	0.	0.	0.	7.800E 00	0.	
MASS ABSORPTION COEFFICIENTS (LAST REGION 13 AIR)						
	7.382E 00	7.382E 00	5.415E 02	9.576E 01	6.036E-04	0,
	3.308E 00	3.308E 00	1.928E 02	4.434E 01	3.233E-04	0.
	1.582E 00	1.582E 00	9.202E 01	2.055E 01	2.505E-04	0.
	8.961E-01	8.964E-01	5.262E 01	1.135E 01	2.219E-04	0.
	5.878E-01	5.878E-01	3.489E 01	7.574E 00	2.073E-04	0.
	2.477E-01	2.847E-01	2.507E 01	3.918E 00	1.891E-04	0.
	2.152E-01	2.152E-01	2.853E 01	3.111E 00	1.831E-04	0.
	3.030E-01	3.030E-01	1.564E 01	1.591E 00	1.591E-04,	0.
	1.027E-01	1.027E-01	6.339E 00	1.069E 00	1.360E-04,	0.
	5.556E-02	5.556E-02	3.476E 00	7.784E-01	1.211E-04,	0.
	3.258E-02	3.258E-02	2.013E 00	6.825E-01	1.092E-04	0.
	1.962E-02	1.962E-02	1.452E 00	5.616E-01	1.032E-04	0.
	1.425E-02	1.425E-02	9.923E-01	4.969E-01	8.291E-05	0.
	1.167E-02	1.167E-02	8.233E-01	4.586E-01	7.575E-05	0.
	9.594E-03	9.594E-03	7.008E-01	4.001E-01	6.835E-05	0.
	8.019E-03	8.019E-03	6.056E-01	3.666E-01	6.143E-05	0.
	7.375E-03	7.375E-03	5.534E-01	3.479E-01	5.702E-05	0.
	6.917E-03	6.917E-03	5.250E-01	3.237E-01	5.368E-05	0.
	6.616E-03	6.616E-03	5.024E-01	3.136E-01	5.070E-05	0.
	6.444E-03	6.444E-03	4.854E-01	2.972E-01	4.855E-05	0.
	6.315E-03	6.315E-03	4.751E-01	2.948E-01	4.617E-05	0.
	6.186E-03	6.186E-03	4.661E-01	2.769E-01	4.044E-05	0.
	0.	0.	0.	0.	0.	0.
	0.	0.	0.	0.	0.	0.
	0.	0.	0.	0.	0.	0.

EXP UNDERFLO AT LOCATION 005335
EXP UNDERFLO At LOCATION 005335
EXP UNDERFLO AT LOCATION 005335
EXP UNDERFLO AT LOCATION 005335
EXP UNDERFLO AT LOCATION 005335
EXP UNDERFLO AT LOCATION 005335
EXP UNDERFLO AT LOCATION 005335
EXP UNDERFLO At LOCATION 005333
EXP UNDERFLO AT LOCATION 005333
EXP UNDERFLO AT LOCATION 005335
EXP UNDERFLO AT LOCATION 005339
EXP UNDERFLO AT LOCATION 005936
EXP UNDERFLO At LOCATION 005335
EXP UNDERFLO AT LOCATION 005335
EXP UNDERFLO AT LOCATION 016420
EXP UNDERFLO AT LOCATION 005335
EXP UNDERFLO At LOCATION 005335
EXP UNDERFLO AT LOCATION 005335
EXP UNDERFLO AT LOCATION 005335
EXP UNDERFLO AT LOCATION 005335
EXP UNDERFLO AT LOCATION 005335

(LEFT BLANK)

GAMMA ATTENUATION CALCULATION HIFER OUTER CORE SUBTRACTED CYLINDER IN 2000 CASK, 1 M. FROM MIDSIDE

CYLINDRICAL SOURCE CYLINDRICAL SHIELDS DIST TO DETECTOR 1.616E 02 CM, LENGTH 5.080E 01 CM. VOL. = 3.352E 04CC

INTEGRATION SPECS NTHETA = 21 NPSI = 21 DELR 0.7250E 00

TAYLOR BUILDUP DATA FOR SHIELD 3 WITH EFFECTIVE ATOMIC NUMBER OF 82.0 USED

SHIELD THICKNESS 1.449E 01 6.646E 00 1.016E 01 1.508E 01

GROUP	GROUP PRODUCTION RATE PHOTONS	GROUP AVERAGE ENERGY MEV	ENERGY FLUX AT DOSE POINT MEV/CMS/SEC	DOSE RATE AT DOSE POINT ROENTGENS/HOUR
1	5.150E 10	2.500E-02	5.960E-36	0.
2	2.220E 11	3.500E-02	3.750E-35	0.
3	3.360E 09	4.500E-02	7.596E-37	0.
4	2.740E 09	5.500E-02	7.812E-37	0.
5	8.310E 01	6.300E-02	2.877E-37	0.
6	2.010E 13	8.500E-02	9.491E-33	1.535E-31
7	4.170E 01	9.500E-02	2.250E-37	0.
8	1.080E 14	1.500E-01	5.164E-31	8.924E-37
9	3.550E 11	2.500E-01	4.622E-31	9.060E-37
10	7.080E 10	3.500E-01	1.132E-16	2.333E-22
11	9.630E 13	4.750E-0I	5.663E-06	1.155E-11
12	3.850E 14	6.500E-01	7.620E-02	1.585E-07
13	4.750E 13	8.250E-01	6.312E 00	1.262E-05
14	6.920E 12	1.000E 00	1.280E 01	2.470E-05
16	3.010E 12	1.225E 00	5.818E 01	1.071E-04
16	4.390E 12	1.475E 00	4.680E 02	8.238E-04
17	5.050E 10	1.700E 00	1.141E 01	2.463E-05
18	3.950E-01	1.900E 00	2.575E-10	4.275E-16
19	6.780E 12	2.100E 00	7.236E 03	1.158E-02
20	4.070E 11	2.300E 00	7.224E 02	1.113E-03
21	1.890E-02	2.500E 00	4.159E-11	6.321E-17
22	6.930E-04	3.000E 00	2.560E-12	3.661E-18
TOTAL	6.792E 14		9.518E 03	1.368E-02

GAMMA ATTENUATION CALCULATION HIFER OUTER CORE SUBTRACTED CYLINDER IN 2000 CASK. 2 M. FROM MIDSIDE

CYLINDRICAL SOURCE CYLINDRICAL SHIELDS DIST TO DETECTOR 2.616E 02 CM. LENGTH 5.080E 01 CM. VOL. = 3.352E 04CC

INTEGRATION SPECS NTHETA = 21 NPSI = 21 DELR = 0.7250E 00

TAYLOR BUILDUP DATA FOR SHIELD 3 WITH EFFECTIVE ATOMIC NUMBER OF 82.0 USED

SHIELD THICKNESS 1.449E 01 6.646E 00 1.016E 01 1.508E 01

GROUP	GROUP PRODUCTION RATE PHOTONS	GROUP AVERAGE ENERGY MEV	ENERGY FLUX AT DOSE POINT MEV/CMS/SEC	DOSE RATE AT DOSE POINT ROENTGENS/HOUR
1	5.130E 10	2.500E-02	2.278E-36	0.
2	2.220E 11	3.500E-02	1.433E-35	0.
3	3.360E 09	4.500E-02	2.903E-37	0.
4	2.740E 09	5.500E-02	2.985E-37	0.
5	8.310E 01	6.500E-02	1.100E-37	0.
6	2.010E 13	8.500E-02	3.627E-33	5.863E-39
7	4.170E 00	9.500E-02	8.597E-38	0.
8	1.080E 14	1.500E-01	1.964E-31	3.395E-37
9	3.550E 11	2.500E-01	2.075E-31	4.067E-37
10	7.080E 10	3.300E-01	4.765E-17	9.815E-23
11	9.630E 13	4.750E-01	2.302E-06	4.695E-12
12	3.830E 14	6.500E-01	3.048E-02	6.939E-08
13	4.750E 13	8.250E-01	2.490E 00	4.992E-06
14	6.920E 12	1.000E 00	5.037E 00	9.721E-06
15	3.010E 12	1.225E 00	2.279E 01	4.194E-05
16	4.390E 12	1.475E 00	1.828E 02	3.218E-04
17	5.050E 10	1.700E 00	5.618E 00	9.607E-06
18	3.930E-01	1.900E 00	1.003E-10	1.665E-16
19	6.780E 12	2.100E 00	2.816E 03	4.506E-03
20	4.070E 11	2.300E 00	2.809E 02	4.326E-04
21	1.890E-02	2.500E 00	1.617E-11	2.457E-17
22	6.930E-01	9.000E 00	9.949E-13	1.423E-18
TOTAL	6.792E 14		3.316E 03	5.326E-03

GAMMA ATTENUATION CALCULATION HIFER OUTER CORE SUBTRACTED CYLINDER IN 2000 CASK. SIDE OF TRUCK

CYLINDRICAL SOURCE CYLINDRICAL SHIELDS DIST TO DETECTOR 1.219E 02 CM. LENGTH 5.080E 01 CM. VOL. = 3.352E 04CC

INTEGRATION SPECS NTHETA = 21 NPS 1 = 21 DELR .0.7250E 00

TAYLOR BUILDUP DATA FOR SHIELD 3 WITH EFFECTIVE ATOMIC NUMBER OF 82.0

SHIELD THICKNESS 1.449E 01 6.646E 00 1.016E 01 1.508E 01

GROUP	GROUP PRODUCTION RATE PHOTONS	GROUP AVERAGE ENERGY MEV	ENERGY FLUX AT DOSE POINT MEV/CMS/SEC	DOSE RATE AT DOSE POINT ROENTGENS/HOUR
1	5.150E 10	2.500E-02	1.042E-35	0.
2	2.220E 11	3.500E-02	6.558E-35	0.
3	3.360E 09	4.500E-02	1.328E-36	0.
4	2.740E 09	5.500E-02	1.366E-36	0.
5	8.340E 01	6.500E-02	5.031E-37	0.
6	2.010E 13	8.500E-02	1.660E-32	2.684E-31
7	4.170E 08	9.500E-02	3.934E-37	0.
8	1.080E 14	1.500E-01	9.084E-31	1.570E-36
9	3.550E 11	2.500E-01	6.793E-31	1.331E-36
10	7.080E 10	3.500E-01	1.763E-16	3.633E-22
11	9.630E 13	4.750E-01	9.145E-06	1.866E-11
12	3.850E 14	6.500E-01	1.253E-01	2.606E-07
13	4.750E 13	8.250E-01	1.053E 01	2.106E-05
14	6.920E 12	1.000E 00	2.147E 01	4.144E-05
15	3.010E 12	1.225E 00	9.820E 01	1.807E-04
16	4.390E 12	1.475E 00	7.932E 02	1.396E-03
17	5.050E 10	1.700E 00	2.447E 01	4.184E-05
18	3.950E-01	1.900E 00	4.383E-10	7.275E-16
19	6.780E 12	2.100E 00	1.233E 04	1.973E-02
20	4.070E 11	2.300E 00	1.232E 03	1.898E-03
21	1.890E-02	2.500E 00	7.097E-11	1.079E-16
22	6.930E-04	3.000E 00	4.372E-12	6.252E-18
TOTAL	6.792E 14		1.451E 04	2.331E-02

GAMMA ATTENUATION CALCULATION HIFER OUTER CORE SUBTRACTED CYLINDER IN 2000 CASK. 2 M. FROM. TRUCK

CYLINDRICAL SOURCE CYLINDRICAL SHIELDS DIST TO DETECTOR 3.219E 02 CM. LENGTH 5.010E Of CM. VOL. = 3.352E 04CC

INTEGRATION SPECS NTHETA = 21 NPSI -= 21 DELR -0.7250E 00

TAYLOR BUILDUP DATA FOR SHIELD 3 WITH EFFECTIVE ATOMIC NUMBER Of 82.0 USED

SHIELD THICKNESS 1.449E 01 6.646E 00 1.016E 01 1.508E 01

GROUP	GROUP PRODUCTION RATE PHOTONS	GROUP AVERAGE ENERGY MEV	ENERGY FLUX AT DOSE POINT MEV/CMS/SEC	DOSE RATE AT DOSE POINT ROENTGENS/HOUR
1	5.150E 10	2.500E-02	1.505E-36	0.
2	2.220E 11	3.500E-02	9.468E-36	0.
3	3.360E 09	4.500E-02	1.918E-37	0.
4	2.740E 09	5.500E-02	1.972E-37	0.
5	8.340E 08	6.500E-02	7.264E-31	0.
6	2.010E 13	8.500E-02	2.396E-33	3.875E-39
7	4.170E 08	9.500E-02	5.680E-31	0.
8	1.080E 14	1.500E-01	1.297E-31	2.241E-37
9	3.550E 11	2.500E-01	1.413E-31	2.769E-37
10	7.080E 10	3.500E-01	3.197E-17	6.586E-23
11	9.630E 13	4.750E-01	1.533E-06	3.128E-12
12	3.850E 14	6.500E-01	2.024E-02	4.210E-08
13	4.750E 13	8.250E-01	1.655E 00	3.310E-06
14	6.920E 12	1.000E 00	3.338E 00	6.442E-06
15	3.010E 12	1.225E 00	1.510E 01	2.778E-05
16	4.390E 12	1.475E 00	1.210E 02	2.130E-04
17	5.050E 10	1.700E 00	3.719E 00	6.359E-06
18	3.950E-01	1.900E 00	6.637E-11	1.102E-16
19	6.780E 12	2.100E 00	1.864E 03	2.982E-03
20	4.070E 11	2.300E 00	1.859E 02	2.863E-04
21	1.890E-02	2.500E 00	1.070E-11	1.626E-17
22	6.930E-04	3.000E 00	6.585E-13	9.417E-19
TOTAL	6.792E 14		2.194E 03	3.525E-03

GAMMA ATTENUATION CALCULATION HIFER OUTER CORE FUEL CORE SUBTRACTED CYL. IN 2000 CASK IN TRUCK CAB

CYLINDRICAL SOURCE CYLINDRICAL SHIELDS DIST TO DETECTOR 6.394E 02 CM. LENGTH 5.080E 01 VOL. = 3.352E 04CC

INTEGRATION SPECS NTHETA = 21 NPSI = 21 DELR = 0.7250E 00

TAYLOR BUILDUP DATA FOR SHIELD 3 WITH EFFECTIVE ATOMIC NUMBER OF 82.0 USED

SHIELD THICKNESS 1.449E 01 6.646E 00 1.016E 01 1.508E 01

GROUP	GROUP PRODUCTION RATE PHOTONS	GROUP AVERAGE ENERGY MEV	ENERGY FLUX AT DOSE POINT MEV/CMS/SEC	DOSE RATE AT DOSE POINT ROENTGENS/HOUR
1	5.150E 10	2.500E-02	3.830E-37	0.
2	2.220E 11	3.500E-02	2.410E-36	0.
3	3.360E 09	4.500E-02	4.881E-38	0.
4	2.740E 09	5.300E-02	5.020E-38	0.
5	8.340E 08	6.500E-02	1.849E-38	0.
6	2.010E 13	8.500E-02	6.099E-34	0.
7	4.170E 08	9.500E-02	1.446E-38	0.
8	1.080E 14	1.500E-01	3.297E-32	5.698E-38
9	3.550E 11	2.500E-01	3.617E-32	7.089E-38
10	7.080E 10	3.500E-01	8.069E-18	1.662E-23
11	9.630E 13	4.750E-01	3.852E-07	7.859E-13
12	3.850E 14	6.500E-01	5.076E-03	1.056E-08
13	4.750E 13	8.250E-01	4.162E-01	8.324E-07
14	6.920E 12	1.000E 00	8.399E-01	1.621E-06
15	3.010E 12	1.225E 00	3.803E 00	6.997E-06
16	4.390E 12	1.475E 00	3.053E 01	5.373E-05
17	5.050E 10	1.700E 00	9.386E-01	1.605E-06
18	3.950E-01	1.900E 00	1.676E-11	2.783E-17
19	6.780E 12	2.100E 00	7.710E 02	7.536E-04
20	4.070E 11	2.300E 00	4.699E 01	7.237E-05
21	1.890E-02	2.500E 00	2.707E-12	4.114E-18
22	6.930E-04	3.000E 00	1.668E-13	2.385E-19
TOTAL	6.792E 14		5.545E 02	8.907E-04

GAMMA ATTENUATION CALCULATION OUTER CORE. SUBTRACTED C IN 2000. TOPSIDE. JACKET SURFACE

CYLINDRICAL SOURCE CYLINDRICAL SHIELDS DIST TO DETECTOR 6. 101 CM. LENGTH 5.090E 01 CM. VOL. = 3.352E 04CC

INTEGRATION SPECS NTHETA = 21 NPSI = 21 DELR •0.7250E 00

TAYLOR BUILDUP DATA FOR SHIELD 3 WITH EFFECTIVE ATOMIC NUMBER OF 82.0 USED

SHIELD THICKNESS 1.449E 01 6.646E 00 1.016E 01 1.508E 01

GROUP	GROUP PRODUCTION RATE PHOTONS	GROUP AVERAGE ENERGY MEV	ENERGY FLUX AT DOSE POINT MEV/CMS/SEC	DOSE RATE AT DOSE POINT ROENTGENS/HOUR
1	5.150E 10	2.500E-02	3.535E-35	0.
2	2.220E 11	3.500E-02	2.224E-34	0.
3	3.360E 09	4.500E-02	4.505E-36	0.
4	2.740E 09	5.500E-02	4.633E-36	0.
5	8.340E 08	6.500E-02	1.706E-36	0.
6	2.010E 13	8.500E-02	5.629E-32	9.101E-38
7	4.170E 08	9.500E-02	1.334E-36	0.
8	1.080E 14	1.500E-01	3.726E-30	6.438E-36
9	3.550E 11	2.500E-01	7.299E-31	1.431E-36
10	7.080E 10	3.500E-01	2.064E-16	4.253E-22
11	9.630E 13	4.750E-01	1.203E-05	2.454E-11
12	3.850E 14	6.500E-01	1.805E-01	3.754E-07
13	4.750E 13	8.250E-01	1.673E 01	3.346E-05
14	6.920E 12	1.000E 00	3.588E 01	6.925E-05
15	3.010E 12	1.225E 00	1.739E 02	3.199E-04
16	4.390E 12	1.475E 00	1.470E 03	2.587E-03
17	8.050E 10	1.700E 00	4.662E 01	7.973E-05
18	3.950E-01	1.900E 00	8.567E-10	1.422E-15
19	6.780E 12	2.100E 00	2.448E 04	3.916E-02
20	4.070E 11	2.300E 00	2.489E 03	3.832E-03
21	1.890E-02	2.500E 00	1.440E-10	2.189E-16
22	6.930E-04	3.000E 00	8.993E-12	1.286E-17
TOTAL	6.792E 14		2.871E 04	4.608E-02

GAMMA ATTENUATION CALCULATION OUTER CORE. SUBTRACTED CYL IN 2000 CASK. TOPSIDE. 1 M, FROM JACKET

CYLINDRICAL SOURCE CYLINDRICAL SHIELDS DIST TO DETECTOR 1.616E 02 CM. LENGTH 5.080E 01 CM. VOL. = 3.352E 04CC

INTEGRATION SPECS NTHETA= 21 NPSI= 21 . DELR •0.7250E 00

TAYLOR BUILDUP DATA FOR SHIELD 3 WITH EFFECTIVE ATOMIC NUMBER Of 82.0 USED

SHIELD THICKNESS 1.449E 01 6.646E 00 1.016E 01 1.508E 01

GROUP	GROUP PRODUCTION RATE PHOTONS	GROUP AVERAGE ENERGY MEV	ENERGY FLUX AT DOSE POINT MEV/CMS/SEC	DOSE RATE AT DOSE POINT ROENTGENS/HOUR
1	5.150E 10	2.300E-02	5.875E-36	0.
2	2.220E 11	3.500E-02	3.697E-35	0.
3	3.360E 09	4.300E-02	7.487E-37	0.
4	2.740E 09	5.300E-02	7.701E-37	0.
5	8.340E 08	6.500E-02	2.836E-37	0.
6	2.010E 13	8.500E-02	9.355E-33	1.513E-31
7	4.170E 08	9.500E-02	2.218E-37	0.
8	1.080E 14	1.500E-01	5.213E-31	9.008E-37
9	3.550E 11	2.500E-01	2.710E-31	5.311E-37
10	7.080E 10	3.500E-01	7.554E-17	1.556E-22
11	9.630E 13	4.750E-01	4.186E-06	8.540E-12
12	3.850E 14	6.500E-01	5.970E-02	1.242E-07
13	4.750E 13	8.250E-01	5.196E 00	1.039E-05
14	6.920E 12	1.000E 00	1.076E 01	2.077E-05
15	3.010E 12	1.225E 00	4.998E 01	9.196E-03
16	4.390E 12	1.475E 00	4.082E 02	7.184E-04
17	5.050E 10	1.700E 00	1.267E 01	2.167E-05
18	3.950E-01	1.900E 00	2.282E-10	3.789E-16
19	6.780E 12	2.100E 00	6.442E 03	1.031E-02
20	4.070E 11	2.300E 00	6.461E 02	9.951E-04
21	1.890E-02	2.500E 00	3.725E-11	5.662E-17
22	6.930E-04	3.000E 00	2.301E-12	3.291E-18
TOTAL	6.792E 14		7.575E 03	1.217E-02

GAMMA ATTENUATION CALCULATION OUTER CORE. SUBTRACTED CYL IN 2000 CASK. TOPSIDE. TRUCK SIDE, SURFACE

CYLINDRICAL .SOURCE CYLINDRICAL SHIELDS DIST TO DETECTOR 1.209E 02 CM. LENGTH 5.080E 01 CM. VOL. = 3.352E 04CC

INTEGRATION SPECS NTHETA = 21 NPSI = 21 DELR = 0.7250E 00

TAYLOR BUILDUP DATA FOR SHIELD 3 WITH EFFECTIVE ATOMIC NUMBER OF 82.0 USED

SHIELD THICKNESS 1.449E 01 6.646E 00 1.016E 01 1.508E 01

GROUP	GROUP PRODUCTION RATE PHOTONS	GROUP AVERAGE ENERGY MEV	ENERGY FLUX AT DOSE POINT MEV/CMS/SEC	DOSE RATE AT DOSE POINT ROENTGENS/HOUR
1	5.150E 10	2.500E-02	1.010E-35	0.
2	2.220E 11	3.500E-02	6.356E-35	0.
3	3.360E 09	4.500E-02	1.287E-36	0.
4	2.740E 09	5.500E-02	1.324E-36	0.
5	8.310E 08	6.500E-02	4.877E-37	0.
6	2.010E 13	8.500E-02	1.609E-32	2.601E-38
7	4.170E 08	9.500E-02	3.813E-37	0.
8	1.080E 14	1.500E-01	9.174E-31	1.585E-36
9	3.550E 11	2.500E-01	3.627E-31	7.109E-37
10	7.080E 10	3.500E-01	1.030E-16	2.122E-22
11	9.630E 13	4.750E-01	5.907E-06	1.205E-11
12	3.850E 14	6.500E-01	8.660E-02	1.801E-07
13	4.750E 13	8.250E-01	7.752E 00	1.550E-05
14	6.920E 12	1.000E 00	1.627E 01	3.140E-05
15	3.010E 12	1.225E 00	7.669E 01	1.411E-04
16	4.390E 12	1.475E 00	6.332E 02	1.114E-03
17	5.050E 10	1.700E 00	1.978E 01	3.383E-05
18	3.950E-01	1.900E 00	3.583E-10	5.948E-16
19	6.780E 12	2.100E 00	1.015E 04	1.623E-02
20	4.070E 11	2.300E 00	1.021E 03	1.573E-03
21	1.890E-02	2.500E 00	5.894E-11	1.959E-17
22	6.930E-01	3.000E 00	3.651E-12	5.221E-18
TOTAL	6.792E 14		1.192E 04	1.914E-02

GAMMA ATTENUATION CALCULATION OUTER CORE. SUBTRACTED CYLINDER IN 2000 CASK, TOPSIDE 2 M. FROM TRUCK

CYLINDRICAL SOURCE CYLINDRICAL SHIELDS DIST TO DETECTOR 3.219E 02 CM. LENGTH 5.080E 01 CM, VOL. = 3.352E 04CC

INTEGRATION SPECS NTHETA= 21 NPSI = 21 DELR = 0.7250E 00

TAYLOR BUILDUP DATA FOR SHIELD 3 WITH EFFECTIVE ATOMIC NUMBER OF 82.0 USED

SHIELD THICKNESS 1.449E 01 6.646E 00 1.016E 01 1.508E 01

GROUP	GROUP PRODUCTION RATE PHOTONS	GROUP AVERAGE ENERGY MEV	ENERGY FLUX AT DOSE POINT MEV/CMS/SEC	DOSE RATE AT DOSE POINT ROENTGENS/HOUR
1	5.150E 10	2.500E-02	1.509E-36	0.
2	2.220E 11	3.500E-02	9.493E-36	0.
3	3.360E 09	4.500E-02	1.923E-37	0.
4	2.740E 09	5.500E-02	1.978E-37	0.
5	8.340E 08	6.500E-02	7.283E-38	0.
6	2.010E 13	8.500E-02	2.402E-33	3.885E-39
7	4.170E 01	9.500E-02	5.694E-38	0.
8	1.080E 14	1.500E-01	1.308E-31	2.260E-37
9	3.550E 11	2.500E-01	1.140E-31	2.235E-37
10	7.080E 10	3.500E-01	2.801E-17	5.771E-23
11	9.630E 13	4.750E-01	1.405E-06	2.867E-12
12	3.850E 14	6.500E-01	1.895E-02	3.941E-08
13	4.750E 13	8.250E-01	1.575E 00	3.151E-06
14	6.920E 12	1.000E 00	3.199E 00	6.173E-06
15	3.010E 12	1.225E 00	1.456E 01	2.680E-05
16	4.390E 12	1.475E 00	1.173E 02	2.065E-04
17	5.050E 10	1.700E 00	3.613E 00	6.179E-06
18	3.950E-01	1.900E 00	6.463E-11	1.073E-16
19	6.780E 12	2.100E 00	1.817E 03	2.907E-03
20	4.070E 11	2.300E 00	1.815E 02	2.795E-09
21	1.890E-02	2.500E 00	1.045E-11	1.589E-17
22	6.930E-01	3.000E 00	6.439E-13	9.208E-19
TOTAL	6.792E 14		2.139E 03	3.436E-03

GAMMA ATTENUATION CALCULATION OUTER CORE. SUBTRACTED CYL IN 2000 CASK. TOPSIDE IN CAB OF TRUCK

CYLINDRICAL SOURCE CYLINDRICAL SHIELDS DIST T0 DETECTOR 6.394E 02 CM. LENGTH 5.080E 01 CM. VOL. = 3.352E 04CC 0

INTEGRATION SPECS NTHETA = 21 NPSI = 21 DELR = 0.7250E 00

TAYLOR BUILDUP DATA FOR SHIELD 3 WITH EFFECTIVE ATOMIC NUMBER OF 12.0 USED

SHIELD THICKNESS 1.449E 01 6.646E 00 1.016E 01 1 . 508E 01

GROUP	GROUP PRODUCTION RATE PHOTONS	GROUP AVERAGE ENERGY MEV	ENERGY FLUX AT DOSE POINT MEV/CMS/SEC	DOSE RATE AT DOSE POINT ROENTGENS/HOUR
1	5.150E 10	2.500E-02	3.856E-37	0.
2	2:220E 11	3.500E-02	2.426E-36	0.
3	3.360E 09	4.500E-02	4.915E-38	0.
4	2.740E 09	5.500E-02	5.055E-38	0.
5	8.310E 08	6.500E-02	1.862E-38	0.
6	2.010E 13	8.500E-02	6.141E-34	0.
7	4.170E 08	9.900E-02	1.456E-38	0.
8	1.080E 11	1.500E-01	3.325E-32	5.746E-38
9	3.550E 11	2.500E-01	3.424E-32	6.711E-38
10	7.080E 10	3.500E-01	7.832E-18	1.613E-23
11	9.630E 13	4.750E-01	3.787E-07	7.725E-13
12	3.850E 14	6.500E-01	5.019E-03	1.044E-01
13	4.750E 13	8.250E-01	4.134E-01	8.267E-07
14	6.920E 12	1.000E 00	8.357E-01	1.613E-06
15	3.010E 12	1.225E 00	3.790E 00	6.971E-06
16	4.390E 12	1.475E 00	3.047E 01	5.362E-05
17	5.050E 10	1.700E 00	9.374E-01	1.603E-06
18	3.950E-01	1.900E 00	1.675E-11	2.781E-17
19	6.780E 12	2.100E 00	4.708E 02	7.533E-04
20	4.070E 11	2.300E 00	4.699E 01	7.237E-05
21	1.890E-02	2.500E 00	2.707E-12	4.114E-18
22	6.930E-04	3.000E 00	1.669E-13	2.386E-19
TOTAL	6.792E 14		5.542E 02	8.903E-04

GAMMA ATTENUATION CALCULATION OUTER CORE. SUBTRACTED CYL IN 2000. MID-INNER. JACKET SURFACE

CYLINDRICAL SOURCE CYLINDRICAL SHIELDS DIST TO DETECTOR 6.160E 01 CM. LENGTH 5.080E 01 CM. VOL. = 3.352E 04CC

INTEGRATION SPECS NTHETA = 21 NPSI = 21 DELR = 0.7250E 00

TAYLOR BUILDUP DATA FOR SHIELD 3 WITH EFFECTIVE ATOMIC NUMBER OF 82.0 USED

SHIELD THICKNESS 1.449E 01 6.646E 00 1.016E 01 1.508E 01

GROUP	GROUP PRODUCTION RATE PHOTONS	GROUP AVERAGE ENERGY MEV	ENERGY FLUX AT DOSE POINT MEV/CMS/SEC	DOSE RATE AT DOSE POINT ROENTGENS/HOUR
1	5.150E 10	2.500E-02	3.535E-35	0.
2	2.220E 11	3.500E-02	2.224E-34	0.
3	3.360E 09	4.500E-02	4.505E-36	0.
4	2.740E 09	5.500E-02	4.633E-36	0.
5	8.340E 08	6.500E-02	1.706E-36	0.
6	2.010E 13	8.500E-02	5.629E-32	9.101E-38
7	4.170E 08	9.500E-02	1.334E-36	0.
8	1.080E 14	1.500E-01	3.726E-30	6.438E-36
9	3.550E 11	2.500E-01	7.299E-31	1.431E-36
10	7.080E 10	3.500E-01	2.064E-16	4.253E-22
11	9.630E 13	4.750E-01	1.203E-05	2.454E-11
12	3.850E 14	6.500E-01	1.805E-01	3.754E-07
13	4.750E 13	8.250E-01	1.673E 01	3.346E-05
14	6.920E 12	1.000E 00	3.588E 01	6.925E-05
15	3.010E 12	1.225E 00	1.739E 02	3.199E-04
16	4.390E 12	1.475E 00	1.470E 03	2.587E-03
17	5.050E 10	1.700E 00	4.662E 01	7.973E-05
18	3.950E-01	1.900E 00	8.567E-10	1.422E-15
19	6.780E 12	2.100E 00	2.448E 04	3.916E-02
20	4.070E 11	2.300E 00	2.499E 03	3.832E-03
21	1.890E -02	2.500E 00	1.440E-10	2.189E-16
22	6.930E-04	3.000E 00	8.993E-12	1.286E-17
TOTAL	6.792E 14		2.871E 04	4.608E-02

GAMMA ATTENUATION CALCULATION OUTER CORE. SUBTRACTED CYL IN 2000 CASK. MID-INNER. 1 M. FROM JACKET

CYLINDRICAL SOURCE CYLINDRICAL SHIELDS DIST TO DETECTOR 1.616E 02 CM. LENGTH 5.080E 01 CM. VOL. = 3.352E 04CC 0

INTEGRATION SPECS NTHETA = 21 NPSI = 21 DELR = 0.7250E 00

TAYLOR BUILDUP DATA FOR SHIELD 3 WITH EFFECTIVE ATOMIC NUMBER OF 82.0 USED

SHIELD THICKNESS 1.449E 01 6.646E 00 1.016E 01 1.508E 01

GROUP	GROUP PRODUCTION RATE PHOTONS	GROUP AVERAGE ENERGY MEV	ENERGY FLUX AT DOSE POINT MEV/CMS/SEC	DOSE RATE AT DOSE POINT ROENTGENS/HOUR
1	5.150E 10	2.500E-02	5.875E-36	0.
2	2.220E 11	3.500E-02	3.697E-35	0.
3	3.360E 09	4.500E-02	7.487E-37	0.
4	2.740E 09	5.500E-02	7.701E-37	0.
5	8.340E 08	6.500E-02	2.836E-37	0.
6	2.010E 13	8.500E-02	9.3551-33	1.513E-38
7	4.170E 08	9.500E-02	2.218E-37	0.
8	1.080E 14	1.500E-01	5.213E-31	9.008E-37
9	3.550E 11	2.500E-01	2.710E-31	5.311E-37
10	7.080E 10	3.500E-01	7.554E-17	1.556E-22
11	9.630E 13	4.750E-01	4.186E-06	8.540E-12
12	3.850E 11	6.500E-01	5.970E-02	1.242E-07
13	4.750E 13	8.250E-01	5.196E 00	1.039E-05
14	6.920E 12	1.000E 00	1.076E 01	2.077E-05
15	3.010E 12	1.225E 00	1.998E 01	9.196E-05
16	4.390E 12	1.475E 00	1.082E 02	7.184E-04
17	5.050E 10	1.700E 00	1.267E 01	2.167E-05
18	3.950E-01	1.900E 00	2.282E-10	3.789E-16
19	6.780E 12	2.100E 00	6.442E 03	1.031E-02
20	4.070E 11	2.300E 00	6.461E 02	9.951E-01
21	1.8901-02	2.500E 00	3.725E-11	5.662E-17
22	6.930E-04	3.000E 00	2.301E-12	3.291E-10
TOTAL	6.792E 14		7.575E 03	1.217E-02

GAMMA ATTENUATION CALCULATION OUTER CORE. SUBTRACTED CYL IN 2000 CASK. MID-INNER. TRUCK SIDE SURFACE

CYLINDRICAL SOURCE CYLINDRICAL SHIELDS DIST TO DETECTOR 1.219E 02 CM. LENGTH 5.080E 01 CM. VOL. = 3.352E 04CC

INTEGRATION SPECS NTHETA = 21 NPSI = 21 DELR .0.7250E 00

TAYLOR BUILDUP DATA FOR SHIELD 3 WITH EFFECTIVE ATOMIC NUMBER OF 82.0 USED

SHIELD THICKNESS 1.449E 01 6.646E 00 1.016E 01 1.508E 01

GROUP	GROUP PRODUCTION RATE PHOTONS	GROUP AVERAGE ENERGY MEV	ENERGY FLUX A1 DOSE POINT MEV/CMS/SEC	DOSE RATE At DOSE POINT ROENTGENS/HOUR
1	5.150E 10	2.500E-02	1.010E-35	0.
2	2.220E 11	3.500E-02	6.356E-35	0.
3	3.360E 09	4.500E-02	1.287E-36	0.
4	2.740E 09	5.500E-02	1.324E-36	0.
5	8.310E 08	6.500E-02	4.877E-37	0.
6	2.010E 13	8.500E-02	1.609E-32	2.601E-38
7	4.170E 08	9.500E-02	3.813E-37	0.
8	1.080E 14	1.500E-01	9.174E-31	1.585E-36
9	3.550E 11	2.500E-01	3.627E-31	7.109E-37
10	7.080E 10	3.500E-01	1.030E-16	2.122E-22
11	9.630E 13	4.750E-01	5.907E-06	1.205E-11
12	3.850E 14	6.500E-01	8.660E-02	1.801E-07
13	4.730E 13	8.250E-01	7.752E 00	1.550E-05
14	6.920E 12	1.000E 00	1.627E 01	3.140E-05
15	3.010E 12	1.225E 00	7.669E 01	1.411E-04
16	4.390E 12	1.475E 00	6.332E 02	1.114E-03
17	5.050E 10	1.700E 00	1.978E 01	3.383E-05
18	3.950E-01	1.900E 00	3.583E-10	5.948E-16
19	6.780E 12	2.100E 00	1.015E 01	1.623E-02
20	4.070E 11	2.300E 00	1.021E 03	1.573E-03
21	1.890E-02	2.500E 00	5.894E-11	8.959E-17
22	6.930E-01	3.000E 00	3.651E-12	5.221E-18
TOTAL	6.792E 14		1.192E 04	1.914E-02

GAM(.TTENUATION CALCULATION OUTER CORE. SUBTRACTE(YLINDER IN 2000 CASK. MID-INNER. 2 M.FROM TRUCK(

CYLINDER SOURCE CYLINDRICAL SHIELDS DIST TO DETECTOR ???? CM. LENGTH 5.080E O1 CM. VOL. = 3.352E 04CC

INTEGRATION SPECS NTHETA = 21 NPSI = 21 DELR = 0.7250E 00

TAYLOR BUILDUP DATA FOR SHIELD 3 WITH EFFECTIVE ATOMIC NUMBER OF 82.0

SHIELD THICKNESS 1.449E 01 6.646E 00 1.016E 01 1.508E 01

GROUP	GROUP PRODUCTION RATE PHOTONS	GROUP AVERAGE ENERGY MEV	ENERGY FLUX AT DOSE POINT MEV/CMS/SEC	DOSE RATE AT DOSE POINT ROENTGENS/HOUR
1	5.150E 10	2.500E-02	1.509E-36	0.
2	2.220E 11	3.500E-02	9.493E-36	0.
3	3.360E 09	4.500E-02	1.923E-37	0.
4	2.740E 09	5.500E-02	1.978E-37	0.
5	8.310E 08	6.500E-02	7.283E-38	0.
6	2.010E 13	5.500E-02	2.402E-33	3.885E-39
7	4.170E 08	9.500E-02	5.694E-38	0.
8	1.080E 14	1.500E-01	1.308E-31	2.260E-37
9	3.550E 11	2.500E-01	1.140E-31	2.235E-37
10	7.080E 10	3.500E-01	2.801E-17	5.771E-23
11	9.630E 13	4.750E-01	1.405E-06	2.867E-12
12	3.850E 11	6.500E-01	1.895E-02	3.941E-08
13	4.750E 13	8.250E-01	1.575E 00	3.151E-06
14	6.920E 12	1.000E 00	3.199E 00	6.173E-06
15	3.010E 12	1.225E 00	1.456E 01	2.680E-05
16	4.390E 12	1.475E 00	1.173E 02	2.065E-04
17	5.050E 10	1.700E 00	3.613E 00	6.179E-06
18	3.950E-01	1.900E 00	6.463E-11	1.073E-16
19	6.780E 12	2.100E 00	1.817E 03	2.907E-03
20	4.070E 11	2.300E 00	1.815E 02	2.795E-04
21	1.890E-02	2.500E 00	1.045E-11	1.589E-17
22	6.930E-01	3.000E 00	6.439E-13	9.208E-19
TOTAL	6.792E 14		2.139E 03	3.438E-03

GAMMA ATTENUATION CALCULATION OUTER CORE. SUBTRACTED CYL IN 2000 CASK, MID-INNER IN CAB OF TRUCK

CYLINDRICAL SOURCE CYLINDRICAL SHIELDS DIST TO DETECTOR 6.394E 02 CM. LENGTH 5.060E 01 CM. VOL. = 3.352E 04CC

INTEGRATION SPECS NTHETA= 21 NPSI = 21 DELR .0.7250E 00

TAYLOR BUILDUP DATA FOR SHIELD 3 WITH EFFECTIVE ATOMIC NUMBER OF 82.0 USED

SHIELD THICKNESS 1.449E 01 6.646E 00 1.016E 01 1.508E 01

GROUP	GROUP PRODUCTION RATE PHOTONS	GROUP AVERAGE ENERGY MEV	ENERGY FLUX AT DOSE POINT MEV/CMS/SEC	DOSE RATE AT DOSE POINT ROENTGENS/HOUR
1	5.150E 10	2.500E-02	3.856E-37	0.
2	2.220E 11	3.500E-02	2.426E-36	0.
3	3.360E 09	4.500E-02	4.915E-38	0.
4	2.740E 09	5.500E-02	5.055E-38	0.
5	8.340E 08	6.500E-02	1.862E-38	0.
6	2.010E 13	8.500E-02	6.141E-34	0.
7	4.170E 01	9.500E-02	1.456E-38	0.
8	1.080E 14	1.500E-01	3.325E-32	5.746E-38
9	3.550E 11	2.500E-01	3.424E-32	6.711E-38
10	7.080E 10	3.500E-01	7.832E-18	1.613E-23
11	9.630E 13	4.750E-01	3.787E-07	7.725E-13
12	3.850E 14	6.500E-01	5.019E-03	1.044E-08
13	4.750E 13	8.250E-01	4.134E-01	8.267E-07
14	6.920E 12	1.000E 00	8.357E-01	1.613E-06
15	3.010E 12	1.225E 00	3.790E 00	6.974E-06
16	4.390E 12	1.475E 00	3.047E 01	5.362E-05
17	5.050E 10	1.700E 00	9.374E-01	1.603E-06
18	3.950E-01	1.900E 00	1.675E-11	2.781E-17
19	6.780E 12	2.100E 00	4.708E 02	7.533E-04
20	4.070E 11	2.300E 00	4.699E 01	7.237E-05
21	1.890E-02	2.500E 00	2.707E-12	4.114E-18
22	6.930E-04	3.000E 00	1.669E-13	2.386E-19
TOTAL	6.792E 14		5.542E 02	8.903E-04

APPENDIX 5.6.5

ISOSHLD INPUT AND OUTPUT FOR THE ANALYSIS OF THE DOSE RATES AT THE TOP AND BOTTOM OF THE PACKAGE FROM THE OUTER CORE PLUS THE "SUBTRACTED CENTER"

```
$$ ASIS,ROUT(1U),TAB (:,8,16,79).KEYWORD(BMM)
$:IDENT : BMM , VVV18 X4455
$:OPTION:FORTRAN
$:SELECT:ISHLD01
$:LIMITS:100,44K,,30K
$:REMOTE:06.1U
$:DATA:I*
    MODE = 3
2 YR HFIR OUTER CORE IN 2000, CORE-SUBTRACTED, TOP OF JACKET
 $INPUT NEXT = 3, IGEOM = 9, SLTH = 21.14, T(1) = 50.8, T(2) = 13.64.
 T(3) = 10.95, NSHLD = 3. NTHETA = 20, DELR = 2.54,
 JBUF = 2, ISPEC = 1, X = 225.06,
 SOURCE(1,1)=   1.10E+11,   SOURCE(2,1)=  0.025,
 SOURCE(1,2)=   4.72E+11,   SOURCE(2,2)=  0.035,
 SOURCE(1,3 =   7.15E+09,   SOURCE(2,3) =  0.045,
 SOURCE(1,4)=   5.82E+09,   SOURCE(2,4)=  0.055,
 SOURCE(1,5)=   1.77E+09,   SOURCE(2,5)=  0.065,
 SOURCE(1,6)=   4.27E+13,   SOURCE(2,6)=  0.085,
 SOURCE(1,7)=   8.87E+08,   SOURCE(2,7)=  0.095,
 SOURCE(1,8)=   2.30E+14,   SOURCE(2,8)=  0.150,
 SOURCE(1,9)=   7.54E+11,   SOURCE(2,9)=  0.250,
 SOURCE(1,10)=  1.51E+11,   SOURCE(2,10)= 0.350,
 SOURCE(1,11)= 2.05E+14,    SOURCE(2,11)= 0.475,
 SOURCE(1,12)= 8.19E+14,    SOURCE (2,12)= 0.650,
 SOURCE(1,13)= 1.01E+14,    SOUFCE(2,13)= 0.825,
 SOURCE(1,14)= 1.47E+13,    SOURCE(2,14) = 1.000,
 SOURCE(1,15)= 6.40E+12,    SOURCE(2,15)= 1.225,
 SOURCE(1,16)= 9.34E+12,    SOURCE(2,16)= 1.475,
 SOURCE(1,17)= 1.07E+11,    SOURCE (2,17)= 1.700,
 SOURCE(1,18)= 8.41E-01,    SOURCE(2,18)= 1.900,
 SOURCE(1,19)= 1.44E+13,    SOURCE(2,19)= 2.100,
 SOURCE(1,20)= 8.66E-411,   SOURCE(2,20) = 2.300,
 SOURCE(1,21)= 4.02E-02,    SOURCE(2,21)= 2.500,
 SOURCE(1,22)= 1.47E-03,    SOURCE(2,22)= 3.000 $
 LEAD    15   1.432E-01
z LEAD    14                1.134E 01
 IRON     9                             7.800E 00                              1
2 YR HF1R OUTER CORE IN 2000, CORE+SUBTRACTED, 1 m. FROM TOP
 $INPUT NEXT = 4, X = 325.06 $
2 YR HFIR OUTER CORE IN 2000, CORE+SUBTRACTED, 2 m. FROM TOP
 $INPUT NEXT = 4, X = 425.06 $
2 YR HFIR OUTER CORE IN 2000, CORE+SUBTRACTED, BASE SURFACE, 2.125 W
 $INPUT NEXT = 3, T(2) = 5.398, T(3) = 18.42, X = 156.213 $
 URAN    15  1.432E-01
 TUNG    13                1.750E 01
 IRON     9                             7.800E 00                              1
2 YR HFIR OUTER, CORE IN 2000, CORE+SUBTRACTED. 1 m FROM BASE, 2.125 W
 $INPUT NEXT = 4, X = 256.213 $
2 YR HFIR OUTER CORE IN 2000, CORE-SUBTRACTED, 2 m FROM BASE, 2.125 W
 $INPUT NEXT = 4, X = 356.213 $
DUMMY TITLE CARD
 $INPUT NEXT = 6 $
$ : ENDDOB
```

SHIELD COMPOSITION GR/CC	1	2	.3	4	5
URANIUM	1.432E-01	0.	0.	0.	0.
LEAD	0.	1.134E 01	0.	0.	0.
IRON	0.	0.	7.800E 00	0.	0.

MASS ABSORPTION COEFFICIENTS (LAST REGION IS AIR)

7.382E 00	5.415E 02	9.576E 01	6.036E-04	0.	0.
3.308E 00	1.928E 02	4.434E 01	3.233E-04	0.	0.
1.582E 00	9.202E 01	2.055E 01	2.505E-04	0.	0.
8.964E-01	5.262E 01	1.135E 01	2.219E-04	0.	0.
5.878E-01	3.489E 01	7.574E 00	2.073E-04	0.	0.
2.847E-01	2.507E 01	3.918E 00	1.891E-04	0.	0.
2.152E-01	2.853E 01	3.111E 00	1.831E-04	0.	0.
3.030E-01	1.564E 01	1.591E 00	1.591E-04	0.	0.
1.027E-01	6.339E 00	1.069E 00	1.360E-04	0.	0.
5.556E-02	3.476E 00	7.784E-01	1.211E-04	0.	0.
3.258E-02	2.013E 00	6.825E-01	1.092E-04	0.	0.
1.962E-02	1.452E 00	5.616E-01	1.032E-04	0.	0.
1.425E-02	9.923E-01	4.969E-01	8.291E-05	0.	0.
1.167E-02	8.233E-01	4.586E-01	7.575E-05	0.	0.
9.594E-03	7.008E-01	4.001E-01	6.835E-05	0	0.
8.019E-03	6.056E-01	3.666E-01	6.143E-05	0.	0.
7.375E-03	5.534E-01	3.479E-01	5.702E-05	0.	0.
6.917E-03	5.250E-01	3.237E-01	5.368E-05	0.	0.
6.616E-03	5.024E-01	3.136E-01	5.070E-05	0.	0.
6.444E-03	4.854E-01	2.972E-01	4.855E-05	0.	0.
6.315E-03	4.751E-01	2.948E-01	4.617E-05	0.	0.
6.186E-03	4.661E-01	2.769E-01	4.044E-05	0.	0.
0.	0.	0.	0.	0.	0.
0.	0.	0.	0.	0.	0.
0.	0.	0.	0.	0.	0.

EXP UNDERFLO AT LOCATION 016420
EXP UNDERFLO AT LOCATION 016420
EXP UNDERFLO AT LOCATION 016420
EXP UNDERFLO AT LOCATION 016420
EXP UNDERFLO AT LOCATION 016420
EXP UNDERFLO AT LOCATION 016420

GAMMA ATTENUATION CALCULATION 2 YR HFIR OUTER CORE IN 2000. CORE+ SUBTRACTED. TOP OF JACKET

END OF CYL. SOURCE SLAB SHIELDS DIST TO DETECTOR 2.25?E ?? CM VOL. =7. 132E 04 CC

LENGTH • 5.080E 01 CM RADIUS • 2.114E 01 CM

INTEGRATION SPECS NTHETA = 21 NPSI = 0 DELR = 0.2540E 01

TAYLOR BUILDUP DATA FOR SHIELD 2 WITH EFFECTIVE ATOMIC NUMBER OF 82.0 USED

SHIELD THICKNESS 5.080E 01 1.364E 01 1.095E 01

GROUP	GROUP PRODUCTION RATE PHOTONS	GROUP AVERAGE ENERGY MEV	ENERGY FLUX AT DOSE POINT MEV/CMS/SEC	DOSE RATE AT DOSE POINT ROENTGENS/HOUR
1	1.100E 11	2.500E-02	7.959E-36	0.
2	4.720E 11	3.500E-02	4.985E-35	0.
3	7.150E 09	4.500E-02	1.010E-36	0.
4	5.820E 09	5.500E-02	1.037E-36	0.
5	1.770E 09	6.500E-02	3.818E-37	0.
6	4.270E 13	8.500E-02	1.260E-32	2.038E-31
7	8.870E 08	9.500E-02	2.992E-37	0.
8	2.300E 14	1.500E-01	1.032E-30	1.783E-36
9	7.540E 11	2.500E-01	2.831E-33	5.550E-39
10	1.510E 11	3.500E-01	6.470E-20	1.333E-25
11	2.050E 11	4.750E-01	2.553E-07	5.208E-13
12	8.190E 11	6.500E-01	1.233E-02	2.565E-01
13	1.010E 11	8.250E-01	3.356E 00	6.712E-06
14	1.470E 13	1.000E 00	9.798E 00	1.891E-05
15	6.400E 12	1.225E 00	5.126E 01	9.432E-05
16	9.340E 12	1.475E 00	1.806E 02	8.458E-04
17	1.070E 11	1.700E 00	1.596E 01	2.730E-05
18	8.410E-01	1.900E 00	2.835E-10	4.706E-16
19	1.440E 13	2.100E 00	8.161E 03	1.306E-02
20	8.660E 11	2.300E 00	8.044E 02	1.239E-03
21	4.020E-02	2.500E 00	4.722E-11	7.177E-17
22	1.470E-03	3.000E 00	2.773E-12	3.966E-11
TOTAL	1.445E 15		9.526E 03	1.529E-02

EXP UNDERFLO At LOCATION 016420
EXP UNDERFLO AT LOCATION 016420
EXP UNDERFLO AT LOCATION 016420
EXP UNDERFLO AT LOCATION 016420
EXP UNDERFLO At LOCATION 016420
EXP UNDERFLO AT LOCATION 016420

GAMMA ATTENUATION CALCULATION 2 YR HFIR OUTER CORE IN 2000. CORE+SUBTRACTED 1 M. FROM TOP

END OF CYL. SOURCE SLAB SHIELDS DIST TO DETECTOR 3.251E 02 CM. VOL. = 7.132E 04 CC

LENGTH • 5.080E 01 CM RADIUS - 2.114E 01 CM

INTEGRATION SPECS NTHETA = 21 NPSI = 0 DELR = 0.2540E 01

TAYLOR BUILDUP DATA FOR SHIELD 2 WITH EFFECTIVE ATOMIC NUMBER OF 82.0 USED

SHIELD THICKNESS 5.060E 01 1.364E 01 1.095E 01

GROUP	GROUP PRODUCTION RATE PHOTONS	GROUP AVERAGE ENERGY MEV	ENERGY FLUX AT DOSE POINT MEV/CMS/SEC	DOSE RATE AT DOSE POINT ROENTGENS/HOUR
1	1.100E 11	2.500E-02	3.514E-36	0.
2	4.720E 11	3.500E-02	2.201E-35	0.
3	7.150E 09	4.500E-02	4.461E-37	0.
4	5.820E 09	5.500E-02	4.580E-37	0.
5	1.770E 09	6.500E-02	1.685E-37	0.
6	4.270E 13	8.500E-02	5.565E-33	8.998E-39
7	8.870E 08	9.500E-02	1.321E-37	0.
8	2.300E 14	1.500E-01	4.549E-31	7.861E-37
9	7.540E 11	2.500E-01	1.249E-33	2.448E-39
10	1.510E 11	3.500E-01	2.993E-20	6.166E-26
11	2.050E 14	4.750E-01	1.155E-07	2.357E-13
12	8.190E 14	6.500E-01	5.544E-03	1.153E-09
13	1.010E 14	8.250E-01	1.500E 00	3.000E-06
14	1.470E 13	1.000E 00	4.370E 00	8.434E-06
15	6.400E 12	1.225E 00	2.282E 01	4.200E-05
16	9.340E 12	1.475E 00	2.138E 02	3.762E-04
17	1.070E 11	1.700E 00	7.096E 00	1.213E-05
18	8.410E-01	1.900E 00	1.260E-10	2.091E-16
19	1.440E 13	2.100E 00	3.625E 03	5.801E-03
20	8.660E 11	2.300E 00	3.572E 02	5.501E-04
21	4.020E-02	2.500E 00	2.097E-11	3.188E-17
22	1.470E-03	3.000E 00	1.232E-12	1.762E-10
TOTAL	1.445E 15		4.232E 03	6.793E-03

EXP UNDERFLO AT LOCATION 016420
EXP UNDERFLO AT LOCATION 016420
EXP UNDERFLO AT LOCATION 016420
EXP UNDERFLO AT LOCATION 016420
EXP UNDERFLO AT LOCATION 016420
EXP UNDERFLO AT LOCATION 016420
EXP UNDERFLO AT LOCATION 016420

GAMMA ATTENUATION CALCULATION 2 YR HFIR OUTER CORE IN 2000 CORE+SUBTRACTED, 2 M. FROM TOP

END OF CYL. SOURCE SLAB SHIELDS DIST TO DETECTOR 4.25?E 02 CM. VOL.=7.132E 01 CC

LENGTH - 5.080E 01 CM RADIUS - 2.114E 01 CM

INTEGRATION SPECS NTHETA = 21 NPSI = 0 DELR = 0.2540E 01

TAYLOR BUILDUP DATA FOR SHIELD 2 WITH EFFECTIVE ATOMIC NUMBER OF 82.0 USED

SHIELD THICKNESS 5.080E 01 1.364E 01 1.095E 01

GROUP	GROUP PRODUCTION RATE PHOTONS	GROUP AVERAGE ENERGY MEV	ENERGY FLUX AT DOSE POINT MEV/CMS/SEC	DOSE RATE AT DOSE POINT ROENTGENS/HOUR
1	1.100E 11	2.500E-02	1.967E-36	0.
2	4.720E 11	3.500E-02	1.232E-35	0.
3	7.150E 09	4.500E-02	2.497E-37	0.
4	5.820E 09	5.500E-02	2.563E-37	0.
5	1.770E 09	6.500E-02	9.433E-38	0.
6	4.270E 13	8.500E-02	3.115E-33	5.036E-39
7	8.870E 08	9.500E-02	7.392E-38	0.
8	2.300E 14	1.500E-01	2.546E-31	4.400E-37
9	7.540E 11	2.500E-01	6.989E-34	0.
10	1.510E 11	3.500E-01	1.677E-20	3.455E-26
11	2.050E 14	4.750E-01	6.448E-08	1.315E-13
12	8.190E 14	6.500E-01	3.094E-03	6.436E-09
13	1.010E 14	8.250E-01	8.371E-01	1.674E-06
14	1.470E 13	1.000E 00	2.439E 00	4.708E-06
15	6.400E 12	1.225E 00	1.274E 01	2.345E-05
16	9.340E 12	1.475E 00	1.194E 02	2.101E-04
17	1.070E 11	1.700E 00	3.964E 00	6.778E-06
11	8.410E-01	1.900E 00	7.038E-11	1.168E-16
19	1.440E 13	2.100E 00	2.026E 03	3.241E-03
20	8.660E 11	2.300E 00	1.996E 02	3.074E-04
21	4.020E-02	2.500E 00	1.172E-11	1.782E-17
22	1.470E-03	3.000E 00	6.888E-13	9.850E-19
TOTAL	1.445E 15		2.365E 03	3.796E-03

SHIELD COMPOSITION GR/CC	1	2	3	4	5
URANIUM	1.432E-01	0.	0.	0.	0.
W	0.	1.750E 01	0.	0.	0.
IRON	0.	0.	7.800E 00	0.	0.

MASS ABSORPTION COEFFICIENTS (LAST REGION IS AIR)

7.382E 00	6.300E 02	9.576E 01	6.036E-04	0.	0.
3.308E 00	2.256E 02	4.434E 01	3.233E-04	0.	0.
1.582E 00	1.090E 02	2.055E 01	2.505E-04	0.	0.
8.964E-01	6.099E 01	1.135E 01	2.219E-04	0.	0.
5.878E-01	5.278E 01	7.574E 00	2.073E-04	0.	0.
2.847E-01	5.672E 01	3.918E 00	1.891E-04	0.	0.
2.152E-01	5.485E 01	3.111E 00	1.831E-04	0.	0.
3.030E-01	2.585E 01	1.591E 00	1.591E-04	0.	0.
1.027E-01	7.698E 00	1.069E 00	1.360E-04	0.	0.
5.556E-02	4.813E 00	7.784E-01	1.211E-04	0.	0.
3.258E-02	2.537E 00	6.825E-01	1.092E-04	0.	0.
1.962E-02	1.662E 00	5.616E-01	1.032E-04	0.	0.
1.425E-02	1.356E 00	4.969E-01	8.291E-05	0.	0.
1.167E-02	1.146E 00	4.586E-01	7.575E-05	0.	0.
9.594E-03	1.050E 00	4.001E-01	6.835E-05	0.	0.
8.019E-03	8.715E-01	3.666E-01	6.143E-05	0.	0.
7.375E-03	8.400E-01	3.479E-01	5.702E-05	0.	0.
6.917E-03	7.875E-01	3.237E-01	5.368E-03	0.	0.
6.616E-03	7.700E-01	3.136E-01	5.070E-05	0.	0.
6.444E-03	7.613E-01	2.972E-01	4.855E-05	0.	0.
6.315E-03	7.525E-01	2.948E-01	4.617E-05	0.	0.
6.186E-03	7.140E-01	2.769E-01	4.044E-05	0.	0.
0.	0.	0.	0.	0.	0.
0.	0.	0.	0.	0.	0.
0.	0.	0.	0.	0.	0.

EXP UNDERFLO AT LOCATION 016420
EXP UNDERFLO AT LOCATION 016420
EXP UNDERFLO AT LOCATION 016420
EXP UNDERFLO At LOCATION 016420
EXP UNDERFLO At LOCATION 016420
EXP UNDERFLO AT LOCATION 016420

GAMMA ATTENUATION CALCULATION 2 YR HFIR OUTER CORE IN 2000 CORE+SUBTRACTED. BASE SURFACE, 2.125 W

END OF CYL. SOURCE SLAB SHIELDS DIST TO DETECTOR 1.562E 02 CM. VOL.= 7.132E 04 CC

LENGTH • 5.080E 01 CM RADIUS • 2.114E 01 CM

INTEGRATION SPECS NTHETA = 21 NPSI = 0 DELR = 0.2510E 01

TAYLOR BUILDUP DATA FOR SHIELD 2 WITH EFFECTIVE ATOMIC NUMBER OF 74.0 USED

SHIELD THICKNESS 5.080E 01 5.398E 00 1.842E 01

GROUP	GROUP PRODUCTION RATE PHOTONS	GROUP AVERAGE ENERGY MEV	ENERGY FLUX AT DOSE POINT MEV/CMS/SEC	DOSE RATE AT DOSE POINT ROENTGENS/HOUR
1	1.100E 11	2.500E-02	1.906E-35	0.
2	4.720E 11	3.500E-02	1.211E-34	0.
3	7.150E 09	4.500E-02	2.488E-36	0.
4	5.820E 09	5.500E-02	2.525E-36	0.
5	1.770E 09	6.500E-02	8.969E-37	0.
6	4.270E 13	8.500E-02	2.763E-32	4.469E-38
7	8.870E 08	9.500E-02	6.339E-37	0.
8	2.300E 11	1.500E-01	8.075E-31	1.395E-36
9	7.540E 11	2.500E-01	1.917E-21	3.757E-27
10	1.510E 11	3.500E-01	1.103E-12	2.272E-18
11	2.050E 11	4.750E-01	4.425E-03	9.026E-09
12	8.190E 14	6.500E-01	3.264E 01	6.789E-05
13	1.010E 11	8.250E-01	1.010E 02	2.019E-04
14	1.470E 13	1.000E 00	1.204E 02	2.324E-04
15	6.400E 12	1.225E 00	3.350E 02	6.164E-04
16	9.340E 12	1.475E 00	2.895E 03	5.095E-03
17	1.070E 11	1.700E 00	6.449E 01	1.103E-04
18	8.410E-01	1.900E 00	1.184E-09	1.966E-15
19	1.440E 13	2.100E 00	2.938E 04	4.701E-02
20	8.660E 11	2.300E 00	2.750E 03	4.235E-03
21	4.020E-02	2.500E 00	1.511E-10	2.297E-16
22	1.470E-03	3.000E 00	1.089E-11	1.558E-17
TOTAL	1.445E 15		3.568E 04	5.757E-02

EXP UNDERFLO AT LOCATION 016420

**THIS IS THE LAST TIME THE ABOVE MESSAGE WILL APPEAR*

GAMMA ATTENUATION CALCULATION 2 YR HFIR OUTER CORE IN 2000, CORE+SUBTRACTED. 1 M FROM BASE, 2.125 W

END OF CYL. SOURCE SLAB SHIELDS DIST TO DETECTOR 2.562E 02 CM. VOL.=7.131E 01 CC

LENGTH • 5.010E 01 CM RADIUS • 2.114E 01 CM

INTEGRATION SPECS NTHETA = 21 NPSI = 0 DELR = 0.2540E 01

TAYLOR BUILDUP DATA FOR SHIELD 2 WITH EFFECTIVE ATOMIC NUMBER OF 74.0 USED

SHIELD THICKNESS 5.080E 01 5.398E 00 1.842E 01

GROUP	GROUP PRODUCTION RATE PHOTONS	GROUP AVERAGE ENERGY MEV	ENERGY FLUM AT DOSE POINT MEV/CMS/SEC	DOSE RATE AT DOSE POINT ROENTGENS/HOUR
1	1.100E 11	2.500E-02	6.073E-36	0.
2	4.720E 11	3.500E-02	3.859E-35	0.
3	7.150E 09	4.500E-02	7.928E-37	0.
1	5.820E 09	5.500E-02	8.045E-37	0.
5	1.770E 09	6.500E-02	2.858E-37	0.
6	4.270E 13	8.500E-02	8.806E-33	1.424E-38
7	8.870E 08	9.500E-02	2.020E-37	0.
8	2.300E 14	1.500E-01	2.573E-31	4.447E-37
9	7.540E 11	2.500E-01	7.480E-22	1.466E-27
10	1.510E 11	3.500E-01	3.983E-13	8.205E-19
11	2.050E 11	4.750E-01	1.521E-03	3.103E-09
12	8.190E 14	6.500E-01	1.100E 01	2.287E-05
13	1.010E 14	8.250E-01	3.382E 01	6.763E-05
14	1.470E 13	1.000E 00	4.011E 01	7.741E-05
15	6.400E 12	1.225E 00	1.111E 02	2.044E-04
16	9.340E 12	1.475E 00	9.554E 02	1.682E-03
17	1.070E 11	1.700E 00	2.126E 01	3.635E-05
18	8.410E-01	1.900E 00	3.893E-10	6.463E-16
19	1.440E 13	2.100E 00	9.652E 03	1.544E-02
20	8.660E 11	2.300E 00	9.023E 02	1.389E-03
21	4.020E-02	2.500E 00	4.959E-11	7.537E-17
22	1.470E-03	3.000E 00	3.568E-12	5.102E-14
TOTAL	1.445E 15		1.173E 04	1.892E-02

GAMMA ATTENUATION CALCULATION 2 YR HFIR OUTER CORE IN 2000, CORE-SUBTRACTED. 2 M FROM BASE. 2.125 W

END OF CYL. SOURCE SLAB SHIELDS DIST TO DETECTOR 3.56E 02 CM. VOL.=7.132E 04 CC

LENGTH = 5.080E 01 CM RADIUS • 2.114E 01 CM

INTEGRATION SPECS NTHETA = 21 NPSI = 0 DELR •0.254OE 01

TAYLOR BUILDUP DATA FOR SHIELD 2 WITH EFFECTIVE ATOMIC NUMBER OF 74.0 USED

SHIELD THICKNESS 5.080E 01 5.398E 00 1.842E 01

GROUP	GROUP PRODUCTION RATE PHOTONS	GROUP AVERAGE ENERGY MEV	ENERGY FLUX AT DOSE POINT MEV/CMS/SEC	DOSE RATE AT DOSE POINT ROENTGENS/HOUR
1	1.100E 11	2.500E-02	2.935E-36	0.
2	4.720E 11	3.500E-02	1.865E-35	0.
3	7.150E 09	1.500E-02	3.831E-37	0.
1	5.820E 09	5.500E-02	3.888E-37	0.
5	1.770E 09	6.500E-02	1.381E-37	0.
6	4.270E 13	8.500E-02	4.256E-33	6.881E-39
7	8.870E 08	9.500E-02	9.762E-31	0.
1	2.300E 11	1.500E-01	1.244E-31	2.149E-37
9	7.540E 11	2.500E-01	3.679E-22	7.211E-28
10	1.510E 11	3.500E-01	1.940E-13	3.996E-19
11	2.050E 11	4.750E-01	7.367E-04	1.503E-09
12	8.190E 14	6.500E-01	5.320E 00	1.107E-05
13	1.010E 11	8.250E-01	1.638E 01	3.277E-05
14	1.470E 13	1.000E 00	1.943E 01	3.750E-05
1S	6.100E 12	1.225E 00	5.383E 01	9.904E-05
16	9.340E 12	1.475E 00	4.627E 02	8.144E-04
17	1.070E 11	1.700E 00	1.030E 01	1.761E-05
11	8.110E-01	1.900E 00	1.885E-10	3.130E-16
19	1.440E 13	2.100E 00	4.675E 03	7.479E-03
20	8.660E 11	2.300E 00	4.370E 02	6.729E-04
21	4.020E-02	2.500E 00	2.402E-11	3.651E-17
22	1.170E-03	3.000E 00	1.728E-12	2.471E-11
TOTAL	1.445E 15		5.680E 03	9.165E-03

APPENDIX 5.6.6

ISOSHLD INPUT AND OUTPUT FOR THE ANALYSIS OF THE DOSE RATES AT THE TOP AND BOTTOM OF THE PACKAGE FROM THE "SUBTRACTED" CENTER OF THE OUTER CORE

```
$$     ASIS,ROUT   (1U),TAB(:,8,16,79)KEYWORD(BMM)
$:IDENT:BMM,VVV18,X4455
$:OPTION:FORTRAN
$:SELECT:ISHLD01
$:LIMITS:100,44K,,30K
$:REMOTE:06,1U
$:DATA:I*
     MODE = 3
2 YR HFIR OUTER CORE SUBTRACTED CYLINDER IN 2000, TOP OF JACKET
  $INPUT NEXT = 3, IGEOM = 9, SLTH = 14.49, T(1) = 50.8, T(2) = 13.64, T(3) = 10.95,
  NSHLD = 3, NTHETA = 30, DELR = 1.693,
  JBUF = 2, ISPEC = 1, X = 225.06,
  SOURCE(1,1)=    5.15E+10,    SOURCE(2,1)= 0.025,
  SOURCE(1,2)=    2.22E+11,    SOURCE(2,2)= 0.035,
  SOURCE(1,3)=    3.36E+09,    SOURCE(2,3)= 0.045,
  SOURCE(1,4)=    2.74E+09,    SOURCE(2,4)= 0.055,
  SOURCE(1,5)=    8.34E+08,    SOURCE(2,5)= 0.065,
  SOURCE(1,6)=    2.01E+13,    SOURCE(2,6)= 0.085,
  SOURCE(I ,7)=   4.17E+08,    SOURCE(2,7)= 0.095,
  SOURCE(1:8)=    1.08E+14,    SOURCE 2:8)= 0.150,
  SOURCE(1,9)=    3.55E+11,    SOURCE(2,9)= 0.250,
  SOURCE(1,10)=   7.08E+10,    SOURCE(2,10)=    0.350,
  SOURCE(1,11)=   9.63E+13,    SOURCE(2,11)=    0.475,
  SOURCE(1,12)=   3.85E+14,    SOURCE(2,12)=    0.650,
  SOURCE(1,13)=   4.75E+13,    SOURCE(2,13)=    0.825,
  SOURCE(1.14)=   6.92E+12,    SOURCE(2,14)=    1.000,
  SOURCE(1,15)=   3.01E+12,    SOURCE(2,15)=    1.225,
  SOURCE(1,16)=   4.39E+12,    SOURCE(2,16)=    1.475,
  SOURCE(1,17)=   5.05E+10,    SOURCE(2,17)=    1.700,
  SOURCE(1,18)=   3.95E-01,    SOURCE(2,18)=    1.900,
  SOURCE(1,19)=   6.78E+12,    SOURCE(2,19)=    2.100,
  SOURCE(1,20)=   4.07E+11,    SOURCE(2,20)=    2.300,
  SOURCE(1,21)=   1.89E-02,    SOURCE(2,21)=    2.500,
  SOUF;CE(1,22)=  6.93E-04,    SOURCE(2,22)=    3.000 $
  URAN    15        1.432E-01
  LEAD    14                  1.134E 01
  IRON     9                              7.800E 00                                  1
HFIR OUTER CORE IN 2000, SUBTRACTED CENTER, 1 m. FROM TOP
  $INPUT NEXT = 4, X = 325.06 $
HFIR. OUTER CORE IN 2000, SUBTRACTED CENTER, 2 m. FROM TOP
  $INPUT NEXT = 4, X = 425.06 $
HFIR OUTER CORE IN 2000, SUBTRACTED CENTER, BASE SURFACE, 2.125" W
  $INPUT NEXT = 3, T(2) = 5.398, T(3) = 18.42, X = 156.213 $
  URAN    15 1.432E-01
  TUNG    13                  1.750E 01
  IRON     9                              7.800E 00                                  1
HFIR OUTER CORE SUBTRACTED CYLINDER IN 2000, 1 m. FROM BASE, 2.125" W
  $INPUT NEXT = 4, X = 256.213 $
HFIR OUTER CORE SUBTRACTED CYLINDER IN 2000, 2 m. FROM BASE, 2.125" W
  $INPUT NEXT = 4, X = 356.213 $
DUMMY TITLE CARD
  INPUT NEXT = 6 $
$ : ENDDOB
```

SHIELD COMPOSITION GR/CC	1	2	3	4	5
URANIUM	1.432E-01	0.	0.	0.	0.
LEAD	0.	1.134E 01	0.	0.	0.
IRON	0.	0.	7.800E 00	0.	0.

MASS ABSORPTION COEFFICIENTS (LAST REGION IS AIR)

7.382E 00	5.415E 02	9.576E 01	6.036E-04	0.	0.
3.308E 00	1.928E 02	4.434E 01	3.233E-04	0.	0.
1.582E 00	9.202E 01	2.055E 01	2.505E-04	0.	0.
8.964E-01	5.262E 01	1.135E 01	2.219E-04	0.	0.
5.878E-01	3.489E 01	7.574E 00	2.073E-04	0.	0.
2.847E-01	2.507E 01	3.918E 00	1.891E-04	0.	0.
2.152E-01	2.853E 01	3.111E 00	1.831E-04	0.	0.
3.030E-01	1.564E 01	1.591E 00	1.591E-04	0.	0.
1.027E-01	6.339E 00	1.069E 00	1.360E-04	0.	0.
5.556E-02	3.476E 00	7.784E-01	1.211E-04	0.	0.
3.258E-02	2.013E 00	6.825E-01	1.092E-04	0.	0.
1.962E-02	1.452E 00	5.616E-01	1.032E-04	0.	0.
1.425E-02	9.923E-01	4.969E-01	8.291E-05	0.	0.
1.167E-02	8.233E-01	4.586E-01	7.575E-05	0.	0.
9.594E-03	7.008E-01	4.001E-01	6.835E-05	0.	0.
8.019E-03	6.056E-01	3.666E-01	6.143E-05	0.	0.
7.375E-03	5.534E-01	3.479E-01	5.702E-05	0.	0.
6.917E-03	5.250E-01	3.237E-01	5.368E-05	0.	0.
6.616E-03	5.024E-01	3.136E-01	5.070E-05	0.	0.
6.444E-03	4.854E-01	2.972E-01	4.855E-O5	0.	0.
6.315E-03	4.751E-01	2.948E-01	4.617E-05	0.	0.
6.186E-03	4.661E-01	2.769E-01	4.044E-05	0.	0.
0.	0.	0.	0.	0.	0.
0.	0.	0.	0.	0.	0.
0.	0.	0.	0.	0.	0.

EXP UNDERFLO AT LOCATION 016420
EXP UNDERFLO AT LOCATION 016420
EXP UNDERFLO AT LOCATION 016420
EXP UNDERFLO AT LOCATION 016420
EXP UNDERFLO AT LOCATION 016420
EXP UNDERFLO AT LOCATION 016420

GAMMA ATTENUATION CALCULATION 2 YR HFIR OUTER CORE SUBTRACTED CYLINDER IN 2000, TOP OF JACKET

END OF CYL. SOURCE SLAB SHIELDS DIST TO DETECTOR 2.251E 02 CM. VOL.•3.351E 04 CC

LENGTH • 5.080E 01 CM RADIUS • 1.449E 01 CM

INTEGRATION SPECS NTHETA = 31 NPSI = 0 DELR = 0.1693E 01

TAYLOR BUILDUP DATA FOR SHIELD 2 WITH EFFECTIVE ATOMIC NUMBER OF 82.0 USED

SHIELD THICKNESS 5.080E 01 1.364E 01 1.095E 01

GROUP	GROUP PRODUCTION RATE PHOTONS	GROUP AVERAGE ENERGY MEV	ENERGY FLUX AT DOSE POINT MEV/CMS/SEC	DOSE RATE AT DOSE POINT ROENTGENS/HOUR
1	5.150E 10	2.500E-02	3.835E-36	0.
2	2.220E 11	3.500E-02	2.413E-35	0.
3	3.360E 09	4.500E-02	4.887E-37	0.
4	2.740E 09	5.500E-02	5.026E-37	0.
5	8.340E 08	6.500E-02	1.851E-37	0.
6	2.010E 13	8.500E-02	6.106E-33	9.874E-39
7	4.170E 08	9.500E-02	1.447E-37	0.
8	1.080E 14	1.500E-01	4.974E-31	8.591E-37
9	3.550E 11	2.500E-01	1.370E-33	2.684E-39
10	7.080E 10	3.500E-01	3.375E-20	6.953E-26
11	9.630E 13	4.750E-01	1.293E-07	2.637E-13
12	3.850E 11	6.500E-01	6.173E-03	1.284E-08
13	4.750E 13	8.250E-01	1.664E 00	3.328E-06
14	6.920E 12	1.000E 00	4.846E 00	9.352E-06
15	3.010E 12	1.225E 00	2.525E 01	4.646E-05
16	4.390E 12	1.175E 00	2.360E 02	4.154E-01
17	5.050E 10	1.700E 00	7.863E 00	1.344E-05
18	3.950E-01	1.900E 00	1.388E-10	2.304E-16
19	6.780E 12	2.100E 00	4.004E 03	6.406E-03 ,
20	4.070E 11	2.300E 00	3.937E 02	6.062E-01
21	1.890E-02	2.500E 00	2.311E-11	3.513E-17
22	6.930E-01	3.000E 00	1.361E-12	1.946E-18
TOTAL	8.792E 11		4.673E 03	7.500E-03

EXP UNDERFLO AT LOCATION 016420
EXP UNDERFLO AT LOCATION 016420
EXP UNDERFLO AT LOCATION 016420
EXP UNDERFLO AT LOCATION 016420
EXP UNDERFLO AT LOCATION 016420
EXP UNDERFLO AT LOCATION 016420
EXP UNDERFLO AT LOCATION 016420

MA ATTENUATION CALCULATION HFIR OUTER CORE IN 2 SUBTRACTED CENTER, 1 M. FROM TOP

END OF CYL. SOURCE SLAB SHIELDS DIST TO DETECTOR 3.251E 02 CM. VOI.=3.351E 04 CC

LENGTH • 5.080E 01 CM RADIUS • 1.449E 01 CM

INTEGRATION SPECS NTHETA = 31 NPSI = 0 DELR = 0.1693E 01

TAYLOR BUILDUP DATA FOR SHIELD 2 WITH EFFECTIVE ATOMIC NUMBER OF 82.0 USED

SHIELD THICKNESS 5.080E 01 1.364E 01 1.095E 01

GROUP	GROUP PRODUCTION RATE PHOTONS	GROUP AVERAGE ENERGY MEV	ENERGY FLUX AT DOSE POINT MEV/CMS/SEC	DOSE RATE AT DOSE POINT ROENTGENS/HOUR
1	5.150E 10	2.500E-02	1.691E-36	0.
2	2.220E 11	3.500E-02	1.064E-35	0.
3	3.360E 09	4.500E-02	2.156E-37	0.
4	2.740E 09	5.500E-02	2.217E-37	0.
5	8.340E 08	6.500E-02	8.165E-38	0.
6	2.010E 13	8.500E-02	2.693E-33	4.355E-39
7	4.170E 08	9.500E-02	6.384E-38	0.
8	1.080E 14	1.500E-01	2.195E-31	3.793E-37
9	3.550E 11	2.500E-01	6.042E-34	0.
10	7.080E 10	3.500E-01	1.489E-20	3.066E-26
11	9.630E 13	4.750E-01	5.678E-08	1.158E-13
12	3.850E 14	6.500E-01	2.714E-03	5.646E-09
13	4.750E 13	8.250E-01	7.318E-01	1.464E-06
14	6.920E 12	1.000E 00	2.131E 00	4.114E-06
15	3.010E 12	1.225E 00	1.111E 01	2.044E-05
16	4.390E 12	1.475E 00	1.039E 02	1.829E-01
17	5.050E 10	1.700E 00	3.462E 00	5.919E-06
18	3.950E-01	1.900E 00	6.113E-11	1.015E-16
19	6.780E 12	2.100E 00	1.763E 03	2.821E-03
20	4.070E 11	2.300E 00	1.734E 02	2.670E-04
21	1.890E-02	2.500E 00	1.018E-11	1.548E-17
22	6.930E-01	3.000E 00	5.996E-13	8.574E-19
TOTAL	6.792E 14		2.058E 03	3.303E-03

EX1 UNDERFLO AT LOCATION 016420
EXP UNDERFLO AT LOCATION 016420
EXP UNDERFLO AT LOCATION 016420
EXP UNDERFLO AT LOCATION 016420
EXP UNDERFLO AT LOCATION 016420
EXP UNDERFLO AT LOCATION 016420
EXP UNDERFLO AT LOCATION 016420

GAMMA ATTENUATION CALCULATION HFIR OUTER CORE IN 2000 SUBTRACTED CENTER, 2 M. FROM TOP

END OF CYL. SOURCE SLAB SHIELDS DIST TO DETECTOR 4.25?E 02 CM. VOL.=3.351E 04 CC

LENGTH • 5.080E 01 CM RADIUS • 1.449E 01 CM

INTEGRATION SPECS NTHETA = 31 NPSI = 0 DELR =0.1693E 01

TAYLOR BUILDUP DATA FOR SHIELD 2 WITH EFFECTIVE ATOMIC NUMBER OF 82.0 USED

SHIELD THICKNESS 5.080E 01 1.364E 01 1.095E 01

GROUP	GROUP PRODUCTION RATE PHOTONS	GROUP AVERAGE ENERGY MEV	ENERGY FLUX AT DOSE POINT MEV/CMS/SEC	DOSE RATE AT DOSE POINT ROENTGENS/HOUR
1	5.150E 10	2.500E-02	9.487E-37	0.
2	2.220E 11	3.500E-02	5.969E-36	0.
3	3.360E 09	4.500E-02	1.209E-37	0.
1	2.740E 09	5.500E-02	1.244E-37	0.
5	8.310E 08	6.500E-02	4.580E-38	0.
8	2.010E 13	8.500E-02	1.511E-33	2.443E-39
7	4.170E 08	9.500E-02	3.581E-38	0.
1	1.080E 14	1.500E-01	1.232E-31	2.129E-37
9	3.550E 11	2.500E-01	3.390E-31	0.
10	7.080E 10	3.500E-01	8.220E-21	1.693E-26
11	9.630E 13	4.750E-01	3.143E-08	6.411E-14
12	3.850E 14	6.500E-01	1.506E-03	3.133E-09
13	4.750E 13	8.250E-01	4.070E-01	8.140E-07
11	6.920E 12	1.000E 00	1.187E 00	2.290E-06
15	3.010E 12	1.225E 00	6.191E 00	1.139E-05
16	4.390E 12	1.175E 00	5.795E 01	1.020E-01
17	5.050E 10	1.700E 00	1.931E 00	3.303E-06
11	3.950E-01	1.900E 00	3.142E-11	5.664E-17
19	6.780E 12	2.100E 00	9.845E 02	1.575E-03
20	4.070E 11	2.300E 00	9.683E 01	1.491E-01
21	1.890E-02	2.500E 00	5.687E-12	8.645E-11
22	6.930E-01	3.000E 00	3.351E-13	4.792E-19
TOTAL	6.792E 14		1.149E 03	1.844E-03

SHIELD COMPOSITION GR/CC	1	2	.3	4	5
URANIUM	1.432E-01	O.	0.	0.	0.
W	0.	1.750E 01	0.	0.	0.
IRON	0.	0.	7.800E 00	0.	0.

MASS ABSORPTION COEFFICIENTS (LAST REGION IS AIRI

7.382E 00	6.300E 02	9.576E 01	6.036E-04	0.	0.
3.308E 00	2.256E 02	4.434E 01	3.233E-04	0.	0.
1.582E 00	1.090E 02	2.055E 01	2.505E-04	0.	0.
8.964E-01	6.099E 01	1.135E 01	2.219E-04	0.	0.
5.878E-01	5.278E 01	7.574E 00	2.073E-04	0.	0.
2.847E-01	5.672E 01	3.918E 00	1.891E-04	0.	0.
2.152E-01	5.485E 01	3.111E 00	1.831E-04	0.	0.
3.030E-01	2.595E 01	1.591E 00	1.591E-04	0.	0.
1.027E-01	7.698E 00	1.069E 00	1.360E-04	0.	0.
5.556E-02	4.813E 00	7.784E-01	1.211E-04	0.	0.
3.258E-02	2.537E 00	6.825E-01	1.092E-04	0.	0.
1.962E-02	1.662E 00	5.616E-01	1.032E-04	0.	0.
1.425E-02	1.356E 00	4.969E-01	8.291E-05	0.	0.
1.167E-02	1.146E 00	4.596E-01	7.575E-05	0.	0.
9.594E-03	1.050E 00	4.001E-01	6.835E-05	0.	0.
8.019E-03	8.715E-01	3.666E-01	6.143E-05	0.	0.
7.375E-03	8.400E-01	3.479E-01	5.702E-05	0.	0.
6.917E-03	7.875E-01	3.237E-01	5.368E-05	0.	0.
6.616E-03	7.700E-01	3.136E-01	5.070E-09	0.	0.
6.444E-03	7.613E-01	2.972E-01	4.855E-05	0.	0.
6.315E-03	7.525E-01	2.948E-01	4.617E-05	0.	0.
6.186E-03	7.140E-01	2.769E-01	4.044E-05	0.	0.
0.	0.	0.	0.	0.	0.
0.	0.	0.	0.	0.	0.
0.	0.	0.	0.	0.	0.

EXP UNDERFLO AT LOCATION 016420
EXP UNDERFLO AT LOCATION 016420
EXP UNDERFLO AT LOCATION 016420
EXP UNDERFLO AT LOCATION 016420
EXP UNDERFLO AT LOCATION 016420
EXP UNDERFLO AT LOCATION 016420
**THIS IS THE LAST TIME THE ABOVE MESSAGE WILL APPEAR*

GAMMA ATTENUATION CALCULATION HFIR OUTER CORE IN 2000. SUBTRACTED CENTER. BASE SURFACE. 2.125" W

END OF CYL. SOURCE SLAB SHIELDS DIST TO DETECTOR 1.56E 02 CM. VOI.•3.351E 04 CC

LENGTH • 5.080E 01 CM RADIUS • 1.449E 01.CM

INTEGRATION SPECS NTHETA = 31 NPSI = 0 DELR = .0.1693E 01

TAYLOR BUILDUP DATA FOR SHIELD 2 WITH EFFECTIVE ATOMIC NUMBER OF 74.0 USED

SHIELD THICKNESS 5.080E 01 5.398E 00 1.842E 01

GROUP	GROUP PRODUCTION RATE PHOTONS	GROUP AVERAGE ENERGY MEV	ENERGY FLUX AT DOSE POINT MEV/CMS/SEC	DOSE RATE At DOSE POINT ROENTGENS/HOUR
1	5.150E 10	2.500E-02	9.234E-36	0.
2	2.220E 11	3.500E-02	5.895E-35	0.
3	3.360E 09	4.500E-02	1.210E-36	0.
4	2.710E 09	5.500E-02	1.230E-36	0.
5	8.340E 08	6.500E-02	4.374E-37	0.
6	2.010E 13	8.500E-02	1.346E-32	2.177E-38
7	4.170E 08	9.500E-02	3.084E-37	0.
8	1.080E 14	1.500E-01	3.924E-31	6.781E-37
9	3.350E 11	2.500E-01	1.165E-21	2.283E-27
10	7.080E 10	3.500E-01	6.164E-13	1.270E-18
11	9.630E 13	4.750E-01	2.351E-03	4.795E-09
12	3.850E 14	6.500E-01	1.692E 01	3.520E-05
13	4.750E 13	8.250E-01	5.185E 01	1.037E-04
14	6.920E 12	1.000E 00	6.149E 01	1.187E-04
15	3.010E 12	1.225E 00	1.700E 02	3.128E-04
16	4.390E 12	1.475E 00	1.460E 03	2.570E-03
17	5.050E 10	1.700E 00	3.261E 01	5.576E-05
18	3.950E-01	1.900E 00	5.944E-10	9.866E-16
19	6.780E 12	2.100E 00	1.477E 04	2.363E-02
20	4.070E 11	2.300E 00	1.378E 03	2.122E-03
21	1.890E-02	2.500E 00	7.574E-11	1.151E-16
22	6.930E-04	3.000E 00	5.464E-12	7.813E-18
TOTAL	6.792E 14		1.794E 04	2.895E-02

GAMMA ATTENUATION CALCULATION HFIR OUTER CORE SUBTRACTED CYLINDER IN 2000, 1 M. FROM BASE. 2.1'25' W

ENO OF CYL. SOURCE SLAB SHIELDS DIST TO DETECTOR 2.562E 02 CM. VOL.=3.351E 04 CC

LENGTH • 5.080E 01 CM RADIUS • 1.449E 01 CM

INTEGRATION SPECS NTHETA 31 NPSI = 0 DELR = 0.1693E 01

TAYLOR BUILDUP DATA FOR SHIELD 2 WITH EFFECTIVE ATOMIC NUMBER OF 74.0 USED

SHIELD THICKNESS 5.080E 01 5.398E 00 1.842E 01

GROUP	GROUP PRODUCTION RATE PHOTONS	GROUP AVERAGE ENERGY MEV	ENERGY FLUX AT DOSE POINT MEV/CMS/SEC	DOSE RATE AT DOSE POINT ROENTGENS/HOUR
1	5.150E 10	2.500E-02	2.916E-36	0.
2	2.220E 11	3.500E-02	1.861E-35	0.
3	3.360E 09	4.500E-02	3.820E-37	0.
4	2.740E 09	5.500E-02	3.884E-37	0.
5	8.340E 08	6.500E-02	1.381E-37	0.
6	2.010E 13	8.500E-02	4.251E-33	6.871E-39
7	4.170E 08	9.500E-02	9.739E-38	0.
8	1.080E 14	1.500E-01	1.239E-31	2.141E-37
9	3.550E 11	2.500E-01	3.871E-22	7.588E-28
10	7.080E 10	3.500E-01	1.997E-13	4.114E-19
11	9.630E 13	4.750E-01	7.514E-04	1.533E-09
12	3.850E 11	6.500E-01	5.397E 00	1.123E-05
13	4.750E 13	8.250E-01	1.656E 01	3.312E-05
14	6.920E 12	1.000E 00	1.963E 01	3.788E-05
15	3.010E 12	1.225E 00	5.424E 01	9.979E-05
16	4.390E 12	1.475E 00	4.651E 02	8.190E-04
17	5.050E 10	1.700E 00	1.039E 01	1.777E-05
18	3.950E-01	1.900E 00	1.893E-10	3.142E-16
19	8.780E 12	2.100E 00	4.702E 03	7.523E-03
20	4.070E 11	2.300E 00	4.386E 02	6.754E-04
21	1.890E-02	2.500E 00	2.411E-11	3.665E-17
22	6.930E-04	3.000E 00	1.739E-12	2.486E-19
TOTAL	6.792E 14		5.712E 03	9.217E-03

GAMMA ATTENUATION CALCULATION HFIR OUTER CORE SUBTRACTED CYLINDER IN 2000, 2 M. FROM BASE, 2.125" W

END OF CYL. SOURCE SLAB SHIELDS DIST TO DETECTOR 3.56E 02 CM. VOL.•3.351E 04 CC

LENGTH • 5.080E 01 CM RADIUS • 1.449E 01 CM

INTEGRATION SPECS NTHETA = 31 NPSI = 0 DELR = 0.1693E 01

TAYLOR BUILDUP DATA FOR SHIELD 2 WITH EFFECTIVE ATOMIC NUMBER OF 74.0 USED

SHIELD THICKNESS 5.080E 01 5.398E 00 1.842E 01

GROUP	GROUP PRODUCTION RATE PHOTONS	GROUP AVERAGE ENERGY MEV	ENERGY FLUX AT DOSE POINT MEV/CMS/SEC	DOSE RATE AT DOSE POINT ROENTGENS/HOUR
1	5.150E 10	2.500E-02	1.410E-36	0.
2	2.220E 11	3.500E-02	9.002E-36	0.
3	3.360E 09	4.500E-02	1.848E-37	0.
4	2.740E 09	5.500E-02	1.878E-37	0.
5	8.340E 08	6.500E-02	6.679E-38	0.
6	2.010E 13	8.500E-02	2.056E-33	3.324E-39
7	4.170E 08	9.500E-02	4.710E-38	0.
8	1.080E 14	1.500E-01	5.993E-32	1.036E-37
9	3.550E 11	2.500E-01	1.837E-22	3.601E-28
10	7.080E 10	3.500E-01	9.507E-14	1.958E-19
11	9.630E 13	4.750E-01	3.588E-04	7.320E-10
12	3.850E 14	6.500E-01	2.585E 00	5.377E-06
13	4.750E 13	8.250E-01	7.956E 00	1.591E-05
14	6.920E 12	1.000E 00	9.440E 00	1.822E-05
15	3.010E 12	1.225E 00	2.611E 01	4.804E-05
16	4.390E 12	1.475E 00	2.242E 02	3.945E-04
17	5.050E 10	1.700E 00	5.008E 00	8.563E-06
18	3.950E-01	1.900E 00	9.123E-11	1.514E-16
19	6.780E 12	2.100E 00	2.267E 03	3.628E-03
20	4.070E 11	2.300E 00	2.115E 02	3.257E-04
21	1.890E-02	2.500E 00	1.163E-11	1.768E-17
22	6.930E-04	3.000E 00	8.389E-13	1.200E-18
TOTAL	6.792E 14		2.754E 03	4.444E-03

APPENDIX 5.6.7

SUMMARY TABULATION OF THE CALCULATED DOSE RATES FROM THE VARIOUS ISOSHLD MODELS OF THE OUTER AND INNER CORE COMPONENTS

02-Aug-93 Frame 1

SUMMARY OF CALCULATED DOSE RATES FROM 2000 CONTAINER WITH COMPONENTS OF THE ISOSHLD MODEL OF THE BFR--CORE IN THE CAVITY

SOURCE: OUTER CORE IN LOWER POSITION SOURCE: INNER CORE IN UPPER POSITION

AT THE SIDE OF THE CONTAINER:

DOSE RATE LOCATION		TOTAL CYLINDER	(NEGATIVE) CYLINDER	NET DOSE RATE,mR/h	TOTAL CYLINDER	(NEGATIVE) CYLINDER	NET DOSE RATE, mR/h	SUM OF NET DOSE RATES, mR/h
MID-LEVEL	CONTACT	126.4	75.26	51.14	25.31	9.764	15.546	66.686
OF OUTER	ONE METER	22.97	13.68	9.29	6.683	2.563	4.12	13.41
CORE	TRUCK SIDE	39.25	23.31	15.94	10.53	4.042	6.488	22.428
	TWO METERS FROM TRUCK	5.81	3.525	2.385	1.892	0.7263	1.1657	3.5507
	CAB OF TRUCK	1.491	0.8907	0.6003	0.4893	0.186	0.3033	0.9036
BETWEEN	CONTACT	76.82	46.08	30.74	25.31	9.764	15.546	46.286
CORES	ONE METER	20.37	12.17	8.2	6.683	2.563	4.12	12.32
	TRUCK SIDE	32.06	19.14	12.94	10.53	4.042	6.488	19.428
	TWO METERS FROM TRUCK	5.758	3.438	2.322	1.892	0.7263	1.1657	3.4877
	CAB OF TRUCK	1.48	0.8903	0.5897	0.4893	0.186	0.3033	0.893
MID-LEVEL	CONTACT	76.82	46.08	30.74	41.25	15.81	25.44	56.18
OF INNER	ONE METER	20.37	12.17	8.2	7.523	2.876	4.647	12.847
CORE	TRUCK SIDE	32.06	19.14	12.94	12.81	4.899	7.911	20.851
	TWO METERS FROM TRUCK	5.758	3.436	2.322	1.941	0.7452	1.1958	3.5178
	CAB OF TRUCK	1.48	0.8903	0.5897	0.4896	0.186	0.3036	0.8933

AT THE TOP OF THE CONTAINER:

LOCATION	TOTAL CYLINDER	(NEGATIVE) CYLINDER	NET DOSE RATE, mR/h	TOTAL CYLINDER	(NEGATIVE) CYLINDER	NET DOSE RATE, mR/h	
CONTACT WITH TOP	15.29	7.5	7.78	9.116	2.688	6.418	14.208
ONE METER FROM TOP	6.783	3.303	3.48	3.09	0.893	2.197	5.677
TWO METERS FROM TOP	3.786	1.844	1.952	1.517	0.4423	1.0747	3.0267

AT THE BOTTOM OF THE CONTAINER (WITH 2.125" HEVIMET):

LOCATION	TOTAL CYLINDER	(NEGATIVE) CYLINDER	NET DOSE RATE, mR/h	TOTAL CYLINDER	(NEGATIVE) CYLINDER	NET DOSE RATE, d/h	
CONTACT WITH BASE	57.57	28.95	28.62	7.776	2.281	5.495	34.115
ONE METER FROM BASE	18.92	9.217	9.703	3.35	0.9775	2.3725	12.0755
TWO METERS FROG BASE	9.165	4.444	4.721	1.847	0.5381	1.3089	6.0298

INPUT LISTING FOR NORMAL CONDITION MODEL

```
HFIR FUEL/ IF2000/SEP=1.50IN. ACCIDENT COND COLD WFin=0.25 WFout=1.00
    210    /*# BATCHES
1000       /*  # NEUTRONS PER BATCH
        10 /*  # BATCHES TO SKIP
   2123469/*  INITIAL "SEED" (IF NON-ZERO)
       0   /*  "IDUMP"
       0   /*  "NRSTRT"
       0   /*  "NBTED" (NON-ZERO IS PRINT EDITS)
       0   /*  "KRED" (NUMBER OF COMBINED REGIONS IN EDITS)
    0    293      19      8
        5293 0    0 U(93.2)308+0.50WTF-H20 RHOMIX=1.750 g/cc                    MAT1
      2351   3.6260E-04
      2381   2.6120E-05
       131   2.4520E-02
        16   1.7730E-02
         1   3.3380E-02
         5   293 0 0 U(93.2)308+0.50WTF-H20 RHOMIX=1.786 g/cc                  MAT 2
      2351   4.9000E-04
      2381   3.5300E-05
       131   2.4120E-02
        16   1.8090E-02
         1   3.3380E-02
       2   293 0 0    MOD IN CONTAINER       (25$)
       1      1.6690E-02
      16      8.3470E-03
       2   293 0 0    MOD BETWEEN CONTAINERS        (100%)
       1 6.6770E-02
      16 3.3380E-02
         2 293 0 0 FULL DENSITY WATER                                    MAT 5
       1 6.6770E-02
      16 3.3380E-02
         1   293 0 0
   LEAD SHIELDING                                                          MAT 6
      82 3.29890E-02
         7   293 0 0
   304 STAINLESS STEEL                                                     MAT 7
      12 6.82690E-05
      14 8.53360E-04
      24 1.53600E-02
      26 6.04950E-02
      28 6.82690E-03
      55 1.70670E-03
    1316 2.56010E-05
         1   293 0 0 ALUMINUM                                            MAT 8
     131 5.12100E-02
KENO GEOM
       19   /*  "KREFM"
        5   /*  "NBOX"
        1   /*  "NBXMAX"
        1   /*  "NBYMAX"
        1   /*  "NBZMAX"
        0   /*  "NXX"
        0   /*  "NTYPST"
        1   /*  "NEMBRG"
```

```
      0   /* "NGMCHK"
BOX TYPE          1 /*MODEL 20.00 CASK WITH STAINLESS BASKET INSERT
CYLINDER          3   21.91        137.06        0.00      16*0.5
CYLINDER          7   29.36        137.06        0.0       16*0.5
CYLINDER          3   33.65        137.16        0.0       16*0.5
CYLINDER          7   35.85        140.64        0.0       16*0.5
CYLINDER          6   46.34        140.64        0.0       16*0.5
CYLINDER          7   48.56        140.64      -14.90      16*0.5
BOX TYPE          2 /* CASK TOP
CYLINDER          6   30.96        158.42       140.64     16*0.5
CYLINDER          7   48.56        162.23       140.64     16*0.5
BOX TYPE          3 /* HFIR FUEL ASSEMBLY-INNER ANNULUS PORTION
CYLINDER          3   6.439     50.80      0.0     16*0.5
CYLINDER          8   6.916     50.80      0.0     16*0.5
CYLINDER          1   12.813    50.80      0.0     16*0.5
CYLINDER          8   13.443    50.80      0.0     16*0.5
BOX TYPE          4 /* HFIR FUEL ASSEMBLY-OUTER ANNULUS PORTION
CYLINDER          3   14.275    50.80       0.0     16*0.5
CYLINDER          8   14.897    50.80       0.0     16*0.5
CYLINDER          2   21.143    50.80       0.0     16*0.5
CYLINDER          8   21.773    50.80       0.0     16*0.5
BOX TYPE          5   /* OVERALL BOX FOR THE PROBLEM
CUBOID            4   48.60       -48.60      48.60 -48.60 162.23 -15.24 16*0.5
CORE              0   48.60       -48.60      48.60 -48.60 162.23 -15.24 16*0.5
CUBOID            5   79.10       -79.10      79.10 -79.10 192.71 -45.72 16*0.5
5 11111           1   111         1
 BEGIN COMPLEX
 /* PLACE HFIR FUEL ASSEMBLY INTO BASKET INSIDE CASK
COMPLEX     1   3    0.0       0.0     68.21 1 1 1        0.0       0.0       0.0        /* INNER
ASSY
COMPLEX     1   4    0.0       0.0     13.60 1 1 1       0.0       0.0       0.0        /* OUTER
ASS'Y
/*          PLACE LOADED CASK INTOOVERALL PROBLEM BOX
 COMPLEX    5   1   0.0        0.0       0.0     1 1 1     0.0       0.0       0.0
 /* PLACE TOP INTO OVERALL PROBLEM BOX
 COMPLEX    5   2   0.0        0.0       0.0     1 1 1     0.0       0.0       0.0
END GEOM
*END GEMER*
```

INPUT LISTING FOR SINGLE CONTAINER MODEL

```
HFIR FUEL/ IF2000/SEP=1.50IN. NORMAL COND COLD WFin=0.050 WFout=1.00
    210    /*# BATCHES
1000       /*  # NEUTRONS PER BATCH
       10 /*  # BATCHES TO SKIP
   2123469/*  INITIAL "SEED" (IF NON-ZERO)
      0   /*  "IDUMP"
      0   /*  "NRSTRT"
      0   /*  "NBTED" (NON-ZERO IS PRINT EDITS)
      0   /*  "KRED-' (NUMBER OF COMBINED REGIONS IN EDITS)
    0    293      19 8
       5293 0    0 U(93.2)308+0.03WTF-H20 RHOMIX=1.275 g/cc                  MAT1
      2351   3.6260E-04
      2381   2.6120E-05
       131   2.4520E-02
        16   1.8710E-03
         1   1.6690E-03
         5   293 0 0 U(93.2)308+0.03WTF-H20 RHOMIX=1.311 g/cc               MAT 2
      2351   4.9000E-04
      2381   3.5300E-05
       131   2.4120E-02
        16   2.2350E-03
         1   1.6690E-03
       2   293 0 0    MOD IN CONTAINER       (5$)
       1      3.3380E-03
      16      1.6690E-03
       2   293 0 0    MOD BETWEEN CONTAINERS        (100$)
       1 6.6770E-02
      16 3.3380E-02
        2 293 0 0 FULL DENSITY WATER                                  MAT 5
       1 6.6770E-02
      16 3.3380E-02
        1   293 0 0
   LEAD SHIELDING                                                       MAT 6
      82 3.29890E-02
        7   293 0 0
   304 STAINLESS STEEL                                                  MAT 7
      12 6.82690E-05
      14 8.53360E-04
      24 1.53600E-02
      26 6.04950E-02
      28 6.82690E-03
      55    1.70670E-
   03
    1316 2.56010E-05
        1   293 0 0 ALUMINUM                                          MAT 8
     131 5.12100E-02
KENO GEOM
      19   /*  "KREFM"
       5   /*  "NBOX"
       1   /*  "NBXMAX"
       1   /*  "NBYMAX"
       1   /*  "NBZMAX"
       1   /*  "NXX"
       0   /*  "NTYPST"
```

```
      1   /* "NEMBRG"
      0   /* "NGMCHK"
 -1.0 0.0 0.0 0.0 0.0 0.0
BOX TYPE          1 /*MODEL 2000 CASK WITH STAINLESS BASKET INSERT
CYLINDER          3   21.91        137.06        0.00     16*0.5
CYLINDER          7   29.36        137.06        0.0      16*0.5
CYLINDER          3   33.65        137.16        0.0      16*0.5
CYLINDER          7   35.85        140.64        0.0      16*0.5
CYLINDER          6   46.34        140.64        0.0      16*0.5
CYLINDER          7   48.56        140.64      -14.90     16*0.5
BOX TYPE          2 /* CASK TOP
CYLINDER          6   30.96        158.42       140.64    16*0.5
CYLINDER          7   48.56        162.23       140.64    16*0.5
BOX TYPE          3 /* HFIR FUEL ASSEMBLY-INNER ANNULUS PORTION
CYLINDER          3   6.439     50.80     0.0     16*0.5
CYLINDER          8   6.916     50.80     0.0     16*0.5
CYLINDER          1   12.813    50.80     0.0     16*0.5
CYLINDER          8   13.443    50.80     0.0     16*0.5
BOX TYPE          4 /* HFIR FUEL ASSEMBLY-OUTER ANNULUS PORTION
CYLINDER          3   14.275    50.80       0.0     16*0.5
CYLINDER          8   14.897    50.80       0.0     16*0.5
CYLINDER          2   21.143    50.80       0.0     16*0.5
CYLINDER          8   21.773    50.80       0.0     16*0.5
BOX TYPE          5   /* OVERALL BOX FOR THE PROBLEM
 CUBOID           4   48.60       -48.60      48.60 -48.60 162.23 -15.24 16*0.5
 CORE             0   48.60       -48.60      48.60 -48.60 162.23 -15.24 16*0.5
 CUBOID           5   48.60       -79.10      79.10 -79.10 192.71 -45.72 16*0.5
 5 1 1 1 1 1      1   1 1 1       1
BEGIN COMPLEX
/* PLACE HFIR FUEL ASSEMBLY INTO BASKET INSIDE CASK
COMPLEX     1   3    0.0      0.0     68.21 1 1 1        0.0      0.0      0.0       /* INNER
ASSY
COMPLEX     1   4    0.0      0.0     13.60 1 1 1       0.0      0.0      0.0       /* OUTER
ASS'Y
/*PLACE LOADED CASK INTO OVERALL PROBLEM BOX
 COMPLEX     5   1   0.0       0.0      0.0     1 1 1     0.0      0.0      0.0
 /* PLACE TOP INTO OVERALL PROBLEM BOX
 COMPLEX     5   2   0.0       0.0      0.0     1 1 1     0.0      0.0      0.0
 END GEOM
 *END GEMER*
```

6.0 CRITICALITY EVALUATION

A criticality evaluation of the Model 2000 Transport Package with the HFIR spent fuel assembly is given below. The cask has a cavity that is 26.5 inches inside diameter by 54 inches long for holding material including special nuclear material. The cask is of steel encased, lead shielded construction. The purpose of this chapter is to identify, describe, discuss and analyze the principle criticality engineering physics design of the packaging and components important to safety and necessary to comply with the requirements of 10CFR Part 71 [6.1].

6.1 DISCUSSION AND RESULTS

The type of spent fuel proposed for transport in the Model 2000 cask is the High Flux Isotope Reactor (HFIR) fuel which is described in and built in accordance to Reference 6.2. The contents considered include a single assembly (both inner and outer elements) of HFIR fuel supported by the HFIR fuel liner and basket detailed in the previous sections.

To qualify the Model 2000 cask with the HFIR spent fuel and its basket as Fissile Class III packages, the following criteria are met as stated in Sections 71.55 and 71.61 of 10CFR Part 71:

1. At least two times the allowable number of packages (2N) in an undamaged condition must remain subcritical in any arrangement and with optimum interspersed hydrogenous moderation. In the case of the Model 2000 cask with contents, this corresponds to an array of two (2) internally dry casks (taken to be no greater than 5.0% of full density pure water) containing fresh fuel.

2. A single container demonstration of subcriticality under optimum moderation conditions (both internal and external moderation) is required. In the case of the Model 2000 cask with contents, this corresponds to one (1) cask with HFIR fuel with full flooding of the fuel element region with pure water, introduction of an intermediate amount of internal interspersed moderation (25% of full water density) inside the cask and surrounding the cask with a reflector of full density water.

3. The allowable number of packages (N) must remain subcritical if the packages are subjected to hypothetical accident conditions and are stacked together in any arrangement, closely reflected on all sides by water, and with optimum interspersed hydrogenous moderation. In the case of only one container, the hypothetical accident condition array is a subset of the above described single container demonstration.

The HFIR liner and basket (see Figure 6.1) consists of a 304 stainless steel cask liner and a basket which constrains the location of the inner fuel element relative to the outer fuel element. This basket is normally supported from the top of the cask liner and has lateral support rings so as to prevent the intrusion of the inner fuel element and basket into the outer fuel element region. An extra degree of assurance of axial separation between the elements under axial load is added by the center column support. This separation of fuel elements provides the basis for safe geometric arrangement of the fuel and does not depend on the fuel elements themselves to provide such configuration control. No neutron poison is required to maintain the HFIR fuel subcritical during normal operation and under hypothetical accident conditions with optimum moderation by water.

The GEMER01V Monte Carlo neutron transport computer program [Reference 6.3], is used to demonstrate subcriticality of the Model 2000 cask with HFIR fuel. GEMER is an enhanced version of the MERIT Monte Carlo code, incorporating the cross-section processing of MERIT and the geometry handling capabilities of KENO-IV [Reference 6.4]. Previous analyses of the criticality safety of the Model 2000 cask have been performed using the MERIT computer code and associated ENDF/B library set [Reference 6.5]. Critical benchmark experiments verify the accuracy of the calculational method chosen for the present analyses and provide the basis for the calculational bias. Table 6.1 summarizes the results of the criticality evaluation.

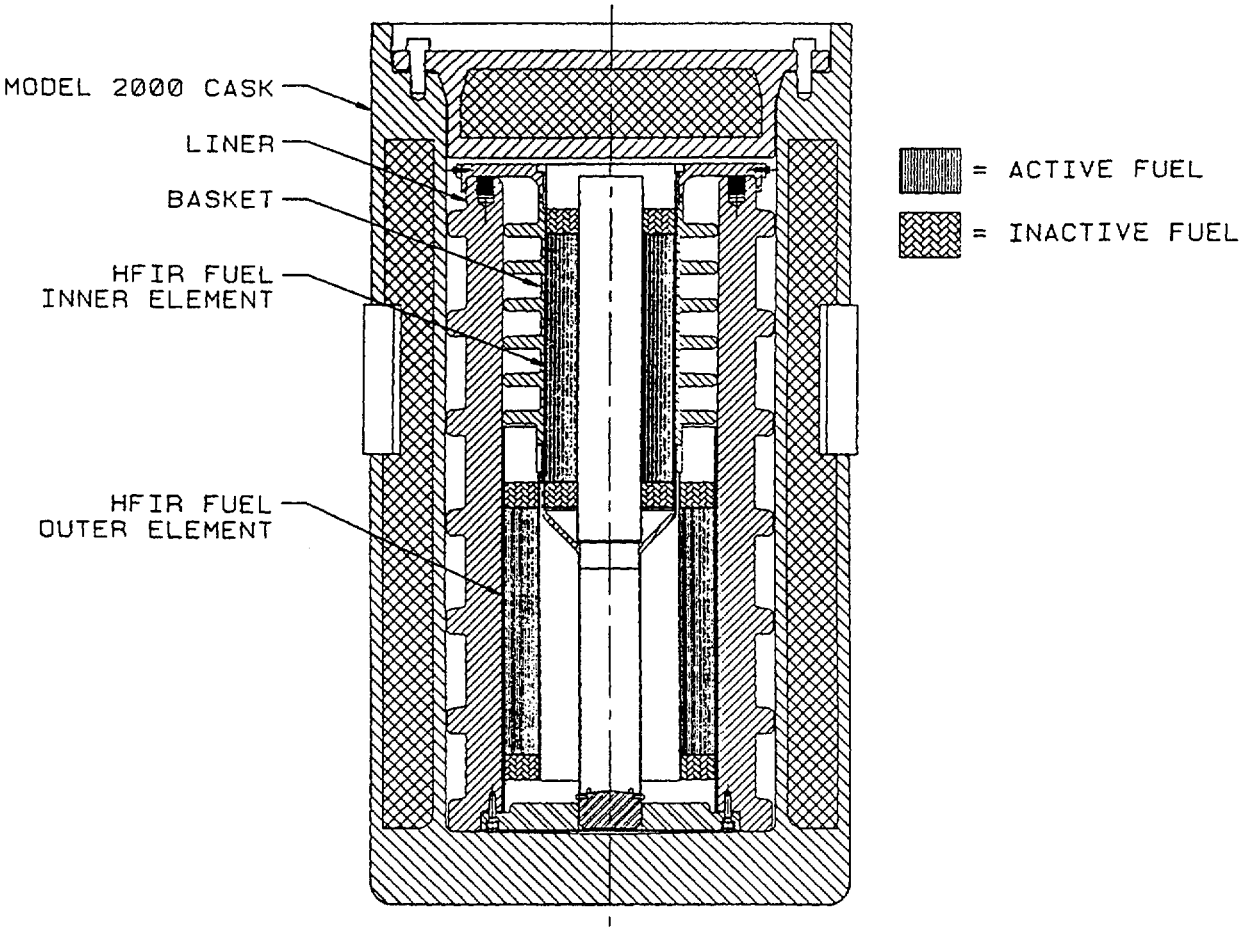

Figure 6.1. Model 2000 Shipping Cask with HFIR Fuel Elements, Liner and Basket

The maximum k_{eff} calculated for a cask containing HFIR fuel is 0.9241 ± 0.0019(1σ). The highest value with two standard deviations and bias is k_{eff} + 2σ + bias = 0.9278. See Figure 6.2 for the model that was used in the criticality analysis.

This effective multiplication factor (including two standard deviations and calculational bias) is significantly lower than the design limit for the multiplication factor, 0.95. Thus, the Model 2000 shipping cask has more than adequate criticality safety for the liner and basket design for the HFIR (either spent or fresh) considered under both normal conditions of transport and hypothetical accident conditions of Fissile Class III packages.

Structural analysis of the package and fuel basket (Chapter 2.0) shows that geometry of the cask contents remains unchanged throughout the hypothetical accident. Thus, no reduction is assumed in the total effective volume of the packaging on which nuclear criticality is assessed.

Condition/Parameter	HFIR Fuel
Normal conditions of transport	
Number of undamaged packages calculated to be subcritical	2
Optimum interspersed hydrogenous moderation	Pure Water (75% Full density between casks)
Water reflection boundary condition	1 ft water reflector
Package interior volume, cm^3	4.879×10^5
Maximum effective multiplication factor, k_{eff} + 2σ + bias	0.2597
Hypothetical accident conditions	
Number of damaged packages calculated to be subcritical	1
Optimum interspersed hydrogenous moderation	25% Full Density Water inside cask 100% Full Density Water outside cask
Water reflection boundary condition	1 ft Water reflector
Package interior volume cm^3	4.879×10^5
Maximum effective multiplication factor, k_{eff} + 2σ + bias	0.9278

Table 6.1. Summary of Criticality Evaluation Fissile Class III

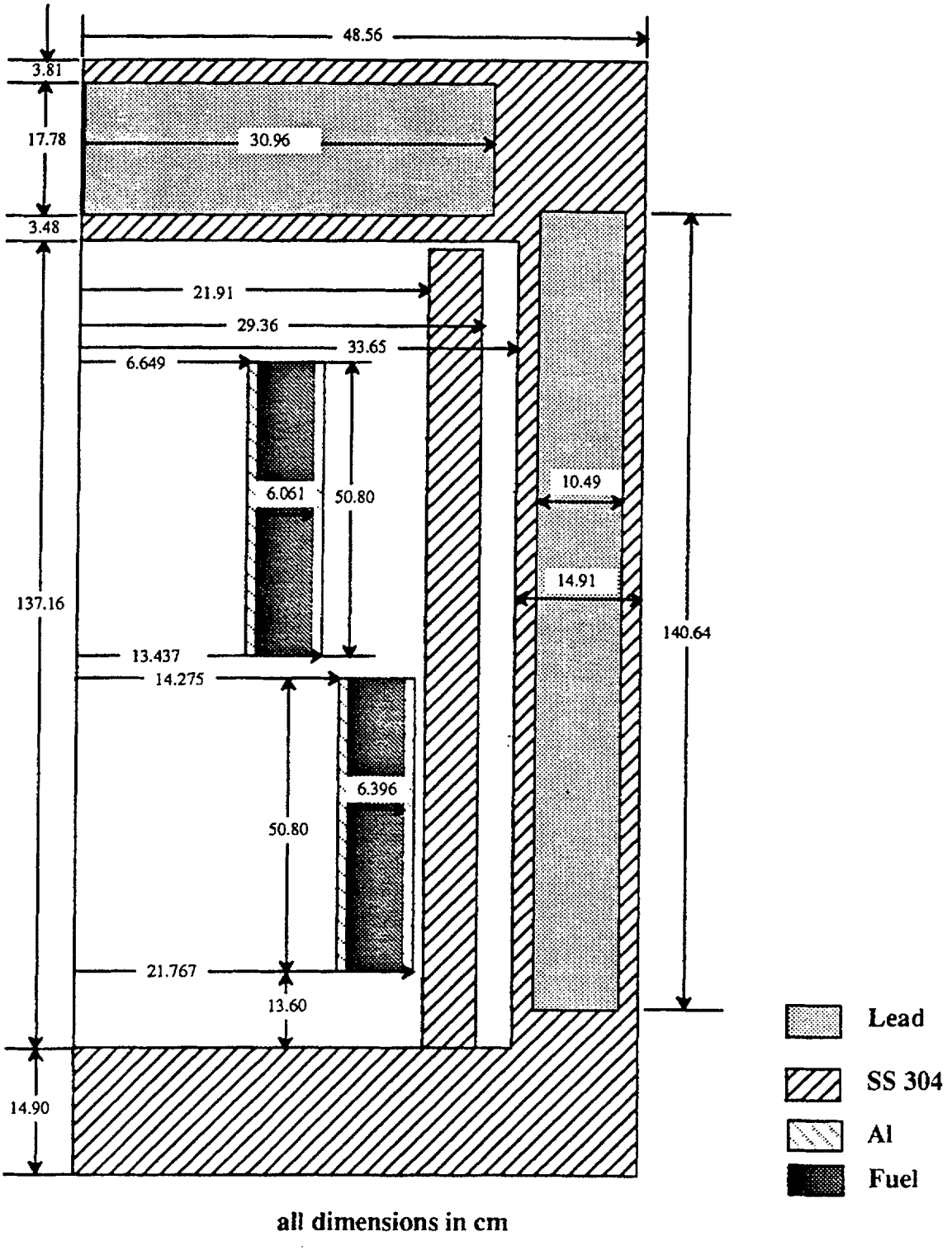

Figure 6.2. Model 2000 Cask with HFIR Fuel: Geometry for Criticality Calculations

6.2 PACKAGE FUEL LOADING

Table 6.2 summarizes the maximum fuel loading and fuel parameters for the package for both normal conditions of transport and hypothetical accident conditions for HFIR fuel, respectively. Because the fuel and basket remains unchanged throughout the hypothetical accident, fuel and basket parameters for normal conditions of transport and single container/hypothetical accident conditions are identical.

Detailed drawings of the fuel elements appear are given in References 6.6 and 6.7 for the HFIR fuel. The HFIR liner and basket contains one HFIR assembly (both inner and outer elements). For conservatism, all fuels are considered to be fresh (no burnup) and without their as-built neutron poison materials in the criticality calculations.

Parameter (per fuel assembly)*	**Units**	
U-235 content (g)	9500	
U-238 content (g)	693	
Maximum enrichment (%)	93.2	
Aluminum content of the fuel zone (kg)	58,988	
Uranium oxide density (g/cm^3) (in the form of U_3O_8)	8.22	
Aluminum density (g/cm^3)	2.699	
Number of plates per inner assembly	171	
Number of plates per outer assembly	369	
	Units	
	Inches	**mm**
Length	30.2	768
Length of active zone	20.0	508
Inner assembly, inner radius of fuel	2.72	64.4
Inner assembly, outer radius of fuel	5.29	134.4
Outer assembly, inner radius of fuel	5.62	142.7
Outer assembly, outer radius of fuel	8.57	217.7
*Note: The maximum fuel loading is one HFIR assembly.		

Table 6.2. Description of HFIR Fuel (Both Normal Conditions of Transport and Single Container/Hypothetical Accident Conditions)

The loading specified qualifies as Fissile Class III under the provisions of 10CFR71.61, and the maximum number of packages per shipment is one (1). The U-235 mass is determined by the maximum (nominal plus tolerance) U-235 mass allowed by the design specification for the HFIR fuel in both the inner and the outer elements [Reference 6.2]. These masses are corroborated by the construction records of the individual fuel elements.

6.3 MODEL SPECIFICATION

6.3.1 Description of the Calculational Models

Two calculational models are used in evaluating the criticality safety of the Model 2000 cask. The two models are identical except in their representation of the number of casks and the interspersed moderation. One of the models assumes that there is one cask loaded with one HFIR assembly (accident condition) and the other assumes that there are two (2) casks each loaded with one HFIR assembly and the casks are in direct contact with each other on one side. Both models assume fresh, undepleted fuel in the active fuel region, neglecting any as-built or burnup poisons. All models omit the overpack from consideration, which conservatively brings the water reflector closer to the fissile material, adding a degree of conservatism to the analysis.

The model for normal conditions is two loaded casks side by side and touching. This places the units of fissile material inside each cask nearest each other for the most reactive configuration. The hydrogen-to-fissile ratio outside each cask is varied to find the peak k-effective value for the normal condition model. The inside of each cask is dry in the undamaged condition, which is conservatively modeled as having 5 wt% interspersed water in the fuel region and inside the remainder of container. The two-cask array is surrounded by 12 inches of full density water reflection on all sides. The cask with fuel is highly undermoderated in both the normal and hypothetical accident conditions, as will be seen from the results.

The model for the single container/accident condition is one cask that is filled with partial density water. Even though it has been shown that the cask remains water-tight under hypothetical accident conditions, the requirement that a single cask be shown safe under optimum moderation conditions covers the hypothetical accident condition array (of one unit) as well. The fissile material unit inside the cask is placed near the lead. The hydrogen-to-fissile ratio within the fissile material units and the interspersed moderation inside the cask are varied to find the peak k-effective for the damaged condition. The outside of the cask is surrounded by a 12 inch thick water reflector.

Both normal condition and hypothetical accident condition models utilize the same basic interior geometry. The two elements inside the cask are radially centered within the cask. The outer and inner elements are coaxial (in the radial direction only). The liner and the basket do not allow lateral movement of the elements. The separation between the active fuel regions of the inner and outer elements is maintained by the configuration of the liner and basket. The separation is taken to be the minimum allowed by the manufacturing and assembly tolerances of the liner/basket. This minimum separation distance between the fuel zones is 1.5 inches (3.81 cm).

Figure 6.2 shows the cask geometry and pertinent dimensions used for modeling the cask loaded with HFIR fuel. The fuel is homogenized by distributing the maximum mass of U-235 allowed throughout the entire active fuel region. The only portion of the liner and basket actually considered in the model is the 3 inch wall of the liner. Neither the stainless steel liner ribs nor the basket material is considered (other than in determining the relative positioning of the elements to one another) in the model. This is conservative, since the stainless steel surrounding the active fuel region acts as a neutron absorber. Figure 6.2 shows the bottom of the active region of the outer fuel element to be separated by 13.60 cm from the bottom of the inside cavity of the cask. No material (other than the interspersed moderator inside the cask) is shown in this region.

Two types of geometry were modeled to account for the liner bottom. The first is as shown in the figure, with only interspersed moderator in the region between the outer fuel element and the bottom of the cask. The second includes a 2.5 inch (6.35 cm) thick tungsten plate resting on the bottom of the stainless steel cask. Two models were investigated for the worst-case conditions (which turn out to be the single container with optimum moderation) because the libraries for tungsten are not benchmarked against a large number of critical experiments and tungsten itself is not a code material so specifications on alloying elements are not necessarily well documented. To take this into account, the liner bottom was modeled both as interspersed moderator and separately with solid, full density tungsten. The actual Heavymet alloy of tungsten used will produce results in between these two models. The analysis will show, however, that there is little difference between the results for these two models and that this cautious approach is probably unnecessary.

The fuel elements were likewise conservatively modeled such that only about 85% of the mass of the aluminum present is considered. This is a conservative approach, since aluminum acts as a slight parasitic absorber within the fuel region. Figure 6.3 shows the fuel assembly geometry of the HFIR fuel. This figure shows the basic dimensions used to homogenize the aluminum and moderator (in the coolant channels) into the description of the active fuel regions.

The Model 2000 cask is modeled in three dimensions. Only the cask, without the overpack, the liner and fuel are modeled. The cask has a cylindrical cavity cross section. The cask has a cavity of 26.5 inches in diameter and 54 inches in height. The cask outside diameter is 38.5 inches. The total cask radial wall and bottom plate thickness is 6.0 inches. The Model 2000 cask consists of a layered radial wall design composed of 1.0 inch of 304 stainless steel, 4.0 inches of lead, and then another 1.0 inch of 304 stainless steel. The cask bottom consists of 6 inches of 304 stainless steel. The top of the cask was modeled as having a 1.5 inch thick 304 stainless steel plate inside the cask at the top, then 4.5 inches of lead, and then a 1.75 inch thick 304 stainless steel plate on the top of the cask. For conservatism, the model reduces the wall thickness of stainless steel portions of the cask and liner in areas where neutron absorption in the stainless steel reduces the neutron multiplication (i.e., cask walls and cask top).

6.3.2 Package Regional Densities

The HFIR fuel assembly model assumes the maximum possible fissile content of 9500 g of U-235 per fuel assembly with a maximum enrichment of 93.2%.

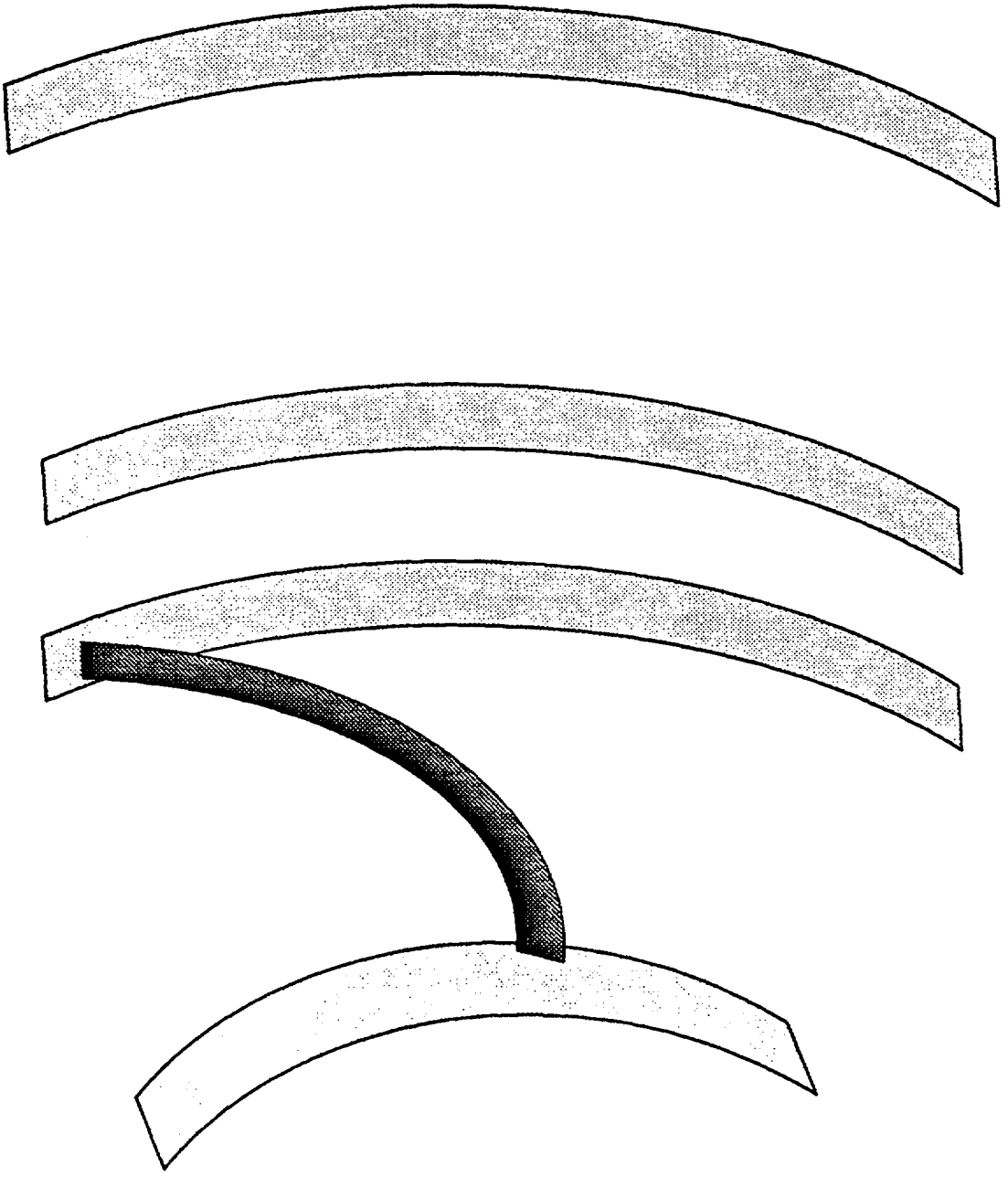

Figure 6.3. HFIR Fuel Assembly Geometry for Criticality Calculations

Material densities and corresponding number densities are based on standard material specifications. The composition for 304 stainless steel is taken as the minimum alloy content (since these alloys all tend to be excellent neutron absorbers) from the specifications given in Reference 6.8. Aluminum is modeled as pure aluminum since the alloying agents for the 6061 again tend to be neutron absorbers and so are conservatively omitted from consideration. These standard compositions are multiplied by the volume fractions of each material present within each region in the models. Table 6.3 presents the material densities, volume fractions, and number densities for substances (materials) within each region in the HFIR criticality model. Substances composed of more than one element are broken into their elemental number densities in the number density column. These are consistent with the densities shown in Reference 6.9.

Region	Material	Volume Fraction	Density (g/cm^3)	Number Density (atoms/barn-cm)
Fuel	U-235	0.0074	0.1415	3.626E-4
(Inner assembly)	U-238	0.0006	0.0106	2.612E-5
	Aluminum	0.4067	1.098	2.452E-2
	Water	0.5000	0.500	3.338E-2 (H)
				1.772E-2 (O)
Fuel	U-235	0.0100	0.1916	4.900E-4
(Outer assembly)	U-238	0.0008	0.0144	3.530E-5
	Aluminum	0.4000	1.080	2.412E-2
	Water	0.5000	0.500	3.338E-2 (H)
				1.809E-2 (O)
Stainless Steel	SS304	0.9848	7.800	1.716E-2 (Cr)
				1.710E-3 (Mn)
				5.846E-2 (Fe)
				7.601E-3 (Ni)
Lead	Lead	1.00	11.350	3.2989E-2
Aluminum (assembly structure)	Aluminum	0.8500	2.294	5.121E-2
Tungsten Liner Bottom (in some models)	Tungsten	1.00	19.3	6.3217E-2

Table 6.3. Material Densities and Atomic Number Densities Within the HFIR Cask with HFIR Fuel Criticality Model

6.4 CRITICALITY CALCULATION

The HFIR elements are represented in the calculation by multi-group and resonance parameter cross sections for fuel/cladding/moderator and are spatially homogenized separately for inner and outer fuel elements. The supporting aluminum walls are discretely modeled, with the homogenized fuel/cladding/moderator region being defined by these boundaries. The neutron statistics for determining the multiplication factor k_{eff} with the GEMER01V program are based on 210 iterations of 1000 neutrons each, in which the first ten iterations are not counted. Flux-weighted estimates of k_{eff} are reported throughout this analysis.

The calculational methods used to determine the nuclear reactivity for the fuel loadings chosen for this package are described below. This is followed by a presentation of the k_{eff} results obtained using these methods and a discussion of these results.

6.4.1 Calculational Methods

The computational tool used in this evaluation is the GE MERIT code (GEMER). A brief description of this computational tool is given below.

The GEMER program is a Monte Carlo program for solving the linear neutron transport equation as a fixed source or an eigenvalue problem in three space dimensions. The cross sections in GEMER are processed from the ENDF/B-IV library in the multi-group and resonance parameter formats. Thermal scattering in water is represented by the Haywood Kernel obtained from the ENDF/B library. The GEMER program utilizes 190 full spectrum cross section energy groups. The types of reactions considered in GEMER are fission, elastic, inelastic and (n,2n) reactions. Absorptions are implicitly treated by applying the non-absorption probability to neutron weights on each collision.

The geometry treatments available in GEMER include the specialized (regular) and generalized geometry options from the KENO-IV code and a complex embedded option.

In the specialized (regular) geometry treatment, a spatial description is generated by defining boxes each of which contains an increment of the desired system. Within each box, the description consists of a nested series of shapes such as CYLINDERS, SPHERES, and CUBOIDS. Within each box, each region defined must completely enclose all previously defined regions. Arrays of the boxes can be put together to describe the entire system and surrounded by reflecting materials or boundaries as required.

In the generalized geometry treatment, a system is represented by writing the equations of the surfaces involved and then specifying where the various media lie relative to these surfaces. This geometry option allows one to describe very complicated systems, but it becomes inefficient when used to describe a system in which small units are repeated a large number of times, as in a rod lattice.

In the complex embedded geometry treatment, boxes, as defined in the specialized (regular) geometry treatment, may be placed inside of one or more other boxes. For example: if Box Type 1 describes the HFIR inner fuel element, Box Type 2 describes the HFIR outer fuel element and Box Type 3 describes the shipping cask, then Box Type 1 can be embedded into Box Type 2 to represent an assembled HFIR element pair and this can be embedded directly into the shipping cask (Box Type 3). The boxes which result from the embedding operation may be assembled into arrays as described in the specialized (regular) geometry treatment to from complex systems.

The three geometry options described above may be used in any combination to describe a system. In the present analysis, the specialized (regular) geometry treatment is used to describe the cask and separately to describe the inner fuel element, the outer fuel element and the cask top, as well as the outer model boundaries with full density water reflector. The complex embedded option is used to assemble the components of the model into the proper geometric relationships.

6.4.2 Fuel Loading or Other Contents Loading Optimization

Fuel assemblies are held within the basket structure during both normal conditions of transport and during the hypothetical accident, so the geometry to be analyzed is well defined. Like other light water reactor fuels, the fuels considered here are substantially subcritical when placed in air due to a lack of neutron moderation. Increasing the moderation within an assembly by adding water to it results in an increase in k_{eff}.

During the hypothetical accident conditions in the Model 2000 cask, the fuel is calculated to be confined in each fuel element and located in the positions defined by the liner and basket geometry as shown in Figure 6.2, as it is under normal shipping conditions.

The boundary condition around the cask in all criticality calculations is a leakage boundary condition with 12" water reflection surrounding all sides of the arrays. This corresponds to a finite array of casks in their most reactive array configuration with full reflection by water.

6.4.3 Criticality Results

Table 6.4 shows the effective multiplication factors calculated for a variety of situations. The first portion of the table is for the normal condition array. This is an array of two containers, which are dry on the inside and are touching each other. The dry fuel and interior of the cask is modeled as 5% of normal full density water. Usually, dry conditions in humid atmospheres may be modeled as 0.5% of full density water, so this treatment clearly allows for a large safety margin with respect to container "dryness".

The next set of values in Table 6.4 are those for the single container/accident array under optimum moderation conditions. These results are for the case where the tungsten bottom of the liner is not considered. The highest neutron multiplication is highlighted in bold typeface. As described in Section 6.4.1, the model is constructed with an axial separation between the fuel elements of 1.5 inches (3.81 cm). The values shown here are given as a function of interspersed moderator density. The highest $k_{eff} + 2\sigma$, (0.9278) is that for full water density (100%) inside the fuel region (which allows for a water volume fraction of 50% in the fuel plate region), 25% of full density water inside the remainder of the cask and 100% full density water reflector outside the cask.

Condition*	Separation Between Elements	Moderator in Fuel	Moderator Inside Cask	Moderator Outside Cask	K_{eff}	σ	$K_{eff} + 2\sigma$
Normal	1.5"	5%	5%	50%	0.2569	0.0011	0.2591
Normal	1.5"	5%	5%	75%	0.2575	0.0011	0.2597
Normal	1.5"	5%	5%	100%	0.2547	0.0011	0.2569
Accident	1.5"	5%	5%	100%	0.2541	0.0010	0.2562
Single Container	1.5"	100%	10%	100%	0.8938	0.0020	0.8977
Single Container	1.5"	100%	20%	100%	0.9197	0.0019	0.9236
Single Container	**1.5"**	**100%**	**25%**	**100%**	**0.9241**	**0.0019**	**0.9278**
Single Container	1.5"	100%	30%	100%	0.9189	0.0018	0.9226
Single Container	1.5"	100%	50%	100%	0.8734	0.0018	0.8770
Single Container	1.5"	100%	75%	100%	0.8289	0.0018	0.8324
Single Container	1.5"	100%	100%	100%	0.7985	0.0019	0.8023
Single Container	1.5"	90%	25%	100%	0.8916	0.0021	0.8959
***Conditions marked with a (W) include the Tungsten line bottom.**							

Table 6.4. Criticality Analysis Results for Normal and Hypothetical Accident Conditions

The above cases were repeated with the model which accounts for the tungsten bottom of the HFIR liner. The results are shown in Table 6.5. The highest $k_{eff} + 2\sigma$ for these cases (0.9283) is obtained with 20% internal interspersed moderator. This result is not statistically different than the case where no tungsten is considered and results can be obtained either by including or excluding this portion of the liner. This is not unexpected since, although a strong reflecting (scattering) material, tungsten is also a relatively strong neutron absorbing medium.

Condition*	Separation Between Elements	Moderator in Fuel	Moderator Inside Cask	Moderator Outside Cask	K_{eff}	σ	$K_{eff} + 2\sigma$
Single Container (W)	1.5"	100%	10%	**100%**	0.8895	0.0019	0.8933
Single Container (W)	**1.5"**	**100%**	**20%**	**100%**	**0.9240**	**0.0022**	**0.9283**
Single Container (W)	1.5''	100%	25%	100%	0.9238	0.0020	0.9278
Single Container (W)	1.5"	100%	30%	100%	0.9168	0.0020	0.9207
Single Container (W)	1.5"	100%	50%	100%	0.8712	0.0018	0.8748
Single Container (W)	1.5"	100%	75%	100%	0.8285	0.0018	0.8321
Single Container (W)	1.5"	100%	100%	100%	**0.8004**	0.0018	0.8041
***Conditions marked with a (W) include the Tungsten liner bottom.**							

Table 6.5. Criticality Analysis Results for Single Container with Tungsten Bottom of Liner

All of the $k_{eff} + 2\sigma$ values are well below the design limit of 0.95. Thus, any mechanical tolerances not explicitly accounted for, deviations in material specifications, or possible temperature effects will not cause criticality to exceed the design limit.

Another set of cases was considered, partly as a basket design aid and partly as anticipatory to concerns as to the sensitivity of the criticality safety margin to changes in geometry. A number of cases were run at the optimum interspersed water density where the separation between the fuel elements was varied. The model was altered to allow the active fuel region of the fuel elements to overlap. The results of this sensitivity study are summarized in Table 6.6. The separation is given in inches and is positive for positive separation. Overlap of the active fuel regions of the elements is denoted by a negative separation. As shown by the table, the worst-case conditions (single container with optimum moderation) does not result in a k_{eff} greater than 0.95 until the fuel elements have over 1.0 inches of overlap of the active fuel regions. This corresponds to a relative movement of over 2.5 inches from where the elements are constrained by the liner and basket. Further, the configuration does not achieve a k_{eff} of 0.97 until the elements have a 3.00 inch overlap of active regions. Thus, although the basis for criticality safety depends on the axial separation of elements, the system is not highly sensitive to this parameter.

Condition*	Separation Between Elements	Moderator in Fuel	Moderator Inside Cask	Moderator Outside Cask	K_{eff}	σ	$K_{eff} + 2\sigma$
Accident	2.00"	100%	25%	100%	0.9156	0.0019	0.9194
Accident	1.75"	100%	25%	100%	0.9221	0.0019	0.9259
Accident	1.50"	100%	25%	100%	0.9241	0.0019	0.9278
Accident	1.25 "	100%	25%	100%	0.9286	0.0020	0.9325
Accident	1.00"	100%	25%	100%	0.9294	0.0019	0.9332
Accident	0.50"	100%	25%	100%	0.9347	0.0019	0.9385
Accident	0.00"	100%	25%	100%	0.9398	0.0020	0.9438
Accident	-0.25 "	100%	25%	100%	0.9370	0.0018	0.9406
Accident	-0.50"	100%	25%	100%	0.9390	0.0020	0.9430
Accident	-0.75"	100%	25%	100%	0.9439	0.0020	0.9479
Accident	-1.00"	100%	25%	100%	0.9449	0.0020	0.9489
Accident	-2.00"	100%	25%	100%	0.9614	0.0019	0.9652
Accident	-3.00"	100%	25%	100%	0.9676	0.0019	0.9715
Accident	-4.00"	100%	25%	100%	0.9756	0.0020	0.9795
***Conditions marked with a (W) include the Tungsten liner bottom.**							

Table 6.6. Criticality Analysis Results as a Function of Fuel Element Separation/Overlap

6.5 CRITICAL BENCHMARK EXPERIMENTS

6.5.1 Benchmark Experiments and Applicability

6.5.1.1 Critical Experiments with IIFIR Fuel. Reference 6.10 presents results of experiments of using HFIR fuel assemblies to determine the critical spacing between assemblies when moderated and reflected by water. These experiments showed that two assembled assemblies are subcritical until they are brought to within 3.60 inches of each other. Similarly, three assemblies are subcritical until they are brought within 5.05 inches of each other in a triangular pattern. Thus, one assembly, such as the contents of the Model 2000 cask, will always be subcritical when fully moderated and reflected by water.

6.5.1.2 Other Critical Experiments. The GEMER01V code has been validated by comparison against 123 critical experiments. These experiments form the database from which the GEMER bias is calculated.

Validation of GEMER01V against experimental data was performed using the same cases which were developed for benchmarking the original GEMER. The validation consisted of performing a set of 123 calculations that were taken from the following:

Name of Experiment	Reference Document No.	No. used in Benchmark
Handley-Hopper (Y-1948)	6.12	40
Handley-Hopper (Y-1858 Set A)	6.11	21
Handley-Hopper (Y-1858 Set B)	6.11	22
Bierman (NUREG/CR-0796)	6.16	19
Rocky Flats (NUREG/CR-0674)	6.15	10
RSIC	6.13	9
TRX (WAPD-TM-931)	6.14	2

Because calculational biases are normally due to the cross-section treatment rather than the geometry treatment, good agreement with the original validation and critical experiment is expected. The experimental parameters are described very briefly below. Consult the appropriate Reference Document for further information on the experiments themselves.

Handley-Hopper Critical Experiments

- Fuel forms of UF_4, UO_2F_2, U-metal or UNH
- Enrichments ranging from 1.4 wt% to 93.8 wt%
- Moderators of water, paraffin or none
- Reflectors of water, graphite, oil or bare

Bierman et. al. Critical Experiments

- Fuel form is UO_2
- Enrichments of 2.35 wt% to 4.29 wt%
- Moderator and reflectors of water

Rocky Flats Critical Experiments

- Uranium form of U_3O_8
- Enrichment is 4.46 wt%
- Moderator is water
- Reflectors of concrete, plastic or steel

RSIC Critical Experiments

- Fuel form is UO_2
- Enrichment of 2.35 wt%
- Moderator and reflectors of water

TRX Critical Experiments

- Fuel form is U-metal
- Enrichment of 1.3 wt%
- Moderator and reflectors of water

The comparison with these experiments is reported in more detail in Reference 6.3.

6.5.2 Details of Benchmark Calculations

6.5.2.1 Critical Experiments with HFIR Fuel. The model used for the simulation of critical lattices of FIR fuel are essentially the same as for the present analysis for the Model 2000 shipping cask. The model involves the homogenization of the fuel plate region and the same annular and axial dimensions as the current analysis. However, the difference is that the nominal amount of U-235 has been included in the fuel elements and the boron in the inner fuel element is also considered. Fuel elements have axially coincident active fuel regions and account has been taken for the aluminum and moderator inactive fuel regions which are immediately above and below the active fuel regions.

6.5.2.2 Other Critical Experiments. Details of the benchmark calculations for the GEMER criticality code are provided in Reference 6.3.

6.5.3 Results of Benchmark Calculations

6.5.3.1 Critical Experiments with HFIR Fuel. The results of the four HFIR fuel benchmark cases run are shown in Table 6.7. The four benchmark cases run show typical overestimation of the reactivity of the elements for the HFIR fuel. Descriptions of the critical experiments in Reference 6.10 are not complete and there are most likely errors in the amount of leakage involved in the models. That is, the actual experiments have been performed much closer to a leakage boundary than implied in the description. In addition, the modeling of the active fuel region of the fuel elements as being uniform throughout the defined annulus is somewhat conservative, since actual fuel plate manufacture calls for a region where fuel is not present at the outer periphery of each plate. The actual fuel projects much less area and for a highly enriched system, the expected neutron multiplication would then be lower. Similar results were obtained in Reference 6.17 for the same configurations modeled with the SCALE system of codes. At any rate, the model used thus shows conservatism with respect to the criticality safety of the HFIR fuel as modeled in the Model 2000 shipping cask.

6.5.3.2 Other Critical Experiments. Detailed results of the benchmark calculations for the GEMER criticality code are provided in Reference 6.3.

The results of the validation cases are compared to experiment and a calculational bias is determined from this comparison. Validation cases have been developed previously and were not created anew for this test. Obviously, for critical experiments, the value of k-effective is 1.000. No attempt has been made to include the experimental uncertainties into the models or the development of the calculated bias.

Condition	No. of Assemblies Used	Assemblies Used	Pitch	Separation Between Assemblies	K_{eff} (σ)	Experiment
CFG 1	2	Both	Linear	3.60"	1.03456 (.00180)	1.00114
CFG 2	3	Both	Triang.	5.05"	1.02878 (.00148)	1.00068
CFG 3	7	Both	Triang.	6.37"	1.02714 (.00148)	1.00000
CFG 4	7	Outer	Triang.	1.5"	1.03905 (.00148)	1.00000

Table 6.7. Criticality Analysis Results for Critical Experiments with HFIR Fuel

K-effectives for these cases have been selected based on the following selection technique. A Monte Carlo code begins with a source distribution and generates a new source distribution from each subsequent batch of neutrons. This allows the solution to converge to a correct distribution at a rate which is dependent upon the neutronic coupling of the model. K-effective is determined by discarding an appropriate number of initial batches so that the remaining batches are all representative subsets of the converged source distribution. The user generally specifies the number of initial batches to be skipped. However, since models do not converge at the same rate, the user is responsible for ensuring that the k-effective selected is a conservative one for criticality analyses. An approach to ensure this is to choose k-effective such that:

$$K_{effective} = \max \left[\sum_{i=n}^{m} \frac{(k_i - 3\sigma_i)}{(m-n)} \right]$$

providing that $\sigma_i \geq 0$ and

$$\sigma_i \leq \sigma_{i+1} ,$$

where m is the number of the last batch and
n is the number of batches skipped.

Since the validation cases fit into the category of criticality calculation and the models were developed with such guidelines as are used in criticality analyses, this selection technique was used to develop the bias, so it is not necessary to further include uncertainty into the bias since it is already included in the bias correlation.

The bias calculated for GEMER01V is identical to the bias developed for the PRIME version of GEMER. The differences in k-effective calculated by skipping the first two batches between the two codes are calculated and an average value and spread of this difference is found. The differences in k-effectives selected as described above are also found and the average of these is calculated.

The GEMER critical benchmark bias, which is known as a function of hydrogen-to-235-U ratio was used to determined the +0.23 percent bias from the critical experiments. Since the bias is positive (i.e., overpredictsthe neutron multiplication) it is conservative to omit this positive bias as a reduction in k_{eff}.

K-effective results for the cross sections set used by GEMER have also been benchmarked using the original MERIT code for the ORAL, PNL, TRX, and B&W critical experiments. In the TRX cases, MERIT and the associated ENDF/B-IV cross-section set was used to compute k_{inf} and the leakage corrections from Reference 6.18 were applied to obtain k_{eff}. For all other calculations, the MERIT models used full three-dimensional geometric representations. For the Cross Section Evaluation Working Group (CSEWG) problems [Reference 6.19], the cross section processing is generally in agreement within statistics with the other calculations agreeing especially well with the detailed BAPL (Bettis Atomic Power Laboratories) Monte Carlo calculations. For the two B&W critical experiments with boron curtains and gadolinia rods, the cross sections underpredict the eigenvalue by approximately 0.3 to 0.5 percent. The previous CSEWG evaluations of the ENDF/B-IV files [Reference 6.19] concluded that the experimental k_{eff} is generally overpredicted by 1-2% for plutonium nitrate systems and underpredicted by approximately 0.5 percent for high moderator-to-fuel ratios to approximately 1.5 percent for low moderator-to-fuel ratios in water moderated uranium lattices. The MERIT results confirm these biases, thus supporting the CSEWG conclusions. More details on these results are found in Reference 6.5.

6.6 REFERENCES

6.1. Code of Federal Regulations, Title 10, Part 71, 1992.

6.2. "Specifications for High Flux Isotope Reactor Fuel Elements HFIR-FE-3", March 1, 1991, ORNL/TM-9220.

6.3. GEMER01V User's Manual, K.R. Fletcher, June 1993, NEDE-32172P.

6.4. KENO-IV: An Improved Monte Carlo Criticality Program, L. M. Petrie and N. F. Cross, ORNL4938 (November 1975).

6.5. Safety Analysis Report for Packaging: Model 2000 Radioactive Transport Package, R. J. Pomares and P. A. Peterson, NEDO-31581, (April 1988).

6.6. ORNL Drawing M-11524-OH-101-D: *HFIR Fuel Inner Element.*

6.7. ORNL Drawing M-11524-OH-102-D: *HFIR Fuel Outer Element.*

6.8. Metals Handbook, 10th ed., Vol.1, ASM International Handbook Committee, 1990.

6.9. Safety Analysis Report for Packaging: The ORNL HFIR Spent-Fuel-Element Shipping Cask, J. H. Evans, K. K. Chipley, R. E. Eversole, R. A. Just, G. H. Llewellyn, ORNL/ENG/TM-12 (1977).

6.10. "Critical Lattices of High Flux Isotope Reactor Fuel Elements", E. B. Johnson, Oak Ridge National Laboratory, March 20, 1967, ORNL-TM-1808.

6.11. Y-1858, "Validation Checks of the 'ANISN' and 'KENO' Codes by Correlation with Experimental Data", G.R. Handley and C. M. Hopper, ORNL, November 20, 1972.

6.12. Y-1948, "Validation of the 'KENO' code for Nuclear Criticality Safety Calculations of Moderated Low-Enriched Uranium Systems", G. R. Handley and C. M. Hopper, ORNL, June 13, 1974.

6.13. RSIC, "Documentation for SCALE-08/CESAR11, (Critical Experiment Storage and Retrieval Program).

6.14. WAPD-TM-931, "A Study of Physics Parameters in Several Water-Moderated Lattices of Slightly Enriched and Natural Uranium", J. Hardy, D. Klein, J. J. Volpe, BAPL, March 1976.

6.15. NUREG/CR-0674, "Benchmark Critical Experiments on Low-enriched Uranium Oxide Systems with H/U=0.77", G. Tuck, I. Oh, Rockwell International, August, 1979.

6.16. NUREG/CR-0796, "Criticality Experiments with Subcritical Clusters of 2.35 wt% 235-U Enriched UO_2 Rods in Water with Uranium or Lead Reflecting Walls", S. R. Bierman, B. M. Durst, E. D. Clayton, Batelle Pacific Northwest Laboratory, April 1979.

6.17. "HFIR Spent Fuel Rack Criticality Safety Analysis", R. D. Dabbs, ORNL/C-HFIR-91-021, October 4, 1991.

6.18. Hardy, J., Jr., et al., Nuclear Science Engineering, 40, 101 (1970).

6.19. "Benchmark testing on ENDF/B-IV", E. M. Bohn (ed.), et al., ENDF-230, Vol. I, March 1976.

6.7 APPENDIX

This appendix includes the program input listings for the most reactive normal and single container cases. Since the input is similar to that used in the popular KENO program and deviations from this were described in an earlier section, no further explanation of these listings are necessary.

7.0 OPERATING PROCEDURES

The operating procedures for the Model 2000 Transport Package are provided in Chapter 7 of the Package Safety Analysis Report (SAR), NEDO-31581, April 1988. The procedures in the SAR include those for loading, unloading, and preparation of the empty container for transport. These procedures are also applicable to the transportation of the HFIR fuel using the basket and liner which are the subject of this Safety Analysis Report.

Separate operating procedures will be developed (prepared) for installation of the basket and liner and the loading and unloading of the HFIR fuel assemblies. These are not considered as part of this SAR for the HFIR fuel, as their specific procedures will meet applicable operating conditions and constraints established in Chapter 7, Model 2000 SAR (NEDO-31581).

8.0 ACCEPTANCE TESTS AND MAINTENANCE PROGRAM

The acceptance tests and maintenance program for the Model 2000 Transport Package are provided in Chapter 8 of Package Safety Analysis Report (SAR), NEDO-31581, April 1988. The acceptance tests and maintenance program are also applicable to the HFIR fuel basket and liner described in this Safety Analysis Report.

The non-destructive examinations required during fabrication of the HFIR fuel basket and liner are shown in Section 1.3.2. Routine inspection (prior to each loading) of the basket consists of visual examination for physical damages of all surfaces and bail components. Periodic or once a year inspection includes visual examination of the basket and liner, penetrant inspection of the basket welds, and replacement of all non-safety related components.